



<https://theses.gla.ac.uk/>

Theses Digitisation:

<https://www.gla.ac.uk/myglasgow/research/enlighten/theses/digitisation/>

This is a digitised version of the original print thesis.

Copyright and moral rights for this work are retained by the author

A copy can be downloaded for personal non-commercial research or study, without prior permission or charge

This work cannot be reproduced or quoted extensively from without first obtaining permission in writing from the author

The content must not be changed in any way or sold commercially in any format or medium without the formal permission of the author

When referring to this work, full bibliographic details including the author, title, awarding institution and date of the thesis must be given

Enlighten: Theses

<https://theses.gla.ac.uk/>  
[research-enlighten@glasgow.ac.uk](mailto:research-enlighten@glasgow.ac.uk)

A Study of  
IMPULSE VOLTAGE BREAKDOWN  
with reference to  
THE INITIATION OF FOLLOW CURRENT

By

Liviu L. Alston,  
B.Sc.(Eng.), A.R.T.C., A.M.I.E.E.

Thesis presented for the Degree of Ph.D.  
of the University of Glasgow.

- September 1955 -

ProQuest Number: 10656258

All rights reserved

INFORMATION TO ALL USERS

The quality of this reproduction is dependent upon the quality of the copy submitted.

In the unlikely event that the author did not send a complete manuscript and there are missing pages, these will be noted. Also, if material had to be removed, a note will indicate the deletion.



ProQuest 10656258

Published by ProQuest LLC (2017). Copyright of the Dissertation is held by the Author.

All rights reserved.

This work is protected against unauthorized copying under Title 17, United States Code  
Microform Edition © ProQuest LLC.

ProQuest LLC.  
789 East Eisenhower Parkway  
P.O. Box 1346  
Ann Arbor, MI 48106 – 1346

## SUMMARY

The mechanism of follow current has been studied using a synthetic power source in conjunction with a Marx impulse generator circuit, and air gaps of up to 1.5 cm. The performance of the circuit has been established analytically and experimentally, and the suitability of synthetic power circuits for follow current studies has been confirmed by the results of this investigation.

A resistance divider with inherent voltage limiting characteristics was essential for recording the discharge voltage between the electrodes. A method was devised and was shown, both by analysis and experiment, to have the required characteristics (Appendix I; also reference 17).

The experimental technique having been established, a study has been carried out of the effects of variation in power and impulse circuit parameters, and in electrode material, shape, spacing, and surface condition. Three types of follow current have been defined, and their mechanisms have been explained. A close relation has been shown to exist in many cases between the conditions under which the establishment of follow current is just possible, and those required for arc-glow and glow-arc transitions in the test gap.

Criteria which determine the establishment of follow current have been derived. A large number of variables has been shown to be involved in this problem, and their relative importance has been discussed. Recommendations have been made for further studies, as well as for the control of variables in industrial tests.

## 1. INTRODUCTION

It is known, as a matter of practical experience, that impulse voltage breakdowns on electrical power equipment sometimes, but not always result in the establishment of a power frequency arc. The terms 'Power Follow', 'Power Follow On', 'Follow Current', etc., are used to describe a power arc initiated in this manner.

It is the purpose of this investigation to study the mechanism of follow current and to determine critical conditions under which follow current can just be established. The importance of the phenomena investigated lies in the fact that in many cases the initial impulse discharge does not cause damage to equipment, while follow current may do so, because of the thermal and magnetic forces involved. In the case of transmission systems, follow current constitutes a short circuit, and even if no permanent damage is done, the system is disturbed when the circuit breakers are opened to clear the fault.

Conclusions from a study of follow current phenomena would also find application in the laboratory. In industrial research, follow current is involved in tests on lightning arrestors and in the impulse testing of energised transformers. In fundamental researches, impulse discharges are sometimes used to initiate heavy current arcs, and the mechanism involved is similar to that of follow current.

### 1.1 Previous Work.

Previous follow current experiments were carried out to determine or compare the performance of items of equipment, such as

insulators or arrestors, under specific operating conditions. There was insufficient variation of circuit and test gap parameters to provide data on the fundamental mechanism of follow current: in many tests, no attempt was made to determine the critical conditions under which follow current was just possible, it being sufficient that it was, in fact, established - and that the item under test cleared it after a certain number of half-cycles. When oscillograms were taken, the sweep was usually sufficiently slow to accommodate a full half cycle of the power voltage: little information was therefore available regarding events occurring during and immediately after the end of the impulse.

E.R.A. (1936-40)<sup>1,2</sup> reports the results of follow current tests on insulators and surge arrestors. The significant information provided by those tests was that follow current was independent of the impulse and power voltage polarities in the case of insulators, and occurred more readily when the impulse and power voltages were of opposite polarity in the case of surge arrestors. Provoost (1952)<sup>5</sup> argues that in the case of full-wave impulse tests on energised transformers, follow current is more likely when the impulse and power voltages are of the same polarity. The apparent contradiction between these conclusions, is due to the fact that the relative polarity of the impulse and power voltages affects the establishment of follow current in a complex way, as will be shown in section 14.

Similar work has been carried out by Jones and Garrard (1950)<sup>3</sup> on surge diverters; by Ackermann (1951)<sup>4</sup> on expulsion type lightning arrestors; and by Baumann (1954)<sup>6</sup> on copper electrodes in air, and

separated by solid insulation, the electrode arrangement being of the type used on 250 Volt and 380 Volt distribution systems in Switzerland. These papers contain little data relevant to the fundamental mechanism of follow current, though they describe experimental techniques suitable for follow current tests.

Edels (1951)<sup>7</sup> carried out an analytical investigation of a circuit suitable for the initiation of a d.c. arc. The circuit differed from fig. 1, in that L and C formed a filter protecting the d.c. source (not shown in fig. 1), the high voltage terminal of which was connected to C through a resistor. No experimental data was given, other than a set of values of circuit parameters with which satisfactory impulse initiation was obtained. Certain assumptions had therefore to be made regarding the characteristics of the test gap<sup>7</sup>; these assumptions were satisfactory for the stated object of the investigation, namely for showing qualitatively the effect of variation of circuit parameters (and the permissible limits of their values) on the probability of arc initiation, on the protection of the power source, and on the flashover of the test gap. Now, in order to determine the fundamental mechanism of follow current it is necessary to investigate the test gap characteristics and to set the circuit and test gap parameters so that follow current is only just possible. In this condition, the test gap characteristics cannot be predicted without considerable experimental work; furthermore, their importance is much greater in this limiting case, than when conditions are more favourable for follow current. For these reasons, the paper<sup>7</sup> throws little light on fundamental follow current phenomena, though the following points

are worthy of note:

(1) Effect of polarity. It is stated<sup>7</sup> that the impulse and arc source voltages should be of the same polarity for successful initiation of the arc. This is true if the current circulated by the impulse in the L.V. circuit (i.e. in L) before the test gap flashes over (see section 2.9, current  $I_0$ ) is negligible. It will be seen in section 14.3 that if that current is taken into account, arc initiation will be more likely when the impulse and arc source voltages are of the same or of opposite polarities, depending on the parameters of the circuit and test gap.

(2) Prediction of Current Waveform. A prediction of the waveform of the current flowing in L is given<sup>7</sup>. This waveform was similar to that obtained in the present investigation under corresponding conditions (fig.10(b),  $I_t$  waveshape) except that the initial current  $I_0$  was ignored in the paper<sup>7</sup>.

(3) Arc-glow Transitions. It is stated<sup>7</sup> that, as the impulse discharged, the test gap current would eventually decay to a value,  $I$ , at which an arc-glow transition would occur: the impulse discharge would then cease, and the d.c. arc source would be just able to maintain the discharge. Tests carried out by the present author, and reviewed in this thesis, confirmed that arc-glow transitions do, in fact, occur under certain limiting conditions but it is probable that they are caused by the cessation of the impulse (which terminates when the output gap of the impulse generator ceases to pass current) rather than that the cessation of the impulse is brought about by arc-glow transitions. Be that as it may, one of the conclusions (maximum value of L) derived in the paper<sup>7</sup> from these

considerations, is difficult to follow. Application of Kirchhoff's current law to fig. 1, gives

$$(\text{Test Gap Current}) = (\text{Current in L}) + (\text{Current in } R_F),$$

the potential divider current being negligible. The current in L is the current flowing from the d.c. arc source, and the current in  $R_F$  is the impulse current. If the test gap current and the impulse current each equal I (as is implied by the appropriate equation given in the paper<sup>7</sup>) at the instant at which the impulse discharge ceases, the current in L must equal zero. However, it is stated in the paper<sup>7</sup> that the current in L must equal I immediately after the end of the impulse, and the equation already mentioned<sup>7</sup> implies that that current increases gradually from zero as the discharge proceeds. Hence the current in L must be very nearly equal to I when the impulse discharge ceases. It is difficult to see how these two contradictory requirements may be reconciled.

Experiments carried out by the present author under similar conditions show firstly, that the current in L does, in fact increase gradually and, secondly, that before the impulse ends, that current also contributes to the test gap current, i.e., the statement of Kirchhoff's current law given above was verified by experiment.

In view of the relatively scant information available from follow current investigations, attention was turned to experiments in which the deionisation of a test gap was studied by applying probing voltage pulses some time after the gap had been subjected to an ionising current discharge<sup>8-12</sup>. The essential difference between the deionisation and follow current experiments was that in

the former the test gap was almost always allowed a finite time in which it could deionise: in the latter case, the test gap is given an opportunity to deionise only if the impulse and power voltages are of opposite polarity (section 14.3).

The present author carried out in 1953, a survey of tests on the deionisation of airgaps<sup>11</sup>. So far as the present thesis is concerned, the most significant information available at that date was contained in a paper by McCann and Clark (1943)<sup>8</sup>, who showed that the rate of deionisation of impulse arcs varies little with impulse magnitude and duration (this is discussed by the present author elsewhere<sup>11</sup>) whilst later work (data by McCann, Conner and Ellis (1950)<sup>9</sup> and Wildt (1951)<sup>10</sup> analysed by the present author (1954)<sup>11</sup>) showed that impulse arcs deionised much more rapidly than power arcs. McCann and Clark (1943)<sup>8</sup> also discussed the probability of lightning strokes producing follow current, taking the special case of the impulse flashover occurring when the system voltage is near its zero value. The scope of the discussion is too limited to elucidate the fundamental follow current phenomena.

Kelham (1954)<sup>12</sup> carried out a comprehensive study of the deionisation of test gaps similar to those used in the present work. Two important results emerge from his work:

(1) When there is residual ionisation in the test gap and it is flashed over by the probing voltage, a glow is established immediately after flashover: this is maintained for a little while before degenerating to an arc. Consequently, the arc would not be established if the energy associated with the probing pulse were insufficient for the transition (alternatively, a glow condition

would not have been recorded if the probing circuit had circulated too high a current at flashover). These conditions are similar to those covered by the present investigation in that a follow current arc was preceded by a glow under certain limiting conditions, as will be seen in the following sections.

(2) The voltages required to flash over the test gap shortly after the end of the ionising discharge were of the same order (between 100 and 1,000 Volts) as the voltages required to establish follow current in similar gaps.

Finally, reference will be made in section 13.3 to a paper by Gambling and Edels (1954)<sup>13</sup> dealing with arc and glow discharges at atmospheric pressures.

## 1.2 Statement of the Problem.

Fundamentally, the problem of follow current resolves itself to the following factors:

When an impulse flashover occurs on an electrical power system, a discharge is maintained for a short time,  $t_1$ , by the energy associated with the impulse. During  $t_1$ , power-frequency current may flow through the ionised path provided by the impulse. After  $t_1$ , the impulse energy is dissipated and ionisation can only be maintained if the power fed by the system is sufficient to overcome the losses associated with the discharge. If ionisation is maintained for a sufficient time, a power arc will be established, i.e. power follow will occur.

In addition to the power-frequency current, relatively high frequency currents (up to some 10 kc/s) may be circulated in the

path of an impulse flashover by the discharge of the stray capacitances associated with the system. Thus the impulse may initiate two main types of follow current: power-frequency follow current, and high-frequency follow current. In order to analyse the two types of follow current, it is necessary to treat them separately, that is to say, it is necessary to study the effect of impulse flashovers on single-frequency electrical systems, at frequencies of 50 c/s to 10 kc/s.

The bulk of the present work was devoted to the study of the power-frequency follow current mechanism. The case of high-frequency follow current is of secondary importance, as shown in section 10: it was, therefore, the subject of a limited study only.

## 2. THE TEST CIRCUIT

### 2.1 The Low Voltage Circuit.

The circuit used in this investigation is shown in fig. 1. The single-frequency electrical network, which will be referred to as the 'Low Voltage Circuit', consisted essentially of the capacitor C and the inductor L. It was energised by charging C to a voltage  $V_0$  before applying the impulse.

It will be shown in section 2.9 that a current was circulated by the impulse in the L.V. circuit, between the time at which the impulse was applied and that at which the test gap flashed over; that current was sufficiently small to be ignored at present. Flashover therefore occurred when the voltage on C was  $V_0$ . If follow current became established, the voltage on C oscillated after flashover, the value of its first peak being  $V_0$ . Hence, with the method adopted in this investigation, flashover always occurred at the peak of the voltage wave. The circuit could be adapted for 'point-on-wave' tests by the method suggested in section 16.2.

Three main advantages ensue from the use of a synthetic L.V. circuit. Firstly, variables are easily controlled; a single frequency output is readily obtained and the frequency ( $f = \frac{1}{2\pi\sqrt{LC}}$ ) and the output impedance ( $Z = \sqrt{L/C}$ ) can be varied independently of each other by varying L and C simultaneously. Secondly, a large impedance can be presented to the impulse voltage even though the output impedance, Z, is relatively low. Thirdly, the only part of the L.V. circuit which need withstand the H.V. impulse, is the inductor L, so that insulation problems are restricted to its design.

The inherent limitation of synthetic circuits is that no energy

is generated in them and, consequently, the current and voltage pulses available are of relatively short duration. This has little effect on the present investigation, since the critical events which determine the establishment of follow current will be seen to occur during the first half period of the L.V. circuit (i.e. within a time of not more than 10 milliseconds).

2.2 Values of L.V. Circuit Parameters.

The available values of L.V. circuit frequency ( $f$ ) and output impedance ( $Z$ ), and the corresponding values of  $L$  and  $C$ , are given in Table 1. Maximum use was made of available equipment by selecting these values in geometric progression, as shown by the Table.

TABLE 1.

Available values of  $f$  and  $Z$ , and corresponding values of  $L$  and  $C$ .

$Z \Omega$ $f$ c/s	40	126	400	1260	4000	12600
50	0.126 H 79 $\mu$ F	0.40 H 25 $\mu$ F				
158	0.040 H 25 $\mu$ F	0.126H 7.9 $\mu$ F	0.40 H 2.5 $\mu$ F			
500	0.0126H 7.9 $\mu$ F	0.040H 2.5 $\mu$ F	0.126H 0.79 $\mu$ F	0.40 H 0.25 $\mu$ F		
1580	0.0040H 2.5 $\mu$ F	0.0126H 0.79 $\mu$ F	0.040 H 0.25 $\mu$ F	0.126H 0.079 $\mu$ F	0.40 H 0.025 $\mu$ F	
5000	0.00126H 0.79 $\mu$ F	0.004 H 0.25 $\mu$ F	0.0126H 0.079 $\mu$ F	0.040H 0.025 $\mu$ F	0.126H 0.0079 $\mu$ F	0.40H 0.0025 $\mu$ F
15800		0.00126H 0.079 $\mu$ F	0.004H 0.025 $\mu$ F	0.0126H 0.0079 $\mu$ F	0.040H 0.0025 $\mu$ F	0.126H 0.00079 $\mu$ F

The resistances of the inductor  $L$ , of the shunts  $R_g$  and  $R_{sg}$  (fig. 1) and of the connecting leads, inevitably introduced an ohmic resistance,  $R$ , in the L.V. circuit.  $R$  did not exceed one sixteenth of the critical damping resistance of the L.V. circuit and was usually less than 14 Ohms. Its effect on the establishment of follow current could therefore be ignored within the accuracy of these tests.

The L.V. circuit used in any experiment can be specified fully without reference to the discharge resistance. The value of that resistance is not a function of the L.V. circuit alone; it is, in fact, one of the discharge characteristics which are studied experimentally in this work. Considerations of discharge resistance were therefore not included in this section.

### 2.3 Tests on L.V. Circuit Elements.

The following sets of measurements were taken to determine the frequency,  $f$ , the output impedance,  $Z$ , and the resistance of the inductors,  $R_I$ :

- (1) The impedance presented by the inductors to a 50 c/s sine wave was measured by the ammeter-voltmeter method.
- (2) The resistance  $R_I$  of the inductors was measured on a d.c. bridge.
- (3) The frequency of the L.V. circuit was measured by recording oscillographically the voltage across  $C$  when it was discharged through  $L$  (and the small, but inevitable winding resistance  $R_I$ , associated with  $L$ ).

The value of frequency,  $f$ , was directly available from test (3).

The inductance  $L$  was calculated from the results of tests (1) and (2):  $f$  and  $L$  being known, the output impedance  $Z$  could be calculated. It was found that  $f$  and  $Z$  were within 1% of their nominal values (Table 1) when  $f = 50$  c/s (nominal), and within 5% at other frequencies.

The value of  $R_I$  was obtained from the decrement of the voltage across  $C$  (recorded in test (3)) and was within 10% of the value obtained in test (2).

The ability of the inductors to withstand the voltage output of the impulse generator, both chopped and full wave, was verified in a further series of tests. Results were satisfactory.

#### 2.4 L.V. Charging Source: Effect on Circuit during Tests.

The capacitor  $C$  was charged from an electronic power pack, giving a maximum value for  $V_o$  of 900 Volts (fig. 2). A 100 Henry (nominal) iron cored reactor was inserted between  $C$  and the power pack to separate the latter from the rest of the circuit during the time that the test gap was conducting.

The complete follow current test circuit (fig. 2) was used in a series of tests carried out to ensure that the current flowing from the power source charging  $C$  was negligible while the test gap was conducting, whether follow current occurred or not. Results showed that:

- (1) During the critical period which determined whether or not follow current would occur, the current from the L.V. charging source (i.e. the current in  $R_{sDC}$ , fig. 2) did not exceed about 2% of the current in  $R_s$ .

(2) In the event of follow current being established, the value of the L.V. circuit frequency,  $f$ , was not affected by the charging source.

### 2.5 The High Voltage Circuit.

A 33 kV peak voltage pulse was obtained from a three stage Marx impulse generator having an output capacitance of 0.083 microfarads. Wavefront control was by means of series resistance only. The stray capacitance associated with the test gap was of the order of 20 micro-microfarads. A separate wave tail resistance was provided only in tests 15 - 17 (section 8.4). In all other tests, the tail resistance consisted of the charging resistors of the impulse generator, and had a value of 75 kilohms. The voltage and current waveforms of the generator are discussed in sections 2.6 and 2.7.

Fig. 3 shows the circuit used for tripping the impulse generator and associated oscillograph. A conventional three electrode gap was connected across the first stage of the impulse generator. The central electrode consisted, in fact, of two separate spheres, so that the two halves of the three electrode gap irradiated one another. A 50 megohm; 50 megohm potential divider was used to energise the central electrode.  $R_1$  and the 550 micro-microfarad capacitor formed a delay circuit; the 1 kilohm resistor was inserted to damp out a high frequency oscillation introduced by the delay circuit in the current output wave of the generator. A pulse from the capacitance divider was applied to the 'trigger' terminal of the oscillograph when the switch S was closed and the

time base began to sweep. After a time determined by the delay circuit and the setting of the three electrode gap, the high voltage half of the three electrode gap flashed over; the other half flashed over immediately afterwards and the impulse generator fired.

## 2.6 Voltage output of Impulse Generator Circuit.

The voltage output of the impulse generator circuit (i.e. the voltage at the test gap) was viewed oscillographically, no L.V. circuit being used, and the test gap being set so as not to flash over (fig. 4(a)). The wave front resistance was 400 Ohms (woven wire); there was no separate wave tail resistance and a conventional 9605 Ohm : 52.6 Ohm potential divider was used for recording.

Records showed that the voltage at the oscillograph reached its peak in 0.2 microseconds and that there was a violent oscillation on the wave front. With such a rapidly rising wavefront, special tests would have been necessary to ensure that the oscillograph voltage was a faithful reproduction of the test gap voltage. Now, it will be seen from the following sections that the voltage output of the impulse generator affects the establishment of follow current only in so far as it circulates a current in the L.V. circuit before flashover, and it causes the flashover. Under the conditions of this investigation, the current circulated by the impulse in the L.V. circuit was usually negligible - when it was not, its value was available from oscillograms of  $I_t$  (fig. 1). Furthermore, the test gap spacings used were sufficiently small for flashover to occur on every application of the impulse. An

accurate reproduction of the voltage wavefront was therefore considered unnecessary.

No similar difficulty occurred in recording the wave tail and fig. 4(b) shows typical oscillogram tracings. Their shapes can be explained quantitatively by considering that  $C_{IG}$  discharges through the potential divider and its own charging resistors in the case of curve (i), and that  $C_{IG}$  and  $C$  in series oscillate with  $L$  in the case of curves (ii) and (iii).

### 2.7 Current Output of Impulse Generator Circuit.

The circuit of fig. 5(a) was used to measure the current output of the impulse generator. Two types of shunt ( $R_{sg}$ ) were used in these tests, carbon resistors and short lengths of resistance wire. The current records obtained for a given experimental condition were identical, so that it was assumed that the inductance of the wire and the temperature and resistance coefficients of the carbons were all negligible.

$C_{IG}$  was measured at 50 c/s and  $R_F$  and  $R_T$  were measured on a low voltage Wheatstone bridge. The nominal time constants of several impulse current waveforms (fig. 5(b)) were then calculated from  $T = C_{IG} R_F R_T / (R_F + R_T)$ , and the actual time constants were obtained by noting the time taken for the current wave to decay to 0.368 of its initial value. Results are compared in Table 2 (page 17); agreement is seen to be very good when  $R_F$  and  $R_T$  both consist of woven wire resistors (curve (ii)) and also when  $R_F$  consists of woven wire resistors and  $R_T$  consists of carbon resistors but approximates to an open circuit (i.e.  $R_T \gg R_F$ ).

curves (i) and (iii)). A considerable discrepancy exists when  $R_F$  and  $R_T$  both consist of carbon units (curve (iv)) - due, probably, to the temperature coefficients of the carbons.

Observations made using the complete test circuit (fig. 1) showed that the impulse current waveforms were determined almost entirely by the H.V. circuit, and were substantially independent of the L.V. circuit and test gap.

TABLE 2.

Comparison of the actual and nominal time constants of the impulse current waveforms of fig. 5(b).

Curve No. (see fig.5(b))	Nominal time constant, T	Actual time constant, obtained from oscillograms.
-	Microseconds.	Microseconds.
1	35	35
11	35	32
111	70	72
iv	35	23

2.8 Conventions regarding the test circuit.

Throughout this work,  $I_t$ ,  $I_{IGt}$  and  $I_{gt}$  will be taken as positive when flowing in the direction indicated in fig. 1, and the polarities of  $V_o$  and  $V_{IGo}$  will be taken as their polarities to earth.  $V_o$  and  $V_{IGo}$  were positive in all experiments covered by this work, except for some of the experiments reviewed in

section 14, where polarity effects are discussed.

The current flowing in the potential divider is usually so small that it plays no significant part in the operation of the circuit; it will therefore be ignored throughout this thesis, except where otherwise stated.

### 2.9 The L.V. circuit current at Flashover ( $I_0$ ).

When the impulse is applied - i.e. when IGOG flashes over - an impulse voltage appears across the test gap and L.V. circuit.  $I_t$  will, under these conditions, equal the current circulated by the impulse in the L.V. circuit; if the conventions of fig. 1 are adopted,  $I_t = - I_{IGt}$ . At the instant of flashover,  $I_t$  has the value  $I_0$  and unless otherwise stated,  $I_0$  was sufficiently small to be ignored. The growth of  $I_t$  after flashover will be discussed in later sections.

If  $V_{IGO}$  is positive, therefore,  $I_t$  will be negative immediately after the impulse is applied. Initially,  $I_t$  will increase in magnitude at a rate determined by the complete test circuit (in the present investigation, the rate of growth of  $I_t$  before the test gap flashed over, was determined primarily by  $C_{IG}$ ,  $L$  and  $R_p$ ). If the test circuit is overdamped,  $I_t$  cannot reverse before the test gap flashes over, so that  $I_0$  will be negative. If, however, the test circuit is underdamped,  $I_t$  may reverse before flashover occurs. Provided the frequency of  $I_t$  before flashover is less than some 10 kc/s (as it was throughout this work), flashover is unlikely after  $I_t$  has reversed, because much of the energy associated with the impulse will have dissipated by then, and successive voltage

peaks at the test gap will be of decreasing magnitude. Consequently, if the test gap fails to flash over at or near the first peak, it is not likely to flash over at all. The possibility of flashover occurring after  $I_t$  reversed will therefore be ignored. Consequently, if  $V_{IG_0}$  is positive,  $I_t$  is negative at flashover - i.e.  $I_0$  is negative. Precisely the same reasoning will show that  $I_0$  is positive if  $V_{IG_0}$  is negative. With the conventions adopted, therefore,  $I_0$  is of opposite polarity to the impulse voltage,  $V_{IG_0}$ .

Experiment showed that not only did  $I_t$  not reverse before flashover, but at the instant of flashover,  $I_t$  was increasing in magnitude. This was to be expected, since flashover occurs at or near a voltage peak: consequently,  $\frac{dI_t}{dt}$  could not reverse polarity by the time flashover occurred. Hence the magnitude of  $I_0$  increases with the time-to-flashover of the test gap.

#### 2.10 Effect of Impulse Circuit on L.V. Circuit after flashover.

After the test gap flashes over, the L.V. circuit current is, of course, affected by the discharge voltage: it is not, however, directly affected by the impulse circuit, unless a current zero occurs in the test gap while IGOG (fig. 1) is still conducting. Such a current zero occurred only under the conditions discussed in section 14.3: that was the only case in which the L.V. circuit was directly affected by the impulse circuit after flashover.

IGOG deionises at the end of the impulse; with the exception of test 17 (section 8.4) there were no restrikes of IGOG, so that the impulse circuit was effectively disconnected from the test gap and L.V. circuit after the end of the impulse.

### 2.11 Impulse Duration.

The impulse duration,  $t_1$ , is defined in section 5.6 as the duration of flow of impulse current. It could be measured very accurately by applying the voltage across  $R_{SIG}$  (fig. 1) to the oscillograph through an amplifier (section 4.4).

In most experiments covered by this investigation, the impulse duration was determined primarily by the impulse circuit, the L.V. circuit and test gap having a secondary effect. In all tests in which a value is quoted for  $t_1$ , and also in all experiments involving the Standard Circuit (section 5.9), the scatter in the value of  $t_1$  (due to changes in the L.V. circuit and test gap, and to random conditions) did not exceed  $\pm 5\%$ , except for tests 16 and 17 (section 8.4) in which it did not exceed  $\pm 10\%$ .

### 3. THE TEST GAP.

All experimental work was carried out in air under atmospheric conditions, at electrode spacings of not more than 1.5 cm.

Tungsten, platinum, brass, steel, aluminium and copper electrodes, of commercial purity, were used. The electrodes were of two principal types, according to the relative size of their arcing surface and the area of the arc roots: 'large' electrodes, whose surface was much larger than the arc roots, and 'small' electrodes, whose surface area was of the order as the area of the arc roots.

The 'large' electrodes were themselves of two types. The first, consisted of 2 cm. diameter spheres, which were assembled as shown in fig. 6(a). The frame of the electrode assembly was of bakelite. The adaptor A was fixed to the frame, and the adaptor B was fixed to the micrometer head, M, which was in turn fixed to the frame. The electrode spacing was varied by rotating the micrometer head, which also served to measure it.

The second type of 'large' electrodes consisted of discs, 15 cm. diameter, 1 cm. thick, with edges rounded to 1 cm. radius (fig. 6(b)). They were assembled as shown in fig. 6(c). The electrodes were mounted on metal shafts which were held between bakelite supports. Electrical connections to the electrodes were made through the shafts. The shaft supporting the upper electrode could be moved vertically in grooves cut in the bakelite supports, thus altering the electrode spacing. The spacing was

measured by means of 'feeler' gauges.

The disc electrodes could be used in one of two ways, namely

- (1) They could be rotated about their axes so as to obtain a clean arcing surface. In the tests in which this was done, the electrodes were rotated once every five flashovers; it was found that almost every flashover occurred to virgin metal in that case.

The sides of the electrodes were covered with black paint (fig. 6(c)) and the metal arrows A bore on the paint and scratched it as the electrodes rotated; the angular movement of the electrodes could thus be ascertained.

- (2) They were fixed in space, so that all flashovers occurred on a small fraction of the disc circumference; that fraction of the circumference became heavily oxidised.

These electrodes were used only in experiments aimed at determining the effect of oxidation produced by flashovers on the establishment of follow current (section 12). Those experiments showed that (a) the conditions under which follow current could just be established (i.e. the critical  $V_0$ , sections 12.7 and 12.10) obtained with disc electrodes was the same as that obtained with spheres under the same conditions, and (b) that flashover always occurred centrally on the edges of the discs (see also photographs of figs. 47, 51 and 52).

The 'small' electrodes consisted of rods having a diameter of not more than 0.063 cm. The assembly of fig. 6(a) was used,

except that the adaptors were replaced by a pair suitable for holding rod electrodes. The length of electrode protruding from the adaptor was not less than 2 cm.

## 4. MEASUREMENT TECHNIQUES

### 4.1 A Potential Divider with a Non-Ohmic Resistor. <sup>17</sup>

The recording of the test gap voltage was complicated by the very considerable variation in its amplitude. Before the test gap flashed over (or if it failed to flash over) the voltage across it could attain 33 kV. A divider ratio of the order of 100 : 1 would have been required to apply this voltage to the oscillograph. After flashover, the voltage reduced to the arc (or glow) value, and the deflection on the oscillograph would not have been visible had a 100 : 1 divider ratio been used.

The solution was found in the use of the potential divider shown in fig. 7.  $R_H$  and  $R_L$  are two ohmic resistors, constructed of woven wire resistance ribbon;  $R_M$  is a silicon carbide non-ohmic resistor, the resistance of which has the instantaneous value  $R_{Mt}$ , and  $C_H$  and  $C_L$  represent stray capacitances. A general discussion of this type of divider is given in Appendix I, together with proving tests which were carried out on the actual divider used in this investigation. The principal characteristics of the divider are that  $R_{Mt} \ll R_H$  when the test gap voltage is high, so that the voltage at the oscillograph is limited to a safe value; when the test gap voltage has reduced to the discharge value,  $R_{Mt}$  approximates to an open circuit and the divider ratio is determined essentially by the ohmic units.  $(R_H + R_L)$  was maintained constant at 23 kilohms in follow current tests, and the divider ratio was varied by altering  $R_H$  and  $R_L$  simultaneously, subject to  $R_H \geq 10$  kilohms. Apart from the initial error discussed below, the accuracy of the divider was estimated at  $\pm 1\%$ .

The main limitation of this type of divider is due to the charges which accumulate on the stray capacitances  $C_H$  and  $C_L$  just before flashover. In the present case, the effect of the charge on  $C_L$  predominated and delayed the reduction in  $V_{Lt}$  at flashover. Tests described in section 5.2 of Appendix I showed that the initial charge dissipated in some 5 microseconds, after which the effect of stray capacitances reduced to that on the linear divider  $R_H R_L$  - the conventional case. Now, the voltage waveshape during the first few microseconds is not very important in the present investigation and events recorded in follow current tests always exceeded 200 microseconds duration. Consequently, an increase of 5 microseconds in the time required by the test gap to collapse could hardly be detected from oscillograms, so that no significant error was introduced in follow current test records by the initial charge on the stray capacitances.

#### 4.2 The Amplifier.

It was estimated before tests were carried out that the current flowing in the L.V. circuit during the critical period when it was determined whether or not follow current would be established, would not exceed 1 Amp. The value of the shunt resistor used to record this current had to be less than 10 Ohms in order that  $R$  should be small (section 2.2). Hence it became evident that an amplifier would have to be inserted between the shunt and the oscillograph. These estimates were later substantiated by experiment.

Fig. 8(a) is the circuit diagram of the two stage, RC coupled amplifier used. Feedback was provided on both stages. Either

the input stage alone or the complete amplifier was used, and the overall gain of the amplifier was 81. The amplitude response was linear over the range used, the frequency response for the complete amplifier being given in fig. 8(b).

The amplifier was calibrated after each test in which it was used, the method being given in Appendix II. Variations in gain did not exceed  $\pm 2.5\%$ . This figure could probably have been reduced, but that was not necessary for the present purpose.

#### 4.3 Oscillographic Equipment.

In follow current tests, a double beam oscillograph was used to give a simultaneous record of the test gap voltage and of the current in one of the shunts (fig. 1).

A high speed transient oscillograph (single beam) was used in tests concerned with the H.V. circuit alone (sections 2.6 and 2.7) and to measure the impulse duration in some follow current tests (section 11).

#### 4.4 The Shunts.

The shunts are shown in the circuit diagram (fig. 1); typical records obtained at each shunt are shown in fig. 9.  $R_g$  was used in conjunction with the amplifier to record the current in the L.V. circuit (figs. 9 (g) and (h));  $R_{SIG}$  was used either in conjunction with the amplifier to give a very accurate recording of the impulse duration (see fig. 9(f)) or, without the amplifier, to measure the current in the H.V. circuit (fig. 9(e)). The shunt  $R_{sg}$  could be used to measure the test gap current (figs. 9 (a) - (d)), but use was made of this shunt only to explore the operation of the circuit

and to confirm results obtained without it. It was preferred to short-circuit  $R_{sg}$  during follow current tests and to obtain the test gap current by measuring its components in terms of the voltages across  $R_s$  and  $R_{sig}$ . The reason for so doing is discussed in Appendix II, where the oscillograms traced in fig. 9 (a) - (d) are considered in greater detail.

With the exception of some tests carried out at 500 c/s, when woven wire shunts were used, the shunts used in follow current tests consisted of 1 or 2 watt carbon resistors, the individual values of which did not exceed 10 Ohms; the value of individual shunts did not exceed 6 Ohms.

## 5. PRINCIPAL DEFINITIONS

### 5.1 Symbols.

Principal symbols are defined on the circuit diagram of fig. 1. In the case of quantities which vary in time, the suffix  $t$  is used to denote instantaneous value (i.e. value at any time  $t$ ). When it is intended to represent the value of such a quantity at a specified time, the suffix  $t$  is replaced by the time concerned. Thus  $I_t$  is the instantaneous value of the L.V. circuit current;  $I_0$  is its value at time zero,  $I_{t_1}$  is its value at time  $t_1$ ,  $I_{t_M}$  is its value at time  $t_M$ , and so forth.

Time zero is taken as the instant of flashover.

### 5.2 Follow Current.

It has been shown in section 1.2 that two principal types of follow current may occur on power systems: power-frequency follow current, due to the e.m.f. generated in the system, and high-frequency follow current, due to the discharge of stray capacitances associated with the system. It is now necessary to define these two types of follow current and the conditions which must be satisfied in each case in order that follow current be taken to have occurred; these definitions are given below in terms which are easily interpreted experimentally.

### 5.3 Low-Frequency Follow Current (L.F. Follow Current).

It will be borne in mind firstly, that under the conditions of this investigation flashover occurred when the low voltage circuit current was equal (or approximated) to zero and, secondly, that in the case of power-frequency follow current, the half period  $1/(2f)$  is much longer than the impulse duration,  $t_1$ . Consequently, if power follow current becomes established, a natural current zero

of the L.V. circuit will occur some  $1/(2f)$  seconds from the instant of flashover. During that time, much of the initial ionisation due to the impulse will have dissipated and the state of ionisation of the discharge will depend largely, if not wholly, on the current that has been fed to it by the L.V. circuit. Hence the reignition of the discharge after a natural current zero is effectively independent of the impulse, and is not relevant to the conditions under which an impulse initiated arc develops into a short circuit on a power system. Power-frequency follow current will therefore be taken to have been established if the L.V. circuit has maintained the discharge up to its first natural current zero following upon the end of the impulse.

The mechanism by which an impulse-initiated discharge is maintained up to its first natural current zero after the end of the impulse, is not specific to the usual power frequencies of 50 or 60 c/s. A similar mechanism operates in all cases in which follow current is defined as above and in which  $t_1 < 1/(2f)$ ; this mechanism was, in fact, investigated at frequencies up to 500 c/s in the present work. The term Low-Frequency (L.F.) Follow Current will therefore be used in preference to Power-Frequency Follow Current to describe this type of follow current.

As the frequency,  $f$ , of the follow current is increased under these conditions, the impulse will have an increasing effect on the reignition of the discharge after the first natural current zero. Nevertheless, the mechanism by which the L.V. circuit takes over and maintains the discharge after the impulse has ceased, emerges, as before, from the analysis of events occurring between the end of

the impulse and the first subsequent natural current zero of the L.V. circuit; the reignition of the discharge after that current zero remains irrelevant to the present investigation. The following definitions can therefore be stated:

1. THE TYPE OF FOLLOW CURRENT OPERATING WHEN THE IMPULSE DURATION IS LESS THAN THE HALF PERIOD OF THE L.V. CIRCUIT (i.e.  $t_1 < 1/(2f)$ ) WILL BE KNOWN AS LOW-FREQUENCY FOLLOW CURRENT.

2. Two requirements are defined for the establishment of follow current, viz.:

(i) THE DISCHARGE MUST BE MAINTAINED BY THE L.V. CIRCUIT UP TO ITS FIRST NATURAL CURRENT ZERO AFTER THE END OF THE IMPULSE.

If the effects of  $I_0$  and of the discharge voltage,  $V_{gt}$ , are ignored, this condition becomes that the L.V. circuit current  $I_t$  - and hence the discharge current  $I_{gt}$  - flows for  $1/(2f)$  seconds from the instant of flashover. The effects of  $I_0$  and  $V_{gt}$  are of secondary importance in this instance and are discussed in the Appendix (V).

(ii) THE DISCHARGE HAS AN ARC CHARACTERISTIC FOR MOST OF THE TIME ELAPSING BETWEEN THE END OF THE IMPULSE AND THE FIRST NATURAL CURRENT ZERO.

#### 5.4 High-Frequency Follow Current (H.F. Follow Current).

The establishment of high-frequency follow current was studied from the point of view of its effect on the discharge while the impulse arc was burning, for two reasons. Firstly, the only alternative would have been to study the mechanism by which a high-frequency follow current arc would be maintained by the L.V. circuit after the impulse has ceased. It was considered that the

latter method which was, in fact, adopted in the case of L.F. Follow Current, was unlikely to reveal any significant data not shown by the study of L.F. Follow Current. Secondly, the importance of high-frequency follow current in the case of power systems lies primarily in its effect on the establishment of power-frequency follow current: this will depend very largely on the effect of high-frequency follow current on the state of ionisation of the discharge during the impulse.

The following definitions were therefore adopted:

1. THE TYPE OF FOLLOW CURRENT OPERATING WHEN THE IMPULSE DURATION EXCEEDS THE HALF PERIOD OF THE L.V. CIRCUIT (i.e.  $t_1 > 1/(2f)$ ) WILL BE KNOWN AS 'HIGH-FREQUENCY FOLLOW CURRENT'.
2. H.F. FOLLOW CURRENT WILL BE TAKEN TO HAVE OCCURRED IF THE L.V. CIRCUIT HAS SUPPLIED ANY POWER TO THE DISCHARGE, THAT POWER BEING DRAWN FROM THE INITIAL ENERGY  $\frac{1}{2}V_0^2 C$  STORED ON C AT FLASHOVER.

### 5.5 Natural Current Zero.

A 'Natural Current Zero' of the L.V. circuit will be taken to mean a current zero which has been reached primarily because of the normal reversal of current in a resonant circuit consisting of L and C (fig. 1), the time at which that current zero is reached being substantially independent of the effective resistance of the test gap.

This qualitative definition is satisfactory for the greater part of this investigation. A quantitative interpretation is required only for certain tests and is given in the Appendix (V).

### 5.6 Half Cycle and Half Period.

A 'Half Cycle' of the L.V. circuit will be taken to occur between two natural current zeros. Its nominal duration i.e. the 'Half Period', will therefore be  $1/(2f)$  seconds.

### 5.7 Impulse Duration ( $t_1$ ).

The impulse duration,  $t_1$ , will be taken as the time elapsing between the instant of flashover and the instant at which  $I_{IGt}$  falls to zero for the first (and generally the only) time.

### 5.8 Critical values and ranges.

The term 'critical  $V_0$ ' will be taken to mean the value of  $V_0$  at which the establishment of follow current is just possible in a given experimental condition. The range of critical values of  $V_0$  obtained in a given experimental condition (i.e. the range of values at which follow current occurs after a fraction of flashovers) will be known as the 'critical range of  $V_0$ '.

The values of other variables recorded when  $V_0$  was given its critical value will be known as the 'critical values' of those variables. Their ranges, recorded when  $V_0$  was in its critical range will be known as the 'critical ranges' of those variables.

### 5.9 The Standard Circuit.

The Standard Circuit is defined as a circuit having the following parameters:  $f = 50$  c/s,  $Z = 40$  Ohms,  $C_{IG} = 0.083$  microfarads,  $R_T = 75$  kilohms (carbon),  $R_F = 420$  Ohms (woven wire, unless otherwise stated),  $V_{IG0} = 33$  kV. The value of  $V_0$  is not specified. The impulse current waveshape obtained with the

Standard Circuit is given in fig. 5 (curve iii). Its peak value was 79 Amps and the impulse duration,  $t_1$ , varied between 170 and 180 microseconds.

#### 5.10 The Standard Electrodes.

0.063 cm. diameter Tungsten rods, the tips of which have been heavily oxidised and enlarged to a diameter of some 0.075 cm., will be known as the 'Standard Electrodes'. The oxidation and enlargement of the electrode tips was due to the application of about 1,000 flashovers, the Standard Circuit (section 5.9) being used, with  $V_0$  set to within the critical range, and a gap spacing of 0.5 cm. The electrode surface due to these flashovers was similar to that obtained in a typical test run and did not change significantly in the course of the follow current tests described here (except for the tests discussed in section 12.2, where the effect of oxidation was investigated). The electrodes were cleaned with metal polish and ether before the first flashover was applied and were not cleaned subsequently. (except as stated in section 12.2).

#### 5.11 The Standard Gap.

The gap consisting of the Standard Electrodes, spaced 0.5 cm. apart, will be known as the Standard Gap.

#### 5.12 The Standard Condition.

The Standard Condition will be said to hold when the Standard Gap is used in conjunction with the Standard Circuit.

## 6. PROCEDURE.

The following procedure was adopted in follow current tests: For a given test condition, all variables were fixed, except the voltage  $V_0$ , to which the capacitor C (fig. 1) was charged before the impulse was applied;  $I_0$  being quite small, that voltage can be taken equal to the voltage to which the capacitor was charged at the instant of flashover (section 2.1).

$V_0$  was varied until it had a critical value, i.e. until follow current occurred occasionally. It was then increased until follow current occurred after every one of  $n$  flashovers applied, giving one limit of the range of critical values of  $V_0$ .  $V_0$  was then decreased in order to establish the other limit of the range. Unless otherwise indicated, each limit was established in this way several times in each test.

When near to one of the limits,  $V_0$  was varied in steps of not more than 10%. The quantity  $n$  had the value 5 or 10, as indicated where the appropriate results are presented; if no indication is given,  $n$  had the value 5.

The upper and lower limits of the critical range of  $V_0$  were determined the same number of times; their arithmetic mean was taken as the mean value of critical  $V_0$  for a specific test.

## 7. CLASSIFICATION OF PHENOMENA.

It has been shown that Follow Current is of two principal types: L.F. and H.F. Follow Current (sections 1.2, 5.2, 5.3 and 5.4). Experimental work, which will now be reviewed, has revealed that L.F. Follow Current may itself be of two types which will be known as High-Voltage and High-Current Follow Current. Three main types of Follow Current have, therefore, been identified: High-Voltage, High-Current and High-Frequency Follow Current.

The characteristics of each type of Follow Current are summarised below and a detailed discussion is given in sections 8 - 10. Only the case of  $V_0$  and  $V_{IG0}$  being positive is discussed in these sections; polarity effects are considered in section 14.

### 7.1 High Voltage Follow Current (H.V. Follow Current).

This type of follow current was obtained when  $t_1 < 1/(16f)$  i.e.  $t_1$  was very small compared to the half period of the L.V. circuit. Fig. 10 shows tracings obtained from oscillograms of discharge voltage,  $V_{gt}$ , and L.V. circuit current  $I_t$ ; the tracings are idealised during the period  $t_c$ , as explained below.

Before the impulse is applied, the test gap voltage equals the voltage to which C is charged; it has been seen that that voltage has the value  $V_0$ . Immediately the impulse is applied, the test gap voltage rises but the voltage at the oscillograph does not rise in proportion because of the non-linear unit,  $R_M$  of the potential divider. At the same time, a current is

circulated in the L.V. circuit by the impulse: this current reaches the value  $I_0$  at flashover.  $I_0$  appears to rise instantaneously in fig. 10 because of the time resolution used: its actual rate of growth is discussed in section 2.9. Except where otherwise stated,  $I_0$  was negligibly small.

When flashover occurs, the voltage at the test gap collapses and is maintained at a low value by the impulse current. That current ceases at  $t_1$ , when the L.V. circuit feeds a current  $I_{t1}$  to the discharge. Immediately after  $t_1$ ,  $V_{gt}$  begins to rise, the extent and nature of the rise depending on the power available from the L.V. circuit. The wave shapes of  $V_{gt}$  during the period  $t_c$ , and events occurring during that period, are discussed in detail in section 8. At present, it need only be noted that the voltage and current wave shapes after  $t_c$  are as shown in fig.10(a) or 10(b), depending on whether or not follow current is established and that the principal characteristics of H.V. follow current are:

- (1) The critical  $I_{t1}$  is small, recorded values being between 0.1 and 0.7 Amps. This is of the order of current associated with high-pressure glows and glow-arc transitions.<sup>13,14</sup> Fig. 11 shows  $I_t$  waveshapes obtained when  $I_{t1}$  has the value at which follow current is just possible: follow current is not established after every flashover in that condition.
- (2) The critical value of  $V_0$  is relatively large and approaches that required to maintain a constant current glow in the test gap.
- (3) Either follow current is established or the test gap deionises within a short time (usually of the order of 100 microseconds)

from the end of the impulse.

### 7.2 High Current Follow Current (H.C. Follow Current).

This type of follow current obtained when  $\frac{1}{16f} < t_1 < \frac{1}{2f}$ .

Fig. 12 shows sketches of typical oscillograms recorded when the value of  $V_0$  was in the critical range. They are similar to those of fig. 10, except that  $I_{t1}$  is larger, so that there is little rise in  $V_{gt}$  at  $t_1$ , whether or not follow current is established.

The principal characteristics of H.C. Follow Current are:

- (1) The critical value of  $I_{t1}$  is sufficiently large to maintain an arc after the end of the impulse.
- (2) The critical  $V_0$  is low, being of the order of the arc voltage.
- (3) Current flows for a considerable time after the end of the impulse, whether or not follow current is established.

The time  $t_{LV}$  for which L.V. circuit current flows increases with  $V_0$  (except at very low values of  $V_0$ , as explained in section 9) until  $t_{LV} \approx 1/(2f)$ . This is illustrated in fig.13.

### 7.3 High Frequency Follow Current (H.F. Follow Current).

H.F. Follow Current was obtained when  $t_1 > 1/(2f)$  (section 5.4).

Current and voltage waveforms obtained from oscillograms are sketched in fig. 14. They are shown for two cases: in one,  $V_0$  is well above the value required for follow current, and in the other it is well below it. As  $V_0$  approaches its critical value,  $I_t$  decreases in magnitude. When  $V_0$  reaches the critical value,  $I_t$  is very much smaller than the value of the impulse current  $I_{igt}$ .

Consequently, the main characteristics of this type of

follow current are:

- (1) The discharge is maintained for a time  $\approx 1/(2f)$  whether or not follow current occurs.
- (2) When  $V_0$  is in the critical range, the characteristics of the discharge are determined primarily by the impulse generator output and the test gap: the effect of the L.V. circuit is relatively small.

## 8. ANALYSIS OF H.V. FOLLOW CURRENT CHARACTERISTICS.

Three possibilities arise, depending on the value of  $V_0$ :

- (1) The value of  $V_0$  is less than critical. This case is in every way similar to that of fig. 18 (a)-(b), which is discussed in section 9.
- (2) The value of  $V_0$  is greater than critical. Oscillograms obtained are similar to those of fig. 10(a), except that the rise in  $V_{gt}$  after  $t_1$  is smaller, and the corresponding rise in  $I_t$  is more rapid.
- (3) The value of  $V_0$  is critical.

The characteristics of H.V. Follow Current emerge from an analysis of case (3). The other two cases are not relevant to the present section, and will not be discussed further.

### 8.1 Qualitative discussion.

The mechanism of H.V. Follow Current will be discussed qualitatively, in the first place, referring to the circuit of fig. 1, and to the waveshapes of fig. 10.

The discharge is an arc during the impulse period, when it is maintained by the impulse and L.V. circuits - mainly the former. After the end of the impulse, the power input to the discharge,  $P_{gt} (= I_{gt} V_{gt})$ , is supplied by the L.V. circuit alone: unless  $V_0$  is appreciably larger than its critical value, the discharge will then begin to deionise, and  $V_{gt}$  will increase in value.

Now,  $I_{gt} = I_t$  (Fig. 1) after the impulse. So long as  $V_{gt} < V_t$ ,  $L \frac{dI_t}{dt}$  will be positive, so that  $I_{gt}$  will continue to increase as  $V_{gt}$  rises: consequently,  $P_{gt}$  will also increase, and

a point may be reached at which  $P_{gt}$  will equal the deionising losses. Further increase in  $V_{gt}$  will therefore be checked, but  $I_{gt}$  will continue to increase, increasing  $P_{gt}$ .  $V_{gt}$  then begins to decrease, resulting in a more rapid increase in  $I_{gt}$ , and the outcome of this cumulative process, will be the establishment of follow current. If however, the deionising losses exceed  $P_{gt}$  after  $V_{gt} = V_t$ , then  $V_{gt}$  will rise further and  $L \frac{dI_t}{dt}$  will become negative.  $I_{gt}$  will decrease, resulting in more rapid increase in  $V_{gt}$ , and the discharge will cease without follow current being established. Hence, in the limiting condition in which follow current is just possible,  $\frac{dI_t}{dt} \rightarrow 0$  immediately after the impulse. More specifically if the maximum value of  $V_{gt}$  occurs at time  $t = t_M$ , then

$$\frac{dI_{tM}}{dt} = 0 \dots\dots\dots (I)$$

and consequently, from fig. 1,  $V_{gtM} = V_{tM}$ . Now,  $t_M$  is not much greater than  $t_1$  and is therefore small compared to the half period of the L.V. circuit (follow current being of the H.V. type).

Consequently  $V_{tM} \approx V_0$ , and hence

$$V_0 \approx V_{gtM} \dots\dots\dots (II)$$

Hence, the critical value of  $V_0$  is determined by the fact that it must circulate a sufficiently large current in the discharge at the end of the impulse, for the maximum discharge voltage to be approximately equal to  $V_0$ .

The above discussion may be modified by arc-glow and glow-arc transitions, as will be seen below (section 8.2). It is based on the tacit assumption that the discharge has a negative

characteristic; this assumption is discussed in section 13.4.

## 8.2 Discharge Characteristics - Effects of Transitions to Glow.

The results obtained under different experimental conditions can be divided into three main types, depending on the characteristic of the discharge in the immediate post-impulse period,  $t_c$ .

Type I. The discharge is an arc during  $t_c$  and the  $V_{gt}$  curve is smooth, except that disturbances of very short duration occur after some flashovers (fig. 15(a)). The following reasons give rise to the belief that the disturbances were caused by arc-glow transitions, followed almost immediately by glow-arc transitions:

- (1) The discharge currents were of the order associated with transitions (section 7.1, point 1).
- (2) The disturbances did not occur if the discharge current was increased (by increasing  $V_0$ ).
- (3) Arc-glow transitions, followed after a finite time by glow-arc transitions, have been identified under experimental conditions which differed only slightly from those discussed here (see type II below, and fig. 15(b)).

Because of the short duration of the disturbances, their effect on equations (I) and (II) (section 8.1) can be ignored.

Type II. The discharge is an arc during most of  $t_c$ , but glows are maintained for times of the order of 10 micro-seconds (fig. 15(b)) after some flashovers. The L.V. circuit must therefore be capable of forcing a glow-arc transition in order to

establish follow current, and  $V_0$  must exceed the maximum arc value of  $V_{gt}$ ; it need not, however, equal the maximum glow value of  $V_{gt}$ , because an appreciable fraction of the voltage required to maintain the short duration glow can be supplied by the energy stored in L. Thus the critical  $V_0$  is less than  $V_{gtM}$ .

$\frac{dI_t}{dt}$  is negative during the glow periods, and positive during the arc periods; on the whole, there is little variation in  $I_t$  during the immediate post impulse period.

Type III. The discharge is a glow during most of  $t_c$  after almost every flashover. The glow may have been reached by a gradual increase in voltage (fig. 15 (c)), or by a sudden transition (fig. 15 (d)). Equations (I) and (II) (section 8.1) hold,  $V_{gtM}$  being a glow voltage. This leads to the Glow Criterion, as explained in section 13.2.

### 8.3 Quantitative Analysis - Procedure.

All but three of the tests which will be discussed in section 8.4 were carried out with the Standard Electrodes (section 5.10). In two cases (tests 13 and 14) the electrodes consisted of 0.047 cm. diameter platinum rods. Before being used, these electrodes were cleaned with metal polish and ether and were subjected to some 300 preliminary flashovers, the experimental conditions being as in test 13 (section 8.4) and  $V_0$  having a critical value. The purpose of these flashovers was to produce a surface condition similar to that due to the tests, so that there should be no significant change in electrode conditions as the tests proceeded. The appearance of the electrodes at the end of these tests was similar to that described in section 12.3, where

other tests on platinum electrodes are discussed.

2 cm. brass spheres were used in test 12, immediately after being cleaned with metal polish and ether. Preliminary flashovers were not applied, because other work (section 12.3) has shown that in the case of brass spheres the critical conditions required for H.V. Follow Current do not change with the application of flashovers - i.e. a stable condition exists even when the spheres are clean and untouched by flashovers.

For the analysis, values of  $V_{gt}$  and  $I_{gt}$  were recorded after the end of the impulse, at two specified times,  $t_2$  and  $t_3$ , measured from the instant of flashover. These times were so fixed for a given impulse duration, that when the value of  $V_0$  was critical and follow current was established,  $P_{gt2}$  was slightly smaller than the deionising losses, while  $P_{gt3}$  exceeded them slightly. Corresponding differences between  $I_{gt2}$  and  $I_{gt3}$ , and between  $V_{gt2}$  and  $V_{gt3}$  were small. Also,  $t_2 < t_M < t_3$  and  $V_{gt2}$ ,  $V_{gt3}$ , or both, were nearly equal to  $V_{gtM}$  (except as explained for Test 28).

Recorded values of  $I_{gt}$  and  $V_{gt}$ , and derived values of  $P_{gt}$  and  $R_{gt}$  are given in figs. 16 and 17. In some cases, when results were of type II and the glow duration was particularly short, arc voltages only were entered in figs. 16 and 17, where dotted lines are used to indicate this condition.

The values of  $V_{gt}$  and  $I_{gt}$  were available from about one hundred oscillograms in each one of the tests discussed in section 8.4. It was found, firstly, that in any one test the limits of the critical ranges (section 5.5) of the quantities recorded were

usually available from oscillograms taken at the maximum and minimum values of  $V_o$  used in the test and, secondly, that the difference between the values of any given quantity (e.g.  $I_{gt2}$ ) recorded on different flashovers, but at the same value of  $V_o$ , were usually small compared to the critical range of that quantity. Not more than 20 (and not less than 5) oscillograms were therefore analysed for each test; they included oscillograms taken at the limits of the critical range of  $V_o$ , they were uniformly distributed over that range and their number varied with it (i.e. the greater the critical range of  $V_o$ , the more oscillograms were analysed), and they covered the limits of the critical ranges of all tabulated variables.

#### 8.4 Quantitative Analysis - Discussion of results.

The results of tests 1 - 6 of fig. 16 give an indication of the random variations occurring for a given experimental condition, and can be used as references to show the effect of different variables.  $R_p$  consisted of carbon resistors in tests 1 - 3, and of woven wire resistance ribbon in tests 4 - 6: its 'cold' value was 420 Ohms in both cases. The difference in the constitution of  $R_p$  resulted in  $t_1$  being some 10% smaller when carbon resistors were used. (Impulse current waveshapes obtained with the two types of resistor, are given in fig. 5(b), curves iii and iv).

Increasing  $Z$  (test 7) resulted in a lower rate of rise of  $I_t$ ; consequently, the critical  $V_o$  increased.  $V_o$  being larger, follow current could be established after a higher value of  $V_{gtM}$ ; that is why the critical  $I_{gt2}$  and  $I_{gt3}$  values were lower. At these

low current values, the maintenance of an arc became more difficult so that results were of type II, as against type I in the Standard Condition.

Increasing  $f$  (test 8) increased the rate of rise of  $I_c$ : the critical  $V_0$  therefore decreased, with consequent increase in  $I_{gt2}$  and  $I_{gt3}$ . The reverse happened in tests 9 and 10, in which the rate of rise of current was decreased (with reference to test 8) by increasing  $Z$ . In test 9, the value  $Z/f$ , and hence the rate of rise of current, were the same as in the Standard Condition: results were identical with those of test 3 (which was carried out immediately before test 9).  $V_{gt}$ ,  $P_{gt}$  and  $R_{gt}$  were large in test 10, because they included glow values.

Test 11 shows that all tabulated values except  $R_{gt2}$  and  $R_{gt3}$  increased when the test gap spacing increased. Replacing the Standard Electrodes by 2 cm. diameter brass spheres is shown by test 12 to have no appreciable effect on the values recorded. However, when the electrodes were replaced by 0.047 cm. diameter platinum rods (test 13), a slight but definite increase occurred in all recorded values.

The platinum electrodes were retained in test 14, and the gap spacing was increased to 1.5 cm.: the effect of spacing was qualitatively the same as with Standard Electrodes. Oscillograms showed that in fact  $t_{gt2} \approx t_{gt3}$  in tests 11 and 14, so that  $P_{gt3}$  was very nearly equal to the power input just sufficient to maintain ionisation. Now, when the spacing was increased from 0.5 to 1.5 cm.,  $P_{gt3}$  increased about  $5\frac{1}{2}$  times in the case of Standard Electrodes, and about  $2\frac{1}{2}$  times in the case of platinum electrodes.

This difference points to the Standard Electrodes having a lower work function, so that their importance is reduced as compared to that of the air space between them, in opposing the establishment of follow current. The effect of electrode material, shape and spacing is discussed further in section 12.

The effect of changes in impulse generator parameters, and hence in the waveshape of the impulse current, is shown in fig. 17.  $R_F$  consisted of woven wire resistance ribbon in all tests of fig. 17 so that the current waveform is an exponential decay from the initial value  $I_{IG0}$  (e.g. fig. 5(b), curves i - iii) and becomes zero when IGOG deionises at time  $t_1$ . The waveshape is therefore defined by the maximum value,  $I_{IG0}$  and the impulse duration,  $t_1$ , both of which are entered in fig. 17. Apart from variations in  $R_T$  and  $R_F$ , the Standard Condition held in the tests recorded in fig. 17.

A decrease in impulse duration was obtained by decreasing  $R_T$  (tests 15 - 17). The impulse duration being smaller,  $I_t$  had less time to build up: the critical  $V_0$  increased, with consequent decrease in the critical  $I_{gt}$ .

Test 17 was the only one in which restrikes of IGOG (fig. 1) were recorded. IGOG is connected in series with  $R_F$  and  $R_T$  across the test gap, and  $(R_F + R_T)$  had a low value (565 Ohms) in test 17. When an arc-glow transition occurred at the test gap, and  $V_{gt}$  rose to a relatively high value, the fraction of  $V_{gt}$  appearing across IGOG was sufficiently high to restrike IGOG in some cases. The energy stored in L could then discharge through  $R_F$ , IGOG and  $R_T$ .

so that there was less chance of follow current being established after a glow-arc transition (i.e. as in type II results). Hence the critical  $V_0$  was sufficiently large to prevent arc-glow transitions, and was therefore higher than it would have been, had IGCG not been liable to restriking.

An attempt was made in tests 18 - 20 to maintain a constant impulse duration, while decreasing the impulse current magnitude. Results were modified by the discharge resistance  $R_{gt}$ , and the impulse duration decreased with  $I_{IG0}$ . One effect of the decrease in  $t_1$ , is that  $I_t$  has less time to build up, so that the critical  $V_0$  must increase. It was seen from the tests of fig. 16 that for a given test gap and impulse current, the critical  $I_{gt2}$  and  $I_{gt3}$  decreased when  $V_0$  increased. In test 19, however,  $I_{gt2}$  and  $I_{gt3}$  were larger than in test 18, although the critical  $V_0$  was higher in the former case. Furthermore, results were of type I in test 18 and of type II in test 19 - i.e. it was more difficult to maintain an arc at the higher current. Evidently the variation in impulse current waveform has a marked effect on the state of ionisation of the test gap at  $t_2$  and  $t_3$ : in the present case, the ionisation decreased when the magnitude of the impulse current was reduced. The results of test 20 confirm this:  $I_{gt2}$  was slightly smaller than in test 18, but  $I_{gt3}$  was larger;  $V_0$  was larger than either in test 18 or 19, and results were of type II.

Both the impulse current magnitude, and its duration  $t_1$ , were varied in tests 21 - 28;  $R_p$  was progressively decreased, thereby increasing the critical  $V_0$ . Initially (tests 21 - 26) results were of type I, and the increase in  $V_0$  resulted in smaller values

of  $I_{gt2}$  and  $I_{gt3}$ . In test 27,  $I_{gt2}$  and  $I_{gt3}$  increased slightly and results were of type II - i.e. it became more difficult for the L.V. circuit to maintain an arc, despite the larger current values. Hence the ionisation of the test gap after the end of the impulse was less intense than in previous tests. This decrease in ionisation can only be due to the decrease in impulse current duration, to turbulence due to increase in impulse current magnitude, or to both; the effect of these parameters is discussed in detail in section 11.

Test 28 shows that further increase in  $R_F$  resulted in a low value of  $V_{gt2}$ . This is because  $I_{IGt}$  was very large and resulted in intense ionisation on the one hand; on the other hand, the impulse duration was very short, and there was little time for the ionisation to decrease; consequently  $V_{gt}$  was very low at the end of the impulse. Immediately the impulse ceased,  $V_{gt}$  began to rise smoothly (there were no arc-glow transitions) and its peak value was usually reached by  $t_3$ . In many cases, the discharge was a glow at its maximum voltage, and follow current was established after a glow-arc transition. In a few isolated instances,  $V_{gt}$  continued to rise after  $t_3$  (reaching, in one case, 940 Volts), yet follow current became established after a glow-arc transition eventually occurred. In general, however, the maximum (glow) value of  $V_{gt}$  did not exceed  $V_0$ , so that in this test conditions were those defined by the Glow Criterion (section 13.2).

The characteristics of H.V. follow current emerge from the analysis given in this section: these characteristics have already been stated in section 7.1.

## 9. ANALYSIS OF HIGH-CURRENT FOLLOW CURRENT CHARACTERISTICS

The mechanism of H.C. Follow Current is best explained by considering a wide range of  $V_0$  values. Typical waveshapes of test gap voltage,  $V_{gt}$ , and L.V. circuit current,  $I_t$ , are given in figs. 12 and 18. The value of  $I_0$  has no significant effect on the qualitative discussion given below so that the waveforms of fig. 18 have been sketched for the simplified case of  $I_0$  being negligible.

Fig. 18(a) is typical of the conditions obtaining when  $V_0$  is so small that  $I_{gt1} = 0$  - i.e. the discharge ceases at or before the end of the impulse; follow current is clearly impossible in that case. Before flashover, traces are similar to those of fig. 10 (section 7.1). Immediately after flashover,  $V_t$  exceeds  $V_{gt}$  in the case considered. Application of Kirchhoff's Law to the L.V. circuit gives

$$L \frac{dI_t}{dt} = V_t - V_{gt} \quad (\text{ohmic resistance being negligible, section 2.2})$$

Hence  $L \frac{dI_t}{dt}$  is positive - i.e.  $I_t$  is positive and increasing. Consequently C discharges through the test gap, and  $V_t$  decreases as the discharge proceeds. At the same time,  $I_{IGt}$  decreases exponentially;  $I_t$  is initially much smaller than  $I_{IGt}$  so that  $I_{gt}$  decreases also (fig. 1). The impulse discharge has a negative characteristic, being an arc, so that the decrease in  $I_{gt}$  results in  $V_{gt}$  rising. Eventually, therefore, point A is reached, at which  $V_t = V_{gt}$  and subsequently  $V_{gt}$  becomes greater than  $V_t$  so that  $I_t$  begins to decrease at A; it falls to zero at B and then reverses. After B, therefore, the impulse generator supplies both the discharge and the L.V. circuit currents, i.e.

$$|I_{IGt}| = |I_{gt}| + |I_t|$$

so that the current  $I_{IGt}$  flowing in IGCG exceeds the discharge current,  $I_{gt}$ . Consequently, IGCG continues to conduct after  $I_{gt} = 0$ , i.e. after the test gap discharge has ceased (point C). Between C and D,  $I_t (= - I_{IGt})$ , with the convention of fig. 1) decreases at a rate determined primarily by L and  $C_{IG}$ . IGCG deionises at D and the energy still stored in L at that moment discharges through the resistance of the potential divider.

Figs. 18 (b) - (d) are typical of the condition in which  $V_o$  was sufficiently large for  $I_{gtl}$  to be finite. In this condition,  $I_t$  is positive so that

$$|I_{gt}| = |I_{IGt}| + |I_t|$$

and the discharge is maintained by  $I_t$  after IGCG ceases to conduct current (i.e. after  $I_{IGt} = 0$ ). (Were  $V_o$  significant,  $I_t$  would be negative at the beginning of the impulse only).  $I_{gtl}$  is relatively low in fig. 18 (b), so that  $V_{gt}$  rises appreciably after the end of the impulse, resulting in  $V_{gt} > V_t$ . Hence  $L \frac{dI_t}{dt}$  becomes negative shortly after the impulse and the current begins to decrease; the discharge ends soon afterwards, as in the H.V. case.

The characteristics of H.C. Follow Current emerge when  $V_o$  is larger still, as in fig. 18(c).  $I_{gtl}$  is sufficiently large (> 0.5 Amps) to maintain an arc condition, so that there is little rise in  $V_{gt}$  after the impulse ceases. However,  $V_t$  decreases as the discharge proceeds, and a time,  $t_q$ , is reached after which  $V_{gt}$  exceeds  $V_t$ . Consequently,  $I_t$  begins to decrease after  $t_q$ , and the discharge may be maintained for appreciably less than  $1/(2f)$  - i.e. follow current is not established, although an arc was

maintained for some time after the end of the impulse and there was very little rise in  $V_{gt}$  immediately after the impulse ceased. Increasing  $V_o$ , increases  $V_t$ , and hence  $t_q$ ; this is illustrated quantitatively in figs. 19-21, which will now be considered.

When  $V_o$  is small (dotted parts of curves),  $I_{gt1} = 0$ , and the conditions holding are those of fig. 18(a). Increasing  $V_o$  decreases the current circulated in the L.V. circuit by the impulse. Now, that current maintains IGOG conducting after  $t_1$ . Hence, the smaller it is, the more rapidly will IGOG interrupt it. That is why the duration of flow of L.V. circuit current,  $t_{LV}$ , decreases initially as  $V_o$  increases.

Further increase in  $V_o$ , results in  $I_{gt1}$  becoming finite (e.g. fig. 18(b)) and  $t_{LV}$  increases rapidly at first;  $\frac{dt_{LV}}{dV_o}$  decreases as  $t_{LV}$  approaches  $1/(2f)$ . In some cases,  $t_{LV}$  exceeds slightly  $1/(2f)$  when  $V_o$  is relatively small, but tends to  $1/(2f)$  if  $V_o$  is increased. This is due to the test gap voltage reducing the rate of discharge of C at low values of  $V_o$ .

The test gap discharge must always have some effect, however small, on the duration of the first loop of current flowing from the L.V. circuit, and the actual value of  $t_{LV}$  at which H.C. follow current is taken to have been established is discussed in the Appendix (V).

The conclusion to be drawn from this discussion, is that the establishment of H.C. Follow Current depends primarily on the characteristics of the L.V. circuit and of the discharge, and is substantially independent of the impulse, provided the latter does, in fact, initiate an arc. Experimental confirmation of this conclusion is given in section 11.4.

## 10. ANALYSIS OF HIGH-FREQUENCY FOLLOW CURRENT CHARACTERISTICS.

Two points emerge from what has already been said on High-Frequency Follow Current. Firstly, H.F. Follow Current is best studied from the point of view of its effects during the time that impulse current is flowing. Hence the effects of follow current on the fundamental characteristics of the discharge, may be masked by the impulse current. Now, in the case of L.F. Follow Current, attention is centred particularly on events occurring after the impulse has ceased. Hence the study of H.F. Follow Current is less likely to produce fundamental data on discharge characteristics than the study of L.F. Follow Current. Secondly, in the case of power systems, the establishment of H.F. Follow Current is important only in so far as it affects the establishment of L.F. (power-frequency) Follow Current. Hence H.F. Follow Current is less important a phenomenon than L.F. Follow Current, and will be the subject of a brief study only.

It will be remembered that H.F. Follow Current mechanism held when  $t_1 > 1/(2f)$ . Application of Kirchhoff's Law to the circuit of fig. 1 gives the following expression for the relation between  $I_t$ ,  $V_o$  and  $V_{gt}$  (the ohmic resistance of the L.V. circuit being negligible):

$$V_o - \frac{\int_0^t I_t dt}{C} - L \frac{dI_t}{dt} = V_{gt}$$
$$\therefore \frac{\int_0^t I_t dt}{C} + L \frac{dI_t}{dt} = V_o - V_{gt}$$

To make a simple analysis possible, it will be assumed, in the first place, that  $V_{gt}$  is constant at the value  $V_{go}$  during the impulse and that  $I_o$  is negligible. In that case

$$I_t = \frac{V_o - V_{go}}{Z} \sin \frac{t}{\sqrt{LC}}$$

and

$$V_t = V_o - \frac{\int_0^t I_t dt}{C} = V_{go} + (V_o - V_{go}) \cos \frac{t}{\sqrt{LC}}$$

Fig. 22 shows curves of  $I_t$ ,  $V_t$  obtained from these expressions for the case  $V_o > V_{go}$ . The impedance of the impulse circuit can be taken to be large compared to that of the discharge (which is an impulse arc) so that the fraction of  $I_t$  flowing in the impulse circuit is negligible. Now, it will be noted that during the first half cycle of L.V. current flow

(1) the L.V. circuit current flows through the test gap in the positive direction - i.e. in the same direction as the impulse current - so that the L.V. current feeds power to the discharge,

and (2) the L.V. circuit current flow is due to the charge  $C(V_o - V_{go})$ : this is part of the charge stored on C just before flashover.

Hence power is fed to the discharge from the energy  $\frac{1}{2}V_o^2 C$  stored on C at flashover, and follow current is established, in accordance with section 5.4.

If  $V_o$  is decreased so that  $V_o = V_{go}$ ,  $I_t = 0$ , and there is clearly no follow current.

If  $V_o$  is decreased further, so that  $V_o < V_{go}$ ,  $I_t$  and  $V_t$

waveshapes are as shown in fig. 23. During the first half cycle of L.V. current flow,  $I_t$  is of opposite polarity to  $I_{IGt}$ , so that  $I_t$  decreases  $|I_{gt}| (= |I_{IGt}| - |I_t|$  in this case). Hence the L.V. circuit does not increase the power available to the discharge; on the contrary, power is drawn by the L.V. circuit, in order to charge C to the voltage  $(2V_{go} - V_o)$ .

On the following half cycle,  $I_t$  reverses and increases the power available to the discharge: however, this power comes from the energy stored on C during the first half cycle of current flow (i.e. from energy drawn from the impulse) so that follow current is not established in this case.

Hence, if  $V_{gt}$  is constant, follow current is established if, and only if,  $V_o$  exceeds  $V_{gt}$ . In the general case, however,  $V_{gt}$  varies with time. Now, the definition of H.F. follow current is such (section 5.4) that when the establishment of follow current is just possible, the power fed by the L.V. circuit to the discharge is small, and the discharge characteristics are not substantially affected by it. Consequently,  $V_{gt}$  rises as the impulse current decreases - i.e.  $V_{gt}$  will increase in time.

When  $V_o$  is in its critical range, therefore,  $V_{gt}$  will be a minimum just after flashover, and will equal  $V_{go}$ . If  $V_o > V_{go}$ , and  $I_o$  is negligible, the L.V. circuit will feed some power to the test gap, that power being drawn from the initial energy stored on C. Hence H.F. Follow Current is established if, and only if,  $V_o > V_{go}$ .

If  $I_o$  is finite,  $I_t$  will be initially negative, and the L.V. circuit will not be able to feed power to the discharge until  $I_t$

has reversed. The critical  $V_0$  is then increased, and the condition for the establishment of H.F. Follow Current becomes that  $V_0$  must exceed the value of  $V_{gt}$  at the instant at which  $I_t$  reverses for the first time after flashover.

The above discussion has been verified experimentally. The circuit parameters were:  $f = 6200$  c/s;  $Z = 20$  ohms;  $C_{IG} = 0.083$  microfarads;  $R_F = 4100$  Ohms;  $R_T = 75$  kilohms. The Standard Gap (section 5.11) was used. The burning voltage of the discharge was nearly constant during the first half cycle of the L.V. circuit. Oscillograms were taken of the discharge voltage,  $V_{gt}$ , of the L.V. circuit current,  $I_t$ , and of the L.V. circuit capacitor voltage,  $V_t$ . Good quantitative agreement was obtained with the above analysis.

The principal characteristics of H.F. Follow Current, which emerge from the above discussion, have been summarised in section 7.3.

## 11. EFFECT OF VARIATION IN IMPULSE CURRENT WAVEFORM ON THE ESTABLISHMENT OF L.F. FOLLOW CURRENT.

The effect of variation in impulse current waveform on the establishment of L.F. Follow Current, will be discussed for the condition of  $V_0$  and  $V_{IG0}$  being positive.  $I_0$  was negligible in all experiments reviewed in this section and the Standard Electrodes (section 5.10) were used.

### 11.1 An Approximate Analysis for the Case of H.V. Follow Current.

The impulse current largely determines the ionisation intensity of the discharge during the impulse period,  $t_1$ , and affects it for a considerable time after the impulse has ceased (see section 8.4, tests 15 - 28). The residual effects of the impulse complicate an exact analysis of the separate effects of the impulse duration,  $t_1$ , and the impulse current amplitude, on the conditions required for follow current. An approximate analysis of the effects of these parameters in the case of H.V. Follow Current will be attempted on the assumption that the probability of follow current increases with the value  $I_{t1}$  of the L.V. circuit current at the end of the impulse, and will ignore the residual effects of the impulse. The peak value of the impulse current,  $I_{IG0}$  will be taken as a measure of the amplitude of that current.

Now, it will be shown in section 13.1 that

$$I_{t1} = I_0 + \frac{1}{L} \int_0^{t_1} (V_t - V_{gt}) dt$$

and it is evident from fig. 1 that  $V_t = V_0 - \frac{1}{C} \int_0^t I_t dt$ .

$$\text{Hence, } I_{t_1} = I_0 + \frac{1}{L} \int_0^{t_1} (V_0 - \frac{1}{C} \int_0^t I_t dt - V_{gt}) dt$$

In the case of H.V. Follow Current (section 7.1)  $V_0$  is large compared to the voltage lost by C ( $= \frac{1}{C} \int_0^t I_t dt$ ) during the impulse, since the impulse duration,  $t_1$ , is short compared to the half period,  $1/(2f)$ ; furthermore,  $V_0$ , which tends to a glow voltage, is large compared to  $V_{gt}$  during most of  $t_1$ , since the discharge is an arc during that time. Hence, to a first approximation,

$$I_{t_1} \approx I_0 + \frac{V_0 t_1}{L}$$

Consequently,  $I_{t_1}$  increases with the impulse duration  $t_1$ .  $I_{IG0}$  does not appear in the above expression, because its effect is reflected only in  $V_{gt}$ , and  $V_{gt}$  was sufficiently small to be ignored relative to  $V_0$ .

The conclusion is that the probability of H.V. Follow Current being established increases with the impulse duration, and that the effect of impulse current amplitude can be ignored to a first approximation. The physical interpretation of this statement is that, the longer the impulse duration, the greater the probability of follow current, because the L.V. circuit current has a longer time to build up. The magnitude of the impulse current affects the state of ionisation of the test gap, but this effect is not very important provided the discharge is an arc.

Experimental verification of this analysis is given below.

### 11.2 Variation in Impulse Duration, $t_1$ :

The impulse duration,  $t_1$ , can be varied independently of  $I_{IG0}$ , by altering  $R_T$ , or simultaneously with  $I_{IG0}$ , by altering  $R_F$  (fig. 24). Results obtained in two such experiments are given in

fig. 25. Other aspects of these results have been discussed in section 8.4 (tests 15 - 17 and 24 - 28).

The curves of fig. 25 are in close agreement over the range  $100 < t_1 < 200$  microseconds, confirming the conclusions of section 11.1. The agreement between the two curves remains satisfactory at lower values of  $t_1$ , but it must be remembered (section 8.4, test 17) that in the case of the lower curve,  $V_0$  would have been even smaller had IGOG not been liable to restriking. Hence analysis of the results of fig. 25 shows that in the case of  $t_1 = 55$  microseconds, a higher value of  $I_{IGO}$  requires a higher value of  $V_0$ .

Now an increase in  $I_{IGO}$  results in  $V_{gt}$  having a lower value during the impulse period.  $V_{gt}$  opposes the growth of  $I_{t1}$ ; on these grounds alone, follow current should be established at a lower value of  $V_0$  when  $I_{IGO}$  increases. This is the opposite of the conclusion derived from fig. 25, and the contradiction can only be due to two causes: the ionisation of the discharge after the end of the impulse decreases due to turbulence when  $I_{IGO}$  increases, and/or the scatter or results masks the true effect of  $I_{IGO}$ . Some support is given to the former view by the conclusion arrived at in section 8.4 (test 27), that the state of ionisation of the discharge after the end of the impulse decreased when  $R_F$  was decreased to the value corresponding to  $t_1 = 55$  microseconds, but the decrease in ionisation in that case may have been due to the decrease in  $t_1$ , and not to the increase in  $I_{IGO}$ . Hence, two possibilities remain: the effect of  $I_{IGO}$  is negligible, or an increase in  $I_{IGO}$  may make

follow current less likely, because of the more violent air movement - and consequent deionisation of the test gap - produced by the larger amount of heat generated.

### 11.3 Variation in Impulse Current Magnitude.

An attempt to alter the magnitude, but not the duration of the impulse current was discussed in section 8.4 (Tests 18 - 20). Results were modified by the resistance of the discharge, so that  $t_1$  varied. Taking the Standard Condition as reference,  $t_1$  decreased by 26% when  $I_{IG0}$  decreased by 90%, the resulting rise in critical  $V_0$  being 38%. It is reasonable to assume that the increase in  $V_0$  would have been no greater had  $t_1$  been constant; in fact, it would probably have been smaller. A figure of merit for the effect of  $I_{IG0}$  on  $V_0$  can be obtained by comparing percentage changes: in the present case that figure will not be greater than  $38 \div 90 = 0.42$ .

A similar figure of merit can be obtained from the results of section 11.2. Over the range  $175 < t_1 < 95$  microseconds,  $t_1$  decreases by 46%, with a resulting increase in  $V_0$  of 44%. The figure of merit showing the effect of  $t_1$  on  $V_0$  is therefore  $(44 \div 46) = 0.96$ . The corresponding figure is appreciably greater over the range  $95 < t_1 < 55$  microseconds, but the increase may then be due, in part, to the special factors discussed in section 8.4 (Test 17). However, even at the value of 0.96, the figure of merit shows  $t_1$  to be appreciably more effective than  $I_{IG0}$  in determining the critical  $V_0$ . This constitutes further confirmation of the conclusions reached in section 11.1.

#### 11.4 Variation of Impulse Current Waveshape obtained by varying $R_F$ .

Increasing  $R_F$  increases the impulse current duration (fig. 24) and decreases its amplitude ( $I_{IG0} = \frac{33 \times 10^3}{R_F}$  Amps). A family of curves showing the relation between  $R_F$  and the critical  $V_0$  is given in figs. 26 - 28. All curves are similar, and the critical  $V_0$  decreases as  $R_F$  increases. Follow Current was of H.V. type at  $R_F < \frac{150}{f} \times 10^3$  Ohms, and of H.C. type at higher values of  $R_F$ . (The impulse generator output was aperiodic for all values of  $R_F$  used in this work).

It will be seen from the graphs, that the critical  $V_0$  decreases little when  $R_F$  is decreased below about 100 Ohms. This is because the critical damping resistance of the impulse circuit is of the order of (but less than) 100 Ohms. At  $R_F < 100$  Ohms, therefore, the stray inductance of the impulse circuit is important in controlling the impulse current, and the effect of changes in  $R_F$  is relatively small. When  $R_F$  is increased above 100 Ohms, it becomes more effective in controlling both the magnitude and the duration of the impulse current, and  $V_0$  falls rapidly at first. Eventually, the rate of decrease of  $V_0$  is much reduced; this is because H.C. Follow Current then holds, and an arc may be maintained for a considerable time after the end of the impulse, without necessarily being maintained for a full half cycle of the L.V. circuit. The critical  $V_0$  tends to be determined by the L.V. circuit and the discharge characteristics, rather than by the impulse, and changes in impulse parameters are less important than in the H.V. case (section 9).

The relation between the critical  $V_0$  and  $(R_F f)/50$  is illustrated in fig. 29.

## 12. ELECTRODE EFFECTS.

The object of experiments discussed in this section was to determine the effect of electrode material, spacing, and surface condition on the establishment of Follow Current. They were carried out either with the Standard Circuit (section 5.9) or with a circuit differing from it only in that the output impedance,  $Z$ , was 126 Ohms. The effect of variation in output impedance (as distinct from electrode effects) on the establishment of follow current has been discussed in section 8.4.

Follow Current was of the H.V. type in these experiments.  $V_0$  and  $V_{IG0}$  were positive, and  $I_0$  was negligible unless otherwise stated.

It was necessary to carry out tests with electrodes both relatively unoxidised, and heavily oxidised in order to determine the effect of surface condition. Rod electrodes oxidised so rapidly when flashovers were applied, that experiments with unoxidised rods were unpracticable. In some cases, the effect of oxidation could be ascertained from tests on spherical electrodes, by noting the variation in critical  $V_0$  as flashovers were applied; where these results were inconclusive, disc electrodes (section 3) were resorted to.

### 12.1 Presentation of Results.

The method adopted for presenting experimental results will be explained in this section; the results themselves will be discussed in the following sections.

The effect of electrode shape and surface condition is presented for each material by means of 'Sequence Diagrams' (e.g. fig. 30): these show the excursion in the critical value of  $V_0$  obtained in each follow current test (section 6) and the difference between the conditions holding in each test and the preceding tests. Conditions common to all tests of a diagram are stated in the caption, or in the text. The electrodes were not cleaned between tests, except as stated on the diagrams.

The surface condition of the electrodes was affected primarily by flashovers: the normal action of the atmosphere on the electrode material was very small in comparison. In order to determine the effect of flashovers, and to alter the surface condition, the electrodes were sometimes 'conditioned' by the application of a large number of flashovers.  $V_0$  was set within the critical range for conditioning flashovers, in order to give a surface condition similar to that obtained for a typical test sequence. The number of conditioning flashovers is stated on the Sequence Diagram, where appropriate. In some cases, other follow current tests, not recorded on the Sequence Diagram, were carried out with the same electrodes, between tests which were recorded. Whenever this was done, an estimate of the number of flashovers applied to the electrodes in the other tests was entered on the Sequence Diagram.

The effect of electrode spacing is shown by means of 'Spacing Diagrams' (e.g. fig. 38). In these diagrams vertical lines are used to represent the scatter in the value of  $V_0$  and horizontal lines its mean, obtained at a given spacing. All spacing diagrams have been obtained for 2 cm. diameter spheres which had been

heavily oxidised by conditioning.

Information regarding the characteristics of the discharge may be obtained by examining oscillographic records of the discharge voltage,  $V_{gt}$ , and the L.V. circuit current,  $I_t$ , during the critical period,  $t_0$ , in which the establishment of follow current is determined (section 8.2). The general waveshapes of  $V_{gt}$  and  $I_t$  shown by these records have already been explained (sections 7.1 and 8) in connection with figs. 10 and 15. In the present section, these waveshapes will be examined only to determine electrode effects. To facilitate comparison of the records with figs. 10 and 15, the time covered by the records has been extended to include at least part of the impulse period,  $t_1$ , and salient points (e.g.  $V_{gt} = V_0$ ,  $t = 0$ ,  $t = t_1$ ) have been marked on them. The discussion of waveshapes will be qualitative only, and for that reason current and voltage scales are not given in conjunction with the records. (quantitative analyses are given in sections 7.1, 8.4 and 13.3). The current and voltage scales of different records given on one figure are not necessarily the same. The complete amplifier (section 4.2) was used for recording most current waveforms; in a limited number of cases, however, only the input stage was used, and the resulting waveshape record was then reversed.

In addition to the waveshapes of  $V_{gt}$  and  $I_t$ , most of the oscillograms shown will be seen to contain two 'zero lines'; the manner in which these lines were obtained, and their purpose, is explained in Appendix VI.

## 12.2 Tungsten Electrodes.

The effect of surface condition and electrode shape was

investigated with two types of electrodes, namely:

- (1) The Standard Electrodes - 0.063 cm. diameter rod electrodes, heavily oxidised, and
- (2) Tungsten tipped brass spheres. The spheres were 2 cm. diameter and had a tungsten cap 1 cm. diameter by 0.5 cm. deep. Flashover always occurred on the tungsten cap; there was no evidence of the arc roots ever touching the brass. From the point of view of the experiment, these electrodes were therefore equivalent to 2 cm. tungsten spheres; they had the additional advantage that they were easier to manufacture.

The Sequence Diagram is given in fig. 30. In order to distinguish between individual electrodes, one sphere and one rod were represented in the diagram by a black circle and a black rectangle, respectively, and the other sphere and the other rod were represented by a white circle and a white rectangle.

Tests 29 and 30 show that there is a definite lowering of the critical voltage level as conditioning proceeds. At the end of test 30, when some 2800 flashovers had been applied, there was no indication that a steady voltage level had been reached.

Typical oscillograms obtained in test 29 (i.e. before conditioning) are given in fig. 31. It will be seen that they are of type II (cf. fig. 31 (c) and (d), and fig. 15 (b)). Oscillograms obtained in test 30 differed in that they were of type I; they were similar to figs. 31 (a) and (b), but follow current was never established after a sustained glow period, as in fig. 31 (c) and (d). This difference may be due to the fact that only when the electrodes are relatively unoxidised, is

$V_0$  sufficiently high to maintain a glow for a time of the order of 10  $\mu$ s, and then cause a glow-arc transition: in the case of oxidised electrodes, the discharge ceases shortly after a glow condition has been reached, and there is thus no follow current in that case.

The electrodes appeared smooth to the naked eye at the end of test 30, but the following markings were visible:

At the anode, there were bluish-grey arc roots over a circle of about 0.25 cm. diameter. Around and concentric with these marks, over a 0.5 cm. diameter circle, the electrode had acquired a yellowish tinge. This circle was surrounded by a bluish circle.

The marking on the cathode was much more faint and irregular. There was a central whitish portion, about 0.15 cm. diameter, broken in many places by black arc roots. This was surrounded by contour line at about 0.2 - 0.3 cm. from the centre of the electrode surface, which was in turn surrounded by a bluish line. Unlike the contour lines on the anode, these lines were not circles.

The marking described above did not change significantly in subsequent tests until the electrodes were cleaned (test 44). In order to remove the markings, it was necessary to rub the electrodes with emery paper. In no test was there any evidence of oxide dust being generated at a spherical electrode.

At the end of each test, the anode was warmer to touch than the cathode.

Results obtained with conditioned rod electrodes are given in tests 31 and 33: it will be seen that the critical  $V_0$  is smaller and its range is narrower than in the case of spherical electrodes.

The fact that results obtained with tungsten rod electrodes (i.e. with the Standard Electrodes) can be repeated with consistency, was also noted in tests discussed earlier (e.g. test 1 - 3 and 4 - 6, fig. 16).

It has been explained in the introduction to section 12 that it was not practicable to carry out tests with unoxidised rod electrodes. At the beginning of test 31, the electrodes had been covered with whitish-yellow dust, which could easily be removed by wiping with a cloth. The dust spread some distance axially along the electrode: the oxide-covered region was longer at the anode than at the cathode, indicating that, as in the case of spherical electrodes, heating was more intense at the anode. The tips of both electrodes were slightly enlarged, to a diameter of some 0.075 cm. The appearance of the electrodes did not change in subsequent tests. Typical oscillograms are given in fig. 32: they are of type I (cf. fig. 15 (a)) and will be seen to be much smoother than those obtained with tungsten spheres (fig. 31).

Test 32 shows that when the anode is spherical and the cathode is a rod, the critical  $V_0$  range does not differ much from that obtained with anode and cathode rods. The oscillograms taken in this test were also similar to those of test 31, (fig. 32) the voltage curves being smoother than in tests 29 and 30. This confirms that cathode phenomena are more important than anode phenomena in the establishment of follow current.

Test 33 shows that the critical range of  $V_0$  obtained with rod electrodes has not changed during test 32. The effect of replacing the cathode rod by a sphere, was investigated in test 34.

The critical  $V_0$  then increased, roughly to the value which had been obtained with sphere anode and cathode in test 30 after (f), and the following was noted:

- (1) A white oxide dust was spluttered from the rod anode on to the surface of the spherical cathode. This dust covered the cathode well beyond the region marked by flashovers, and extended onto the brass. The dust could easily be removed by wiping.
- (2) The oscillograms obtained were similar to those taken with rod anode and cathode.

Tests 35 - 38 were carried out successively on the same day. Their purpose was to confirm and extend the information available from tests 30, 32 and 33. The time interval between tests 35 - 38 was kept as short as possible, as a precaution against atmospheric changes, and changes in electrode conditions, occurring between the tests. The oxide dust, which had been spluttered on to the cathode in test 34 was removed by wiping before test 35, which gives the critical  $V_0$  obtained with a spherical anode and cathode.

Test 36 confirms the results of test 32. Additional information is supplied by test 36, because the cathode was initially clean in that test, and two points emerge:-

- (1) When the cathode is relatively clean, the critical  $V_0$  is below that of test 35. This would indicate that the cathode shape, in addition to its surface layer, has considerable

effect on the follow current mechanism. It must, however, be borne in mind that rod electrodes oxidise rapidly, (i.e. after a small number of flashovers) so that there may have been appreciable oxide formation on the cathode while the limits of the  $V_0$  range were being established. It is not possible, therefore, to give a quantitative result for the effect of the shape of the cathode on the follow current mechanism. All that can be said is that follow current is more readily established if the cathode is small compared to the arc root than if it is large: this may be due to temperature or to field effects, or to both.

- (2) The cathode (but not the anode) became covered with oxide dust after conditioning. Thus in the case of rod electrodes, the cathode as well as the anode is raised to a temperature sufficiently high to cause oxidation. This result removes the possibility, which might have been contemplated after test 34 that in the case of anode and cathode rods, the oxide dust on the cathode may have been spluttered from the anode. Test 37 confirms the results of test 35 and shows that the critical range of  $V_0$  has not changed during test 36 for the case in which both anode and cathode were spheres. Test 38 shows that the critical range of  $V_0$  is unchanged for the first few flashovers. As the test proceeded, the anode became oxidised and oxide dust was spluttered on to the cathode. After conditioning the cathode was well covered with oxide and the critical range of  $V_0$  was much lower, but the mean value of the critical  $V_0$  was still somewhat higher than in test 33. (Test 33 was not carried out on the same

day as tests 35 - 38, but experience had shown that there would be little variation in the results of test 33, which could be repeated consistently). Hence the temperature and/or field effects, due to a reduction in cathode diameter, remain important even if the cathode is covered by an oxide layer which lowers the critical  $V_0$ .

Tests 39 and 40 were carried out to investigate further the effect of the oxide layer which had been spluttered on the cathode in test 38. Results were inconclusive, due no doubt to the fact that the two spherical electrodes were not identical (quite apart from the oxide layer on one); differences in the condition of the surfaces were due to the fact that the sphere represented by a black circle had always been used as anode, while the other had been used as cathode. The anode became hotter, and more marked by flashovers than the cathode, as discussed in connection with test 30.

The difference between the condition of the two spherical electrodes was confirmed by tests 41 - 43. The spheres were wiped before test 41 in order to remove the oxide dust. (This did not affect the markings described on page 65, which could only be removed by rubbing with emery paper). It will be seen from the Sequence Diagram, that the critical range of  $V_0$  changed when the spheres were reversed.

At the beginning of test 44, the electrodes were cleaned in an attempt to remove the traces of previous flashovers. After cleaning with rough and fine emery paper, metal polish and ether, the electrode surfaces appeared unmarked and smooth to the naked eye: they were, however, less bright than they had been before

test 29. Evidently minute scratches had been left by the emery paper. These may have resulted in high local field intensity; in any event, the critical  $V_0$  was low. Wiping the electrodes with an ether soaked cloth (point (j) on Sequence Diagram) resulted in an increase in the critical  $V_0$  range. This may have been due to the fact that irregularities produced by flashovers on the electrode surfaces were rubbed into the depressions caused by the emery paper, so that local high field intensity spots were removed.

A photograph of the electrodes taken at the end of these tests is shown in fig. 33.

The following can be concluded from these observations:-

(1) Follow Current occurs at a lower critical  $V_0$  in the case of thin rod electrodes than in the case of relatively large spherical electrodes. This is due to two separate sets of causes;

(a) Quite apart from the formation of oxides, the thin electrodes will be raised to higher temperatures, and the field stress will be higher. Thus the emission of electrons at the cathode will be greater.

(b) Since the thinner electrodes are raised to higher temperatures, larger quantities of oxide are produced at the surface. These oxides lower very appreciably the critical  $V_0$  range.

(2) In the case of the spherical electrodes, a steady critical  $V_0$  range was not reached in these experiments, because of the dependence of the critical  $V_0$  on the surface condition.

(3) In the case of rod electrodes, a steady critical  $V_0$  is reached very readily, because the high temperatures induced by flashovers

result in rapid oxidation of these electrodes.

It has been stated that in the case of spherical electrodes, a steady critical  $V_0$  was not reached i.e. the critical  $V_0$  varied as flashovers were applied. Hence, if a Spacing Diagram had been taken, the critical  $V_0$  recorded at one spacing would have altered, whilst the critical  $V_0$  corresponding to another spacing was being established; the Diagram would therefore have been meaningless. A Spacing Diagram was not obtained for tungsten spheres, for this reason.

The effect of spacing and of changes in circuit parameters has been discussed in detail for tungsten rods in section 8.4.

### 12.3 Platinum Electrodes.

The Standard Circuit was used in a series of tests on 0.047 cm. diameter platinum electrodes, spaced 0.5 cm. apart: the Sequence Diagram is given in fig. 34.

The purpose of these tests was to determine whether the critical range of  $V_0$  was smaller and the consistency greater, than in the case of other rod electrodes: the tests were carried out at several days' interval from one another. It will be seen from the Sequence Diagrams (figs. 30, 35, 39, 43 and 48) that the critical range and consistency of results is of the same order as in other tests on rod electrodes.

The electrodes were cut from platinum wire, before test 45, and the slight increase in critical  $V_0$  which occurred as the tests proceeded was probably due to changes in electrode shape. At the end of test 47, the electrode tips were slightly enlarged, approximating to 0.063 cm. diameter spheres. The tips were

brighter than the rest of the electrodes, and there was a black deposit at the anode, extending axially about 3 mm. and situated about 1 mm. above the tip. The black deposit could easily be removed by scraping. There was no deposit visible to the naked eye at the electrode tips.

The oscillograms taken in tests 45 - 47 were similar to those obtained in the Standard Condition (fig. 32). The effect of spacing has been discussed in detail in section 8.4 for platinum rod electrodes.

#### 12.4 Brass Electrodes.

Both test circuits were used in tests on 2 cm. brass spheres and 0.056 cm. diameter brass rods. Results are given in the Sequence Diagram of fig. 35, which shows that the critical  $V_0$  is not affected by flashovers in the case of spherical electrodes, so that no conditioning is required in order to obtain a steady critical  $V_0$ . In the case of rods, the critical  $V_0$  is raised by conditioning; this is probably due to the fact that sharp edges are left on the electrode tips when they are cut, and conditioning burns them off. It will be seen from the Sequence Diagram that the critical  $V_0$  obtained with conditioned rods, is very nearly the same as that of spheres, at both values of output impedance,  $Z$ . Consequently, the significant information provided by the Sequence Diagram, is that the critical  $V_0$  is substantially independent of surface condition and electrode shape in the case of brass electrodes, provided there are no sharp edges.

The oscillograms obtained in tests on brass rods are similar to those obtained with tungsten rods (fig. 32). Typical

oscillograms obtained with spherical brass electrodes are shown in fig. 36; a quantitative analysis of such oscillograms is given in fig. 16. In some cases (e.g. fig. 36 (b))  $V_{gt}$  decreased rapidly before follow current was established (though less rapidly than at a glow-arc transition). This resulted in a very pronounced peak in the  $V_{gt}$  waveshape. Similar waveshapes have also been obtained with conditioned steel, aluminium and copper spheres. In the case of tungsten spheres, and of all the rod electrodes used in this investigation,  $V_{gt}$  fell much more slowly after reaching its peak value, unless a glow-arc transition occurred.

The appearance of the spherical electrodes at the end of these tests is shown in fig. 37. The anode surface was completely covered by grey-brown spots over a circle about 0.6 cm. diameter, and had remained smooth. The cathode surface was covered with black spots over a circle of about 0.6 cm. diameter, and had been roughened slightly by the arc roots. Apparently clean brass was visible at the bottom of the troughs left by the arc roots on the cathode surface.

The tips of the rod electrodes were covered with a black deposit at the end of these tests. There was also a white deposit on the anode tip situated axially above the black deposit. The tips were not enlarged, but the cathode tip was roughly conical with a pointed end.

The Spacing Diagram for brass is given in fig. 38. The two curves shown were obtained in two separate test runs carried out at an interval of 19 days.

## 12.5 Steel Electrodes.

Both test circuits were used in a series of tests on 2 cm. steel spheres and 0.056 cm. diameter steel rods. The Sequence Diagram of fig. 39 was obtained from these tests.

The electrodes were cleaned with metal polish and ether before tests 55, 57 and 63. In the case of spherical electrodes, a bright surface was obtained after cleaning. The surface became rapidly rusted as flashovers were applied, and the critical  $V_0$  was lowered at the same time. Once the arcing tips of the electrodes were covered in rust over a circle of some 0.6 cm. diameter, the critical range of  $V_0$  was not affected by further flashovers, and results could be repeated consistently. The rapid lowering of the critical  $V_0$  as the oxidation of the electrode surfaces proceeded, was the most significant information presented by the Sequence Diagram.

The appearance of the spherical electrodes at the end of the tests is shown in fig. 40. The central portion of the anode was covered by a black and rusty deposit. The black deposit was formed by a large number of closely spaced points, taken to be arc roots. The deposit on the cathode surface was similar, except that the black spots were larger, less closely spaced, and it was more evident that they were distinct from the rusty layer which surrounded them.

The rod electrodes were very much affected by flashovers: incandescent metal was splattered off when follow current occurred. At the end of the tests, the tips of the rods had acquired a rusty layer extending axially about 0.5 cm. along the anode, and 0.2 cm.

along the cathode. The arcing ends of the rods (at right angles to the axis) were black.

The Sequence Diagram shows that a steady critical  $V_0$  was obtained in the case of rods, after conditioning. The mean critical  $V_0$  was slightly smaller, and its range was narrower, than in the case of spherical electrodes when the standard circuit was used; at the higher Z value, however, the mean critical  $V_0$  was slightly larger in the case of rod electrodes and there was little difference in the width of the two ranges of critical  $V_0$ . It is reasonable to assume that the differences in mean critical  $V_0$  are due to random conditions. On these grounds, therefore, it is concluded that the critical  $V_0$  is substantially independent of electrode shape in the case of heavily oxidised steel electrodes.

Typical oscillograms obtained with steel spheres are shown in fig. 41; they are similar to those obtained with brass spheres, except that there was some roughening of the  $V_{gt}$  waveshape due to short-duration disturbances of the type associated with type I results (section 8.2). Oscillograms obtained with steel rods, were similar to those obtained with tungsten rods (fig. 32).

The Spacing Diagram for heavily oxidised steel spheres is given in fig. 42. Two test runs were carried out, at an interval of seven weeks; it will be noted that there is good agreement between results obtained at large spacings (0.3 cm. or more), but not at low spacings (0.1 cm.). This points to the discrepancy recorded at low spacings being due to electrode effects. Its probable cause was that even after the electrodes had been oxidised by flashovers, and a nominally stable electrode condition

had been reached, flashovers still resulted in random changes in the electrode surface - i.e. ridges were produced or eroded by flashovers. The effect of such ridges is more important at low than at high spacings.

Two spot tests (not recorded in fig. 42) were carried out under the conditions of fig. 42, at a spacing of 0.1 cm. The results obtained lay between those recorded.

### 12.6 Aluminium Electrodes - Spheres.

Both circuits were used in a series of tests, the results of which are shown in the Sequence Diagram of fig. 43. The spheres were cleaned with metal polish and ether and the critical range of  $V_0$  was determined with  $n = 5$  (i.e. only five flashovers were applied at a given value of  $V_0$ ). This small value of  $n$  was chosen in order to have as few flashovers as possible, and so oxidise the electrodes as little as possible during the test. Nevertheless, oxidation proceeded rapidly: at the end of test 67 (fig. 43) the arcing tip of the anode had been covered with a white oxide over a roughly elliptical area, with axes of 0.5 x 0.6 cm. approximately. This area was broken by a large number of black points - presumably arc roots - which had penetrated the metal up to a depth of the order of  $10^{-2}$  cm. The effect of these numerous penetrations was to give the anode a porous appearance.

The appearance of the cathode was similar to that of the anode, except that the white surface was more intense. Its boundaries were more irregular, but lay within a circle 0.5 cm. diameter. The white oxide could be wiped off with a cloth but the black marks could only be removed by scraping.

Test 67 shows an initial trend for  $V_o$  to rise as the test proceeded, but this trend was not maintained after point (a). It is therefore not possible to attribute the initial increase in the critical  $V_o$  to oxidation of the electrodes; it may have been due to other, random factors. To investigate this, the oxide layer was removed by rubbing the electrodes with emery paper, and then cleaning them with metal polish and ether; test 68 was then carried out as a repeat of test 67. There was no increase in the  $V_o$  range in test 68, and it was decided to use the disc electrodes to determine the effect of the oxide layer (section 12.7).

It was noted that oxidation proceeded very rapidly in test 68, the appearance of the electrodes at the end of the test being very nearly the same as at the end of test 67. Subsequent experiments made little difference to the appearance of the electrodes; a photograph of the electrodes was taken at the end of test 73, and is reproduced in fig. 44.

Tests 69-72 were carried out with the electrodes heavily oxidised. They show that there is little variation in the critical range of  $V_o$  and that it is not affected by flashovers.

Typical oscillograms obtained in tests 67-72 are shown in fig. 45. Relatively smooth  $V_{gt}$  waveshapes of the type shown in fig. 45(a), were recorded only when the value of  $V_o$  was near the upper limit of the critical range. In all other cases, the  $V_{gt}$  waveshape was very rough, as illustrated by figs. 45 (b) - (f) (the roughening is illustrated more strikingly by figs. 45 (b) - (d), than in figs. 45 (e) - (f) because the oscillographic sweep was more rapid in the former case). The roughening was due to short

duration disturbances, of the type associated with type I results (section 8.2) which followed upon one another in quick succession in this case. While such disturbances have also been recorded with other electrodes (notably tungsten and copper spheres), they occurred after a greater proportion of flashovers, and were more numerous in the case of aluminium electrodes, experimental conditions being the same.

In addition to these short-duration disturbances, some of the oscillograms showed definite steps in the  $V_{gt}$  curve (e.g. fig. 45(e), point X). The amplitude of these steps was too small to be a transition from a glow to an arc condition.

Increasing the Z value (test 73, fig. 43) made no significant difference to the  $V_{gt}$  and  $I_t$  waveshapes.

The Spacing Diagram is given in fig. 46. When the spacing was 0.05 cm., oscillograms differed from those obtained at 0.5 cm. in that the short-duration disturbances were of greater amplitude at the lower spacing. The magnitude of these disturbances decreased as the test gap spacing increased, but was nearly constant over the range 0.3 - 0.8 cm.

When the test gap spacing was increased above 0.8 cm., the upper limit of the critical range of  $V_0$  was raised very considerably and oscillograms showed that  $I_0$  varied in magnitude from flashover to flashover, and was often very large. The effect of  $I_0$  on the critical  $V_0$ , is evident from fig. 10. It will be seen that the L.V. circuit current,  $I_t$ , builds up from the (negative) value  $I_0$ . Its rate of growth is substantially independent of  $I_0$ , and is determined primarily by  $V_0$ ,  $V_{gt}$  and the circuit parameters. Now,

the establishment of follow current depends on the L.V. circuit current being sufficiently large to maintain the discharge at the end of the impulse, and the bigger  $I_0$ , the smaller will that current be at the appropriate time (i.e. the smaller will  $I_{t_1}$  be). Hence, if  $I_0$  is not negligible, the value of  $V_0$  at which the establishment of follow current is just possible, will vary with  $I_0$  and the upper limit of the critical  $V_0$  will only be reached when  $V_0$  is sufficiently large to establish follow current at the maximum value to which  $I_0$  can rise.

In the case of the Spacing Diagram,  $I_0$  was negligible ( $< 0.05 I_{t_1}$ ) at spacings up to 0.8 cm. At higher spacings,  $I_0$  became significant so that a direct comparison with other results, obtained with a negligible value of  $I_0$ , was no longer possible: that is why the Spacing Diagram was not continued to higher spacings.

The reason for the high value of  $I_0$  must be that the flashover time of the test gap is long, for only in that case has the impulse voltage sufficient time to build up a large current in L. This phenomenon had not been recorded with any other electrode materials, so that it was evidently caused by the particular electrodes used in this test - i.e. heavily oxidised aluminium spheres. Long times-to-flashover are not generally associated with aluminium electrodes, so that the oxide layer was assumed to be their cause: tests with aluminium disc electrodes (section 12.7) showed this assumption to be correct.

It is interesting to note that the effect of the oxide layer is to make follow current less likely in this case: it will be

seen in section 14.3 that a large value of  $I_0$  (and hence the oxide layer) has the reverse effect if  $V_0$  and  $V_{IG0}$  are of opposite polarity to earth.

### 12.7 Aluminium Electrodes - Discs.

The Standard Circuit was used in tests carried out with disc electrodes (section 3) at a spacing of 0.5 cm. A fraction of the periphery of each electrode was then conditioned by the application of a large number of flashovers (see fig. 43, test 74) and the critical range of  $V_0$  was determined. A photograph of the conditioned sections of the electrodes is reproduced in fig. 47(a).

The discs were then rotated after every five flashovers, and the critical value of  $V_0$  was determined for the relatively clean electrode surface (test 75). The photographs of fig. 47 (b) - (c) were obtained in this test: they show that the marking of the cathode is much more intense than on the anode, particularly if there is no follow current. Fig. 47(c) shows that the markings overlap in the case of flashovers which resulted in follow current: the amount of overlap is very slight at the cathode, and is greater at the anode, where the markings extend over a much greater area than in the case of no-follow-current flashovers. Now, it will be remembered that the establishment of H.V. Follow Current is determined shortly after the end of the impulse, when the discharge current is quite small (section 7.1). Hence, at the critical times at which follow current is determined, the area of the electrode surface affected by each arc root is roughly the same as in fig. 47(b) whether or not follow current occurs. Consequently, the area affected by an arc root at these critical times, had not generally been affected by previous flashovers.

Finally, the critical  $V_0$  was again determined for the conditioned part of the electrodes (test 76) as a check against possible changes in  $V_0$  due to random conditions.

It will be seen from the Sequence Diagram (fig. 43) that there is little variation in the critical  $V_0$  obtained in tests 74 - 76; consequently, the oxide layer produced by conditioning has no significant effect on the critical  $V_0$ .

The electrodes were then machined to remove all traces of arc roots and were cleaned with metal polish and ether. An experiment was then carried out to determine the effect of the oxide layer produced by conditioning, on the time-to-flashover (and hence  $I_0$ ) at large gap spacings. The Standard Circuit was used.

In the first place, a fraction of the electrode surfaces was conditioned. The gap spacing was reduced to 0.5 cm. during conditioning so that the upper limit of the critical range of  $V_0$  would not exceed the maximum available value of  $V_0$ ; it will be remembered that the upper limit may be much increased by the high  $I_0$  at large gap spacings. Conditioning consisted of 400 flashovers at  $V_0 = 600$  Volts ( $V_0$  greater than critical) and 300 flashovers at  $V_0 = 260$  Volts (critical  $V_0$ ). The general appearance of the conditioned part of the electrodes was similar to that shown in fig. 47(a) and did not change in the subsequent test.

The spacing was then increased to 1.0 cm. and 20 flashovers were applied at  $V_0 = 600$  Volts (follow current occurred on every flashover) and 10 at  $V_0 = 300$  Volts (follow current occurred after 6 flashovers only). Oscillograms showed that there was considerable variation in the magnitude of  $I_0$ , which was large in many cases (see page 82, table 3, first lot of 30 flashovers). The

experiment was continued by applying flashovers to the unconditioned parts of the electrodes. Oscillograms taken in 20 flashovers ( $V_0 = 300$  volts, 6 cases of follow current) showed that  $I_0$  was negligible in every case. Finally, another test was carried out as a check, by applying to the conditioned parts of the electrodes, 12 flashovers at  $V_0 = 300$  volts (follow current occurred after 6 flashovers only) and 26 flashovers at 600 volts (follow current occurred after every flashover): there was considerable variation in the magnitude of  $I_0$  obtained in these 38 flashovers.

TABLE 3.

Electrode condition	Total number of Flashovers.	Number of flashovers on which the magnitude of $I_0$ lay in the range shown.				
		0 - 0.05 Amps	0.05 - 0.1 Amps	0.1 - 0.25 Amps	0.25 - 0.8 Amps	Over 0.8 Amps
Conditioned, heavily oxidised electrodes	30	8	14	8	-	-
'Clean' electrodes	20	20	-	-	-	-
Conditioned, heavily oxidised electrodes	38	13	8	7	3	7

A quantitative analysis of the results obtained in these tests is given in the above Table. The data of that table proves that the heavy oxide layer, which is caused by repeated flashovers,

results in random and potentially large variations in the value of  $I_0$ , and hence in the time-to-flashover.

The test on the 1.0 cm. gap also provided information on the effect of conditioning on glow-arc transitions. 12 flashovers were applied to the conditioned section of the electrodes at a critical value of  $V_0$  ( $V_0 = 300$  volts, 6 cases of follow current) and 20 flashovers were applied to unconditioned sections of the electrodes at the same value of  $V_0$  (6 cases of follow current). Oscillograms of flashovers to the conditioned section were similar to those obtained with conditioned spheres (section 12.6); they were of type I (section 8.2), and the  $V_{gt}$  waveshape was roughened by a large number of short-duration disturbances. Oscillograms of flashovers to the unconditioned sections, were of type II (section 8.2); glows were maintained in all but one of the twenty oscillograms taken, their duration ranging from a few microseconds to 100 microseconds or more. The  $V_{gt}$  waveshape was smooth while glows were maintained, but it was roughened by short-duration disturbances while the discharge was an arc.

Now, the view has been advanced in section 8.2 (type I results) that the short-duration disturbances are caused by arc-glow transitions followed almost immediately by glow-arc transitions, i.e. that they are short-duration glows. This view is supported in the present instance by the fact that glows were recorded under the same experimental conditions as the short-duration disturbances. Furthermore, if the duration of some of these glows had been halved or quartered, they would have been indistinguishable from the short-duration disturbances.

If, therefore, the disturbances are, in fact, short-duration glows, it follows that the times for which glows can be maintained are much greater in the case of unconditioned electrodes (where transitions to arc often occurred after glow periods of the order of 10 microseconds) than in the case of conditioned electrodes (where the glow durations were so short, that the glows appeared merely as disturbances in the  $V_{gt}$  curve). Hence the oxidation produced by conditioning facilitates glow-arc transitions.

### 12.8 Aluminium Electrodes - Rods.

The Sequence Diagram for rod electrodes is shown in fig. 43. The rods were obtained from 0.051 cm. diameter aluminium wire. They were cut with a razor blade so that their ends were, as nearly as possible, plane and perpendicular to their axes. Before the tests were carried out the rods were cleaned with metal polish and ether, except at the cut surfaces which were cleaned with ether only.

Conditioning resulted in considerable oxidation and deformation of the electrode tips. Metal spikes, up to 0.1 cm. long were jutting out from the electrode tips at right angles to the electrode axis at the beginning of test 78 (fig. 43), and the metal at the electrode tips was porous in appearance. The test gap increased appreciably as flashovers were applied and was reset repeatedly. None of the other materials tested was affected by conditioning in this manner.

It will be seen from the Sequence Diagram (fig. 43) that three separate sets of rod electrodes were used; they all show that there is little variation in the critical range of  $V_0$  when

the electrodes are not heavily deformed and oxidised (i.e. before conditioning). Also results obtained with one set of electrodes could be repeated consistently with another set of electrodes if the experimental conditions were the same (cf. tests 77, 79 and 84).

Conditioning resulted in considerable increase in  $V_0$ . Thus when the Standard Circuit was used,  $V_0$  rose from some 220 - 300 volts (tests 77, 79 and 84) to 300 - 440 volts (test 82) and when the other circuit was used ( $Z = 126$  ohms),  $V_0$  rose from some 320 - 420 volts (test 83) to 400 - 550 volts (test 81). Two distinct factors may contribute to the increase in critical  $V_0$ , namely:-

- (1) Quite apart from the formation of oxide, the considerable enlargement of the electrode tips may result in a decrease in the temperature of, and the voltage gradient at, the electrodes.
- (2) The oxide layer may have thermal and electrical (i.e. work function) properties which would make electron emission more difficult.

The results of sections 12.6 and 12.7 show that the oxide layer does not affect the critical value of  $V_0$  except if the voltage gradient just before flashover is relatively low, so that  $I_0$  can be large. With rod electrodes, and at the spacing considered (0.5 cm.) the voltage gradient was sufficiently high for  $I_0$  to be negligible: hence, on the basis of the results just quoted the increase in the critical  $V_0$  cannot be due to the oxide layer and must be due to the increase in the size of the electrode

tips, and the consequent decrease in temperature and/or voltage gradient. This argument is based on the assumption that the oxide layer has the same composition and electrical and thermal properties in the case of the rods as in that of the spheres. This assumption is supported by the fact that the appearance of the oxide layer was the same in both cases; the possibility, nevertheless, remains that the oxide formation may be different in the two cases, just because the rods become considerably hotter than the spheres.

Oscillograms obtained in tests on rod electrodes showed that the general shape of the  $V_{gt}$  curve was similar to that obtained with tungsten rods (fig. 32) except that the rapid voltage fluctuations associated with heavily oxidised aluminium electrodes (fig. 45) were also present. There was no significant difference in the appearance of oscillograms obtained with relatively unoxidised, and heavily oxidised (conditioned) rod electrodes.

### 12.9 Copper Electrodes - Spheres.

Results obtained with 2 cm. copper spheres spaced 0.5 cm. apart, are given on the Sequence Diagram of fig. 48. Tests 86 and 87 of that Diagram indicate that the critical  $V_0$  was, if anything, slightly larger before than after flashovers were applied: this agrees with the results obtained with disc electrodes (section 12.10). Tests 87-90 and 91-93 show that there is little variation in the critical  $V_0$  obtained with oxidised electrodes in a given experimental condition - i.e. the critical  $V_0$  was unaffected by conditioning once the electrodes were oxidised.

It was not possible to obtain a set of oscillograms for the unoxidised condition in these tests, because the electrodes oxidised as the test proceeded (oscillograms for the unoxidised condition were obtained with disc electrodes, section 12.10). The oscillograms obtained with oxidised electrodes (latter part of test 86, tests 87-90 and 91-93) did not differ in any significant way from those obtained with oxidised disc electrodes under similar conditions (figs. 53 and 55). In the case of  $Z = 40$  Ohms (tests 86-90) results were usually of type I (fig. 53 (a) - (c)) the only exception being one record of type II (as fig. 53(d)). The short-duration disturbances in the  $V_{gt}$  waveshape, which have also been recorded with aluminium electrodes, were present in all cases.

When  $Z$  was increased to 126 Ohms (tests 91-93) results became of type III (fig. 55). The discharge usually degenerated into a glow at the end of the impulse, and follow current could then be established only after a glow-arc transition. During the time that the glow was maintained, the discharge current was nearly constant, so that  $V_{gt} \approx V_t$ . To a sufficiently good approximation  $V_o \approx V_t$  during that time, so that  $V_o \approx V_{gt}$ , as shown by fig. 55. This is an experimental verification of the discussion of section 8.1.

The Spacing Diagram is given in fig. 49. Oscillograms obtained at different spacings were similar to those recorded with a 0.5 cm. gap. In the case of oscillograms obtained at  $Z = 126$  Ohms, the times for which a nearly-constant-voltage glow was maintained, decreased as the spacing increased. Thus the

duration of the constant voltage glows was of the order of 0.1 milliseconds in the case of a 1.0 cm. gap, and of the orders of 1 and 10 milliseconds in the case of a 0.05 cm. gap. It was also noted that in the case of low gap spacings (0.1 or 0.05 cm.) the discharge voltage  $V_{gt}$  remained very nearly constant as  $I_{gt}$  decreased to zero after a glow condition was reached. Such oscillograms were obtained when follow current was not established; in the case of corresponding oscillograms obtained at higher gap spacings,  $V_{gt}$  rose as  $I_{gt}$  fell.

The appearance of the electrodes at the end of these tests is shown in fig. 50. The central portion of the anode was greyish in colour, and could be enclosed in a 2 mm. diameter circle. This was surrounded by a blackened area, extending up to a diameter of 4 mm.; by a green area, extending up to a diameter of 5 mm. and by an area in which the copper was discoloured, extending up to a diameter of 8 mm. On the cathode, there was a central area, which lay within a 4 mm. diameter circle, in which the metal was bright and of the usual copper colour. This was surrounded by a black circle, which was in turn surrounded by a region, 9 mm. diameter, in which the copper was discoloured. The electrode surfaces appeared smooth to the naked eye.

#### 12.10 Copper Electrodes - Discs.

All tests in which disc electrodes were used were carried out at a spacing of 0.5 cm. A photograph of the conditioned sections of the electrodes is given in fig. 51, and photographs of corresponding sections of the electrodes, to which only five

flashovers had been applied, are shown in fig. 52. Close examination shows that a certain amount of overlapping of markings produced by flashovers exists in the case of fig. 52(b), and the remarks made in section 12.7 in connection with fig. 47(c) apply here also.

Results have been summarised in the Sequence Diagram of fig. 48. Tests 94 and 95 show that the oxidation produced by conditioning results in an appreciable lowering in the critical  $V_0$ . Typical oscillograms obtained in those tests are given in figs. 53 and 54. Relatively few (53) oscillograms were taken with oxidised discs, because their results were confirmed by those taken with oxidised spheres. They showed that waveshapes were usually of type I (section 8.2), as illustrated by figs. 53 (a) - (c). In many cases, the  $V_{gt}$  waveshape was roughened by short-duration disturbances which were probably short-duration glows (sections 8.2 and 12.7). A few type II waveshapes were recorded (e.g. fig. 53(d)), and arc-glow transitions occurred frequently in the case of no-follow-current oscillograms (e.g. fig. 53(e)).

85 oscillograms were taken when flashovers were applied to the oxidised part of the electrodes. They differed from those obtained with oxidised electrodes in that glows were maintained for longer times. Type II records (e.g. fig. 54(b)) were more frequent, and type III records were obtained in three cases (e.g. fig. 54(c)), in which nearly-constant-voltage glows were maintained for 300 microseconds or more, before follow current became established. In a fourth instance, a nearly-constant voltage glow was maintained for over 1000 microseconds,

when the end of the oscillograph sweep was reached.

Tests carried out at the higher value of  $Z$  (tests 96 and 97) showed that the effect of oxidation is much smaller than at the lower value of  $Z$ . Oscillograms taken in tests 96 and 97 were of type III (fig. 55 and 56). Thus the oxide layer loses much of its effect on the critical  $V_0$  if the experimental conditions are such that follow current can only be established after a glow has been maintained for a time of the order of 100 microseconds or more (i.e. if the limiting condition of the Glow Criterion has been reached) even though the electrodes are oxidised.

One significant effect of the oxide is maintained at the higher value of  $Z$ : glows precede the establishment of follow current in fewer cases, and last for shorter times, if the electrodes are oxidised, than if they are not. This statement is borne out by the quantitative analysis of Table 4.

TABLE 4.

Electrode Condition	Test No. (Sequence Diagram fig. 48)	Total Number of Flashovers resulting in Follow Current	Number (and %) of flashovers on which Follow Current was preceded by a glow	Mean duration of glows which preceded follow current
Unoxidised	97	33	32 (97%)	2 ms.
Oxidised	96	78	65 (83%)	less than $\frac{1}{2}$ ms.

### 12.11 Copper Electrodes - Rods.

Results obtained with 0.056 cm. diameter copper rods, spaced 0.5 cm. apart, are given in fig. 48 (tests 98 - 101). When  $Z = 40$  Ohms (tests 98 - 100), the lower limit of  $V_0$  is the same as in the case of other electrodes, but the critical range is narrower in the case of rods. When  $Z$  is increased to 126 Ohms (test 101), both limits of  $V_0$  are lower in the case of rods, but the critical range has roughly the same amplitude.

Typical oscillograms obtained in these tests are shown in fig. 57. It will be seen that waveforms are of type I. In no case was the establishment of follow current preceded by long-duration glows of the type recorded with 'large' copper electrodes (i.e. spheres and discs, section 3) under similar conditions.

### 13. CRITERIA OF FOLLOW CURRENT FOR $V_o$ AND $V_{IGo}$ OF SAME POLARITY TO EARTH.

The criteria which determine the establishment of follow current will now be derived in terms of  $V_o$ ,  $I_o$  and the discharge characteristics, for the conditions of sections 6 - 11, - i.e. for the conditions of  $V_o$  and  $V_{IGo}$  being positive to earth. It will be seen from section 14, that these criteria are not affected by the actual polarities of  $V_o$  and  $V_{IGo}$ , and depend only on their relative polarities. When  $V_o$  and  $V_{IGo}$  are of opposite polarities, the criteria are different, and are given in section 14.6.

The criteria derived in this section are stated in Table 5 (page 93), and are illustrated by fig. 58 for the case  $I_o = 0$ .

#### 13.1 L.F. Follow Current; Criteria of No-Follow-Current.

It will be remembered that the L.V. circuit current,  $I_t$ , must flow up to its first natural current zero occurring after the end of the impulse in order that L.F. Follow Current be established (section 5.3). Now, at the instant of flashover, the L.V. circuit voltage has the positive value  $V_o$  and the L.V. circuit current has the negative value  $I_o$ . The first natural current zero of the L.V. circuit (section 5.7) therefore occurs some

$$t_{no}' = \frac{1}{2\pi f} \sin^{-1} \frac{I_o Z}{(V_o^2 + I_o^2 Z^2)^{\frac{1}{2}}} \quad \text{seconds from}$$

the instant of flashover. Under the conditions of this investigation,  $I_o$  was so small compared to  $V_o/Z$ , that the impulse duration,  $t_1$ , exceeded  $t_{no}'$  in all cases in which L.F. Follow Current was established: in other words,  $I_t$  had reversed polarity

TABLE 5.

Criteria of Follow-Current and No-Follow-Current, for  
 $V_o$  and  $V_{IGo}$  of the same polarity to earth.

Follow Current Type	Criterion Type	Statement of Criterion
L.F.	No-Follow-Current. (Arc Criterion)	Follow Current cannot be established if $(V_o^2 + I_o^2 Z^2)^{1/2}$ is less than the mean value of the discharge voltage, taken over the impulse period.
		Follow Current cannot be established if $V_o$ is less than the discharge voltage at the end of the impulse, provided the impulse duration is much less than the half period of the L.V. circuit.
	Follow-Current (Glow Criterion)	Follow Current will be established if $V_o$ exceeds a value approximately equal to that required to maintain a constant current glow in the test gap (a) at a current equal to $I_{gtl}$ , if a constant current glow can be maintained at that current, or (b) at the maximum current at which a glow can be maintained, if that current is less than $I_{gtl}$ .
H.F.	No-Follow-Current (Arc Criterion)	Follow Current cannot be established if $V_o$ is less than the value of the discharge voltage at the first current zero of $I_o$ (i.e. at $t_{no}$ ).
	Follow-Current (Arc Criterion)	Follow Current will be established if $V_o$ exceeds the value of the discharge voltage at the first current zero of $I_o$ (i.e. at $t_{no}$ ).

and had become positive before the end of the impulse.

The criteria of no-follow-current will be derived for the condition which held in these experiments, namely,  $t_1 > t_{no}$ , or

$$t_1 > \frac{1}{2\pi f} \sin^{-1} \frac{I_0 Z}{(V_0^2 + I_0^2 Z^2)^{\frac{1}{2}}}$$

which is satisfied when:

$$(Z I_0)^2 > V_0^2 \tan^2 2\pi f t_1$$

It has been shown above that if this condition is met and L.F. follow current is established,  $I_t$  must

- (a) become positive during the impulse period,  $t_1$ , and
- (b) flow for a half cycle in the positive direction.

Now, the discharge voltage,  $V_{gt}$ , opposes the growth of  $I_t$  (fig. 1) in this condition. Consequently, if  $V_0$  - and hence  $V_t$  - is sufficiently small in relation to  $V_{gt}$ , then  $I_{t1}$  (the value of  $I_t$  and the end of the impulse) may be too small for the discharge to be maintained for a half cycle. In the limit, L.F. follow current will clearly not be established, if  $V_{gt}$  so far affects the L.V. circuit, that  $I_{t1} = 0$ .

Now, referring to fig. 1, and remembering that the ohmic resistance associated with the L.V. circuit is negligible (section 2.2):

$$L \frac{dI_t}{dt} = (V_t - V_{gt})$$

subject to:  $I_t = I_0$  at  $t = 0$

Hence, integrating from zero to  $t_1$

$$L(I_{t1} - I_0) = \int_0^{t_1} (V_t - V_{gt}) dt$$

$$\therefore I_{t_1} = I_0 + \frac{1}{L} \int_0^{t_1} (V_t - V_{gt}) dt$$

so that L.F. Follow Current cannot occur if

$$I_0 + \frac{1}{L} \int_0^{t_1} (V_t - V_{gt}) dt = 0$$

$$\text{i.e. if } \frac{1}{L} \int_0^{t_1} V_t dt = -I_0 + \frac{1}{L} \int_0^{t_1} V_{gt} dt$$

Now, if L.F. Follow Current cannot occur at a given value of  $\int_0^{t_1} V_t dt$ , it will clearly not occur at lower values. Hence, there can be no L.F. Follow Current if

$$\frac{1}{L} \int_0^{t_1} V_t dt \leq -I_0 + \frac{1}{L} \int_0^{t_1} V_{gt} dt$$

Furthermore, the peak value of  $V_t$  cannot exceed  $(V_0^2 + I_0^2 Z^2)^{\frac{1}{2}}$ , consequently,  $\int_0^{t_1} V_t dt < \int_0^{t_1} (V_0^2 + I_0^2 Z^2)^{\frac{1}{2}} dt$

so that there can be no L.F. Follow Current if

$$\frac{1}{L} \int_0^{t_1} (V_0^2 + I_0^2 Z^2)^{\frac{1}{2}} dt \leq -I_0 + \frac{1}{L} \int_0^{t_1} V_{gt} dt$$

$$\text{i.e. if } (V_0^2 + I_0^2 Z^2)^{\frac{1}{2}} \leq -\frac{I_0 L}{t_1} + \frac{1}{t_1} \int_0^{t_1} V_{gt} dt$$

Now,  $I_0$  is negative, so that there can be no L.F. Follow Current if

$$(V_0^2 + I_0^2 Z^2)^{\frac{1}{2}} \leq \frac{1}{t_1} \int_0^{t_1} V_{gt} dt$$

Hence the criterion of no-follow-current is stated in the first column of Table 5.

If  $t_1 \ll \frac{1}{2f}$ , L.F. Follow Current cannot occur even though  $(V_0^2 + I_0^2 Z^2)^{\frac{1}{2}}$  has a higher value than that given by the above

criterion. It will be remembered that  $t_{no}'$ , the time at which  $I_t = 0$  and  $V_t$  is a maximum (if L.F. Follow Current is established) is less than  $t_1$ , i.e.  $V_t$  is decreasing from its maximum value towards the end of the impulse. Now, it has been shown that

$$L \frac{dI_t}{dt} = (V_t - V_{gt})$$

and if  $\frac{dI_t}{dt}$  should become negative during  $t_1$ ,  $I_t$  will begin to decrease;  $I_{IGt}$  decreases exponentially in any case so that  $I_{gt} (= I_t + I_{IGt})$  will decrease: consequently,  $V_{gt}$  will rise (the impulse discharge has a negative characteristic, being an arc).  $V_t$  decreases in any case so that if  $\frac{dI_t}{dt}$  becomes negative, it will remain so until the end of the discharge. Now, if L.F. Follow Current is established,  $\frac{dI_t}{dt}$  should not become negative until some  $(t_{no}' + \frac{1}{4f})$  seconds from the instant of flashover. Hence, if  $t_1 \ll \frac{1}{2f}$  and  $\frac{dI_t}{dt}$  becomes negative at any time  $\leq t_1$ , L.F. Follow Current cannot be established. In the limit, therefore, there will be no L.F. Follow Current if  $\frac{dI_t}{dt}$  becomes negative at  $t_1$ , i.e. at  $t_1$ ,  $\frac{dI_t}{dt} < 0$ , which means that  $(V_{t1} - V_{gt1}) < 0$ .

Now, the maximum value of  $V_t$  will be greater than  $V_0$  if  $I_0$  is finite but will not exceed  $(V_0^2 + I_0^2 Z^2)^{\frac{1}{2}}$ , and two approximations are possible, because  $t_1$  is much smaller than  $1/(2f)$ . Firstly,  $I_0 Z$  will be much smaller than  $V_0$  (since  $(I_0 Z)^2 < V_0^2 \tan^2 2\pi f t_1$  and  $t_1 \ll 1/(2f)$ ), so that  $(V_0^2 + I_0^2 Z^2)^{\frac{1}{2}} \approx V_0$ . Secondly, the capacitor C will have lost only a small fraction of its charge during  $t_1$ , so that  $V_{t1} \approx V_0$ . Hence L.F. Follow Current cannot be established if

$$V_0 < V_{gt1}$$

The second criterion of no-follow-current is therefore entered in Table 5 (second column).

The discharge is an arc during the impulse period, so that both criteria of no-follow-current are expressed in terms of an arc voltage; consequently, these criteria will be known as 'Arc Criteria'.

In no experiment was follow current established at a value of  $V_0$  smaller than that given by the appropriate criterion.

### 13.2 H.V. Follow Current - The Glow Criterion.

The criterion of L.F. Follow Current will be derived for the case of H.V. Follow Current in the first place; it will then be shown to apply also to the case of H.C. Follow Current (section 13.5).

It has been established in the discussion of H.V. Follow Current (section 8) that:

- (1) The establishment of H.V. Follow Current is just possible if  $V_0 \approx V_{gtM}$  (section 8.1): follow current will be established at all higher values of  $V_0$ .
- (2) The discharge may have either an arc or a glow characteristic at time  $t_M$  (section 8.2).

Hence H.V. Follow Current will always be established if  $V_0$  exceeds a value approximately equal to the maximum glow voltage of the discharge.

The maximum glow voltage of the discharge will depend on three factors, namely:

- (1) The test gap.
- (2) The current flowing through the discharge at the time that

the discharge attains its maximum (glow) voltage. That time is denoted by  $t_M$ , so that the appropriate current has the value  $I_{gtM}$ .

Now, it will be remembered (section 8.1) firstly, that  $I_{gt} = I_t$  after  $t_1$ , secondly, that  $t_M$  occurs shortly after  $t_1$ , and thirdly, that if the establishment of H.V. Follow Current is just possible,  $\frac{dI_t}{dt} \rightarrow 0$  shortly after  $t_1$ . Hence,  $I_{gtM} \approx I_{gt1}$ , i.e. the current flowing through the discharge at  $t_M$  can be taken as the current flowing through the discharge at the end of the impulse. It will be shown in Appendix VII that the latter current can be predicted fairly accurately for a given test gap, impulse discharge, and L.V. circuit, provided  $V_0$  does not exceed the maximum critical value.

(3) The past history of the discharge. Let  $V_{gc}$  be the voltage value required to maintain a glow discharge in the test gap at a constant current  $I_{gtM}$ .  $V_{gtM}$  will, in general, differ from  $V_{gc}$ , because in the case of the present experiments, the discharge current had a high (impulse) value before falling to a glow value. The high initial current value could have one of two predominant residual effects at  $t_M$ , namely,

(i) Owing to the high initial ionisation of the discharge, the ionisation at  $t_M$  could be higher than that corresponding to  $V_{gc}$ ; consequently,  $V_{gtM} < V_{gc}$ .

(ii) It is conceivable that turbulence set up during the impulse may result in more rapid deionisation at  $t_M$ , than would be the case had the discharge current been

constant at the value  $I_{gtM}$ . Hence,  $V_{gtM}$  may exceed  $V_{gc}$ .

So far as the author is aware, there is no experimental evidence available to indicate the magnitude of effect (ii) and an investigation aimed at determining it is now being planned (section 16.1). In the light of existing knowledge, therefore, it is reasonable to assume that this effect can be ignored to a first approximation, so that  $V_{gtM}$  will not be substantially greater than  $V_{gc}$ ; hence  $V_0$  need not be substantially greater than  $V_{gc}$  in order to establish H.V. Follow Current.

It follows, therefore, that H.V. Follow Current will invariably be established if  $V_0$  exceeds a value approximately equal to the voltage required to maintain a constant current glow in the test gap, at a current value  $I_{gtl}$ . This criterion will be known as the 'Glow Criterion'.

### 13.3 Experimental Confirmation of the Glow Criterion.

The limiting conditions of the Glow Criterion were reached in two series of experiments discussed below.

#### (1) Tests on Tungsten Rods.

Reference is made to tests 21 - 28 (fig. 17, section 8.4), in which the effect of variation in  $R_f$  (fig. 1) was investigated using 0.063 cm. diameter tungsten rods, spaced 0.5 cm. apart. It will be seen from fig. 17, that as conditions became progressively less favourable for the establishment of follow current, and the critical  $V_0$  increased, the oscillograms obtained changed from type I (tests 21 - 26) to type II (test 27) and finally to type III (test 28). In the case of test 28, therefore, a glow

was established and maintained immediately after the end of the impulse, and follow current could only be established by a glow-arc transition. The duration of the glow period was too long for any substantial part of the voltage required for the transition to be supplied by the energy stored in L (fig. 1), so that  $V_0$  was very nearly equal to  $V_{gtM}$  (section 8.1): in other words, the limiting conditions of the Glow Criterion were reached in test 28.

An estimate of the value of  $V_{go}$  corresponding to test 28, can be obtained from data published by Gambling and Edels<sup>13</sup> for 1.2 cm. diameter tungsten electrodes spaced 0.5 cm. apart; over the current range of test 28,  $V_{go}$  had a value of some 490 - 500 Volts<sup>13</sup>, while the critical  $V_0$  ranged from 440 to 650 Volts. Hence, the critical  $V_0$  is approximately equal (within 33%) to  $V_{go}$  in the limiting case of the Glow Criterion.

Other results obtained with the same electrodes and at the same spacing (tests 1 - 10, fig. 16, and 15 - 27, fig. 17) were analysed in the same way. It was found that in all cases (including test 28), the critical  $V_0$  was less than  $1.33 V_{go}$  - i.e. follow current was invariably established if  $V_0$  exceeded  $1.33 V_{go}$ . This confirms the Glow Criterion.

## (2) Copper Electrodes.

It has been seen that nearly-constant-voltage glows were maintained for times of the order of 1 millisecond after the end of the impulse in the case of un-oxidised copper discs, spaced 0.5 cm. apart and  $Z = 126$  Ohms (test 97, section 12.10). The oscillograms of fig. 56 were obtained in that condition, and they

constitute by far the most striking illustration of the Glow Criterion, since they showed that follow current occurred if  $V_0$  were capable to maintain a glow and to force a transition to arc ( $L \frac{dI_t}{dt}$  was nearly zero during the glow period).

The critical  $V_0$  ranged from 460 to 560 Volts in test 97, and the critical  $I_{gt}$  ranged from 0.12 to 0.14 Amps (approx.). The value of  $V_{go}$  corresponding to that current and spacing in the case of 0.7 cm. diameter copper rod electrodes is given by Gambling and Edels<sup>13</sup> as 510 - 520 Volts. The close agreement between this value and that of the critical  $V_0$  confirms the Glow Criterion.

#### 13.4 Current Ranges over which Glow Criterion is Valid.

The Glow Criterion depends on the fact that so long as  $V_t$  exceeds the maximum discharge voltage, the discharge current must increase, and consequently the discharge voltage must fall; this results in a more rapid increase in current, and hence a further decrease in voltage. In other words, the Glow Criterion depends on the discharge having a negative characteristic.

Now, it is well known, from work carried out at low pressures, that the glow discharge has a positive characteristic at low currents. In the case of discharges in air at atmospheric pressures, a negative characteristic has been recorded at current values down to some 0.01 Amps<sup>13,14</sup>. So far as the author is aware, positive characteristics have not been obtained in the case of glow discharges in air at atmospheric pressures; such characteristics may well hold at lower currents. In the light of available evidence, therefore, the Glow Criterion applies when  $I_{gt}$  has values greater than some 0.01 Amps; its application at lower currents depends on the characteristic of the discharge. In the

present work, the critical  $I_{gtl}$  was not less than 0.1 Amps.

### 13.5 L.F. Follow Current - The Criterion of Follow Current.

It has been shown (sections 7.2 and 9) that the critical  $V_0$  required for the establishment of H.C. Follow Current is of the order of an arc voltage. Hence, if  $V_0$  is given a glow value, H.C. Follow Current will be established, so that the Glow Criterion remains valid; this statement was confirmed by all the experimental evidence reviewed for this thesis, in which follow current was of the H.C. type.

The Glow Criterion defines  $V_0$  in terms of the voltage required to maintain a constant current glow in the test gap at a current equal to  $I_{gtl}$ . Now, in the case of H.C. Follow Current, the critical value of  $I_{gtl}$  may be too large to maintain a constant current glow; the Glow Criterion is therefore stated in the third column of Table 5 in terms which apply equally to H.V. and H.C. Follow Current.

### 13.6 Criteria of H.F. Follow Current.

The conclusions arrived at in section 10 are in fact the criteria of H.F. Follow Current; they are stated in the fourth and fifth columns of Table 5. These criteria are expressed in terms of arc voltages (since the discharge is an arc during the impulse period) and will therefore be known as 'Arc Criteria'.

If  $I_0$  is negligible, the criteria become that H.F. Follow Current will be established if, and only if,  $V_0$  exceeds the minimum value of the discharge during the impulse.

## 14. EFFECT OF POLARITY

It will be shown in this section that two principal cases exist, depending on whether  $V_o$  and  $V_{IGo}$  are of the same, or of opposite polarities to earth. Two possibilities arise in either case, depending on whether  $V_o$  (or  $V_{IGo}$ ) is positive or negative to earth. There are thus four possible combinations of the polarities of  $V_o$  and  $V_{IGo}$ : these are considered individually below.

### 14.1 $V_o$ and $V_{IGo}$ both positive.

This condition held in all but two experiments carried out in this work. Results obtained with it have already been discussed, and it will now be used as reference, to show the effect of changes in the polarities of  $V_o$  and  $V_{IGo}$ .

### 14.2 $V_o$ and $V_{IGo}$ both negative.

Reversal of the polarities of both  $V_o$  and  $V_{IGo}$  affects matters only because the test gap is not symmetrical with respect to the earth plane. In the absence of a discharge, the voltage gradient is smaller at the earthed electrode. When  $V_o$  and  $V_{IGo}$  are of the same polarity (as in this case), there is always a discharge in the test gap at the critical times at which the establishment of follow current is determined. The effect of assymetry is then sufficiently small to be ignored within the order of accuracy of this investigation.

This conclusion was verified experimentally in two tests, carried out in the Standard Condition (section 5.12):  $V_o$  and  $V_{IGo}$

were positive in one and negative in the other. No difference could be detected in the critical ranges of  $V_o$  obtained in the two tests.

14.3  $V_o$  positive and  $V_{IGo}$  negative - The L.F. Follow Current Case.

This case differs from that already discussed (i.e. section 14.1) in that the impulse is negative. The operation of the circuit under this condition will now be considered.

Immediately IGOG begins to conduct, the impulse circulates a current in the L.V. circuit. That current reaches the value  $I_o$  at the instant of flashover of the test gap.  $I_o$  is positive when the impulse is negative (section 2.9);  $I_{IGt}$  is, of course, negative.

The general relation between the discharge, L.V. circuit and impulse currents (fig. 1):

$$I_{gt} = I_{IGt} + I_t$$

Now, the discharge is initiated by a negative impulse, so that  $I_{gt}$  will be negative initially, and  $I_{IGo}$  will exceed  $I_o$  in magnitude. As the discharge proceeds,  $I_{IGt}$  decreases in magnitude, but remains negative.  $V_o$  being positive,  $I_t$  must remain positive towards the end of the impulse if follow current is to be at all possible; otherwise, the L.V. circuit would not circulate a current in the test gap after the end of the impulse. A time  $t_a$  will eventually be reached when the impulse current  $I_{IGt}$  will have fallen to a value numerically equal to that of the L.V.

circuit current,  $I_t$ . The two currents being of opposite polarity,  $I_{gt}$  will then be zero - i.e. a current zero will be induced in the test gap.  $I_{IGt}$  is finite at  $t_a$  so that IGOG is still conducting - hence  $t_a$  is less than the impulse duration,  $t_1$ .

Other effects of reversing the polarity of the impulse, emerge from considerations of the value of  $I_{ta}$  obtained when the impulse duration (and hence  $t_a$ ) is much smaller than the half period of the L.V. circuit. It has been shown in section 13.1 that in general

$$L \frac{dI_t}{dt} = V_t - V_{gt}$$

subject to  $I_t = I_0$  at  $t = 0$ . Now, if  $t_a \ll 1/(2f)$ ,  $V_t$  approximates to  $V_0$  during that period, so that

$$L \frac{dI_t}{dt} = V_0 - V_{gt}, \text{ for } t \leq t_a$$

and therefore

$$I_{ta} = I_0 + \frac{1}{L} V_0 t_a - \int_0^{t_a} V_{gt} dt$$

When the impulse was positive,  $I_0$  was negative and  $V_{gt}$  was positive, so that they opposed the growth of  $I_t$ . In the present case,  $V_{gt}$  is negative during  $t_a$ , and  $I_0$  is positive: hence  $I_{ta}$  may be substantially greater in the case of the negative impulse. It will be remembered that  $I_{ta}$  is the current available from the L.V. circuit to maintain the discharge, subject to the test gap being flashover over after  $t_a$ .

The above discussion depends on the relative polarities of  $V_0$  and  $V_{IG0}$ , but is not affected by the actual polarities of these voltages. The following conclusions can therefore be stated:

(1) A current zero is induced in the test gap towards the end of

the impulse if  $V_o$  and  $V_{IGo}$  are of opposite polarities, but not if they are of the same polarity. In the former case, therefore, follow current can only be established after a restrike.

- (2) The time,  $t_a$ , for which the impulse maintains the discharge when  $V_o$  and  $V_{IGo}$  are of opposite polarities, is shorter than the time,  $t_1$ , for which the discharge would be maintained if  $V_o$  and  $V_{IGo}$  were of the same polarities, other things being equal. The L.V. circuit current therefore has less time to build up in the negative impulse case.
- (3) Owing to the effects of  $I_o$  and  $V_{gt}$ ,  $I_{ta}$  may be larger when  $V_{IGo}$  and  $V_o$  are of opposite polarities, than when they are of the same polarity. A larger current may therefore be available to maintain the discharge at the end of the impulse when  $V_{IGo}$  and  $V_o$  are of opposite polarities, despite effect (2) above.

Thus, when  $V_o$  is positive, follow current will be more likely if the impulse is positive, than if it is negative, provided effects (1) and (2) predominate over (3) (and viceversa). The relative importance of these effects is determined by the specific circuit and gap used; this is the reason for the apparently contradictory results which were obtained by previous investigators, and which have been discussed in section 1.1.

The inhibiting effect of the current zero on the establishment of follow current (effect 1 above), was confirmed experimentally by the author in tests carried out in the Standard Condition (section 5.12), and again, with  $Z = 126$  Ohms.  $V_{IGo}$  was negative,  $V_o$  was positive and  $I_o$  was negligible in both cases,  $I_{IGo}$  was sufficiently

large (79 Amps) compared to the maximum value of  $I_{ta}$  ( $\approx 0.2$  Amps) for  $t_a$  to be very nearly equal to  $t_1$ , and  $V_o$  was sufficiently high for  $V_{gt}$  to be negligible compared to  $V_t$ . In neither test did follow current occur when  $V_o \approx 900$  Volts (i.e. the critical  $V_o$  exceeded that value). The only significant difference between these tests, and tests carried out under the same conditions but with positive  $V_{IGo}$  (e.g. tests 6 and 7, fig. 16) was that the negative impulse induced a current zero; it will be seen from fig. 16, that in the absence of that current zero, the critical  $V_o$  lay between 210 and 250 Volts in the Standard Condition (test 6), and between 380 and 420 Volts when  $Z = 126$  Ohms (test 7).

The conditions required for the establishment of follow current when  $V_o$  and  $V_{IGo}$  are of opposite polarities, can therefore be summarised as follows:

- (I) The recovery voltage due to the L.V. circuit must be capable of restriking the test gap at the end of the impulse, and
- (II) The L.V. circuit must be capable of maintaining a discharge in the test gap after the impulse has ceased.

The above conditions must be satisfied in the sequence in which they have been stated. Once the first is fulfilled, the establishment of follow current depends on the second. Now the second condition is the (only) condition which must be fulfilled when  $V_o$  and  $V_{IGo}$  are of the same polarity. Consequently, both types of L.F. Follow Current mechanism (H.V. and H.C. Follow Current) identified when  $V_o$  and  $V_{IGo}$  were of the same polarity may

operate when  $V_o$  and  $V_{IGo}$  are of opposite polarities. In the latter case, however, it is possible that the critical value of  $V_o$  be determined primarily by the first condition, so that its value may be in excess of that at which the second condition may just be satisfied.

The second condition is specific to the follow current problem, and must be satisfied whatever the polarities of  $V_{IGo}$  and  $V_o$ : there was no significant information on this subject when the present investigation was started. Condition (I) has been studied under similar conditions, in investigations of deionisation of arcs<sup>8-12</sup>. It was therefore decided to concentrate the present investigation on the study of Condition (II), i.e. of the case of  $V_o$  and  $V_{IGo}$  being of the same polarity, and only to show qualitatively the effects of polarity on the results so obtained. This has been done in the present section.

14.4  $V_o$  positive and  $V_{IGo}$  negative - The H.F. Follow Current Case.

The establishment of H.F. Follow Current will be considered for the simplified case of  $V_{gt}$  being constant and equal to  $V_o$  during  $t_1$ , and  $I_o$  and the resistance of the L.V. circuit being negligible. Then, from section 10,

$$I_t = \frac{V_{go} - V_o}{Z} \sin \frac{t}{\sqrt{LC}}$$

Now,  $V_{go}$  is negative in this case, so that,

$$I_t = - \frac{|V_{go}| + |V_o|}{Z} \sin \frac{t}{\sqrt{LC}}$$

Hence,  $I_t$  is negative during the first half cycle, and does

not contribute power to the discharge. During the second half cycle, however,  $I_t$  becomes positive, i.e. it flows through the discharge, and therefore contributes power to it.  $I_t$  increases with  $V_o$ , so that some of that power is drawn from the energy  $\frac{1}{2}V_o^2 C$  stored on C before flashover. Hence, provided the discharge lasts for a sufficient time for the second half cycle of the L.V. circuit to be initiated, H.F. follow current, defined as flow of energy from the L.V. circuit, will be established at any value of  $V_o$ , however small.

By definition, H.F. Follow Current operates when the impulse duration,  $t_1$ , exceeds  $1/(2f)$ . Hence the impulse duration is, in general, sufficient for the second half cycle of the L.V. circuit to be initiated. It must be borne in mind, however, that  $I_t$  and  $I_{IGt}$  flow in opposite directions through the discharge, during the first half cycle of  $I_t$  flow. If  $V_o$  is sufficiently large, a current zero may be induced in the test gap (as in the L.F. case) at a time  $t_a < 1/(2f)$ . The discharge may then cease, without the establishment of follow current. The anomalous position therefore exists, that H.F. Follow Current may be established at low values of  $V_o$ , but not at higher values.

The above conclusion has been arrived at after considering a simplified case. In general, results are more complicated, particularly because  $V_{gt}$  is not constant. It is therefore impossible to generalise about the establishment of H.F. Follow Current when  $V_o$  and  $V_{IGo}$  are of opposite polarities: in all such cases in which the establishment of H.F. Follow Current must be considered, a separate analysis would have to be carried out,

taking into account the specific circuit and test gap used.

14.5  $V_o$  negative and  $V_{IGo}$  positive.

This condition differs from that discussed in the preceding sections (14.3 and 14.4) only because of the asymmetry of the test gap, as explained in section 14.2. This difference does not affect the (qualitative) conclusions arrived at in sections 14.3 and 14.4 so that those conclusions hold without alteration in this case also.

14.6 Criteria of Follow Current for  $V_o$  and  $V_{IGo}$  of opposite polarities.

It follows from section 14.3 that L.F. Follow Current cannot be established if the circuit is not capable of flashing over the test gap at the end of the impulse. This is the criterion of no-follow-current for the L.F. case.

In order to establish a criterion of Follow Current, it is necessary to consider the performance of the circuit after  $t_a$ , when a current zero occurs in the test gap. Until the test gap is re-struck, a path is provided to the L.V. circuit current by the impulse circuit and potential divider only (as against the impulse circuit, potential divider and test gap before  $t_a$ , see fig. 1).  $I_t$  therefore decreases after  $t_a$ , and in so doing increases the recovery voltage of the L.V. circuit at the test gap; that voltage equals  $\left[ V_t - L \frac{dI_t}{dt} \right]$ , stray capacitances being negligible.

If the rate of rise of voltage is sufficiently large, flashover occurs, at time  $t_b$ . The flashover voltage has, associated with it, a current  $I_{tb}$ , and that current is available to be fed into the discharge at flashover (the effective impedance

of the discharge is, in general, much smaller than that of the potential divider and impulse circuit, which can therefore be ignored). After  $t_b$ , conditions are similar to those holding at  $t_1$  when  $V_o$  and  $V_{IGo}$  are of the same polarity to earth, so that the Glow Criterion applies (section 13.5). Hence, the criterion of L.F. Follow Current can be defined as follows for the case of  $V_o$  and  $V_{IGo}$  being of opposite polarity:

L.F. Follow Current will invariably occur if:

- (1) the circuit is capable of restriking the discharge after the current zero which occurs towards the end of the impulse, and
- (2) the voltage  $V_o$  exceeds a value approximately equal to that required to maintain a constant current glow in the test gap
  - (a) at current  $I_{tb}$ , if a glow can be maintained at that current or,
  - (b) at the maximum current at which a glow can be maintained, if that current is less than  $I_{tb}$ .

If the peak value of the impulse current is very large compared to  $I_{ta}$ , then a little consideration will show that  $t_a$  will be nearly equal to  $t_1$ . Furthermore, if the rate of rise of recovery voltage is sufficiently large (after  $t_a$ ), then the time to flashover will be very short, so that  $t_b \approx t_a$ . Under these conditions, therefore,  $I_{t1}$  can replace  $I_{tb}$  in the criterion of follow current. The above discussion has been verified experimentally by the author in an investigation carried out after the experimental work reviewed in this thesis had been completed.

It has been seen in section 14.4 that it is not possible to generalise about the establishment of H.F. Follow Current when  $V_o$

and  $V_{IG0}$  are of opposite polarities, so that criteria cannot be stated for that case. It is worth noting, however, that H.F. Follow Current may occur at very low values of  $V_0$  under certain conditions.

## 15. CONCLUSIONS

A technique for investigating follow current phenomena has been established. Three principal types of follow current (H.V., H.C. and H.F.) have been identified, and the following conclusions can be drawn from the present work.

The initial impulse effects can be divided into voltage and current effects. The impulse voltage affects the establishment of follow current in two ways: firstly, it flashes over the test gap, and secondly, it results in a current  $I_0$  in the L.V. circuit at the instant of flashover.  $I_0$  increases in magnitude with the time-to-flashover of the test gap (section 2.9). Depending on the relative polarities of the impulse and L.V. circuit voltages,  $I_0$  will either oppose or assist the establishment of follow current (section 14.3). In the case of power systems, flashovers are as likely to occur in one condition as in the other, so that little would be gained by designing a means of ensuring a high (or low) value of  $I_0$ .

In the case of routine tests on different items of equipment, however, conditions should be standardised for ease of comparison of results. It is recommended that  $I_0$  be made negligible in those tests: where only one test is carried out on each item,  $V_0$  and  $V_{IG0}$  should be of the same polarity ( $I_0$  being negligible, effects (1) and (2) of section 14.3 are likely to predominate over effect (3), so that follow current will be more likely when  $V_0$  and  $V_{IG0}$  are of the same than of opposite polarity).

To make  $I_0$  negligible, the test gap must be subjected to an

overvoltage by the impulse: the time-to-flashover would then be very short, and  $I_0$  would not have sufficient time to develop. The overvoltage would have no other effect on the establishment of follow current, since the initial ionisation of the test gap depends mainly on the impulse current, not the impulse voltage.

The effect of  $I_0$  on the establishment of follow current is negligible if  $I_0$  is much smaller than  $I_{t_1}$  (see fig. 10 and section 12.6). In the case of H.V. Follow Current,  $I_{t_1}$  was 0.1 to 0.7 Amperes and was therefore much smaller than the maximum value of  $I_t$  (which approximated to  $V/Z$ ). Throughout the present work,  $I_0 \ll V/Z$ ; that is why flashover could always be taken to have occurred at the peak of the L.V. circuit voltage wave (section 2.1): nevertheless,  $I_0$  affected the establishment of follow current in the case of some of the experiments discussed in sections 12.6 and 12.7.

The moment flashover occurs, the impulse voltage waveform ceases to be important, and events are determined by the waveshape of the impulse current. The latter has two principal effects. Firstly, it maintains the discharge for a time  $t_1$  (i.e. for the time that impulse current is flowing) and it therefore provides an opportunity for the L.V. circuit current to build up. Secondly, the state of ionisation of the test gap after the end of the impulse is affected by the ionisation and possible turbulence due to the impulse current.

These effects have been discussed in section 11 in terms of the impulse duration,  $t_1$ , and the peak value of the impulse current,  $I_{IG0}$ . The analysis of section 11.1 showed that the duration is more important than the magnitude of the impulse current in

determining the conditions required for the establishment of H.V. Follow Current; that analysis was confirmed experimentally over the range of variables used. The effect of changes in impulse parameters was seen to be relatively small in the case of H.C. follow current; nevertheless, the critical  $V_0$  continued to decrease when the impulse current magnitude was decreased, and the duration was increased simultaneously, by increasing  $R_F$  (figs. 23 - 28). This indicates that the relative importance of the two parameters, was the same as in the H.V. case.

These conclusions also find application to follow current investigations on electrical equipment (e.g. impulse tests on energised transformers), if it is desired that follow current should be established after every impulse breakdown. The results of section 11.4 are particularly relevant, and they show that  $R_F$  should be large in order to increase the likelihood of follow current occurring (since the critical  $V_0$  decreases as  $R_F$  increases). The maximum permissible value of  $R_F$  is likely to be limited by two sets of conditions: the first, is the required steepness of the voltage wavefront, and the stray capacitance between the low voltage terminal of  $R_F$  and earth. The second, is the maximum voltage required at the test object, the impedance between the low voltage terminal of  $R_F$  and earth, and the impulse generator voltage output.

A third factor, which may limit the value of  $R_F$  under certain conditions, is that if  $R_F$  is too large, the impulse current will be so small that the impulse discharge will be a glow, instead of an arc. The value of  $V_{gt}$  will then be greater during the impulse

period than if  $R_F$  were smaller, and the impulse duration itself may be smaller (because the smaller impulse current due to the higher  $R_F$ , is more readily interrupted by IGOG). If  $R_F$  is increased, therefore, a value is likely to be reached beyond which further increase in  $R_F$  will not increase the probability of follow current being established and may, in fact, have the opposite effect.

Electrode effects are discussed in section 12. It will be seen that in the case of brass and steel, the critical  $V_0$  was substantially independent of electrode shape, provided the electrodes were heavily oxidised. In the case of copper and tungsten, the critical  $V_0$  was smaller, and its range was narrower, when the arcing surface of the electrodes was of the same order as the arc roots (rods) than when it was much larger (spheres and discs). In the case of aluminium, progressive deformation of the electrode tips caused a continuous increase in the critical  $V_0$  when the arcing surface of the electrodes was initially of the same order as the arc root (rods), and the upper limit of the range of critical  $V_0$  was therefore not reached in those tests.

The effect of flashovers, and subsequent oxidation, on large electrodes, was to lower the critical  $V_0$  in the case of tungsten, steel and copper; in the case of copper, oxidation lost most of its effect on  $V_0$  if conditions were close to the Glow Criterion. Oxidation had no effect on the critical  $V_0$  in the case of brass and aluminium electrodes, provided, in the latter case, that the test gap was subjected to an overvoltage sufficient to ensure a very short time-to-flashover. In the case of aluminium electrodes,

heavy oxidation may introduce long times-to-flashover; consequently the oxide layer may prevent a flashover if the impulse voltage has a short duration tail. If the impulse voltage has a long wavetail, the oxide layer results in high values of  $I_0$ .

The Spacing Diagrams obtained in section 12 are compared in fig. 59. It will be seen that there is little difference between the critical  $V_0$  obtained with aluminium, brass and steel at spacings of some 0.2 cm. or less; the corresponding  $V_0$  is much higher in the case of copper. As the spacing is increased, the aluminium curve approaches the copper curve. In general, the percentage differences between the curves decrease as the spacing increases indicating that electrode effects become relatively less important than effects associated with the air space between the electrodes, as the air space is increased.

Other tests on electrode effects have shown that the critical  $V_0$  range obtained with platinum electrodes is not substantially different from that obtained with other electrodes in similar conditions, and tests on tungsten electrodes (section 12.2) have confirmed that cathode phenomena are more important than anode phenomena for the establishment of follow current.

The criteria which determine the establishment of all three types of follow current are compared in fig. 58, for the case of  $V_0$  and  $V_{IG_0}$  having the same polarity to earth, and  $I_0$  being negligible. It will be seen that under these conditions H.F. Follow Current is invariably established even when H.V. and H.C. Follow Current cannot occur. Hence, when the latter types of follow current are possible, H.F. Follow Current will certainly

occur: in other words, the discharge of stray capacitances will increase the probability of Power Follow under these conditions. This statement does not take into account that the interaction of impulse, H.F. and power frequency follow currents may result in current zeros and, furthermore, the additional currents supplied by the discharge of line capacitances, may result in turbulence and thus accelerate the deionisation of the test gap. These effects will vary from system to system and are best studied by means of site tests: a laboratory investigation (section 16.3) could, however, provide some data, as well as extending the present experimental technique to the case of multi-frequency L.V. circuits. The conclusion to be drawn from the diagram of criteria, therefore, is that H.F. Follow Current may in many cases increase the probability of power follow.

The suitability of synthetic power circuits for follow current investigations has been confirmed by the results reviewed in this thesis. Possible extensions of synthetic circuit techniques are suggested in sections 16.2 and 16.3.

## 16. FURTHER WORK

### 16.1 Voltage characteristics of impulse-initiated constant-current discharges.

If the L.V. circuit of fig. 1 is replaced by a constant current source, a constant current will circulate in the test gap after the end of the impulse. For a given test gap, the voltage ( $V_{gt}$ ) will then be determined primarily by

- (1) the magnitude of that current, and
- (2) the impulse current waveshape,

both of which could easily be controlled.

The effect of the initial impulse discharge on the voltage required to maintain a constant current glow could be observed, and results so obtained would find application to the Glow Criterion (section 13.2).

In view of the results of section 7.1 (critical  $I_{t1}$ ) the constant current values should cover the range 0.1 - 1 Amp at gap spacings of the order used in the present investigation. The discharge would probably be an arc at the higher values of current.

### 16.2 Synthetic Circuit Techniques: 'Point-on-Wave' Tests.

If the discharge voltage is ignored, the L.V. circuit voltage is given by

$$V_t = \sqrt{V_o^2 + I_o^2 Z^2} \cos \left( \omega t + \tan^{-1} \frac{I_o Z}{V_o} \right)$$

with the usual conventions regarding symbols and polarities.

In the present investigation,  $V_o \gg I_o Z$ , so that the above expression approximated closely to

$$V_t = V_o \cos \omega t$$

and flashover always occurred at the crest of the voltage wave. Now, if a current,  $I_0$ , were circulated in L before flashover, the maximum value of  $V_t$  ( $= (V_0^2 + I_0^2 Z^2)^{1/2}$ ) could be maintained constant, but the instant of flashover could be varied with respect to the  $V_t$  waveshape (i.e. the 'point-on-wave' could be varied) by altering  $V_0$  and  $I_0$  simultaneously.

A current could be circulated in L by using the arrangement of fig. 60. B is a battery, and L' is a large inductance, which isolates B from the test circuit while the test gap conducts.  $I_0$  can be altered by varying either the resistor  $R_B$ , or the output voltage of the battery.

### 16.3 Synthetic Circuit Techniques: Studies involving H.F. and L.F. Follow Current.

It has been seen in section 15 that the effect of H.F. Follow Current on the establishment of L.F. (power-frequency) Follow Current is best studied by means of experiments in which both types of follow current may occur simultaneously. The use of synthetic circuits in this connection should be investigated, and fig. 61 illustrates a possible arrangement: L and C are tuned to 50 c/s, and  $L_1$  and  $C_1$  are tuned to a high frequency to produce H.F. Follow Current.

### 16.4 Extension of Follow Current Tests.

Follow Current tests should be carried out to obtain quantitative data on the establishment of follow current over a wide range of voltages, currents, and gap spacings, of the order of the magnitudes met with on power systems. Investigation of gap effects should include experiments on air gaps at different

pressures, experiments in oil, and experiments involving surface flashover. Point-on-wave tests should be carried out, using either synthetic (section 16.2) or a.c. power circuits.

Some of the work outlined in this subsection has already been completed, and will be the subject of a separate publication.

17. ACKNOWLEDGEMENTS

The author wishes to acknowledge his indebtedness to Professor F.M. Bruce for his interest and encouragement in this work, and for his advice in the preparation of the thesis; to Mr. A.S. Husbands, and to members of the Electrical Engineering Department, for many helpful discussions, and to the staff of the Electrical Engineering Workshop, who built the equipment used in this investigation.

18. BIBLIOGRAPHY

1. The British Electrical and Allied Industries Research Association: 'Surge Phenomena - Seven Years' Research for the Central Electricity Board (1933/40)' (Book), p.326.
2. Ibid., p.352-4.
3. H.F. Jones and C.J.O. Garrard: 'The Design, Specification and Performance of High-Voltage Surge Diverters', Proc. I.E.E., Vol. 97 (1950), part II, p.368.
4. O. Ackermann: 'The Power Interruption Testing of Lightning Arrestors', Trans. A.I.E.E., Vol. 70, (1951), part I, p.1.
5. P.G. Provoost: 'Impulse Testing of Transformers', C.I.C.R.E., 14th Convention, 1952, Vol. II, Paper No. 123.
6. W. Baumann: 'Wechselstrom-Lichtbogen in Niederspannungs-Installationen als Folge von Stossentladungen', Bulletin de l'Association Suisse des Electriciens, 1954, p.465.
7. H. Edels: 'A Technique for Arc Initiation', Brit. J. App. Phys., Vol. 2, (1951), p.171.
8. G.D. McCann and J.J. Clark: 'Dielectric Recovery Characteristics of Large Air Gaps', Trans. A.I.E.E., Vol. 62, (1943), p.45.
9. G.D. McCann, J.E. Connor and H.M. Ellis: 'Dielectric Recovery of Power Arcs in Large Air Gaps', Trans. A.I.E.E., Vol. 69, (1950), Part I, p.616.
10. P. Wildi: 'Uber den Verlauf der Verfestigung von Lichtbogenstrecken', (Thesis), Eidgenossische Technische Hochschule, Zurich (1951).
11. L.L. Alston: 'The Deionisation of Long Air Gaps', J.I.E.E., February 1954, p.61.
12. W.O. Kolham: 'The Recovery of Electric Strength of an Arc-Discharge Column Following Rapid Interruption of the Current', Proc. I.E.E., Vol. 101, (1954), Part II, p.321.
13. W.A. Gambling and H. Edels: 'The High Pressure Glow Discharge in Air', Brit. J. App. Phys., Vol. 5, (1954), p.36.
14. J.M. Meek and J.D. Crages: 'Electrical Breakdown of Gases', (Book) Clarendon Press, 1953, pp. 463, 468 and 469.

Bibliography (Cont'd).

15. F. Ashworth, W. Needham and R.W. Sillars: 'Silicon Carbide Non-Ohmic Resistors', J.I.E.E., Vol. 93, Part I, p.385 and p.596.
16. J.D. Higham and J.H. Meek: 'Voltage Gradients in Long Gaseous Spark Channels', Proc. Phys. Soc., Vol. 63, B, p.632.
17. L.L. Alston: 'A Potential Divider Containing a Non-Linear Unit', Proc.I.E.E., Part A, to be published.

## APPENDIX I

### A Potential Divider with a Non-Ohmic Resistor. 17

#### 1. Introduction:

A potential divider containing a non-linear unit has been developed for applications such as the measurement of a relatively low arc or glow voltage, whilst providing protection of the measuring apparatus against high overvoltages used to initiate the discharge by sparkover between electrodes.

Two possible methods for achieving this characteristic were considered and rejected. Firstly, an amplifier could be connected between the low voltage arm of a conventional divider and the measuring equipment, the output voltage of the amplifier being limited to a safe value determined by the HT voltage. In addition to screening problems, the initial saturation of the amplifier introduces serious distortion in the output waveform. Secondly, a gas diode could be connected across the low voltage arm of the divider, which would then be shorted out at all voltages in excess of the striking voltage of the diode. This is a technique familiar to H.V. engineers, but requires a knowledge of the volt-time characteristic for ionisation or deionisation of the diode for given waveforms.

The method adopted is shown in fig. 7.  $R_H$  and  $R_L$  constitute a conventional resistance divider, having stray capacitances  $C_H$  and  $C_L$ .  $R_M$  is a silicon carbide non-ohmic resistor<sup>15</sup>; its resistance has the instantaneous value  $R_{Mt}$ , and decreases instantly when the

voltage across it rises. During the preparation of this paper, the author found that a similar divider had been used by Higham and Meek<sup>16</sup>, but a critical analysis of its performance was not given.

2. Theoretical Considerations:

Ignoring, for the moment, the stray capacitances, the relation between  $V_{gt}$  and  $V_{Lt}$  for the divider of fig. 7 is given by

$$V_{Lt} = \frac{V_{gt}}{\left(1 + \frac{R_H}{R_L} + \frac{R_H}{R_{Mt}}\right)} \dots\dots\dots (I)$$

When  $V_{gt}$  is large,  $R_{Mt}$  must be much smaller than  $R_H$  in order to limit  $V_{Lt}$  to a safe value. When  $V_{gt}$  has a relatively low value,  $R_{Mt}$  should be much greater than  $R_H$  in order that  $V_{Lt}$  be substantially independent of  $R_M$  over the measuring range. These conflicting requirements can be satisfied because of the non-linear characteristic of  $R_M$ , and the corresponding ratios of  $R_H/R_{Mt}$ . It will be noted that for a given  $R_M$ , a high value of  $R_H$  improves protection, but a low value of  $R_H$  decreases the effect of  $R_M$  in the measuring range. This is illustrated in fig. 62, which shows characteristics of dividers having different  $R_H$  and  $R_L$  values.

Ignoring  $R_M$ , the divider ratio is  $n_{\infty} = \frac{R_H + R_L}{R_L}$ . The effect of  $R_M$  is to introduce a percentage error

$$v_t' = \frac{100}{1 + R_{Mt} \left(\frac{1}{R_{Mt}} + \frac{1}{R_L}\right)} \% \dots\dots\dots (II)$$

in the measurement of  $V_{gt}$ . Even if allowance has to be made for this,  $R_M$  need not be known to a high degree of accuracy, since

$R_{Mt} \gg R_H$  in the measuring range. In the most adverse case, when  $R_L = \infty$ , a percentage error  $\alpha$  in  $R_{Mt}$  will result in a percentage error of less than  $\frac{\alpha R_H}{R_{Mt} (1 + \frac{\alpha}{100})}$  in the calculated value of  $V_{gt}$ .

2.1 Effect of Stray Capacitance:

$V_{Lt}$  is limited to a safe but nevertheless much greater value before flashover than after. Consequently, a relatively large charge,  $q_{Lo}$ , is stored on the stray capacitance  $C_L$  (fig. 7) before flashover: the corresponding charge on  $C_H$  is  $q_{Ho}$ . The construction of high voltage resistance dividers is such that  $C_L$  is much larger than  $C_H$ , so that  $q_{Lo}$  is usually larger than  $q_{Ho}$ . This condition ( $q_{Lo} > q_{Ho}$ ) will be considered in the present case, but a similar treatment would apply if  $q_{Lo} < q_{Ho}$ .

Flashover connects  $C_H$  and the arc in parallel with  $C_L$ , and the charges  $q_{Lo}$  and  $q_{Ho}$  then contribute a component  $V_{Lt}'$  to  $V_{Lt}$ .  $V_{Lt}'$  has the maximum value  $V_{Lo}' = \frac{|q_{Lo}| - |q_{Ho}|}{C_L + C_H}$  and decays as the

residual charge,  $q_o = (|q_{Lo}| - |q_{Ho}|)$ , discharges through  $R_H$ ,  $R_L$  and  $R_M$ . The residual charge,  $q_o$ , being positive, the reduction in  $V_L$  which should occur at flashover, is delayed by  $V_{Lt}'$ . Now,  $R_M$  is much greater than  $R_H$  when  $V_{Lt}'$  is still quite large, so that further discharge of  $q_o$  is possible, in effect, only through  $R_H$  and  $R_L$ .

Recording will therefore be inaccurate for a time of the order of the time constant  $T' = (C_L + C_H) R_H R_L / (R_H + R_L)$  ( $\approx R_H R_L C / (R_H + R_L)$ , since  $C_L \gg C_H$ ). After  $V_{Lt}'$  becomes negligible, the error due to stray capacitances falls to that due to their effect on the linear divider  $R_H R_L$  - the conventional case.

One method of eliminating  $V_{Lt}'$ , is suggested by the expression

for  $V_{Lo}'$ .  $C_H$  could be increased deliberately, so that  $C_{Ho} = C_{Lo}$  and  $V_{Lo}' = 0$ . The appropriate value of  $C_H$  is  $C_H' = C_L / (n_o - 1)$ , where  $n_o$  is the divider ratio at flashover.

The value of  $C_H$  required to eliminate the error due to the effect of stray capacitances on the linear divider  $R_H R_L$ , is  $C_H'' = C_H / (n_{\infty} - 1)$ , as in conventional mixed dividers. Now,  $n_{\infty} < n_o$ , so that  $C_H''$  is larger than  $C_H'$ . Consequently, if  $C_H = C_H'$ , recording would be more accurate than in the case of the linear divider  $R_H R_L$ .

If  $C_H = C_H''$ , recording would inaccurate immediately after flashover, though very accurate recording would be obtained eventually. The protective action of the divider would be complicated by the relatively high value of  $C_H$ .

5. Design Procedure:

The following procedure is advocated for a first design.

$R_H$  is selected first; it should be small, in order to keep  $V_t'$  small in the measuring range, and to provide a low resistance discharge path to the stray capacitances.  $R_H$  is therefore given the minimum value,  $R_{Hm}$ , which does not interfere unduly with the performance of the test circuit.

$R_M$  is next selected such that  $V_{Lt}$  shall not exceed a safe value at the maximum value of  $V_{gt}$ ,  $v_t'$  shall be small at the maximum  $V_{Lt}$  corresponding to the measuring range, in the most adverse case of  $R_L = \infty$ , and the stray capacitance of  $R_M$  (which increases  $C_L$ ) shall have the minimum value consistent with the rating of  $R_M$ .

Finally,  $R_L$  is selected to give a suitable deflection on the oscillograph in the measuring range. If several divider ratios

are required, it may be of advantage to vary  $R_H$  and  $R_L$ , while maintaining  $(R_H + R_L) = 2R_{Hm}$ , and  $R_H \geq R_{Hm}$ . In that case,  $v_t'$  and  $T'$  will not exceed half the value they would have if  $R_H = R_{Hm}$  and  $R_L = \infty$ .

#### 4. Divider Data:

The divider was designed to record an event having a peak voltage of 33 kV. at flashover, and lasting for 150  $\mu$ S to 10 mS.  $V_{Lt}$  had to be limited to 3 kV. in the protective range; in the measuring range,  $V_{Lt} < 500$  Volts and  $v_t' < 0.1\%$ .

In this particular case the divider parameters were:

$R_H = 10 \text{ k}\Omega$  and  $R_L = \infty$ , or  $R_H \geq 10 \text{ k}\Omega$  and  $(R_H + R_L) = 23 \text{ k}\Omega$ ;  
 $R_{Mt} = 940 \Omega$  at 3 kV. and  $R_{Mt} = 1 \text{ M}\Omega$  at 500 Volts. The time constant  $T'$  did not exceed 1  $\mu$ S (i.e.  $\ll 150 \mu$ S), so that no lumped  $C_H$  was used.

$R_H$  and  $R_L$  were constructed from identical woven wire resistance ribbon, and the estimated accuracy of the divider was within  $\pm 1\%$  after  $V_{Lt}'$  had become negligible (i.e. some 5  $\mu$ S after flashover).

#### 5. Proving Tests:

##### 5.1 Effect of $R_H$ on protection of oscillograph.

A 35 kV. long duration pulse was applied to the divider, and the maximum value of  $V_{Lt}$  corresponding to different  $R_H$  was obtained by recording the voltage appearing across a fraction of  $R_L$ . Results are given in fig.63. The resistance characteristic of  $R_M$  was calculated from this data, and also from d.c. measurements at low voltages. It was found that over the range  $0.5 < V_{Lt} < 7.2 \text{ kV.}$  (i.e. over a considerably greater voltage range than that of fig.63),

TABLE 6.

R H k $\Omega$	Time Constant T' $\mu$ S
1	0.18
10	0.83

TABLE 7.

Time Constants,  $\mu$ S.

T' = $\frac{R C}{H L}$	T' (values obtained from oscillograms)
40	42
50	50
79	79

$R_{Mt} \approx 7.6 V_{Lt}^{-3.32} \times 10^{14} \Omega$ . This expression was then used to calculate the relation between  $R_H$  and the maximum value of  $V_{Lt}$ . The values of  $V_{Lt}$  obtained in this way were within  $\pm 10\%$  of those given by direct experiment, as shown in fig. 63. This justifies the use of an equation of the type  $R_{Mt} = kV_{Lt}^{-m}$  to predict the operation of the divider for design purposes, as was done in connection with fig. 62.

### 5.2 Effect of $R_H$ and $C_L$ after flashover.

The circuit of fig. 7 was used to verify experimentally the analysis of section 2.1 of this Appendix.  $C_H$  consisted only of stray capacitance and was so small that its effect and that of  $q_{Ho}$  were negligible. Also,  $R_H \ll R_L$ , so that  $T' \approx R_H C_L$ .

The gap was flashed over by a 33 kV. voltage impulse, and oscillograms obtained with different  $R_H$  are given in fig. 64 ((a) - (c)). They confirm that  $V_{Lt}$  falls more rapidly when  $T'$  is small (i.e. when  $R_H$  is small). An approximate quantitative analysis was attempted assuming  $V_t$  to fall suddenly at flashover, and to remain at the constant value  $n_{\infty} V_x$  until  $V_{Lt}'$  had become negligible.  $V_{Lt}$  therefore tends to the constant value  $V_x$ , obtained from fig. 64(b). The time constant  $T'$  was then taken as the time required for  $V_{Lt}$  to fall from any value  $(V_x' + V_x)$  to  $(0.368 V_x' + V_x)$ . Results obtained from the two curves of fig. 64(a) are given in Table 6: they show that  $T'$  decreases less rapidly than  $R_H$  - due, in all probability, to stray self inductance becoming effective in controlling the discharge of  $C_L$  at the lower value of  $R_H$ .

More consistent results were obtained in a similar test in which  $R_H$  was constant, and  $C_L$  was increased by lumped capacitance.

Curves from typical oscillograms are given in fig. 64(d), and  $T'$  was measured as above. The stray capacitance component of  $C_L$  was then measured by Q-meter ( $C_L = 40 \mu\text{F}$ ) and time constants were estimated to within some 20% from  $T' = R_H C_L$ , the percentage error being nearly the same for all  $T'$ . Experimental and estimated results are compared in Table 7 and will be seen to be in close agreement. This justifies the discussion relating to the effect of  $V_{Lt}'$  (section 2.1 of this Appendix).

### 5.3 Effect of $C_H$ on the performance of a divider.

The circuit of fig. 7 was used to verify qualitatively the effect of increasing  $C_H$  on the performance of the divider after flashover. Lumped  $C_H$  consisted of two 5" x 5" aluminium plates: its value was varied by altering the distance between them and by introducing a sheet of bakelite dielectric. Fig. 64(e) shows tracings obtained from oscillograms. Curves 1 + 3 show that the values of  $V_{Lt}$  immediately after flashover, decrease when  $C_H$  increases: this is because  $V_{Lo}'$  decreases (section 2.1 of this Appendix). When  $C_H$  is given values greater than that at which  $V_{Lo}' = 0$ , further increase in  $C_H$  results in  $V_{Lo}$  increasing in magnitude, its polarity being reversed; this is illustrated by curve 4.

The above confirms qualitatively the discussion relating to the effect of  $C_H$  (section 2.1 of this Appendix).

### 5.4 Comparison of non-ohmic resistor with gas diode.

A test was carried out with the circuit of fig. 7, but with the non-ohmic resistor replaced by a gas diode. Oscillograms

showed that during the first 2 or 3  $\mu\text{s}$  after flashover there was some variation in the voltage curves recorded on successive shots, the experimental conditions being the same. This inconsistency was ascribed to variations in the state of ionisation of the gas diode (section 1 of this Appendix). However, when the oscillograph sweeps were sufficiently slow to record the whole of the event for which the divider was designed, no difference could be detected between records obtained under the same conditions, when the gas diode or the non-ohmic resistor was used. This was taken as additional confirmation of the performance of both types of non-linear divider.

## 6. Conclusions:

The analysis of a divider incorporating a non-linear resistor has been given, and has been verified experimentally.

Further work should aim at overcoming the main limitation of this type of divider, i.e. the voltage introduced immediately after flashover by the residual charges on the stray capacitances. The use of lumped capacitance  $C_H$  has been discussed (section 2.1 of this Appendix), where it was seen that if  $C_H$  had the appropriate value, the divider could be more accurate than a conventional resistance divider; alternately, a discharge path might be provided to the net residual charge,  $q_0$ , by connecting a rectifier valve, having an interelectrode capacitance smaller than  $C_H'$ , in parallel with  $R_H$ .

(While this thesis was being typed the author was informed that a paper based on this Appendix had been accepted for publication in Part A of the Proceedings of the Institution of Electrical Engineers<sup>17</sup>).

## APPENDIX II

### Calibration of the Amplifier used for Current Measurement (section 4.2).

It was desirable to calibrate the amplifier using an input signal similar to that it would have to amplify in follow current tests. To achieve this requirement, the follow current test circuit (fig. 1) was used, except that a large resistor,  $R'$ , was inserted between  $R_s$  and C, the potential divider being removed. Had R not have had to be limited to a low value (section 2.2),  $R'$  could have been used as a shunt in follow current tests, and the amplifier could have been dispensed with.

When calibrating the amplifier, the voltage across  $(R' + R_s)$  was applied directly to the  $Y_1$  plate of a double beam oscillograph, and the voltage across  $R_s$  was applied via the amplifier to the  $Y_2$  plate of the oscillograph. Fig. 65 shows a sketch of an oscillogram so obtained; it is found that a deflection  $s_1$  on beam 1 corresponds to a deflection  $Y_2$  on beam 2.

The amplifier was then disconnected from beam 2 and  $Y_1$  and  $Y_2$  were connected together, and the test was repeated in order to obtain the relative sensitivities of the two beams. The oscillograms obtained were similar to that shown in fig. 65, and it was found that a deflection  $h_1$  on beam 1 corresponded to a deflection  $h_2$  on beam 2. Hence, the gain of the amplifier was

$$G = \frac{(R' + R_s)s_2h_1}{R_s h_{s12}}$$

The same double beam oscillograph was used in follow current tests, the output of the potential divider being applied to beam 1, and that of the amplifier being applied to beam 2. Then,

if 1 cm. deflection on beam 1 =  $k_1$  volts, it follows that

$$1 \text{ cm. deflection on beam 2} = (k_1 h_1) / h_2 \text{ volts}$$

$$\text{so that 1 cm. deflection on beam 2} = (k_1 h_1) / (h_2 G R_s) \text{ Amps}$$

$$= \frac{k_1 h_1}{h_2 \frac{R' + R_s}{R_s} \frac{s_2}{s_1} \frac{h_1}{h_2} R_s} \text{ Amps}$$

$$= \frac{k_1 s_1}{(R' + R_s) s_2} \text{ Amps}$$

This expression is only valid if  $h_1/h_2$  is constant; numerous tests have shown it to be. It will be noted that the expression is independent of the sensitivity of beam 2. This is an advantage, since the sensitivity of beam 1 is available from numerous oscillograms taken throughout follow current experiments. Beam 1 was generally used to record the test gap voltage in those experiments, and it has been seen (e.g. fig. 10) that the test gap voltage equalled  $V_0$  before flashover. Now, the value of  $V_0$  was read from a voltmeter, and recorded in all tests. Hence  $k_1$  could be obtained from the deflection corresponding to  $V_0$  on the oscillograph, the potential divider ratio, and the value of  $V_0$ . Had the sensitivity of beam 2 been required, special tests would have had to be carried out to determine it, and its variation as the oscillograph heated up and the mains voltage fluctuated.

It will also be noted that the above expression is practically

independent of  $R_s$ , since  $R_s \ll R'$ . This is an advantage, because it is easier to measure accurately the value of the relatively large resistor,  $R'$ , than that of the small shunt  $R_s$ .

### APPENDIX III

#### Reasons for Shortcircuiting $R_{sg}$ (fig. 1) during Follow Current Tests.

The shunt  $R_{sg}$  (fig. 1) was used in exploratory tests only and was shortcircuited in actual follow current tests for the following reasons:

- (1) The voltage across  $R_{sg}$  during the impulse period was of the same order as, and initially considerably greater than, the test gap voltage  $V_{gt}$ . Consequently, when  $R_{sg}$  was not shortcircuited, the voltage across the L.V. circuit was determined not by the test gap alone, but by the test gap and the shunt. Thus, if  $I_t$  was taken to be positive when C discharged through the test gap (fig. 1), then
$$V_t - L \frac{dI_t}{dt} = V_{gt} + (\text{instantaneous voltage across } R_{sg}), \text{ if } R_{sg} \text{ was finite, while } V_t - L \frac{dI_t}{dt} = V_{gt}, \text{ if } R_{sg} = 0.$$
Consequently,  $R_{sg}$  could have significant effects on the follow current mechanism; one of these effects would be similar to that of a large value of  $I_o$ .
- (2) The low voltage end of the test gap is no longer at earth potential, resulting in a slight complication in the measurement of test gap voltage, if  $R_{sg}$  is not shortcircuited.
- (3) The magnitude of the current in  $R_{sg}$  varies considerably.  $R_{sg}$  has to be small, to keep the ohmic resistance of the L.V. circuit to a low value (section 2.2). If no amplifier were used, then a record of the impulse current,  $I_{IGt}$ , would be obtained (fig. 9 (a) - (b)), but the deflection on the

oscillograph would be too small to be measured accurately after  $t_1$ . If an amplifier were used (with the same value of  $R_{sg}$ , fig. 9 (c) - (d)) a record would be obtained of the current flowing in the test gap after  $t_1$ . During  $t_1$ , the relatively large impulse current,  $I_{IGt}$  is flowing in  $R_{sg}$ , so that the amplifier would be driven to cut off. Thus, two separate recordings would be necessary to obtain the test gap current during and after  $t_1$ .

Inspection of fig. 1 will show that the current in  $R_{sg}$  can be obtained, by applying Kirchhoff's Law, if the currents in  $R_s$  and  $R_{SIG}$  are known; this is illustrated by fig. 9. It will be seen that if the voltage on  $R_{SIG}$  is recorded without using the amplifier (fig. 9 (e)), the current  $I_{IGt}$  is obtained. If the amplifier is used (fig. 9 (f)), the current wave record is severely distorted by the saturation of the amplifier, but the impulse duration,  $t_1$ , is obtained very accurately. If the amplifier is used to record the voltage across  $R_s$  (fig. 9 (g) - (h)) the current  $I_t$  is obtained both during and after  $t_1$ . Thus more information than would be available by recording on  $R_{sg}$  can be obtained, without additional difficulty, by recording on  $R_s$  and  $R_{SIG}$ .

#### APPENDIX IV

##### Ammeter-Voltmeter Errors in Measuring $I_{gt}$ and $V_{gt}$ .

It will be seen from fig. 1 that the method used for the measurement of the test gap voltage and current suffers from the inherent errors of ammeter-voltmeter resistance measurements. Corrections can be applied, but the errors could be made negligible by making the connections carefully. Thus, the connections of fig. 1 give accurate recording when the voltage across  $R_s$  is small compared to the voltage across  $R_L$ , i.e. when  $I_{gt}$  is relatively small. When the voltage across  $R_s$  was large, accurate recording could be obtained by connecting the earthy end of the potential divider to the common earth point.

## APPENDIX V

### Effect of $I_0$ and $V_{gt}$ on the Duration of Current Flow in the Case of L.F. Follow Current.

The definition 2 (1) of section 5.3 required the L.V. circuit to maintain the discharge up to its first natural current zero occurring after the end of the impulse, in order that L.F. follow current be established. In order to apply this definition experimentally, it is necessary to decide the time interval which elapses between the instant of flashover and the natural current zero(s) of the L.V. circuit.

Ignoring, for the moment, the effect of the discharge, the times elapsing between the instant of flashover and the natural current zeros of  $I_t$ , are given by

$$t_{no} = \frac{1}{2\pi f} \sin^{-1} \frac{I_0 Z}{V_0} + \frac{k}{2f}, \quad \text{where } k \text{ has any integral value}$$

(the ohmic resistance of the L.V. circuit is negligible).

Under the conditions of this investigation, the term  $\frac{1}{2\pi f} \sin^{-1} \frac{I_0 Z}{V_0}$  never exceeded  $(1/f) \times 10^{-2}$  and was usually very much smaller: the effect of  $I_0$  on  $t_{no}$  can therefore be ignored. By definition,  $t_1 < 1/(2f)$  in the case of Low Frequency Follow Current, so that the first natural current zero occurring after the end of the impulse, occurs  $1/(2f)$  seconds from the instant of flashover. Hence the definition referred to above, requires an L.V. circuit current flow lasting not less than  $1/(2f)$  seconds.

It is now necessary to consider the effect of the discharge on this statement.

The H.V. Follow Current Case.

In the case of H.V. follow current, the critical  $V_0$  is relatively high, so that the mean value of the discharge current, taken over a half cycle, is high also. Hence the mean value of  $V_t$ , taken over a half cycle, is large compared to the corresponding value of  $V_{gt}$ .  $V_{gt}$  has therefore very little effect on the frequency of the discharge: tests did, in fact, show that the duration of a current loop differed very little from  $1/(2f)$  in all cases in which H.V. Follow Current became established.

The only exception to this rule occurred in those tests of sections 12.9 and 12.10 in which a constant current glow was maintained for times of the order of 1 millisecond before H.V. Follow Current became established. Whenever that happened, the duration of the current loop exceeded  $1/(2f)$  by a time approximately equal to that for which constant current glows had been maintained. Now, it follows from point 3 of section 7.1 that under the conditions in which H.V. Follow Current mechanism operated, the duration of current flow was very much smaller than  $1/(2f)$  if follow current did not become established. There was therefore no difficulty in determining whether or not follow current became established, in all cases in which the H.V. mechanism held.

The H.C. Follow Current Case.

It will be seen from figs. 19 - 21 that if follow current is of the H.C. type, and  $I_{t1}$  is positive, the duration  $t_{LV}$  for which current  $I_t$  flows, increases rapidly with  $V_0$ , until  $t_{LV} \approx 0.9/(2f)$ . Subsequent increase in  $V_0$ , results in a smaller increase in  $t_{LV}$ :

$t_{LV}$  may exceed slightly the value  $1/(2f)$ , and further increase in  $V_0$  then results in a decrease in  $t_{LV}$ .

A note of arbitrariness must therefore be introduced in this case in the definition of L.F. follow current, referred to above; it was decided that that definition be taken to require a duration of flow of  $I_t$  of not less than  $0.9/(2f)$  seconds, in order that H.C. Follow Current be established.

To apply this definition, oscillograms have to be taken in follow current tests and the duration of the  $I_t$  loop obtained at different values of  $V_0$  has to be measured from them. A less laborious, but less accurate way of determining the critical  $V_0$  depends on the fact that  $t_{LV}$  increases rapidly with  $V_0$  until it reaches a value of some  $0.9/(2f)$ , and the rate of change of  $t_{LV}$  with  $V_0$  becomes small at higher values of  $V_0$ . The value of  $V_0$  at which further increase in  $V_0$  results in little increase in  $t_{LV}$  can be determined fairly accurately, by viewing the  $I_t$  waveshape on the screen of an oscillograph. This method was used in the tests of section 11.4; an error of not more than 10% was therefore introduced in the critical  $V_0$  recorded in those tests, when follow current was of the H.C. type.

## APPENDIX VI

### 'Zero Lines' for Oscillograms of $I_t$ and $V_{gt}$ .

'Zero Lines', from which the deflections of the beams could be measured, were obtained for all the oscillograms of  $I_t$  and  $V_{gt}$  used for quantitative analyses, and for many of the others. To obtain the 'zero lines', the low voltage arm of the potential divider and the shunt  $R_g$  were shortcircuited simultaneously through the same switch; the circuit (fig. 1) was not otherwise altered. The impulse generator was then tripped in the usual way (section 2.5), so that oscillograph began to sweep. Two traces were obtained, each due to one of the two beams; these traces were straight lines, except as explained below.

Owing to the characteristic of the shortcircuiting switch, a voltage pulse having a peak of the order of 100 millivolts, and a duration of some 50 microseconds appeared at the switch when the impulse generator fired. This pulse had negligible effect in the case of the 'zero line' corresponding to  $V_{gt}$ . In the case of the 'zero line' corresponding to  $I_t$ , however, the pulse was magnified by the amplifier and caused a small but visible deflection (e.g. see 'zero lines' of fig. 36(a)). This deflection was used to distinguish between the 'zero lines', i.e. to determine whether the upper or the lower line was associated with  $I_t$  (or  $V_{gt}$ ) in a given test.

The impulse generator was usually tripped before being fully charged when 'zero lines' were obtained. The flashover-delay was therefore not the same as in the case of flashovers from which  $I_t$

and  $V_{gt}$  waveshapes were recorded, so that the small deflection on the current 'zero line' did not necessarily occur near the beginning of the sweep, and in some cases it was not recorded at all.

In the case of sketches of oscillograms (e.g. fig. 10) it was considered that the use of two 'zero lines' would result in unnecessary complication. Only one 'zero line' was therefore shown, and the waveforms recorded on both beams were referred to it.

## APPENDIX VII

### Prediction of $I_{t1}$ .

The problem of follow current is, in fact, the problem of the growth of current in the L.V. circuit. A simple mathematical analysis is not possible because of the non-linear relation between the test gap voltage and current. However, observations made in this investigation have shown that  $V_{gt}$  is substantially independent of the L.V. circuit during the impulse period, provided  $V_0$  does not exceed the critical range; thus the waveshapes of  $V_{gt}$ , which can be obtained oscillographically for a given impulse and test gap, apply whatever the L.V. circuit used. A mathematical analysis can therefore be used to predict the value of  $I_{t1}$ .

It has been shown in section 13.1 that

$$I_{t1} = I_0 + \frac{1}{L} \int_0^{t1} (V_t - V_{gt}) dt$$

so that 
$$I_{t1} = I_0 + \frac{1}{L} \int_0^{t1} V_t dt - \frac{1}{L} \int_0^{t1} V_{gt} dt$$

Now, from fig. 1, 
$$V_t = V_0 - \frac{1}{C} \int_0^t I_t dt$$

The last two expressions determine  $I_{t1}$ ; a simple solution is possible in many cases by using an approximate expression for  $V_t$ . The specific case of the standard Condition (section 5.12) will now be considered as an illustration,  $V_0$  and  $V_{IG0}$  being of the same polarity to earth. In that case - as, indeed, in the general case of impulse flashovers to an energised system - the impulse

duration,  $t_1$ , was small compared to the half period,  $1/(2f)$ , so that  $V_t \approx V_0$  during the impulse. Oscillograms of  $V_{gt}$ , taken in the Standard Condition, have been traced in fig. 66(b) for the impulse period;  $\int_0^{t_1} V_{gt} dt \approx 0.011$  volt-seconds represents a good approximation, obtained from these oscillograms. Also, in the Standard Condition,  $t_1 \approx 180$  microseconds and  $L = 129$  millihenries, so that the relation between  $I_{t_1}$  (amps) and  $V_0$  (volts) becomes

$$I_{t_1} = \frac{1}{0.129} (180 \times 10^{-6} V_0 - 0.011) = 1.40 \times 10^{-3} V_0 - 0.085$$

This straight line has been drawn in fig. 66(a) where it is seen to be in good agreement with results obtained by direct experiment.

# INDEX

	<u>Page No.</u>
<u>SUMMARY</u>	1
1. <u>INTRODUCTION</u>	2
1.1 Previous Work.	2
1.2 Statement of the Problem.	8
2. <u>THE TEST CIRCUIT</u>	10
2.1 The Low Voltage Circuit.	10
2.2 Values of L.V. Circuit Parameters.	11
2.3 Tests on L.V. Circuit Elements.	12
2.4 L.V. Charging Source: Effect on Circuit during Tests.	13
2.5 The High Voltage Circuit.	14
2.6 Voltage Output of Impulse Generator Circuit.	15
2.7 Current Output of Impulse Generator Circuit.	16
2.8 Conventions regarding the Test Circuit.	17
2.9 The L.V. Circuit Current at Flashover ( $I_0$ ).	18
2.10 Effect of Impulse Circuit on L.V. Circuit after Flashover.	19
2.11 Impulse Duration.	20
3. <u>THE TEST GAP</u>	21
4. <u>MEASUREMENT TECHNIQUES</u>	24
4.1 A Potential Divider with a Non-Ohmic Resistor.	24
4.2 The Amplifier.	25
4.3 Oscillographic Equipment.	26
4.4 The Shunts.	26
5. <u>PRINCIPAL DEFINITIONS</u>	28
5.1 Symbols.	28
5.2 Follow Current.	28
5.3 Low-Frequency Follow Current (L.F. Follow Current).	28
5.4 High-Frequency Follow Current (H.F. Follow Current).	30
5.5 Natural Current Zero.	31
5.6 Half Cycle and Half Period.	32
5.7 Impulse Duration ( $t_1$ ).	32
5.8 Critical Values and Ranges.	32
5.9 The Standard Circuit.	32
5.10 The Standard Electrodes.	33
5.11 The Standard Gap.	33
5.12 The Standard Condition.	33
6. <u>PROCEDURE</u>	34

(Contd.)

<u>Index (Continued).</u>	<u>Page No.</u>
7. <u>CLASSIFICATION OF PHENOMENA</u>	35
7.1 High-Voltage Follow Current (H.V. Follow Current).	35
7.2 High-Current Follow Current (H.C. Follow Current).	37
7.3 High-Frequency Follow Current (H.F. Follow Current).	37
8. <u>ANALYSIS OF H.V. FOLLOW CURRENT</u> <u>CHARACTERISTICS</u>	39
8.1 Qualitative Discussion.	39
8.2 Discharge Characteristics - Effects of Transitions to Glow.	41
8.3 Quantitative Analysis: Procedure.	42
8.4 Quantitative Analysis: Discussion of Results.	44
9. <u>ANALYSIS OF H.C. FOLLOW CURRENT</u> <u>CHARACTERISTICS</u>	49
10. <u>ANALYSIS OF H.F. FOLLOW CURRENT</u> <u>CHARACTERISTICS</u>	52
11. <u>EFFECT OF VARIATION IN IMPULSE CURRENT</u> <u>WAVEFORM ON THE ESTABLISHMENT OF L.F.</u> <u>FOLLOW CURRENT</u>	56
11.1 An Approximate Analysis for the Case of H.V. Follow Current.	56
11.2 Variation in Impulse Duration, $t_1$ .	57
11.3 Variation in Impulse Current Magnitude.	59
11.4 Variation in Impulse Current Waveshape obtained by varying $R_p$ .	60
12. <u>ELECTRODE EFFECTS</u>	61
12.1 Presentation of Results.	61
12.2 Tungsten Electrodes.	63
12.3 Platinum Electrodes.	71
12.4 Brass Electrodes.	72
12.5 Steel Electrodes.	74
12.6 Aluminium Electrodes - Spheres.	76
12.7 Aluminium Electrodes - Discs.	80
12.8 Aluminium Electrodes - Rods.	84
12.9 Copper Electrodes - Spheres.	86
12.10 Copper Electrodes - Discs.	88
12.11 Copper Electrodes - Rods.	91
13. <u>CRITERIA OF FOLLOW CURRENT FOR <math>V_0</math> AND <math>V_{IG0}</math></u> <u>OF SAME POLARITY TO EARTH</u>	92
13.1 L.F. Follow Current - Criteria of No-Follow-Current.	92
13.2 H.V. Follow Current - The Glow Criterion.	97

(Contd.)

Index (Continued)

Page No.

13.3	Experimental Confirmation of Glow Criterion.	99
13.4	Current ranges over which the Glow Criterion is valid.	101
13.5	L.F. Follow Current - The Criterion of Follow Current.	102
13.6	Criteria of H.F. Follow Current.	102
14.	<u>EFFECT OF POLARITY</u>	103
14.1	$V_o$ and $V_{IGo}$ both positive.	103
14.2	$V_o$ and $V_{IGo}$ both negative.	103
14.3	$V_o$ positive and $V_{IGo}$ negative - The L.F. Follow Current Case.	104
14.4	$V_o$ positive and $V_{IGo}$ negative - The H.F. Follow Current Case.	108
14.5	$V_o$ negative and $V_{IGo}$ positive.	110
14.6	Criteria of Follow Current for $V_o$ and $V_{IGo}$ of opposite polarities.	110
15.	<u>CONCLUSIONS</u>	113
16.	<u>FURTHER WORK</u>	119
16.1	Voltage Characteristics of Impulse-Initiated Constant Current Discharges.	119
16.2	Synthetic Circuit Techniques: 'Point-on-Wave' Tests.	119
16.3	Synthetic Circuit Techniques: Studies involving H.F. and L.F. Follow Current.	120
16.4	Extension of Follow Current Tests.	120
17.	<u>ACKNOWLEDGEMENTS</u>	122
18.	<u>BIBLIOGRAPHY</u>	123

APPENDICES

Appendix I	A Potential Divider with a Non-Ohmic Resistor.	125
Appendix II	Calibration of Amplifier used for Current Measurement (section 4.2).	134
Appendix III	Reasons for Shortcircuiting $R_{sg}$ (fig. 1) during Follow Current Tests.	137

(Contd.)

Index (Continued)

Page No.

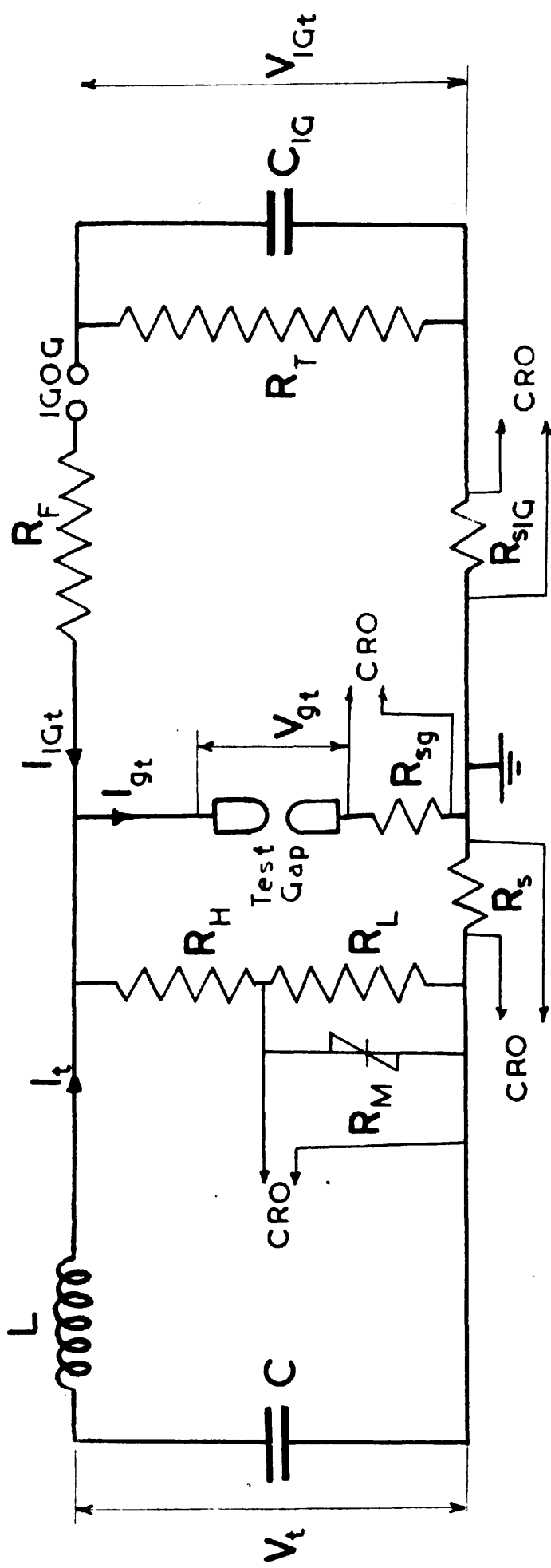
Appendix IV	Ammeter-Voltmeter Errors in Measuring $I_{gt}$ and $V_{gt}$ .	139
Appendix V	Effect of $I_0$ and $V_{gt}$ on the Duration of Current Flow in the Case of L.F. Follow Current.	140
Appendix VI	'Zero Lines' for Oscillograms of $I_t$ and $V_{gt}$ .	143
Appendix VII	Prediction of $I_{t1}$ .	145

Illustrations for Thesis on

"A Study of Impulse Voltage Breakdown with Reference to the  
Initiation of Follow Current".

by

Liviu L. Alston.



$$f = \frac{1}{2\pi\sqrt{LC}} ; Z = \sqrt{\frac{L}{C}} ; t_1 = \text{impulse duration.}$$

**Fig. 1. The Test Circuit.** The principal symbols used are defined on this diagram. In the case of quantities which vary in time, the suffix  $t$  is used to denote instantaneous value; the use of other suffixes is explained in section 5.1.

Except where otherwise stated, the current flowing in the potential divider was negligibly small, and was ignored in the discussions given in the text.

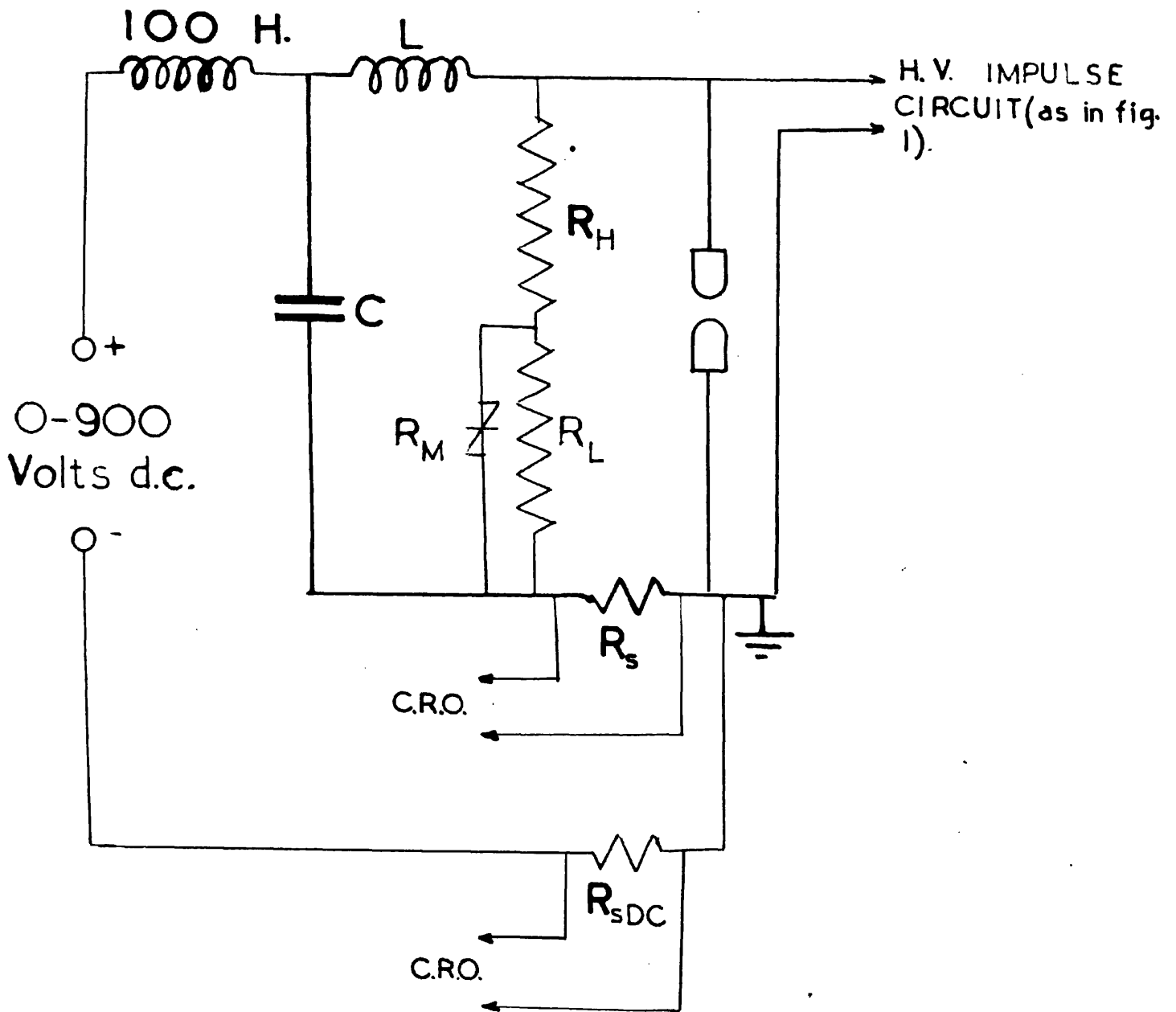


FIG. 2

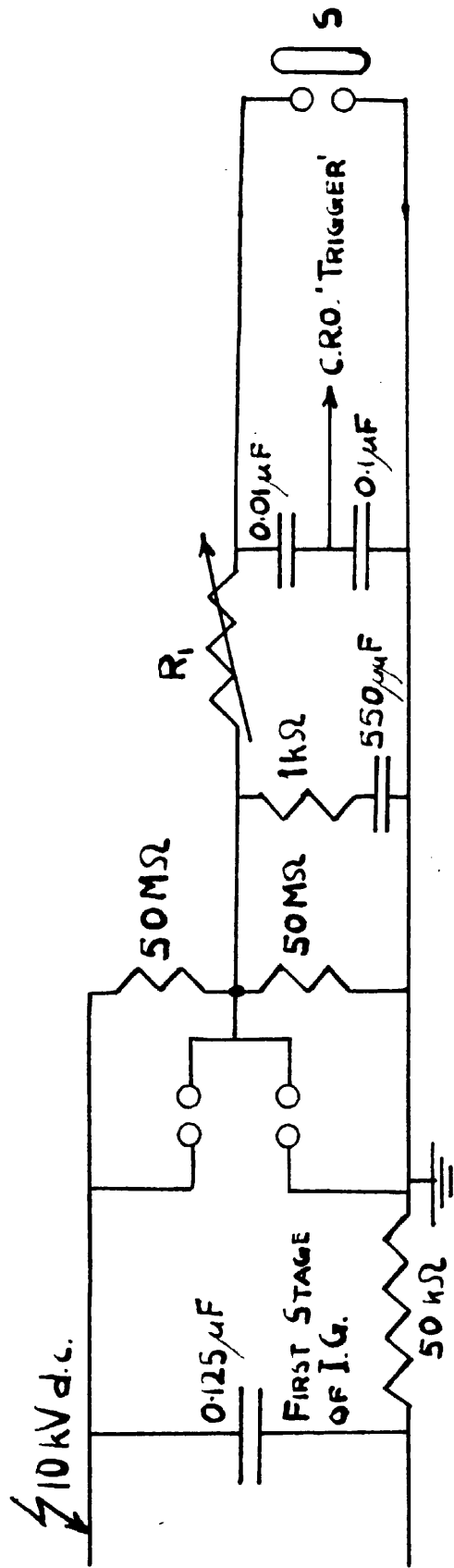


FIG. 3. CIRCUIT USED FOR TRIPPING THE IMPULSE GENERATOR AND THE OSCILLOGRAPH.

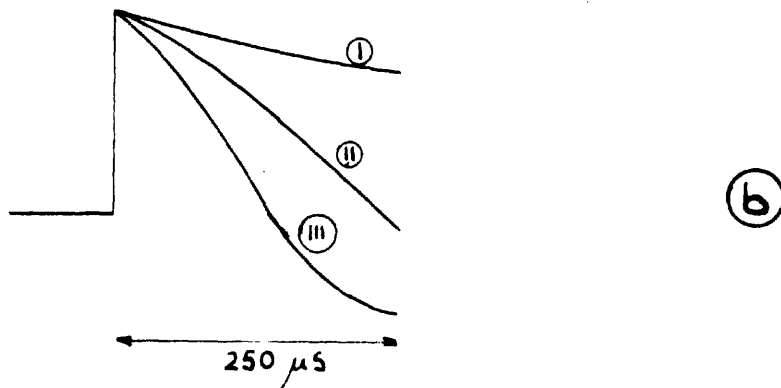
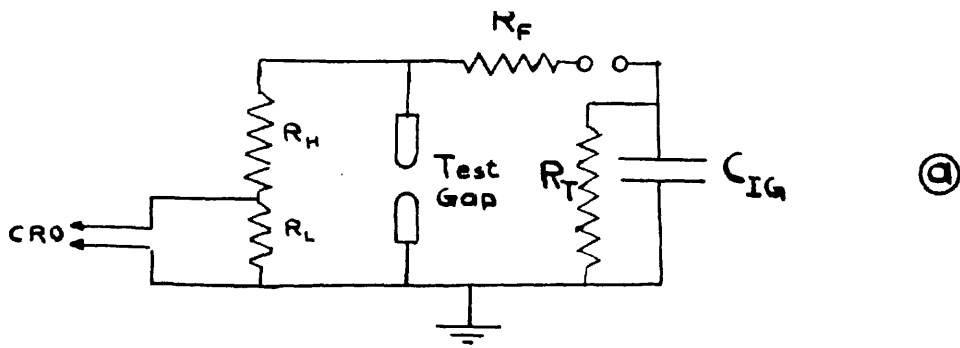
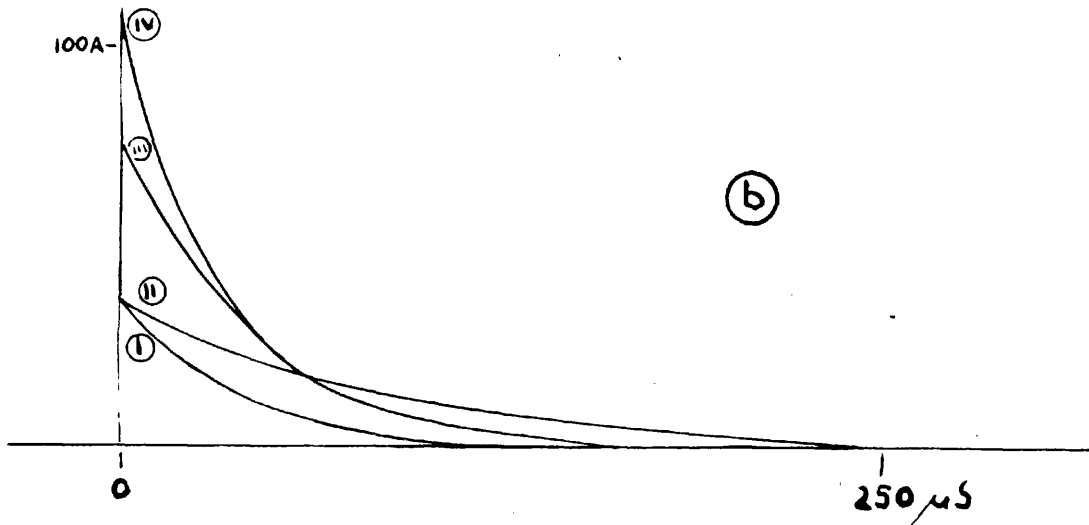
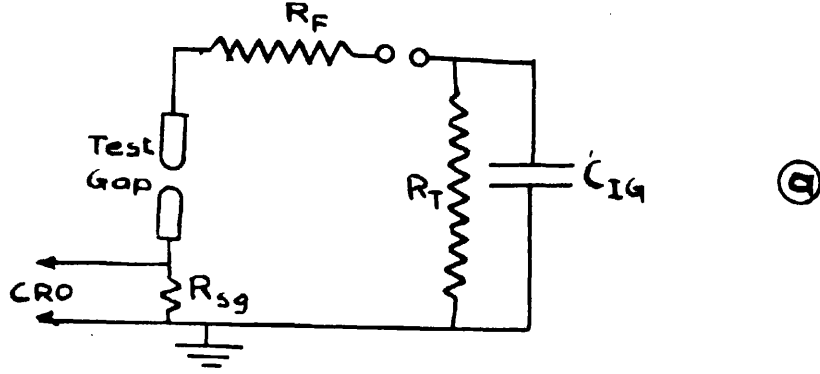


FIG. 4. (a) CIRCUIT USED FOR DETERMINING IMPULSE VOLTAGE WAVEFORM. PARAMETER VALUES WERE:  $C_{IG} = 0.083 \mu\text{F}$ ;  $R_F = 400 \Omega$  (WOVEN WIRE);  $R_H = 9605 \Omega$  (WOVEN WIRE);  $R_L = 52.6 \Omega$  (WOVEN WIRE); THE TEST GAP WAS SET SO AS NOT TO FLASH OVER;  $R_T = 75 \text{ k}\Omega$  (CARBON).

(b) TRACINGS FROM OSCILLOGRAMS OBTAINED

- (i) WITH THE ABOVE CIRCUIT;
- (ii) WITH THE ABOVE CIRCUIT, BUT WITH THE L.V. CIRCUIT CORRESPONDING TO  $f = 50 \text{ Hz}$  AND  $Z = 126 \Omega$  CONNECTED ACROSS THE TEST GAP;
- (iii) AS (ii), EXCEPT THAT  $Z = 40 \Omega$ .



**FIG. 5 (a) CIRCUIT USED FOR MEASURING THE CURRENT OUTPUT OF THE IMPULSE GENERATOR**

**(b) CURRENT WAVESHAPES WITH THE ABOVE CIRCUIT.**

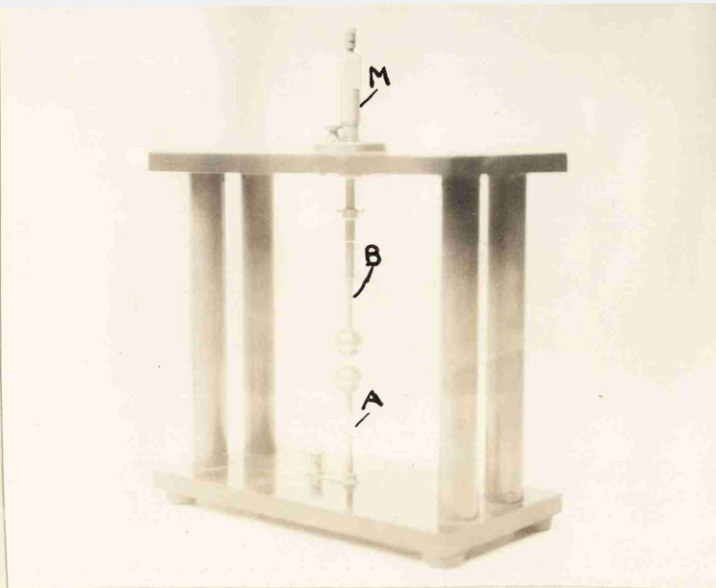
$$C_{IG} = 0.083 \mu F; R_{Sg} = 4.34 \Omega \text{ (WIRE)}$$

The test gap spacing was 0.5 cm; current waveshapes were substantially independent of the test gap, provided it flashed over.  $R_F$  and  $R_T$  are given below: they

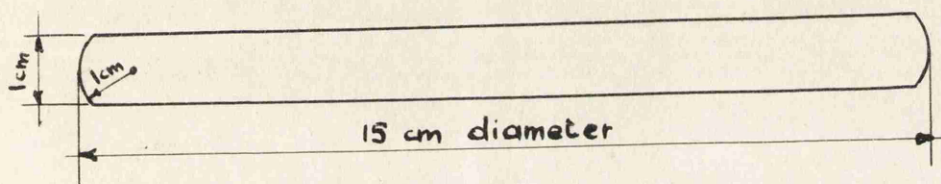
Curve No	$R_F$ $\Omega$	$R_T$ $\Omega$
I	841 (w.w.)	833 (w.w.)
II	841 (w.w.)	$75 \times 10^3$ (c.)
III	419 (w.w.)	$75 \times 10^3$ (c.)
IV	420 (c.)	$75 \times 10^3$ (c.)

are nominal values, measured on a low voltage d.c. bridge. (The currents used in the present investigation were not limited to those given above).

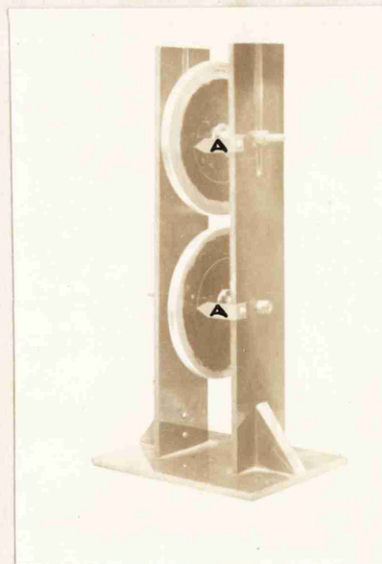
W.W. = WOVEN WIRE; C. = CARBON



(a)  
Electrode  
Assembly -  
Spheres.



(b)  
Disc Electrode.



(c)  
Electrode  
Assembly -  
Discs.

Fig. 6. Test Gap Data.

In the case of rod electrodes, the assembly of fig. 6(a) was used, the adaptors A and B being replaced by a pair suitable for rods (section 3).

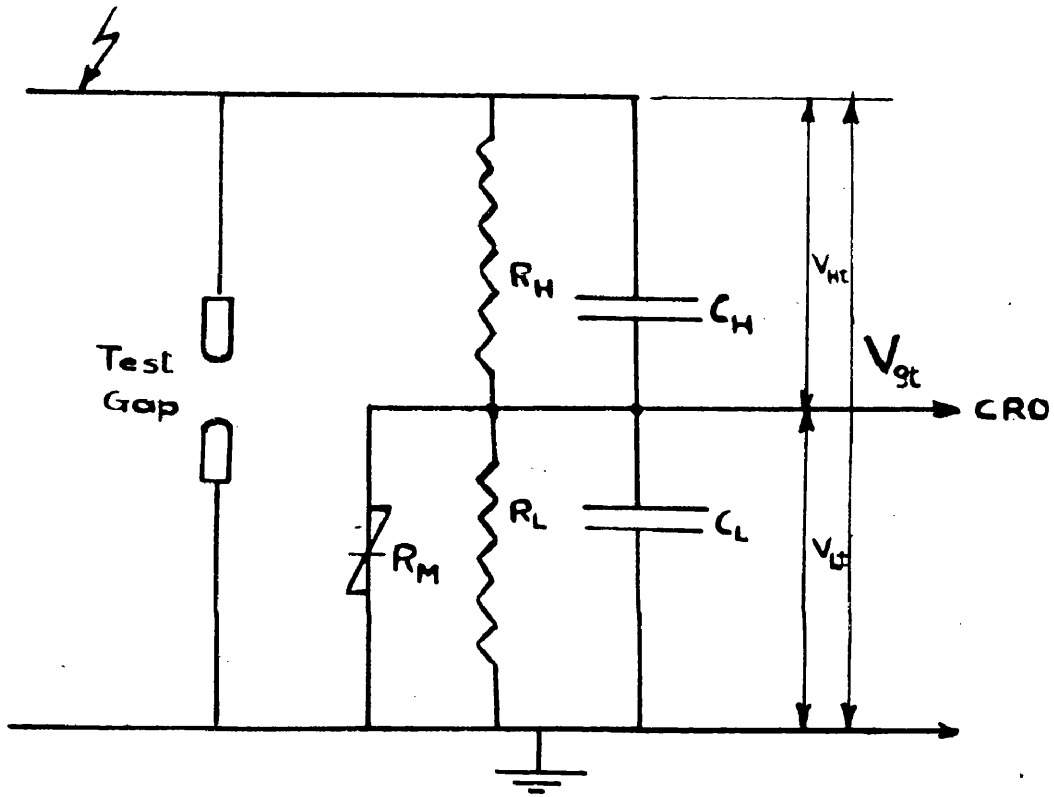
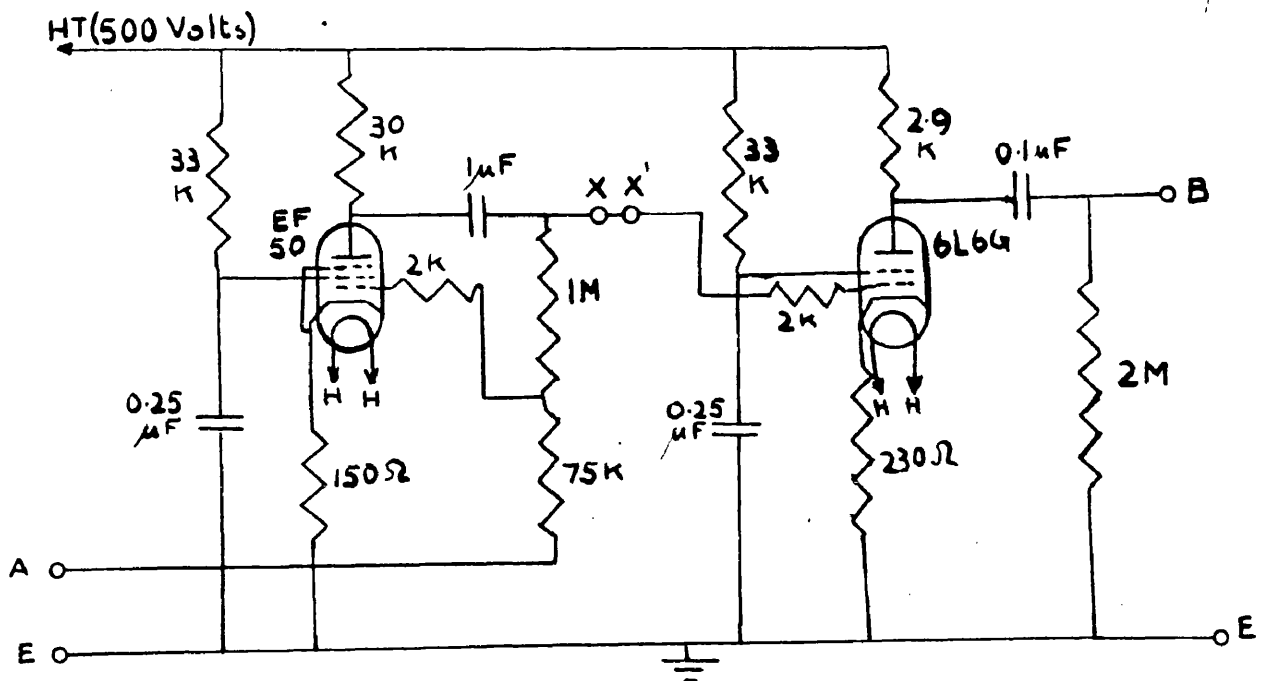
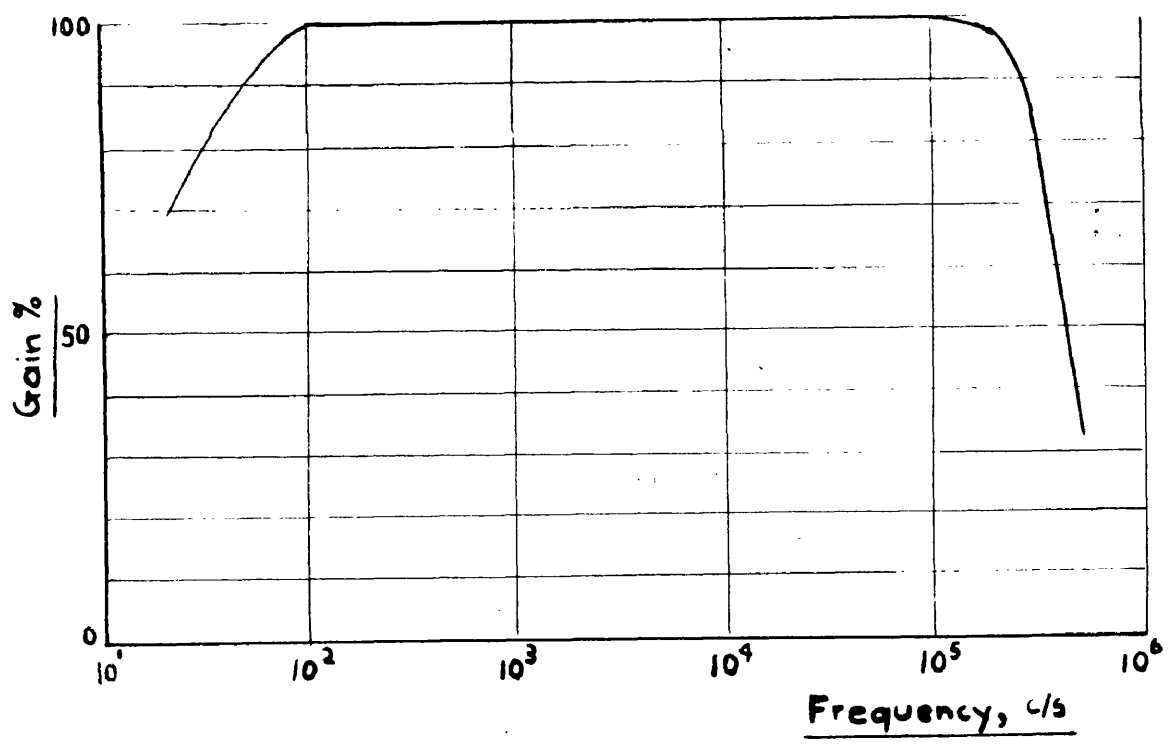


FIG. 7

The voltage-limited potential divider, shown connected across the test-gap.



(a)



(b)

**FIG 8. AMPLIFIER USED FOR CURRENT MEASUREMENT.**

- (a) Circuit Diagram. The input is applied between A and E, and the output is obtained between B and E. When the input stage only is used, the link XX' is removed, X' is earthed, and the output is obtained between X and E.
- (b) Frequency response.

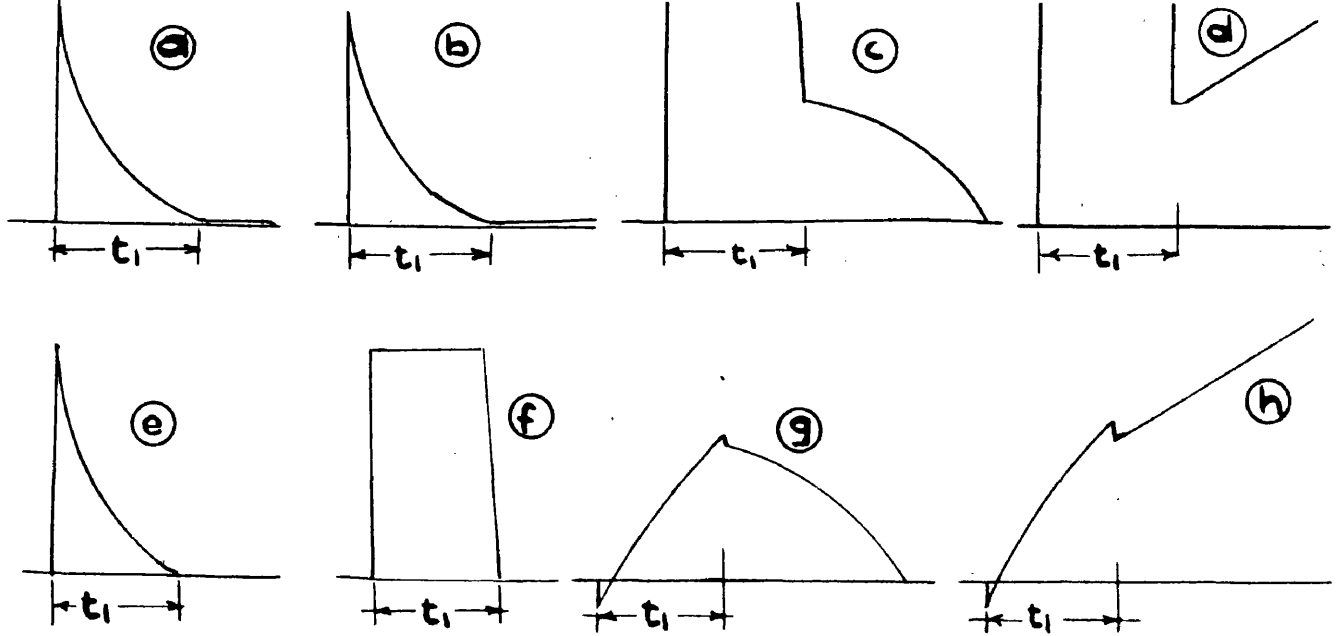


**FIG. 9. TYPICAL OSCILLOGRAPHIC TRACES OBTAINED BY RECORDING AT THE SHUNTS OF FIG. 1, WHEN FOLLOW CURRENT WAS OF L.F. TYPE. A horizontal 'zero line' is shown on each tracing.**

TRACING	SHUNT AT WHICH RECORDING (fig. 1)	WHETHER AMPLIFIER USED (BETWEEN SHUNT AND CRO)	REMARKS
a	$R_{sg}$	No	Follow Current not established.
b			Follow Current established.
c		Yes	Follow Current not established.
d			Follow Current established.
e	$R_{sig}$	No	The traces are independent of the establishment of follow current.
f		Yes	
g	$R_s$	Yes	Follow Current not established.
h			Follow Current established.

THE AMPLIFIER WAS DRIVEN TO CUT OFF BY THE HIGH INITIAL CURRENT IN TRACINGS c, d AND f.

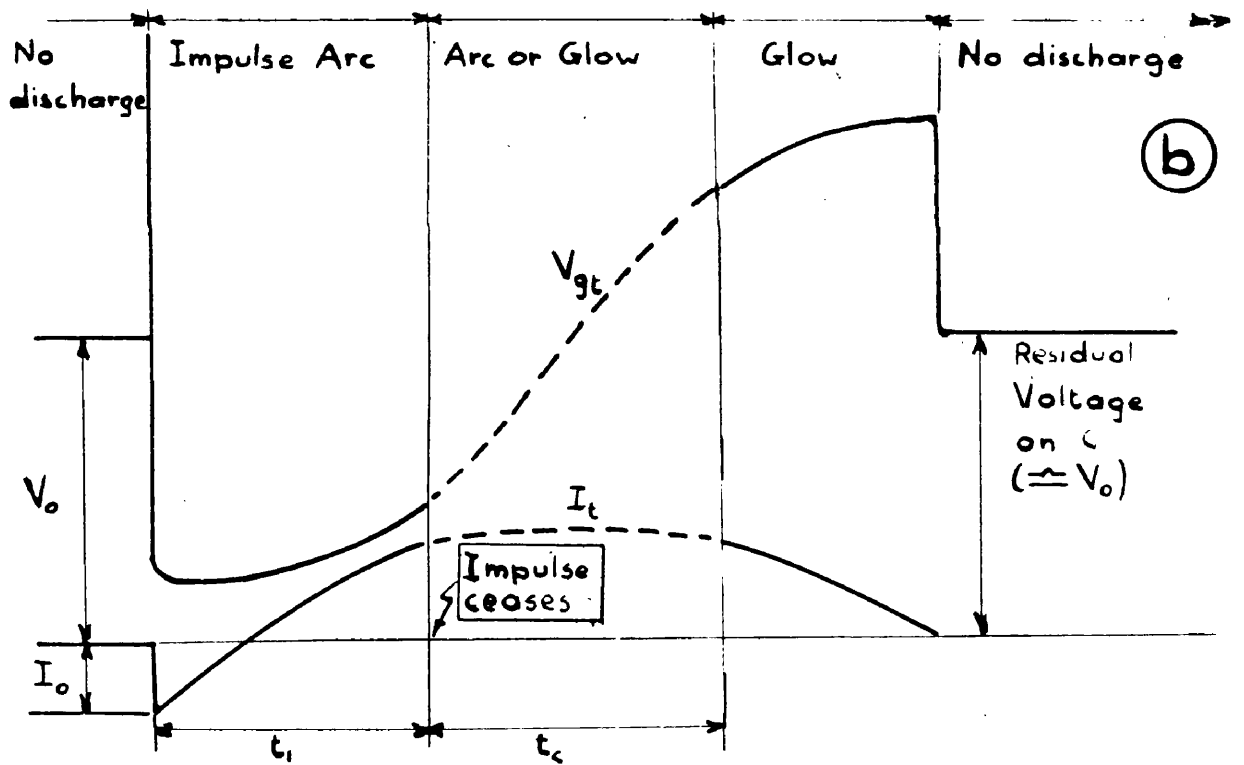
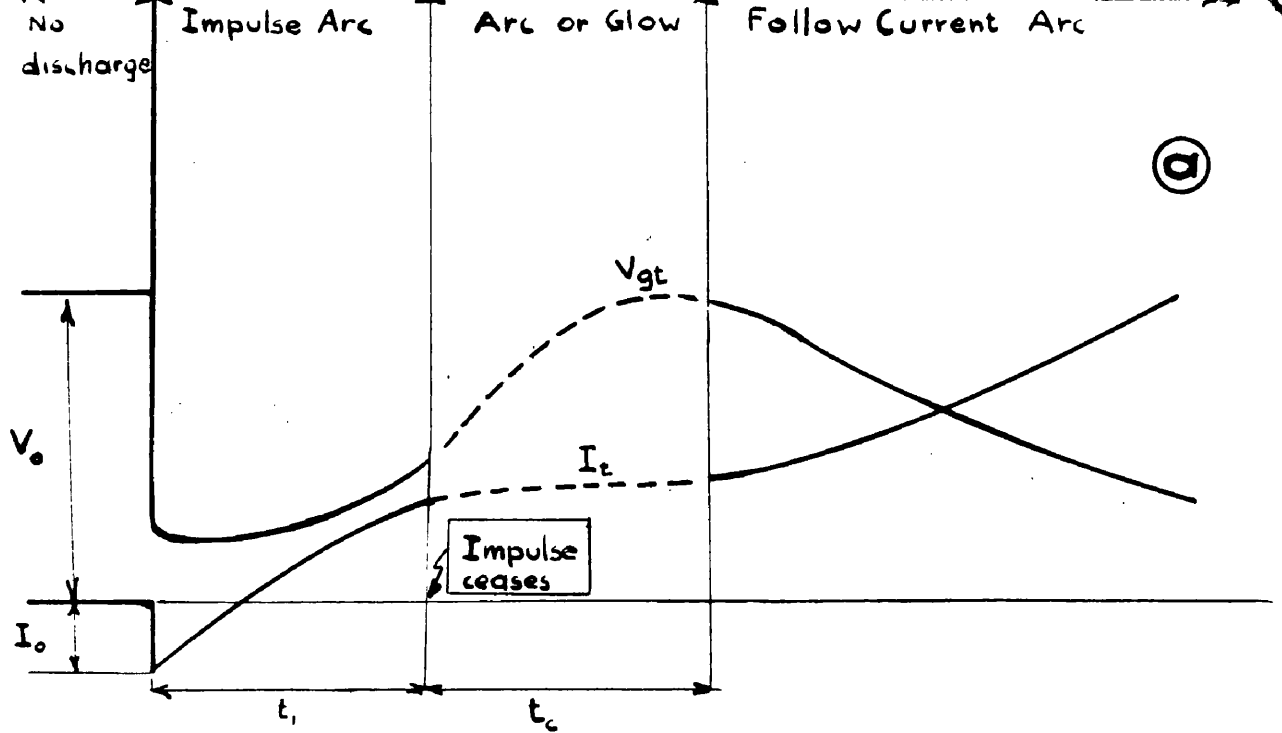


**FIG. 10. H.V. FOLLOW CURRENT ( $t_i \ll \frac{1}{2f}$ ).**

Idealised tracings from oscillograms of discharge Voltage,  $V_{gt}$ , and L.V. circuit current,  $I_t$ . If potential divider current is ignored,  $I_t = I_{gt}$  (fig.1) after  $t_i$ .

(a) FOLLOW CURRENT ESTABLISHED.

(b) FOLLOW CURRENT DOES NOT OCCUR.

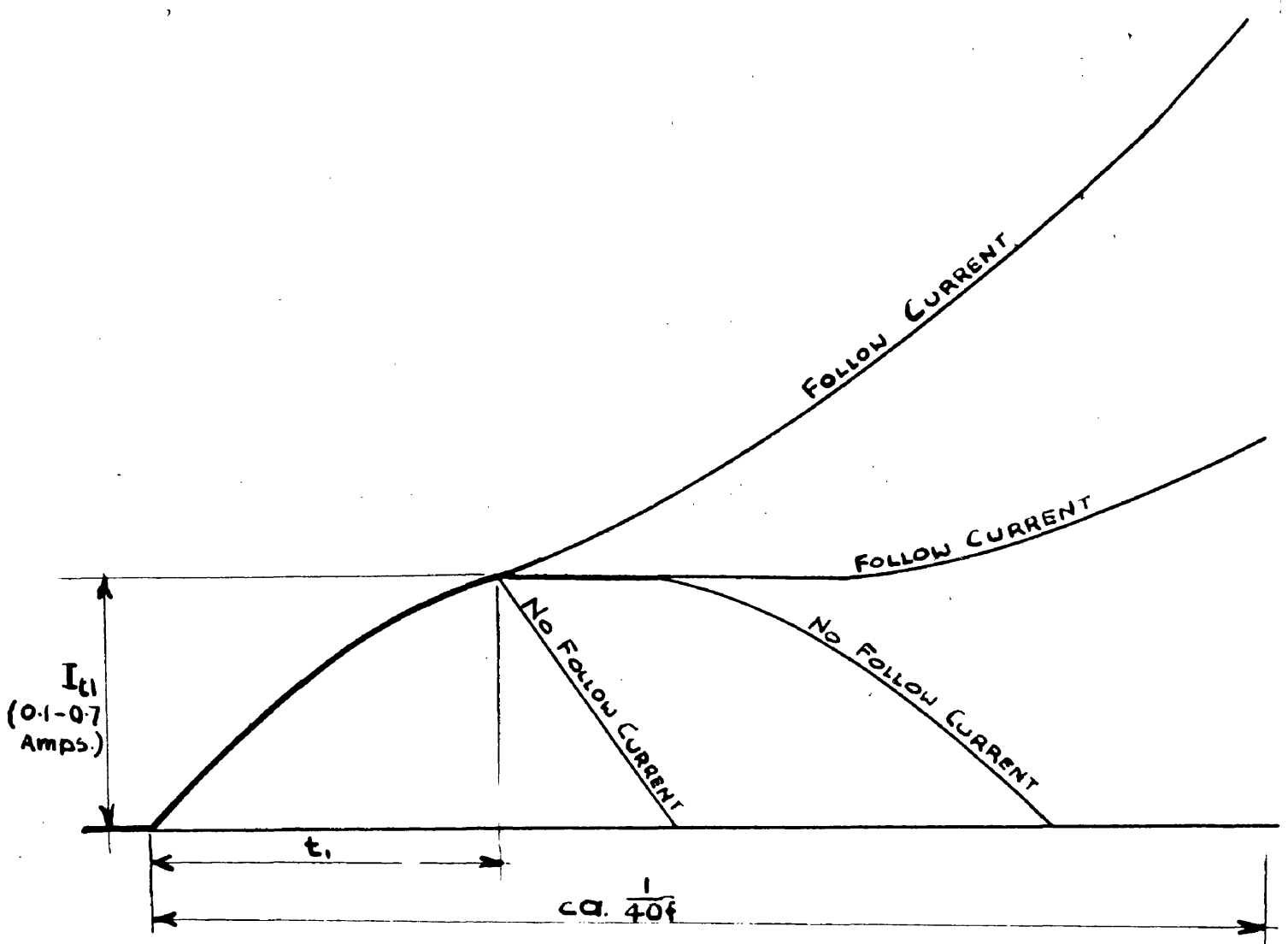


FIG. II. H.V. FOLLOW CURRENT.

Sketches of waveshapes of L.V. circuit current,  $I_t$ , obtained when  $V_0$  had a critical value and  $I_0$  was negligible.

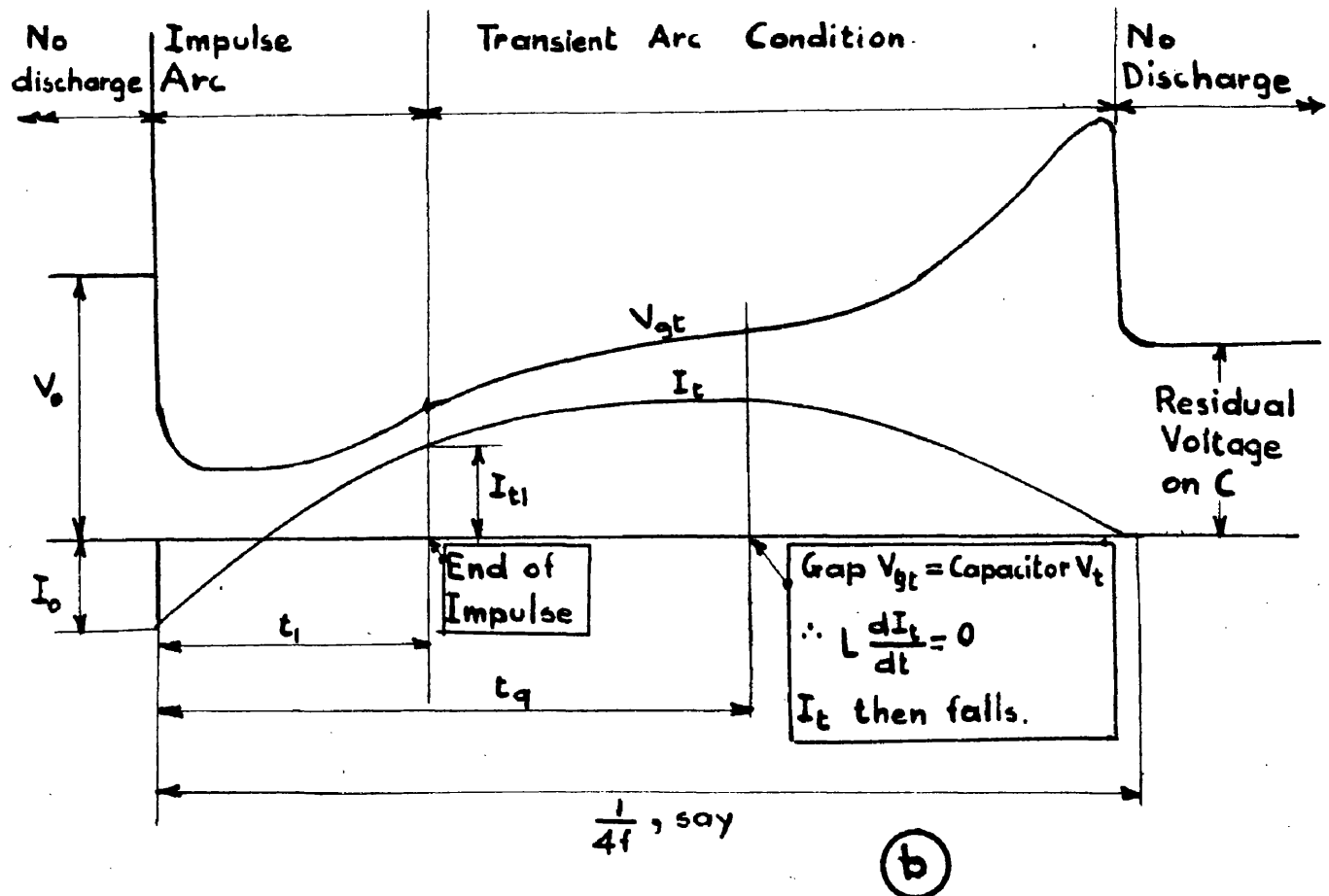
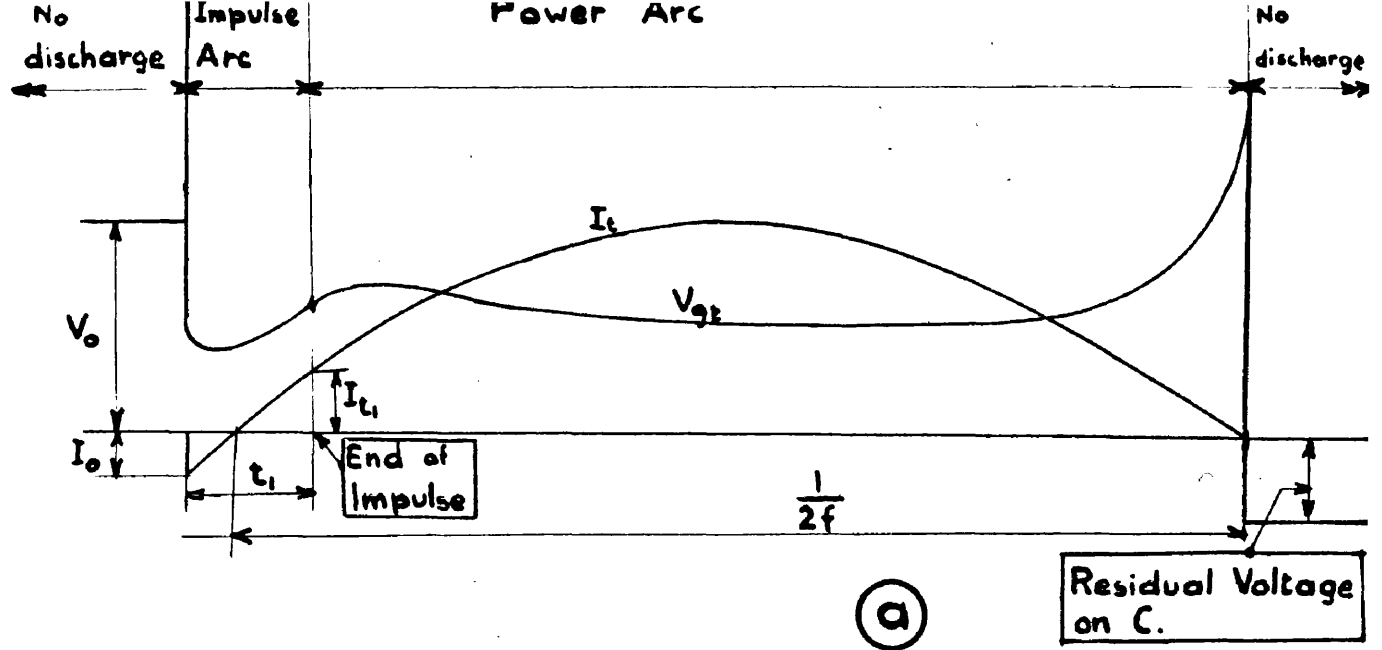


FIG. 12. H.C. FOLLOW CURRENT.

Sketches of waveshapes of discharge voltage,  $V_{gt}$ , and L.V. circuit current,  $I_t$ . If potential divider current is ignored,  $I_t = I_{gt}$  (fig. 1) after  $t_1$ .

(a) Follow Current established.

(b) Follow Current did not occur.

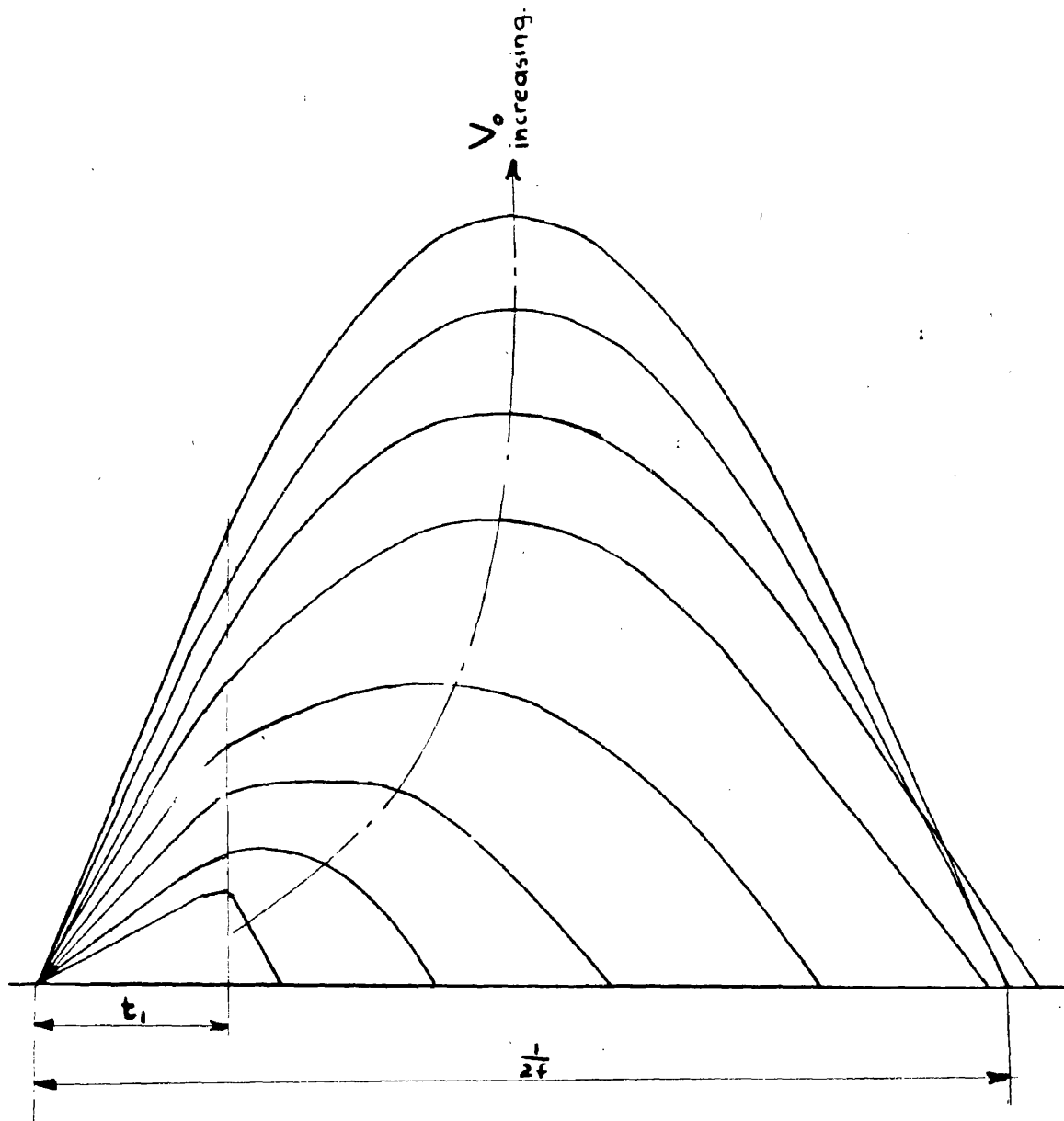
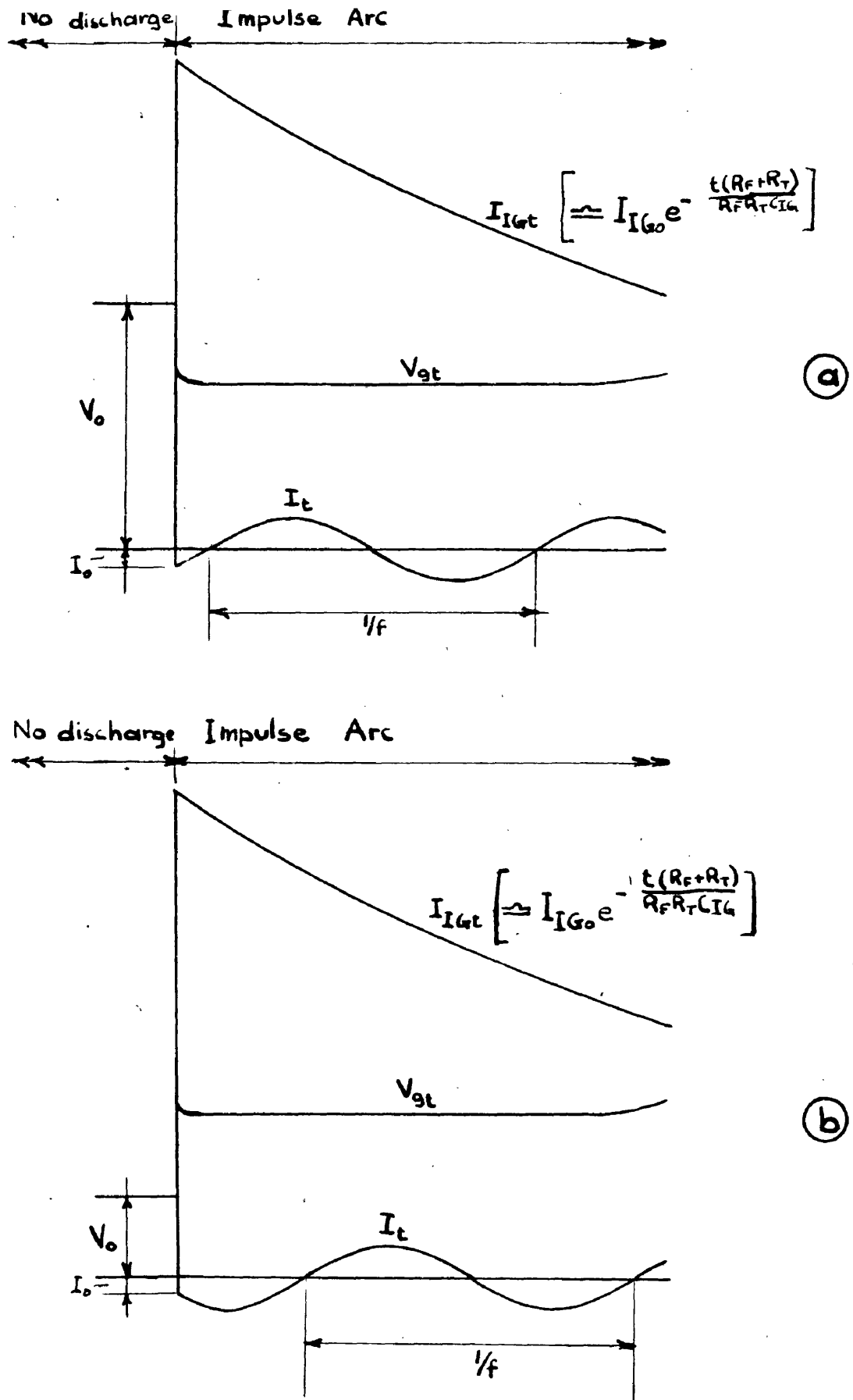


FIG. 13. H.C. FOLLOW CURRENT.

Sketches of  $I_t$  waveshapes illustrating the effect of changes in  $V_0$  on the time for which  $I_t$  is maintained ( $t_{LV}$ ).  
(Negligible  $I_0$ ).



**FIG. 14. H.F. Follow Current.**

Sketches of waveshapes of discharge voltage,  $V_{gt}$ , impulse current,  $I_{igt}$ , and L.V. Circuit current,  $I_t$ .

- (a) Follow Current established.
- (b) Follow Current did not occur.

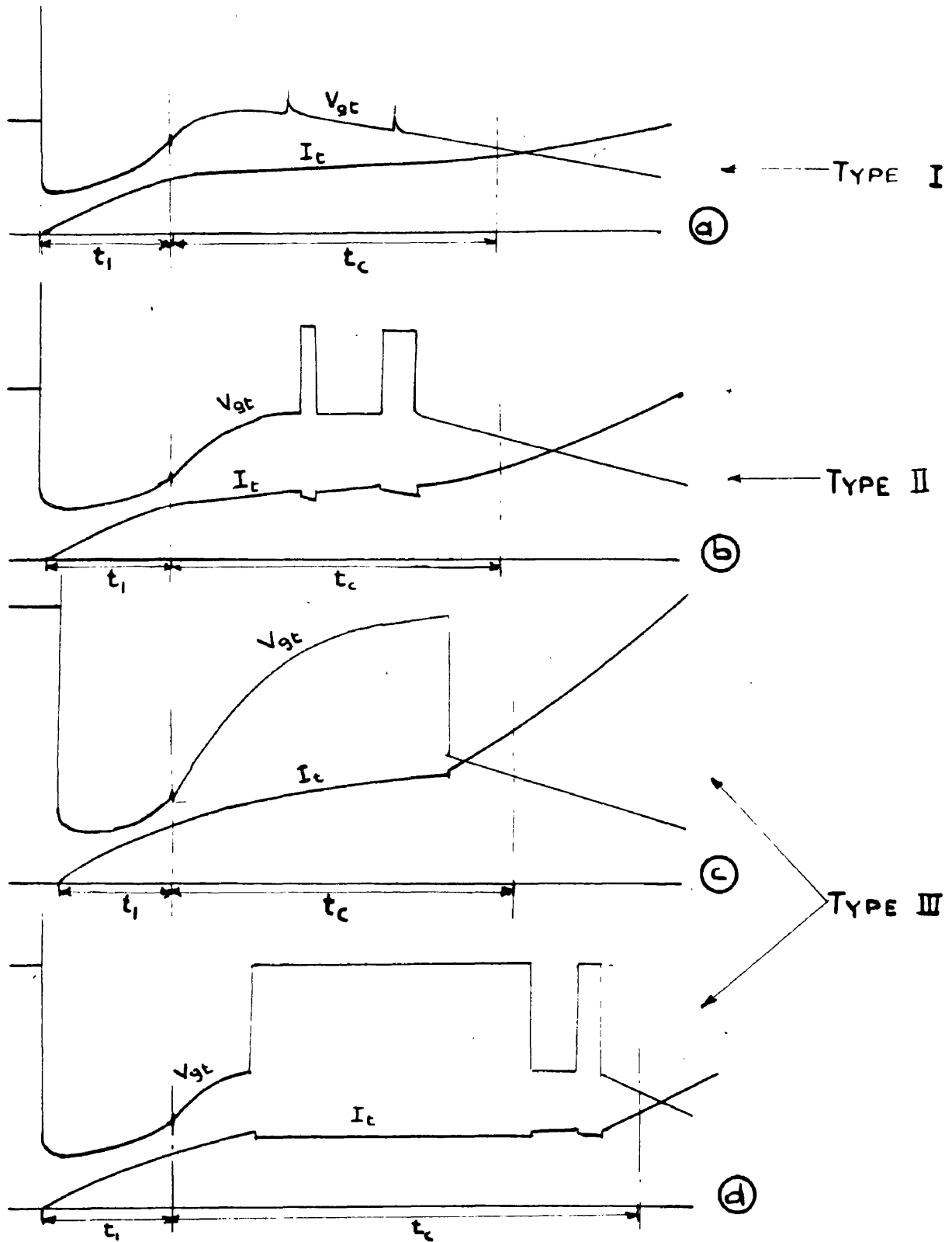
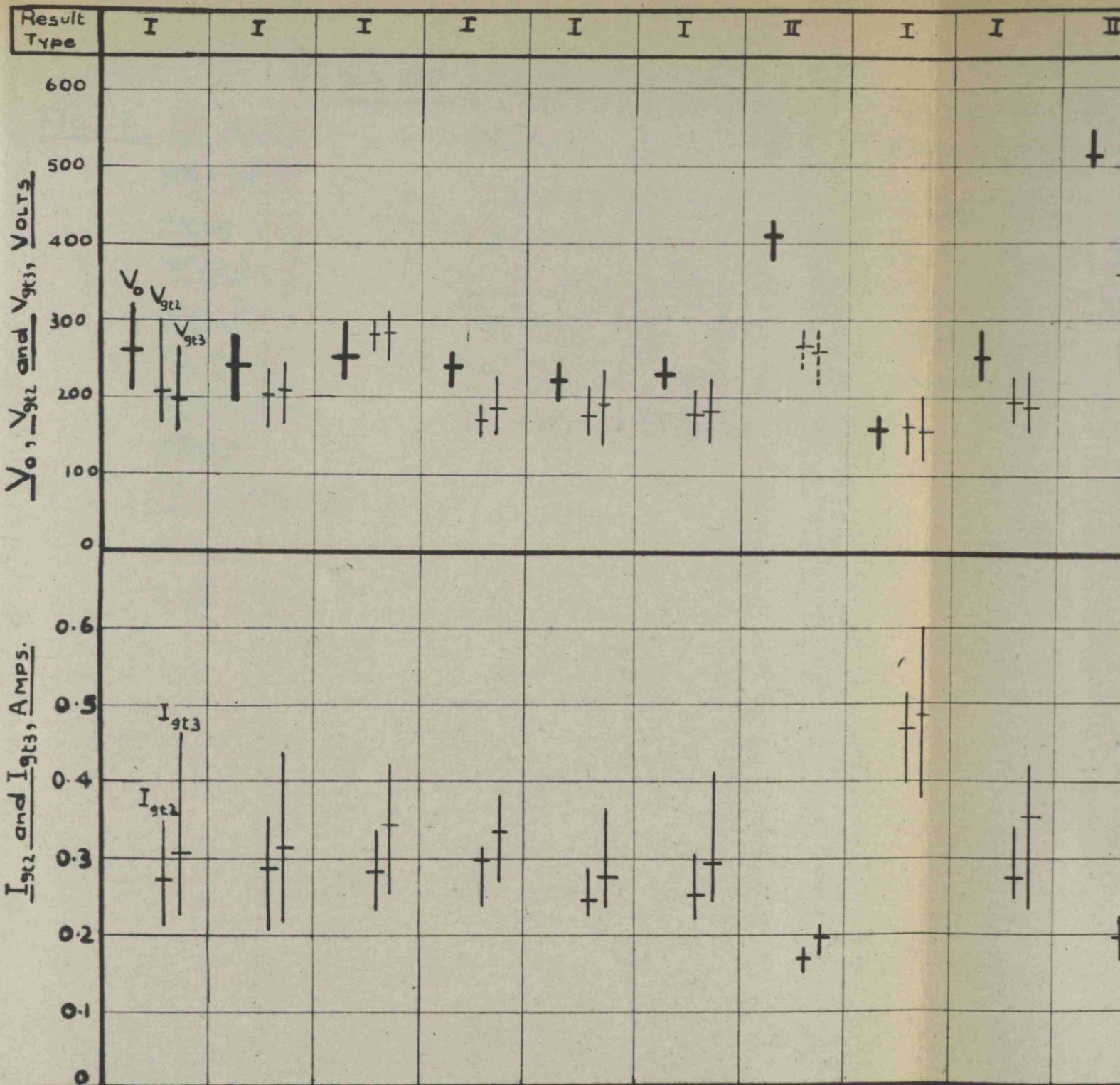


FIG. 15. CLASSIFICATION OF H. V. FOLLOW CURRENT OSCILLOGRAMS IN ACCORDANCE WITH THE WAVESHAPES OF  $V_{gt}$  DURING  $t_c$  (SEE ALSO FIG. 10). SUDDEN CHANGES IN  $V_{gt}$  INDICATE TRANSITIONS FROM ARC TO GLOW AND FROM GLOW TO ARC.

$I_t$  WAVESHAPES HAVE BEEN DRAWN ABOVE FOR THE CONDITION  $I_0 = 0$ : THIS HELD IN MOST EXPERIMENTS COVERED BY THE PRESENT INVESTIGATION. THE POTENTIAL DIVIDER CURRENT BEING NEGLIGIBLE,  $I_t = I_{gt}$  AFTER  $t_1$ .



TEST No.

(CARBON  $R_F$ )

(WOVEN WIRE  $R_F$ )

$Z=126\Omega$

$f=158\text{ c/s}$

$f=158\text{ c/s}$

$f=158\text{ c/s}$

$Z=126\Omega$

$Z=400\Omega$

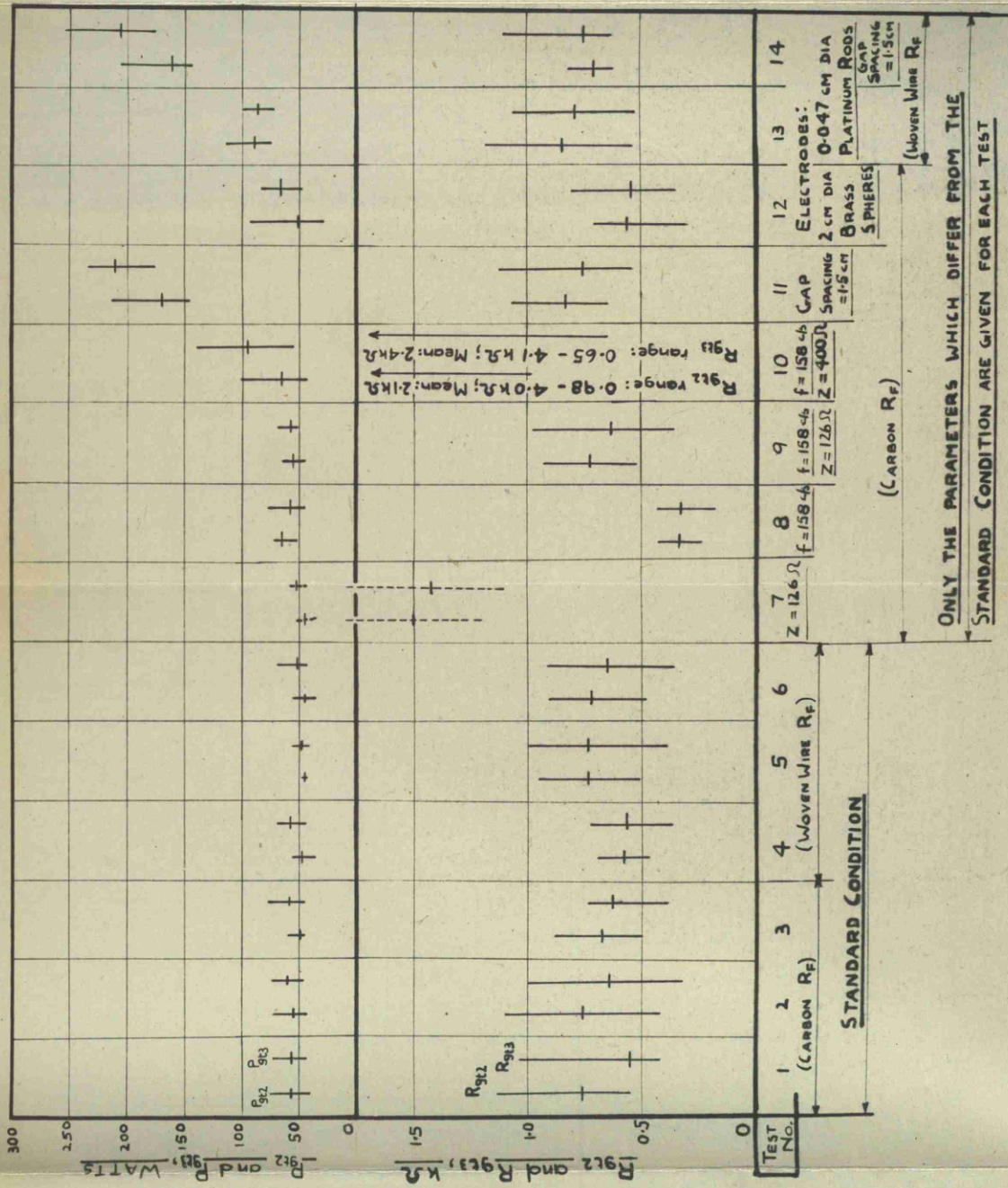
(SAME  $Z/f$  VALUES AS IN STANDARD CONDITION, TESTS 1-6)

(CARBON  $R_F$ )

STANDARD CONDITION:  $f = 50\text{ c/s}$ ;  $Z = 40\Omega$ ;  
 $C_{IG} = 0.083\mu\text{F}$ ;  $R_F = 420\Omega$  (Carbon or Woven Wire);  $R_T = 75\text{k}\Omega$ ; Test Gap Electrodes: 0.063 cm dia. tungsten rods, heavily oxidised; Test Gap Spacing: 0.5 cm;  $t_2 = 200\mu\text{s}$ ;  $t_3 = 300\mu\text{s}$

ONLY THE PARAMETERS W  
CONDITION ARE GIVEN FOR

FIG. 16. CRITICAL VALUES OF  $V_0$ ,  $V_{gt}$ ,  $I_{gt}$ ,  $P$  AND  $R_{gt}$  OBTAINED WITH H.V. FOLLOW CURRENT. Values recorded at  $t_2$  are shown in every test at the left of values recorded at  $t_3$  and the values of  $V_0$  are indicated by heavier lines (see test). Vertical lines give the scatter and horizontal lines give the mean values of the recorded data.



ONLY THE PARAMETERS WHICH DIFFER FROM THE STANDARD CONDITION ARE GIVEN FOR EACH TEST

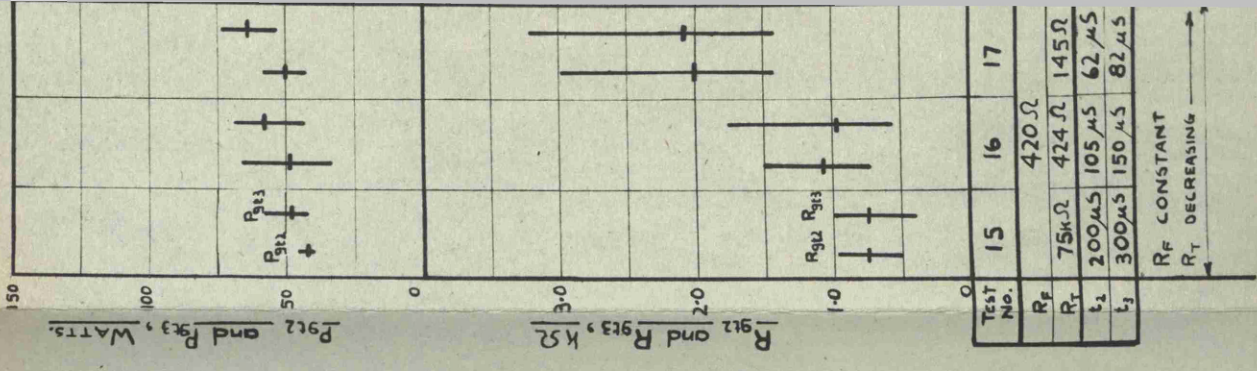
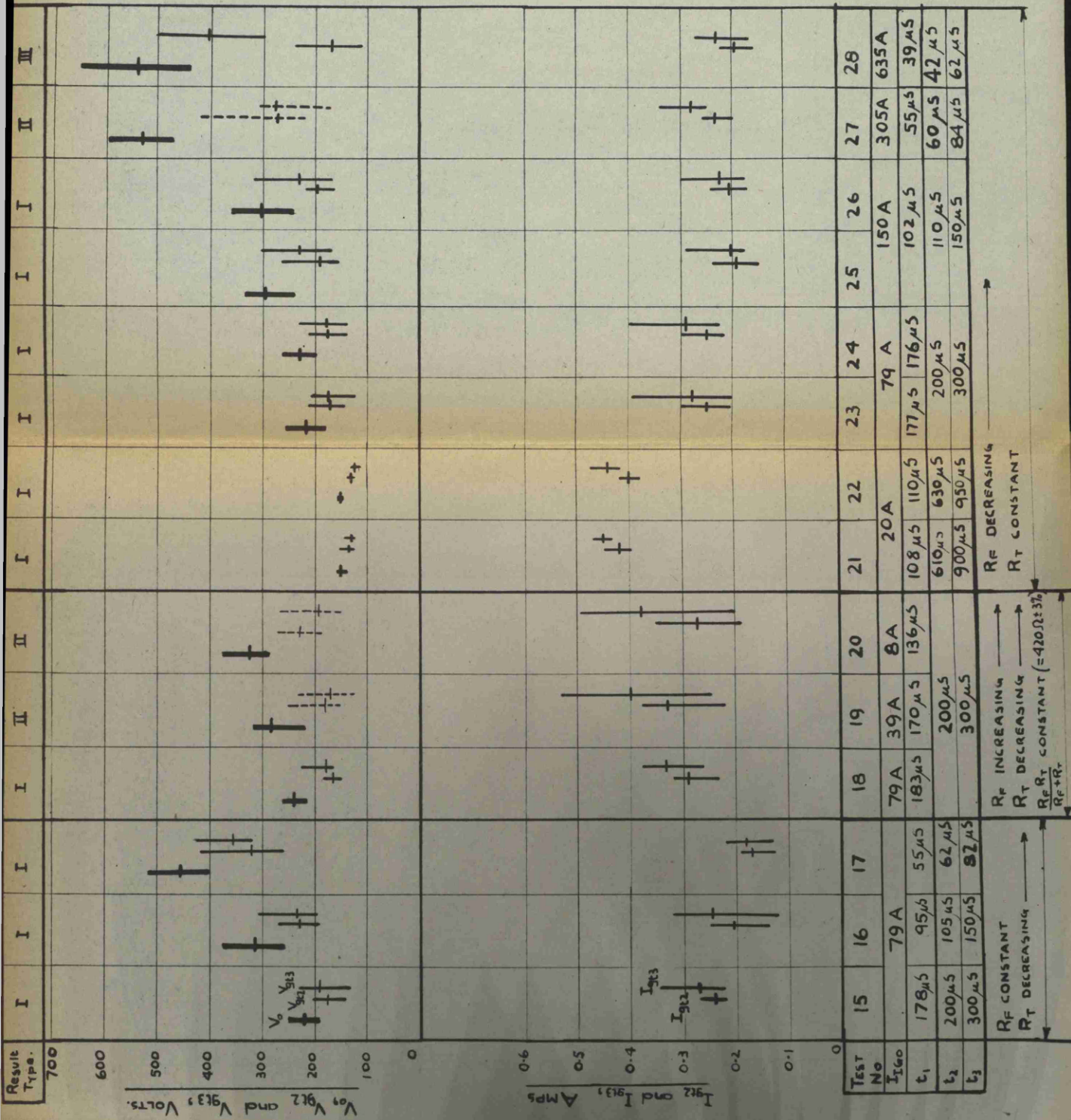
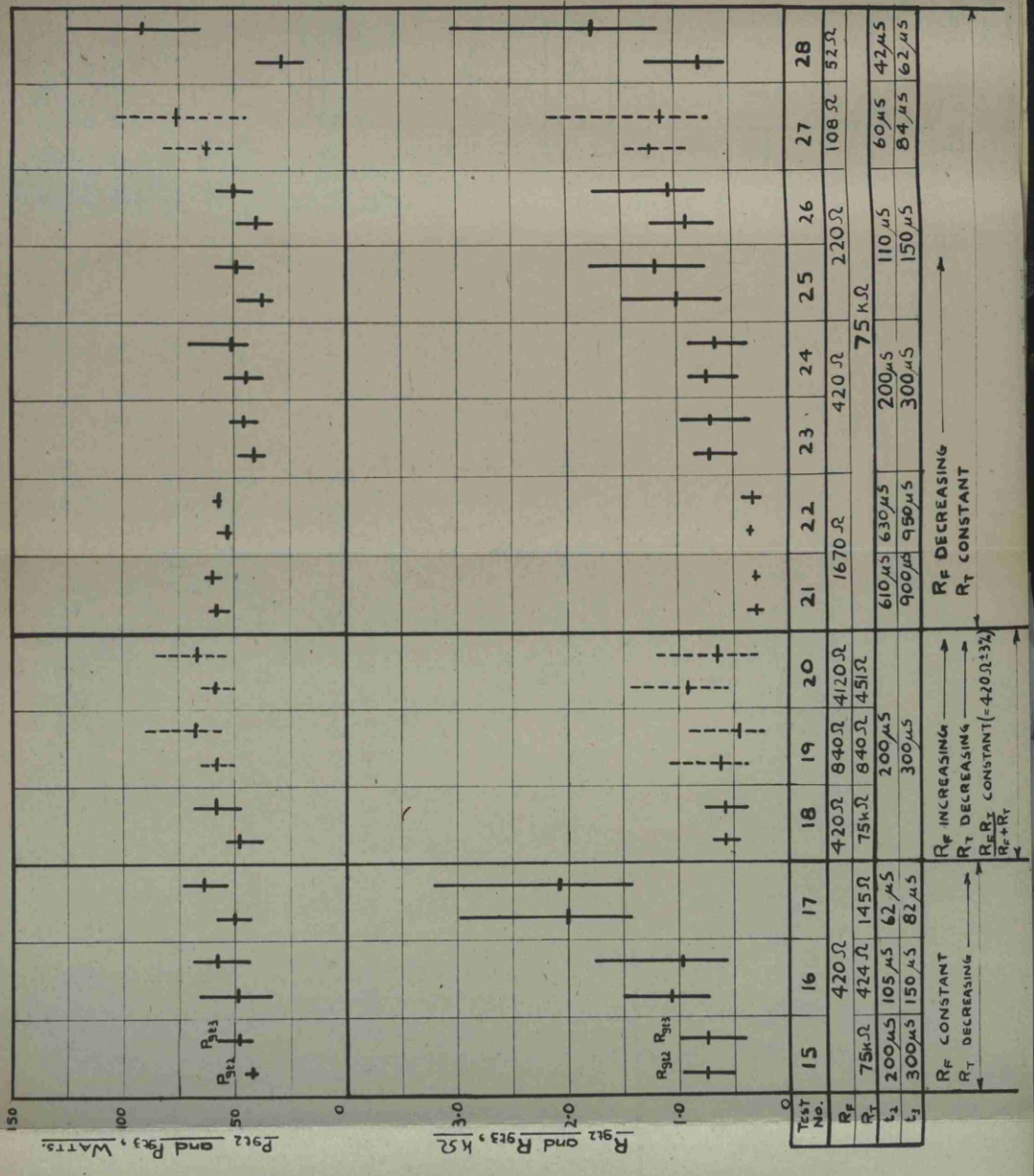


Fig. 17. CRITICAL VALUES OF  $V_0$ ,  $V_{gt}$ ,  $I_{gt}$ ,  $P_{gt}$  AND  $R_{gt}$  OBTAINED WITH H.V. FOLLOW CURRENT.

Values recorded at  $t_2$  are shown in every test at the left of values recorded at  $t_3$ , and the values of  $V_0$  are indicated by heavier lines (see test 15). Vertical lines give the scatter and horizontal lines give the mean values of the recorded data.

The STANDARD CONDITION held in tests 15, 18, 23 and 24.  $R_F$  consisted of woven wire resistance ribbon in all tests.



$P_{gt2}$  and  $P_{gt3}$ , WATTS

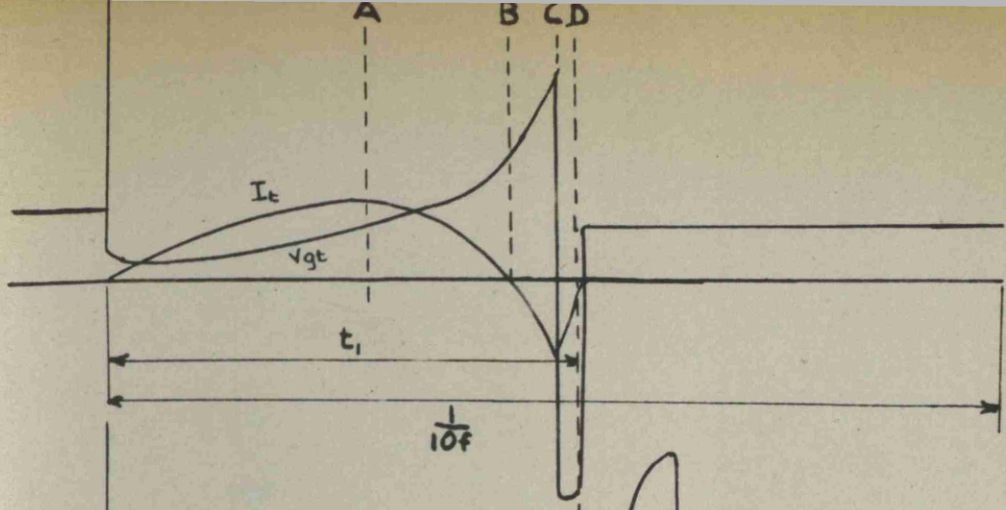
$R_{gt2}$  and  $R_{gt3}$ , k $\Omega$

$R_F$  INCREASING  
 $R_T$  DECREASING  
 $R_{gt}$  CONSTANT (-470  $\Omega$   $\pm$  3%)  
 $R_F + R_T$

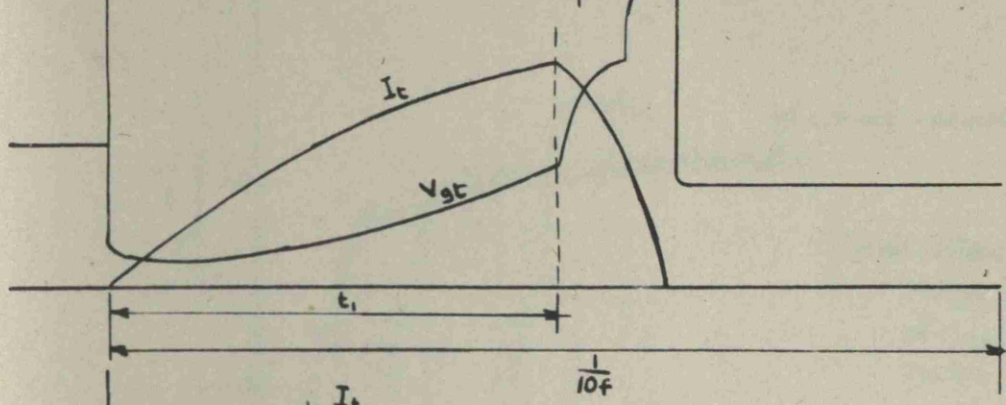
$R_F$  CONSTANT  
 $R_T$  DECREASING

$R_F$  DECREASING  
 $R_T$  CONSTANT

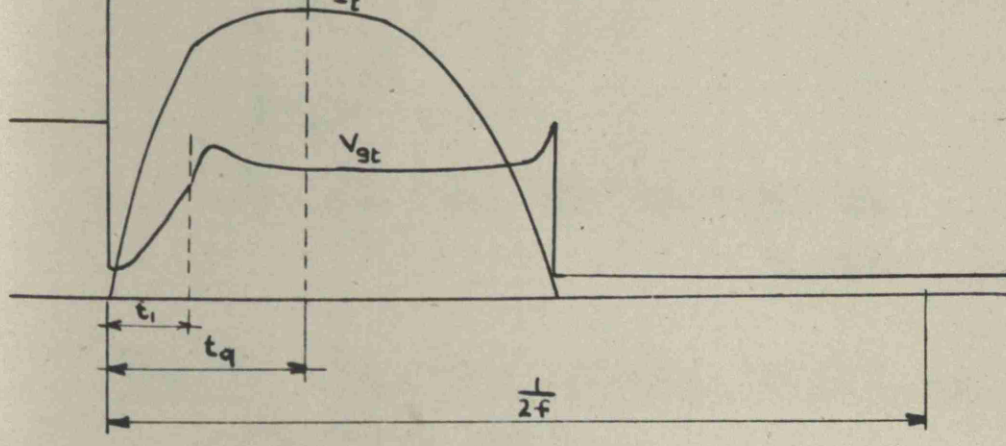
75 k $\Omega$



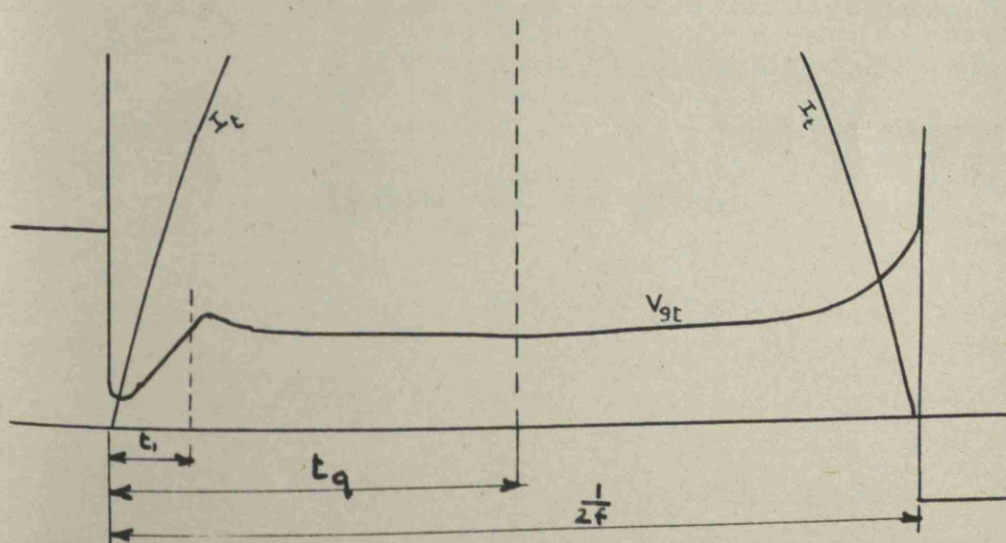
(a)



(b)



(c)



(d)  
 [The  $I_t$  waveshape approximates to a sine wave. Its peak is reached at  $t_q$  and is not shown in this sketch.]

FIG. 18. Sketches of waveshapes of  $I_t$  and  $V_{gt}$ , illustrating the mechanism of H.C. Follow Current. (See also fig. 12)

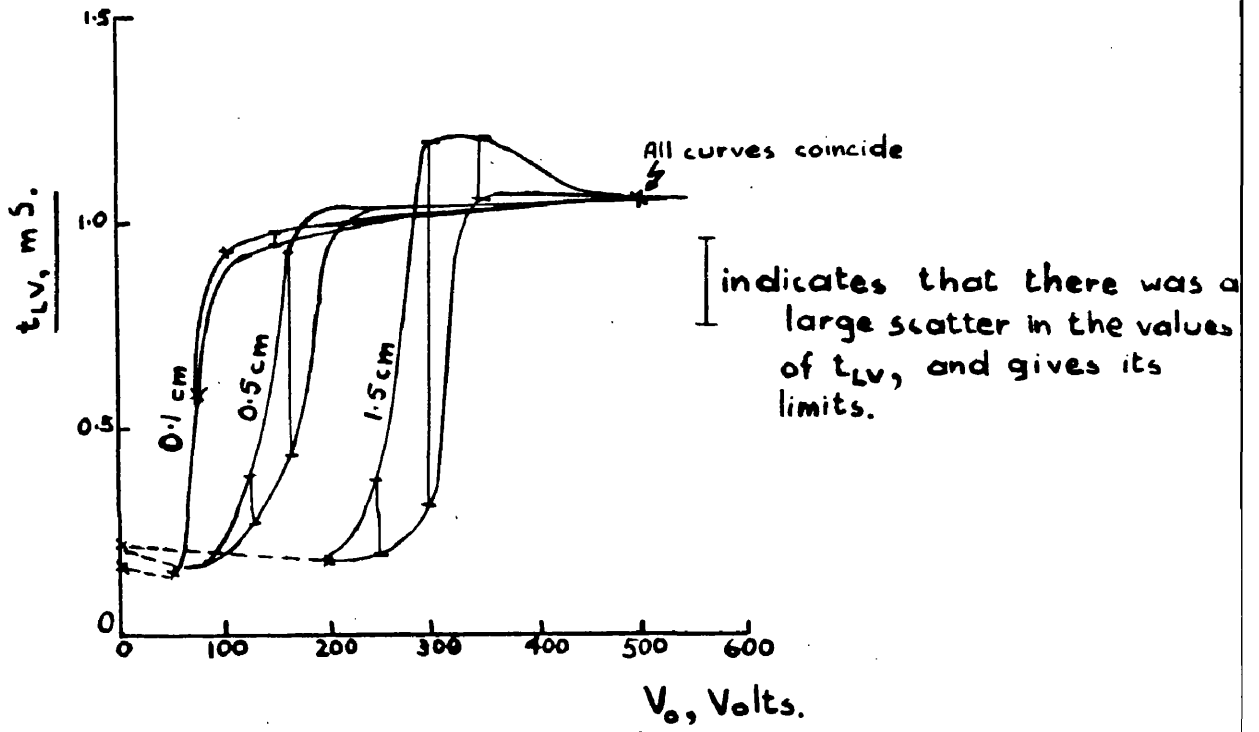


FIG. 19. RELATIONS BETWEEN THE TIME,  $t_{LV}$ , FOR WHICH  $I_t$  FLOWS AND  $V_0$ .

$f = 500 \text{ } \mu\text{s}$ ;  $Z = 40 \text{ } \Omega$ ;  $t_i \approx 160 \text{ } \mu\text{s}$ ;  $I_{IG_0} = 79 \text{ Amps}$ ;

$I_0 = 0$ ;  $R_F = 420 \text{ } \Omega$  (carbon);  $R_T = 75 \text{ k}\Omega$  (carbon);

$C_{IG} = 0.083 \text{ } \mu\text{F}$ ;  $V_{IG_0} = 33 \text{ kV}$ ; standard Electrodes,

spaced as indicated.

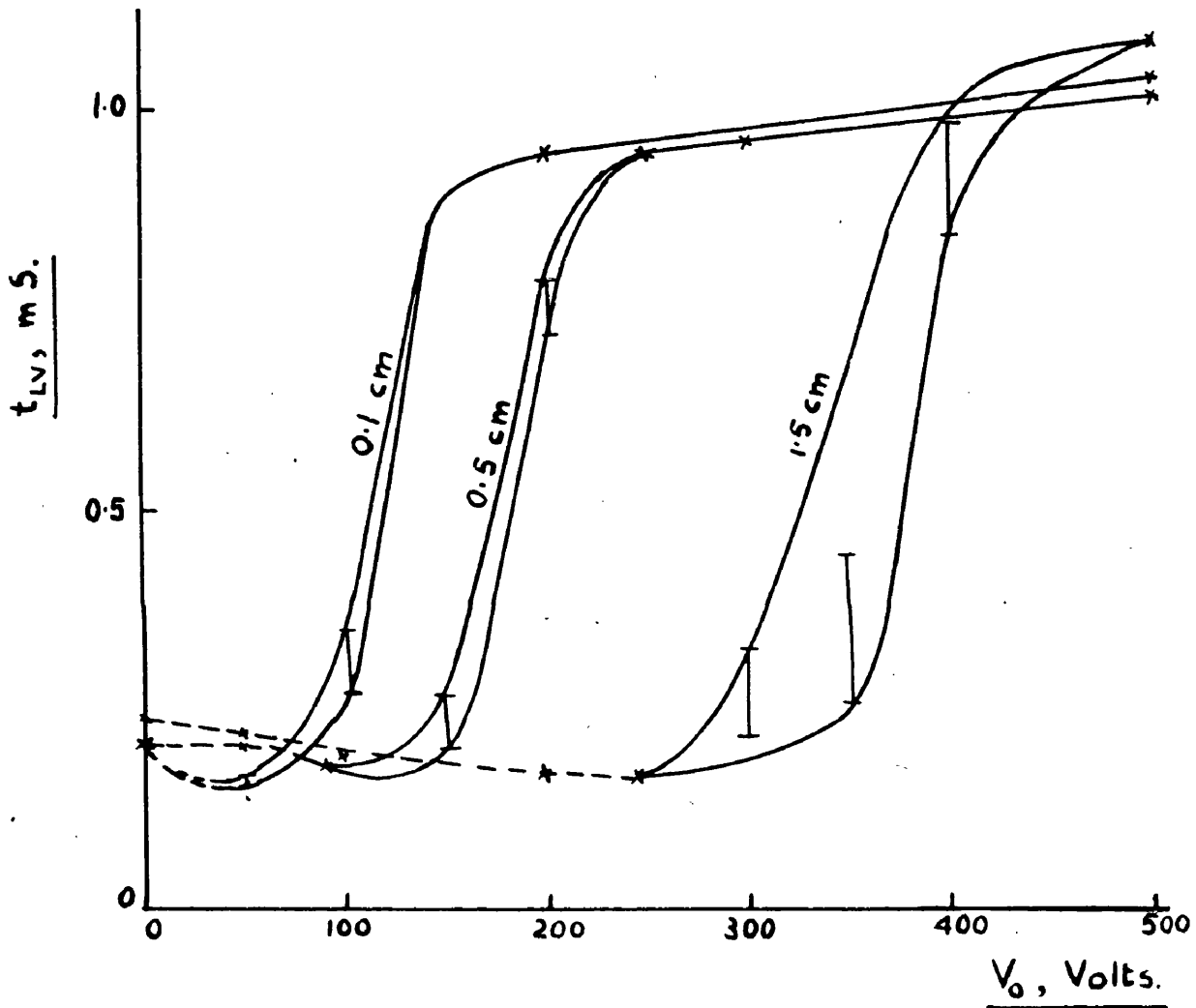


FIG. 20. RELATIONS BETWEEN THE TIME,  $t_{LV}$ , FOR WHICH  $I_t$  FLOWS, AND  $V_0$ .

$Z = 126 \Omega$ . Other data, and convention regarding the scatter in  $t_{LV}$ , as on Fig. 19.

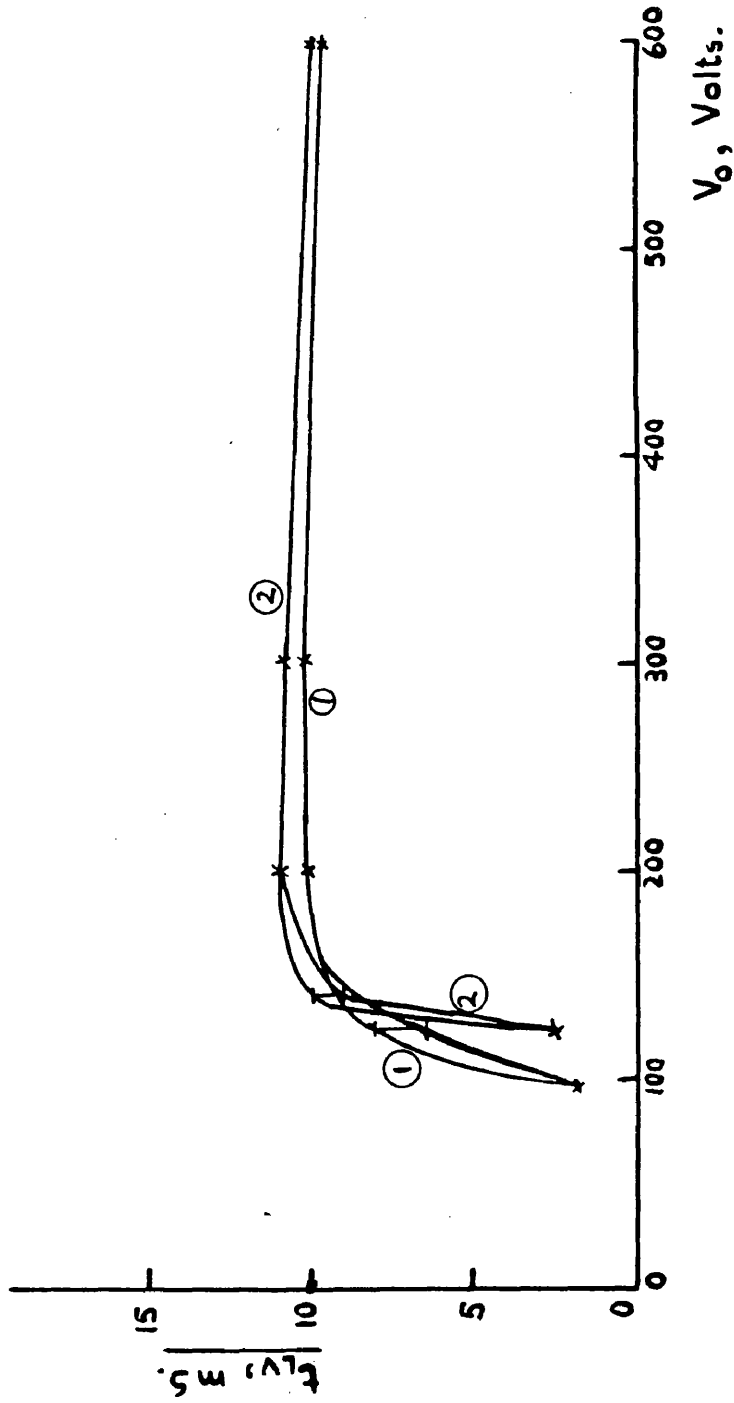


FIG. 21. RELATIONS BETWEEN THE TIME,  $t_{LV}$ , FOR WHICH  $I_t$  FLOWS, AND  $V_o$ .  
 $f = 50$  c/s;  $Z = 40 \Omega$ ;  $V_{IG_0} = 33$  kV;  $C_{IG} = 0.083 \mu\text{F}$ ;  $R_T = 75 \text{ k}\Omega$  (carbon);  $I_0 = 0$ ;  
Standard Test Gap; and  
Curve 1:  $t_1 \approx 1.2$  ms;  $I_{IG_0} = 8$  Amps;  $R_F = 4120 \Omega$  (woven wire).  
Curve 2:  $t_1 \approx 2.2$  ms;  $I_{IG_0} = 3.4$  Amps;  $R_F = 9600 \Omega$  (woven wire).

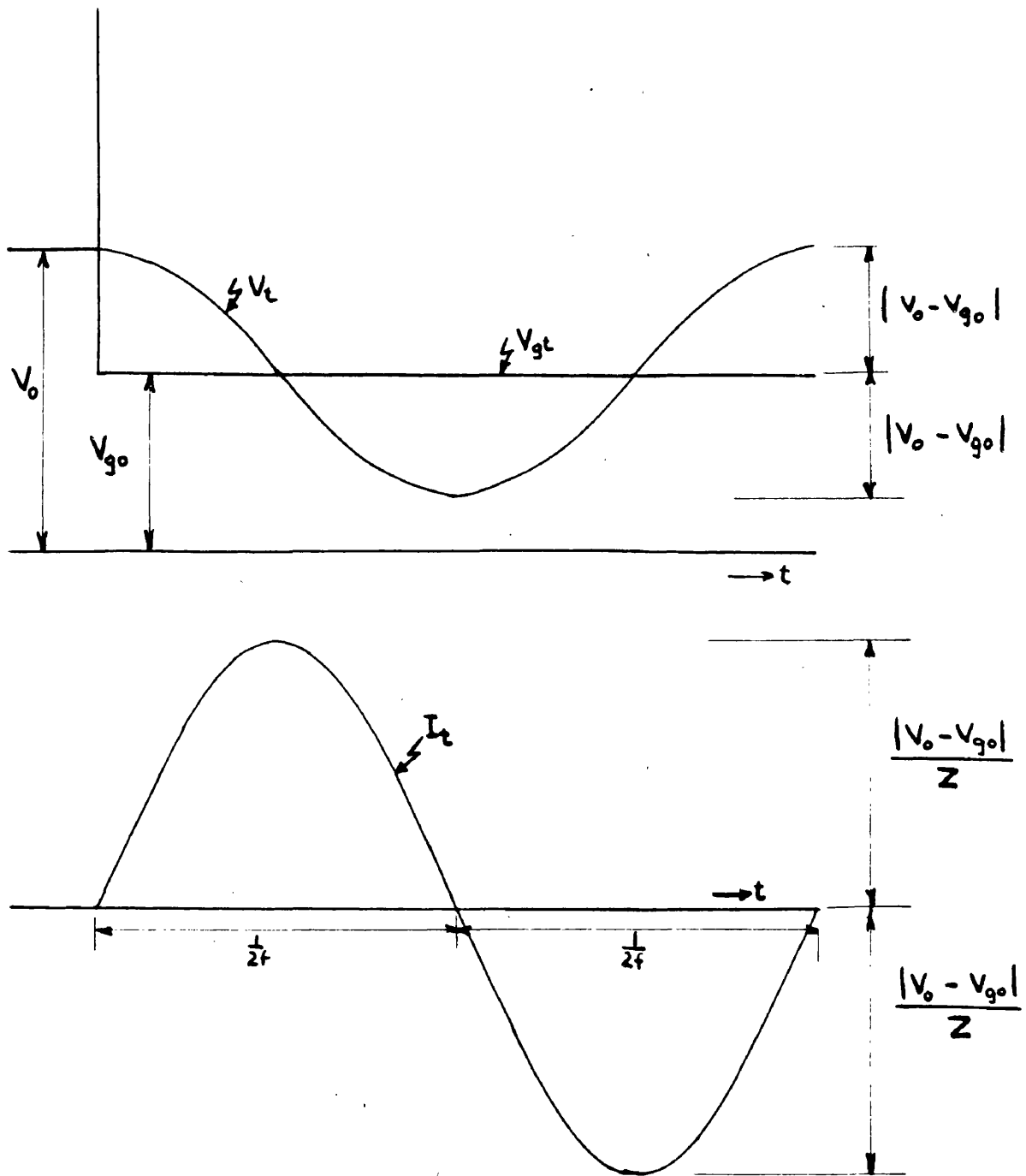


FIG. 22. ANALYSIS OF THE H.F. FOLLOW CURRENT MECHANISM FOR THE CASE  $V_0 > V_{g0}$ .

Assumptions:  $V_{gt} \equiv V_{g0}$  (constant);  $I_0$  and  $R$  negligible.

See also Figs. 14 and 23.

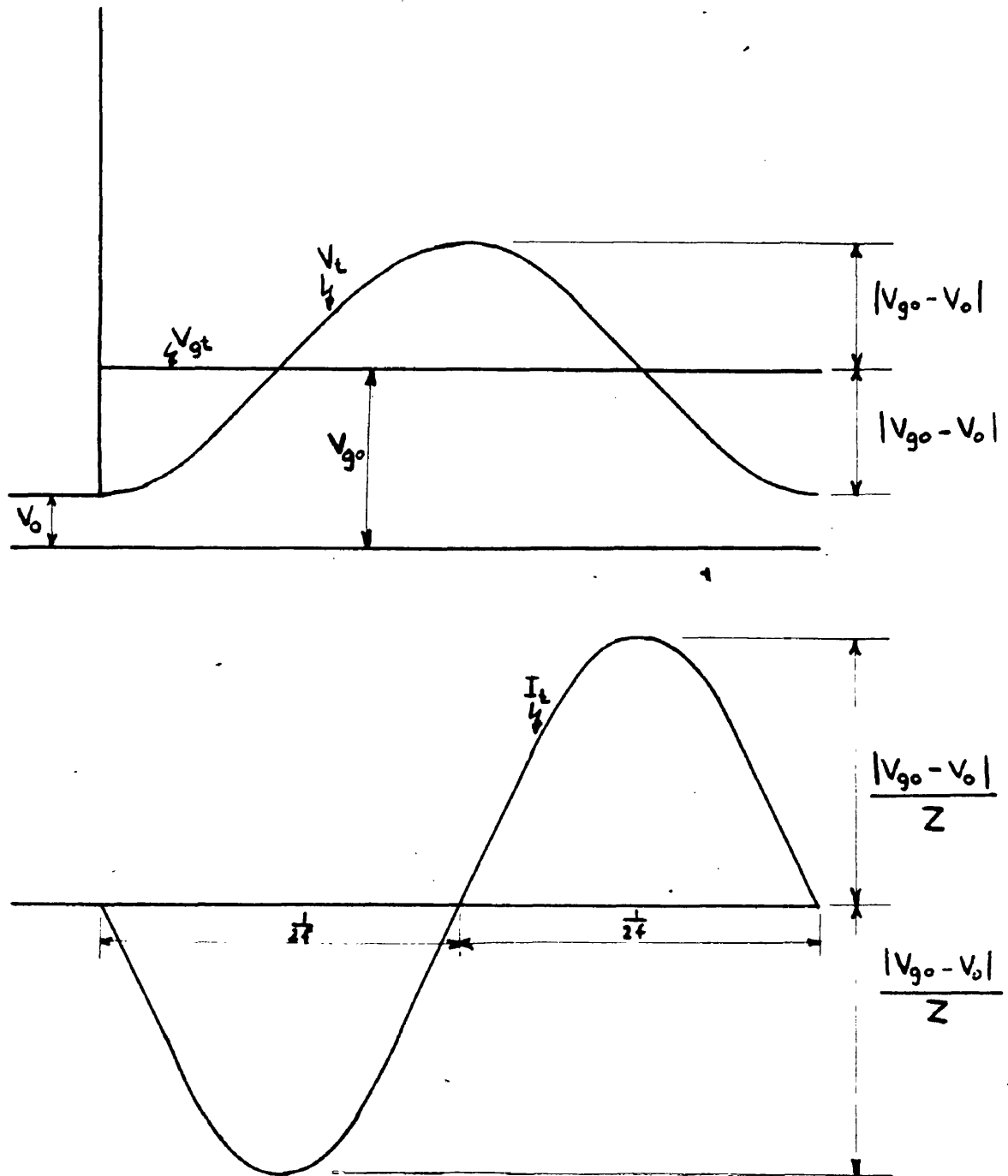


FIG. 23. ANALYSIS OF THE H.F. FOLLOW CURRENT MECHANISM FOR THE CASE  $V_0 < V_{g0}$ .

Assumptions:  $V_{gt} = V_0$  (constant);  $I_0$  and  $R$  negligible

See also Figs. 14 and 22.

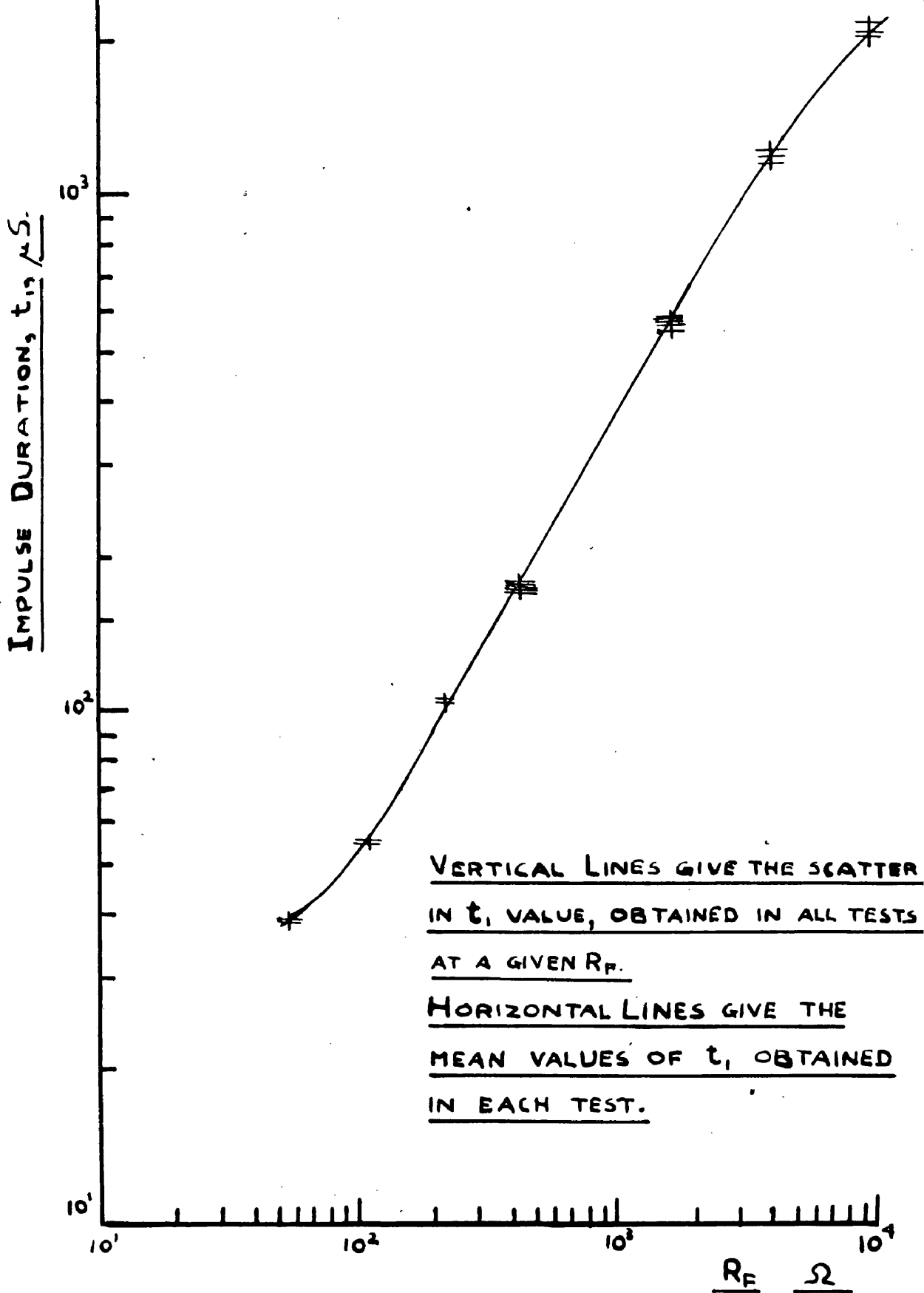


FIG. 24. RELATION BETWEEN IMPULSE DURATION,  $t_i$ , AND  
WAVE FRONT RESISTANCE,  $R_F$ .

$R_T = 75 \times 10^3 \Omega$ ;  $C_{IG} = 0.083 \mu F$ ;  $V_{IG_0} = 33 kV$ ,

Under the conditions of this investigation,  $t_i$  was substantially  
independent of test gap and L.V. circuit, provided  $I_{t_i} > 0$ .

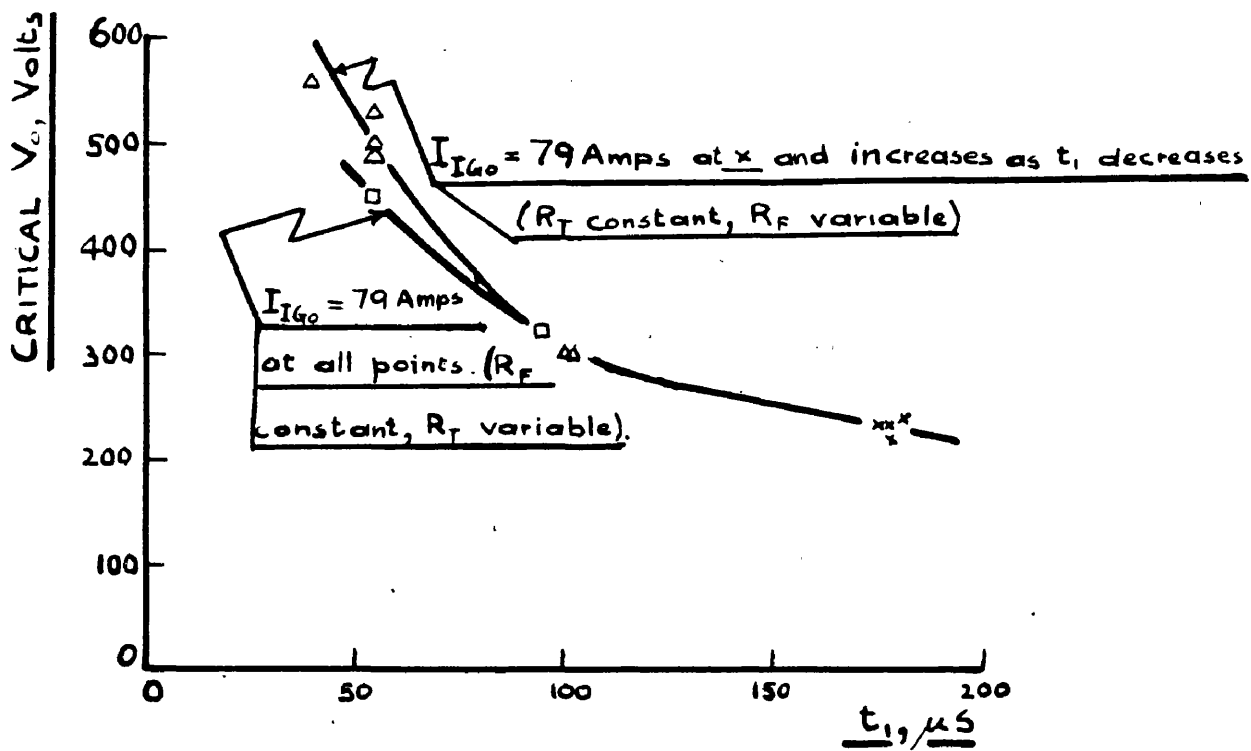


FIG. 25. RELATION BETWEEN THE MEAN VALUES OF CRITICAL  $V_c$  AND IMPULSE DURATION  $t_i$ .

The scatter was less than  $\pm 20\%$  in  $V_c$  and less than  $\pm 10\%$  in  $t_i$ .

$f = 50 \text{ Hz}$ ;  $Z = 40 \Omega$ ;  $C_{IG} = 0.083 \mu F$ ;  $V_{IG0} = 33 \text{ kV}$ ;  
 $0.5 \text{ cm gap}$ .

$\square R_F = 420 \Omega$ ;  $145 \Omega < R_T < 75 \times 10^3 \Omega$

$\Delta R_T = 75 \times 10^3 \Omega$ ;  $50 \Omega < R_F < 420 \Omega$

$\times$  Common to both above conditions ( $R_F = 420 \Omega$ ;  $R_T = 75 \times 10^3 \Omega$ )

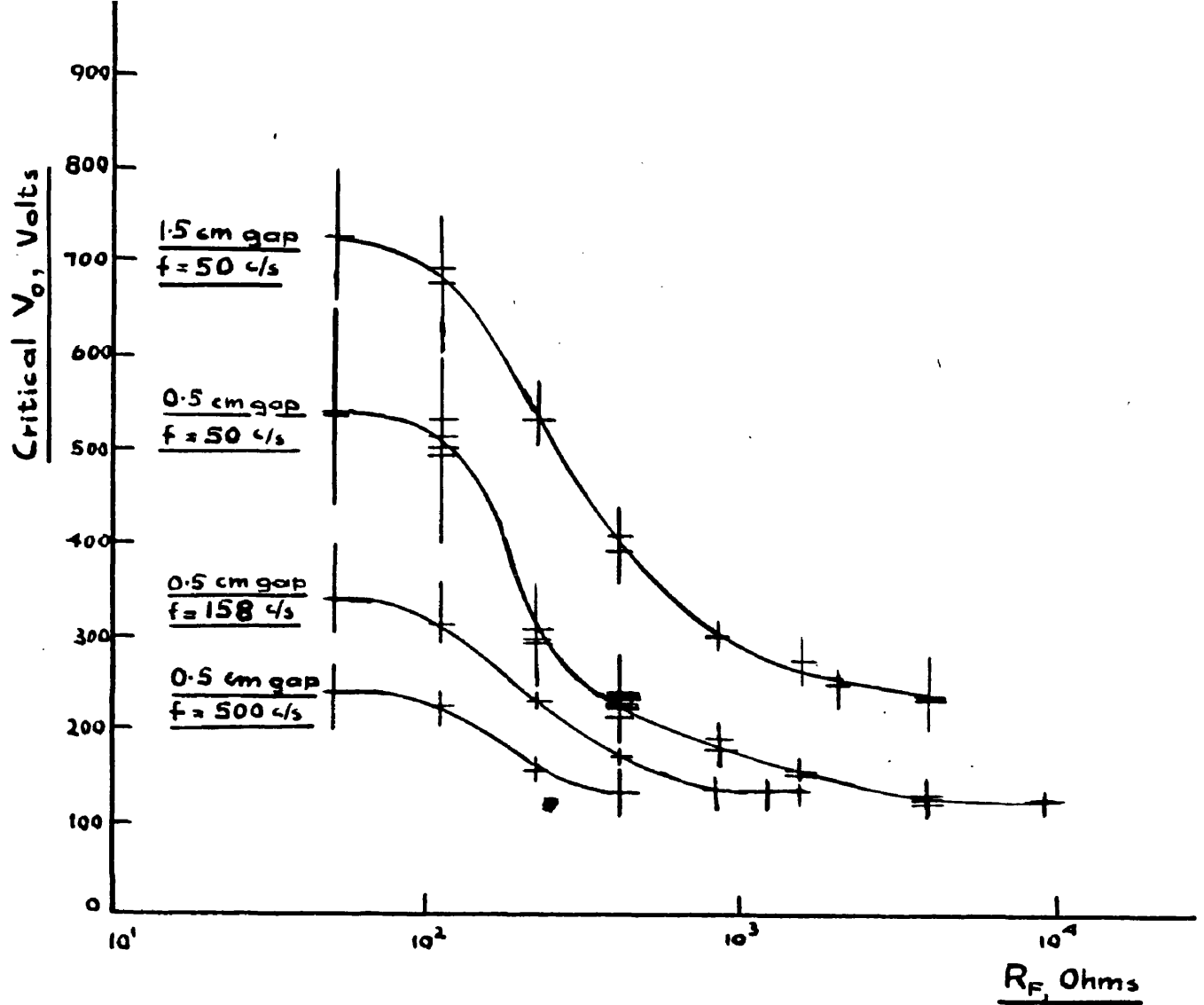


Fig.26: Effect of  $R_F$  on Critical  $V_0$  at different L.V. circuit frequencies and gap spacings.

$Z = 40$  Ohms;  $R_T = 75 \times 10^3$  Ohms;  $C_{IG} = 0.083 \mu F$ ;  $V_{IG0} = 33$  KV.

The vertical lines give the scatter obtained in all tests carried out at a given  $R_F$ . The horizontal lines give the mean values of critical  $V_0$  obtained in each test.

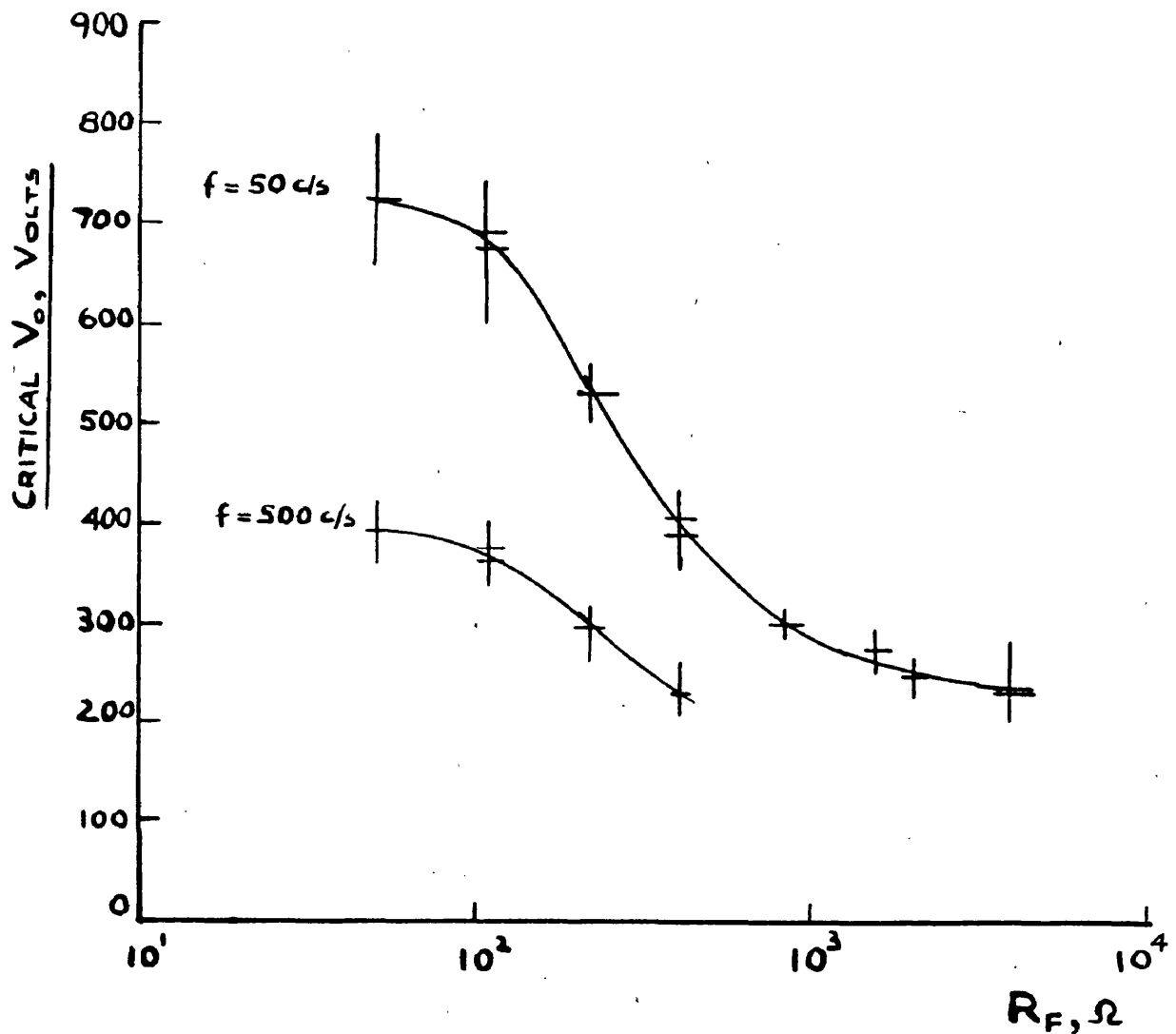


FIG.27. EFFECT OF  $R_F$  ON CRITICAL  $V_0$  AT DIFFERENT L.V. CIRCUIT FREQUENCIES.

$Z = 40 \Omega$ ;  $R_T = 75 \times 10^3 \Omega$ ;  $C_{IG} = 0.083 \mu F$ ;  $V_{IG0} = 33 \text{KV}$ ;

GAP SPACE = 1.5 CM.

THE VERTICAL LINES GIVE THE SCATTER OBTAINED IN ALL TESTS CARRIED OUT AT A GIVEN  $R_F$ . THE HORIZONTAL LINES GIVE THE MEAN VALUE OF CRITICAL  $V_0$  OBTAINED IN EACH TEST.

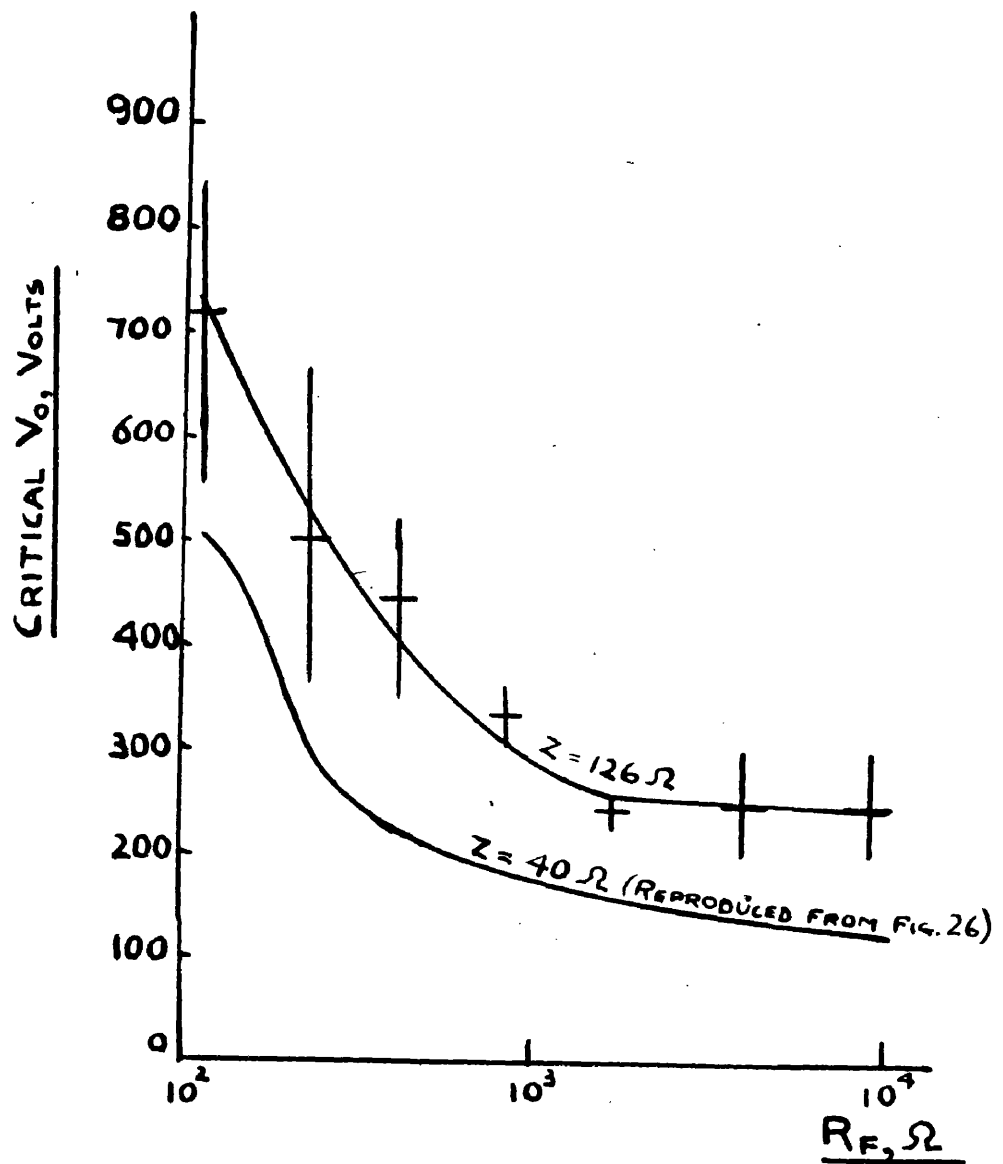


FIG. 28. EFFECT OF  $R_F$  ON CRITICAL  $V_0$  AT DIFFERENT L.V.

CIRCUIT OUTPUT IMPEDANCE VALUES.

$f = 50$  c/s;  $R_T = 75 \times 10^3 \Omega$ ;  $C_{IG} = 0.083 \mu F$ ;  $V_{IG_0} = 33$  kV; 0.5 cm GAP.

THE VERTICAL LINES GIVE THE SCATTER, AND THE HORIZONTAL LINE GIVE THE MEAN, OF THE CRITICAL  $V_0$  OBTAINED IN EACH TEST.

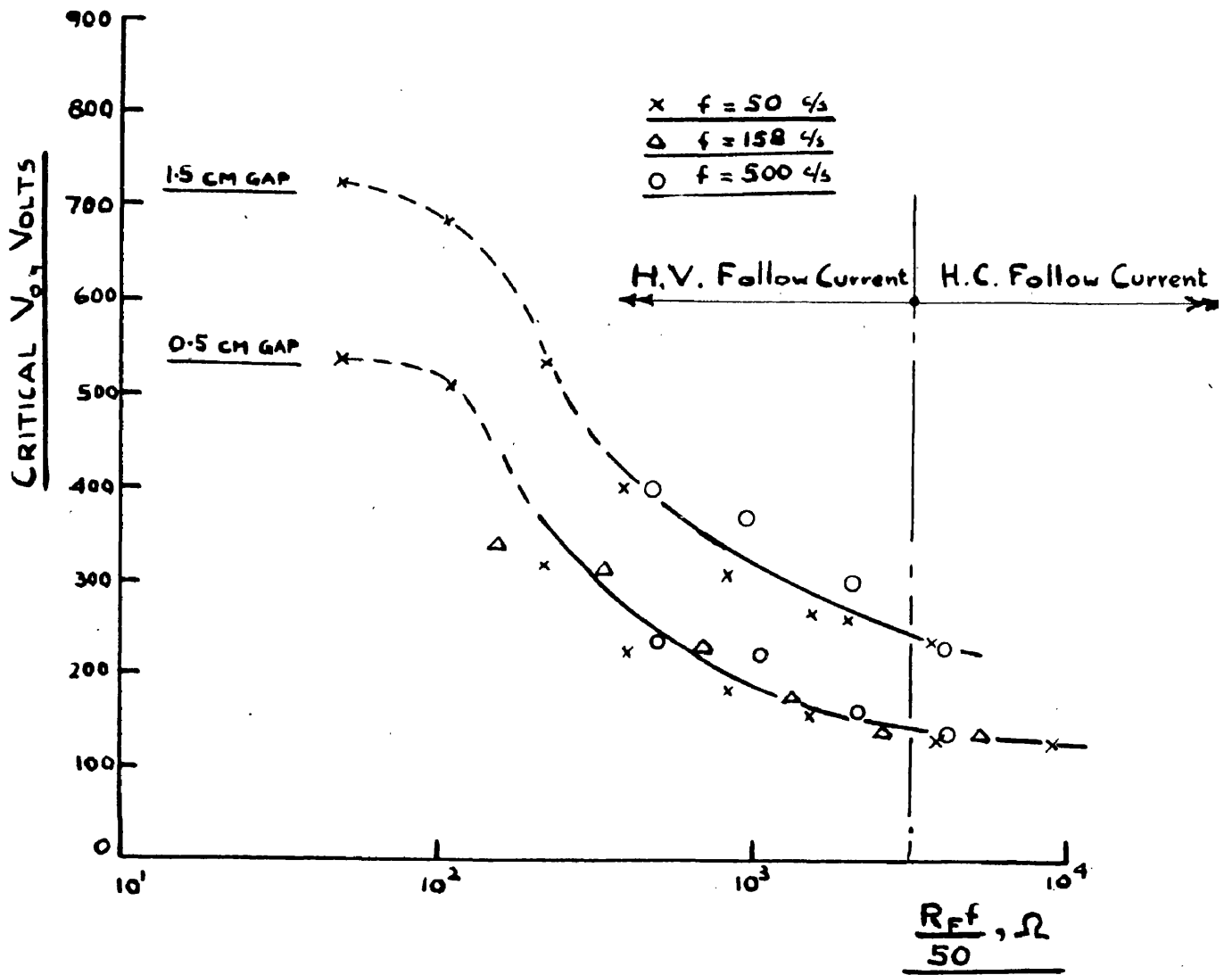


FIG. 29. RELATION BETWEEN  $\frac{R_{ff}}{50}$  AND THE CRITICAL  $V_{0c}$  AT DIFFERENT GAP SPACINGS.

$Z = 40 \Omega$ ;  $R_T = 75 \times 10^3 \Omega$ ;  $C_{IG} = 0.083 \mu F$ ;  $V_{IG0} = 33 kV$ .

THE POINTS SHOWN HAVE BEEN OBTAINED FROM THE APPROPRIATE CURVES OF FIGS. 26-28.

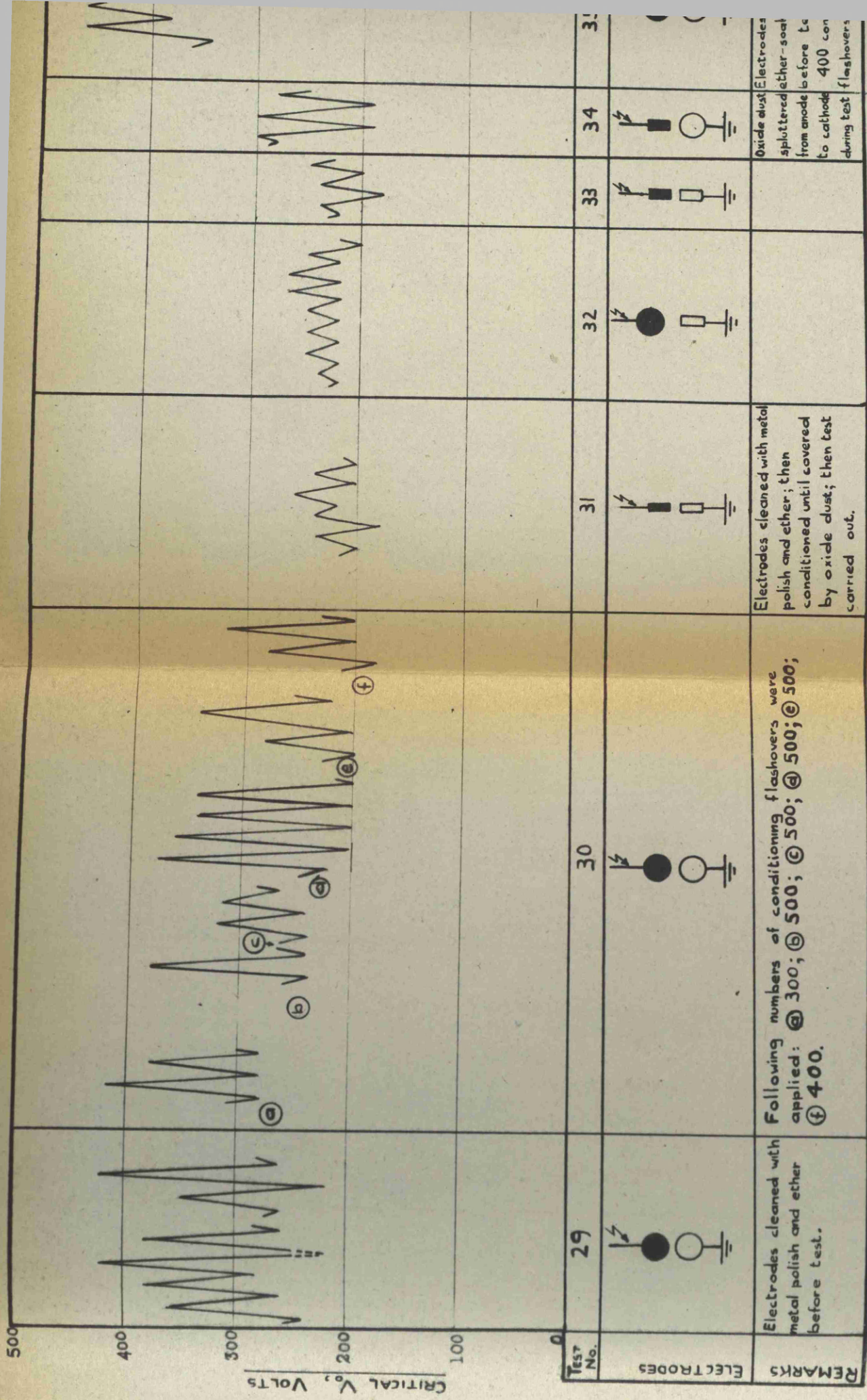


FIG. 30. SEQUENCE DIAGRAM FOR TUNGSTEN ELECTRODES SPACED 0.5 CM APART.

Spherical Electrodes consisted of 2 cm dia. brass spheres having a Tungsten cap 1 cm dia. and 0.5 cm deep.  
 The rods consisted of 0.063 cm dia. Tungsten wire.  
 The Standard Circuit was used

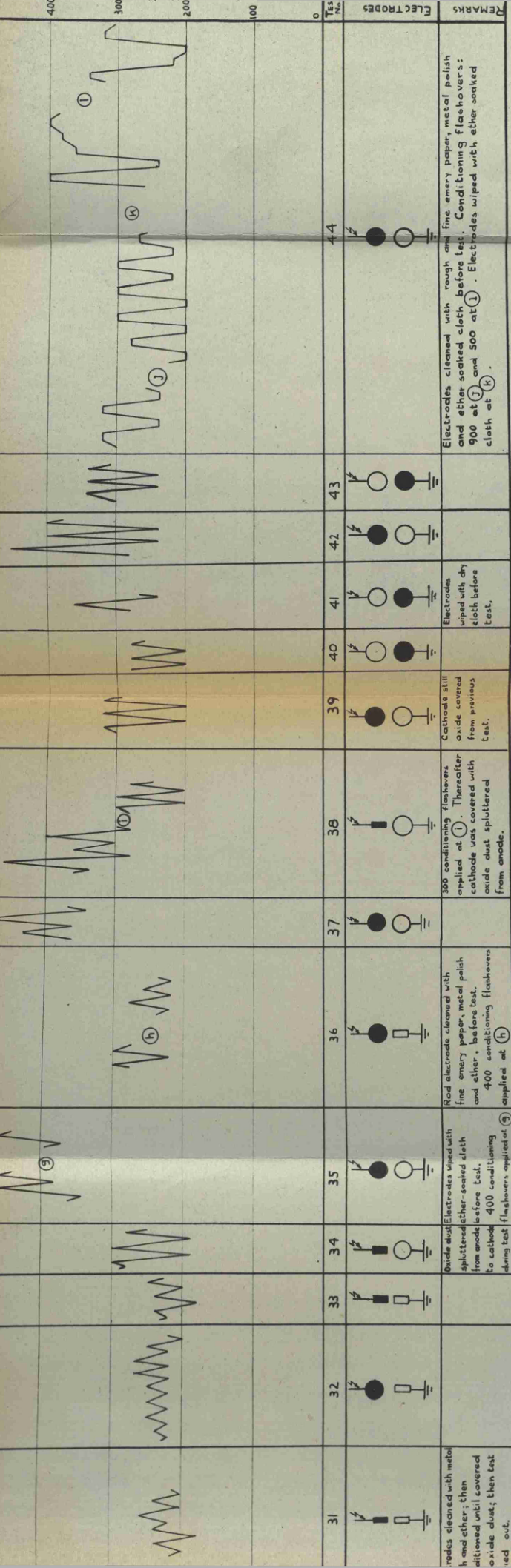
Test No.	Electrodes	Remarks
31		Electrodes cleaned with metal h and other; then conditioned until covered oxide dust; then test red out.
32		
33		
34		Oxide dust splattered from anode before test. to cathode during test flashovers applied at (g)
35		Electrodes wiped with other-soaked cloth before test. 400 conditioning flashovers applied at (g)
36		Red electrode cleaned with fine emery paper, metal polish and other, before test. 400 conditioning flashovers applied at (h)
37		300 conditioning flashovers applied at (i). Thereafter cathode was covered with oxide dust splattered from anode.
38		Cathode still oxide covered from previous test.
39		Electrodes wiped with dry cloth before test.
40		
41		
42		
43		
44		Electrodes cleaned with rough and fine emery paper, metal polish and other soaked cloth before test. Conditioning flashovers: 900 at (j) and 500 at (k). Electrodes wiped with ether soaked cloth at (k)

**Conventions:**

- $\wedge$  Follow Current occurred on each of five successive flashovers.
- $\vee$  Follow Current occurred on none of five successive flashovers.
- $\sphericalangle$  Follow Current occurred on each of five successive flashovers, but not on each of 10 successive flashovers.
- $\sphericalangle$  Follow Current occurred on none of five successive flashovers, but occurred on some of 10 successive flashovers.

0.5 CM APART.  
Langsten cap 1 cm dia. and 0.5 cm deep.

5  
400  
300  
200  
100  
0



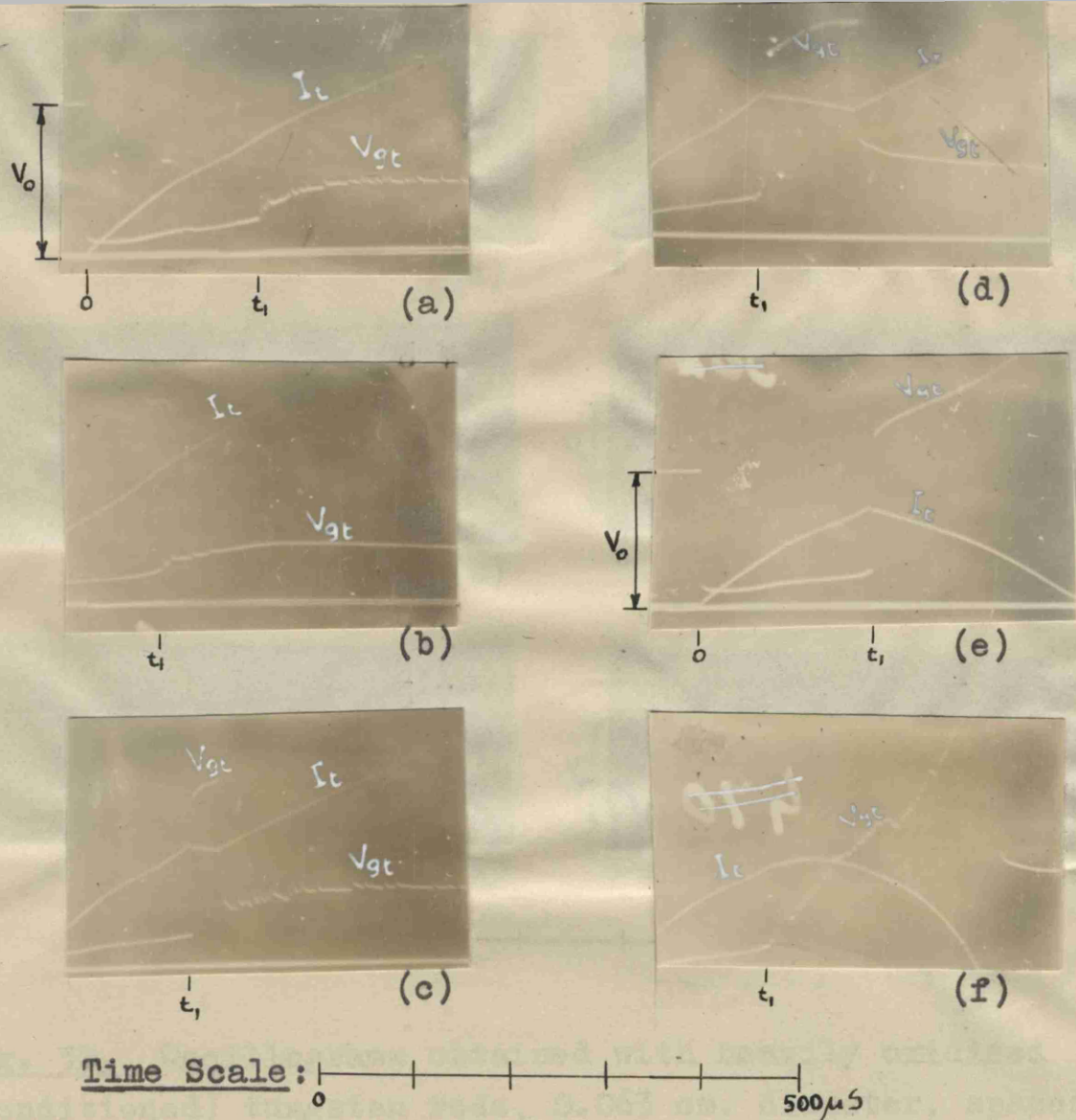


**Fig. 31.** Oscillograms obtained with unconditioned tungsten capped spheres, 2 cm. diameter, spaced 0.5 cm. apart, when  $V_0$  was in the critical range. Standard Circuit.

(a)-(d) Follow Current established.

(e)-(f) Follow Current did not occur.

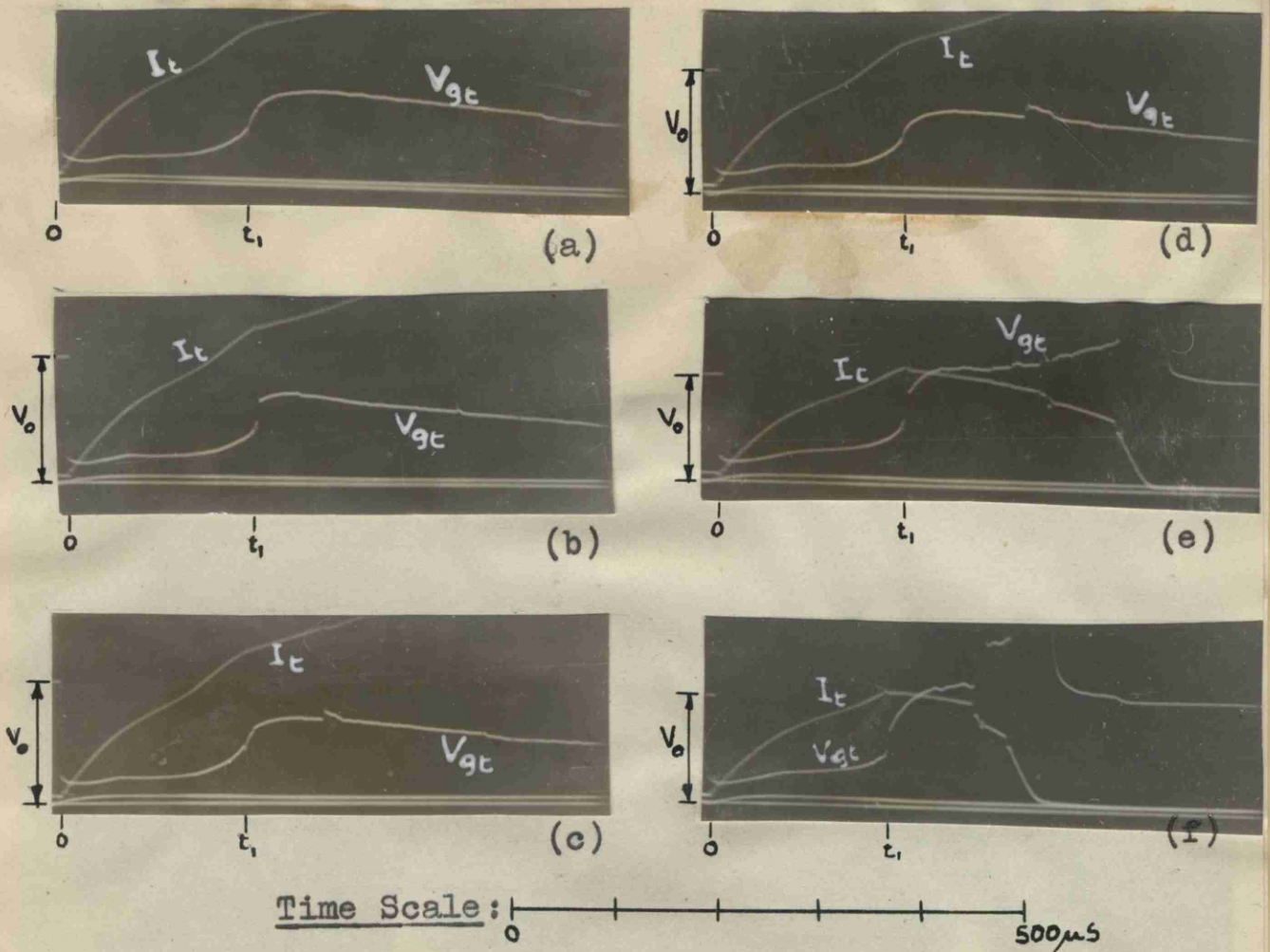


Fig. 32. Oscillograms obtained with heavily oxidised (conditioned) tungsten rods, 0.063 cm. diameter, spaced 0.5 cm. apart, when  $V_0$  was in the critical range. Standard Condition.

(a)-(d) Follow Current established.

(e)-(f) Follow Current did not occur.

Fig. 33. Photograph of 2 cm. diameter tungsten capped spheres, showing arcing surface.

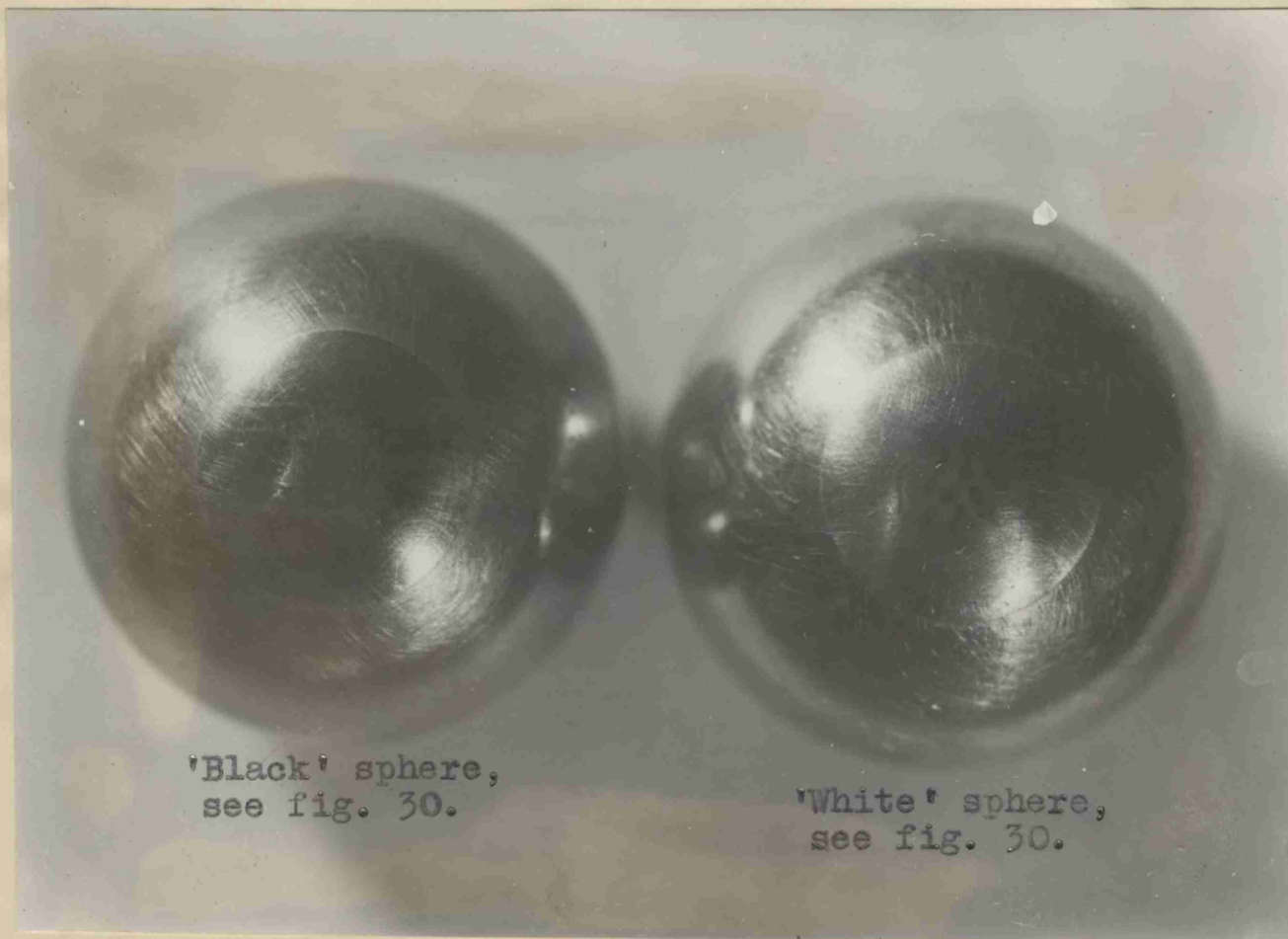


Fig. 33. Photograph of 2 cm. diameter, tungsten capped spheres, showing arcing surfaces.

Fig. 34. Sequence Diagram for 0.047 cm diameter tungsten  
Electrodes, spaced 0.5 cm apart, 100000 volt/cm

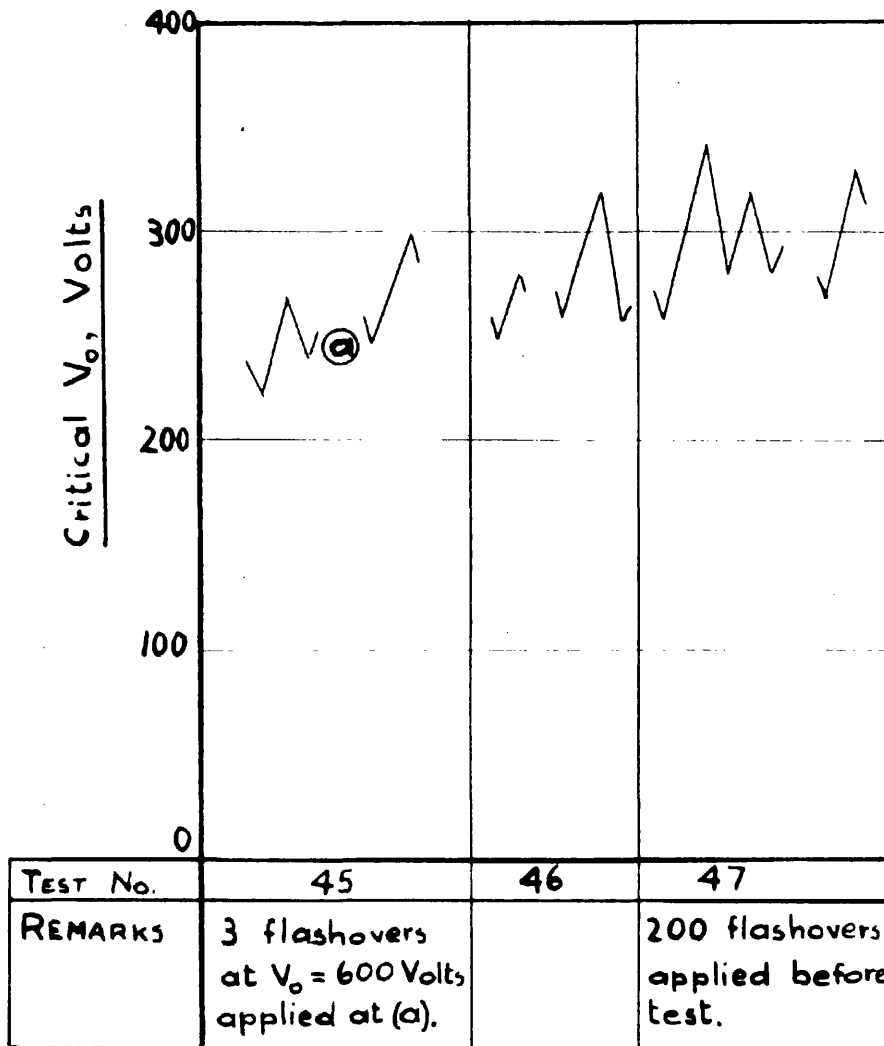


FIG.34. SEQUENCE DIAGRAM FOR 0.047 CM DIAMETER PLATINUM ELECTRODES, SPACED 0.5 CM APART. Standard Circuit.



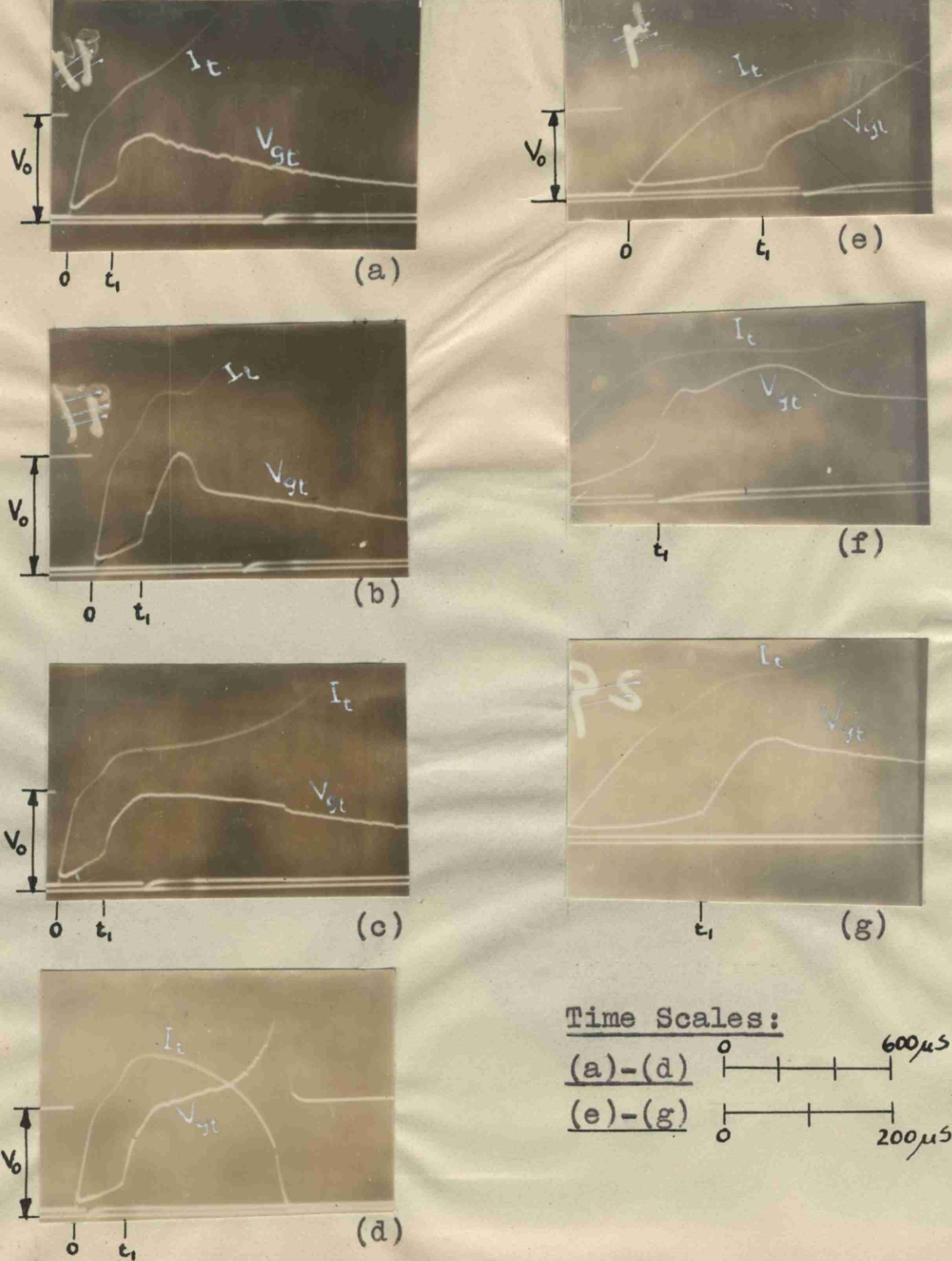


Fig. 36. Oscillograms obtained with conditioned brass spheres, 2 cm. diameter, spaced 0.5 cm. apart, when  $V_0$  was in the critical range. Standard Circuit.

(a)-(c) and (f)-(g) Follow Current established.

(d)-(e) Follow Current did not occur.

The two curves are obtained in two test runs  
carried out at an interval of 14 days.

Vertical lines give the scatter in  $\%$ , and horizontal  
lines the mean, for each test.

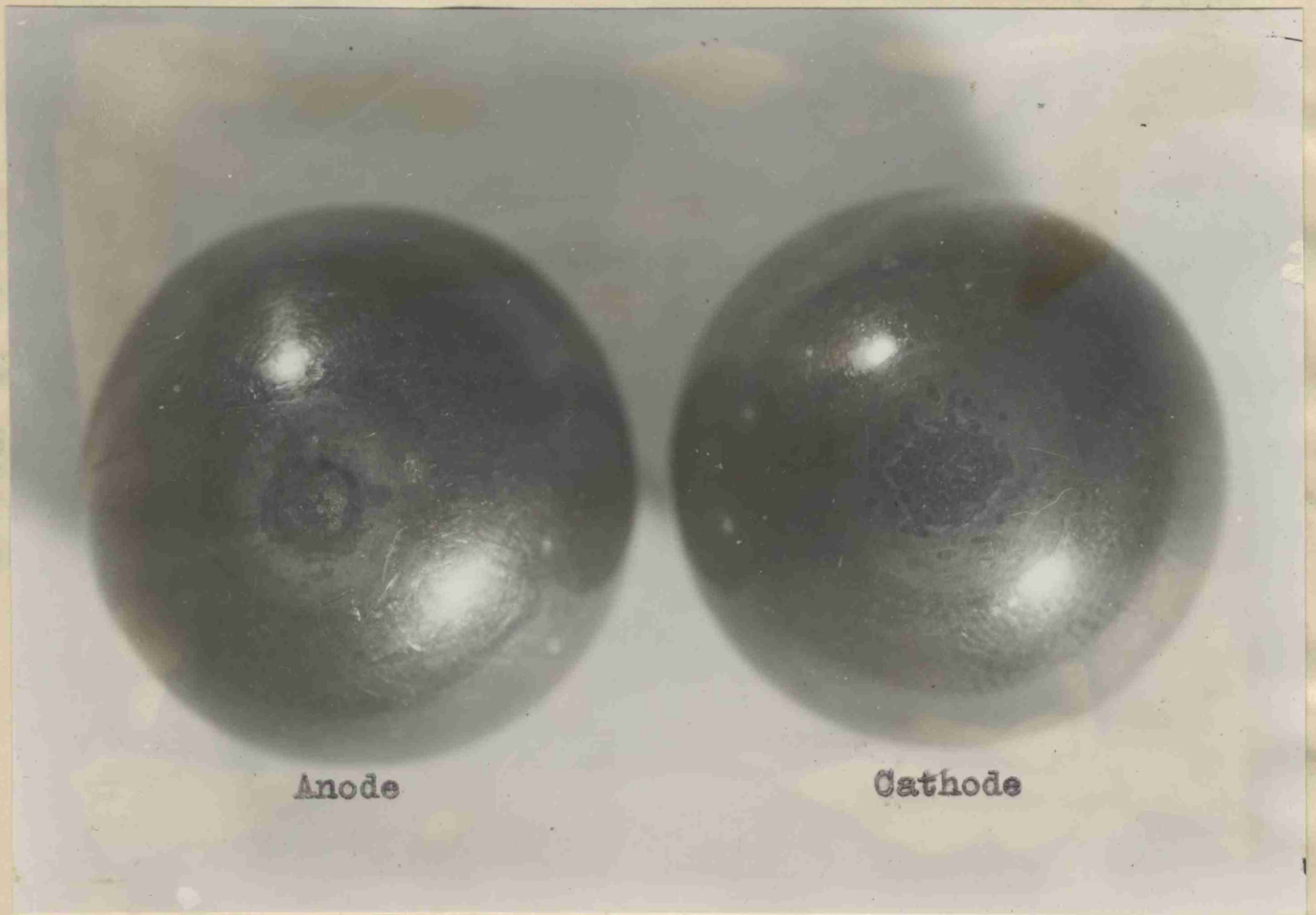
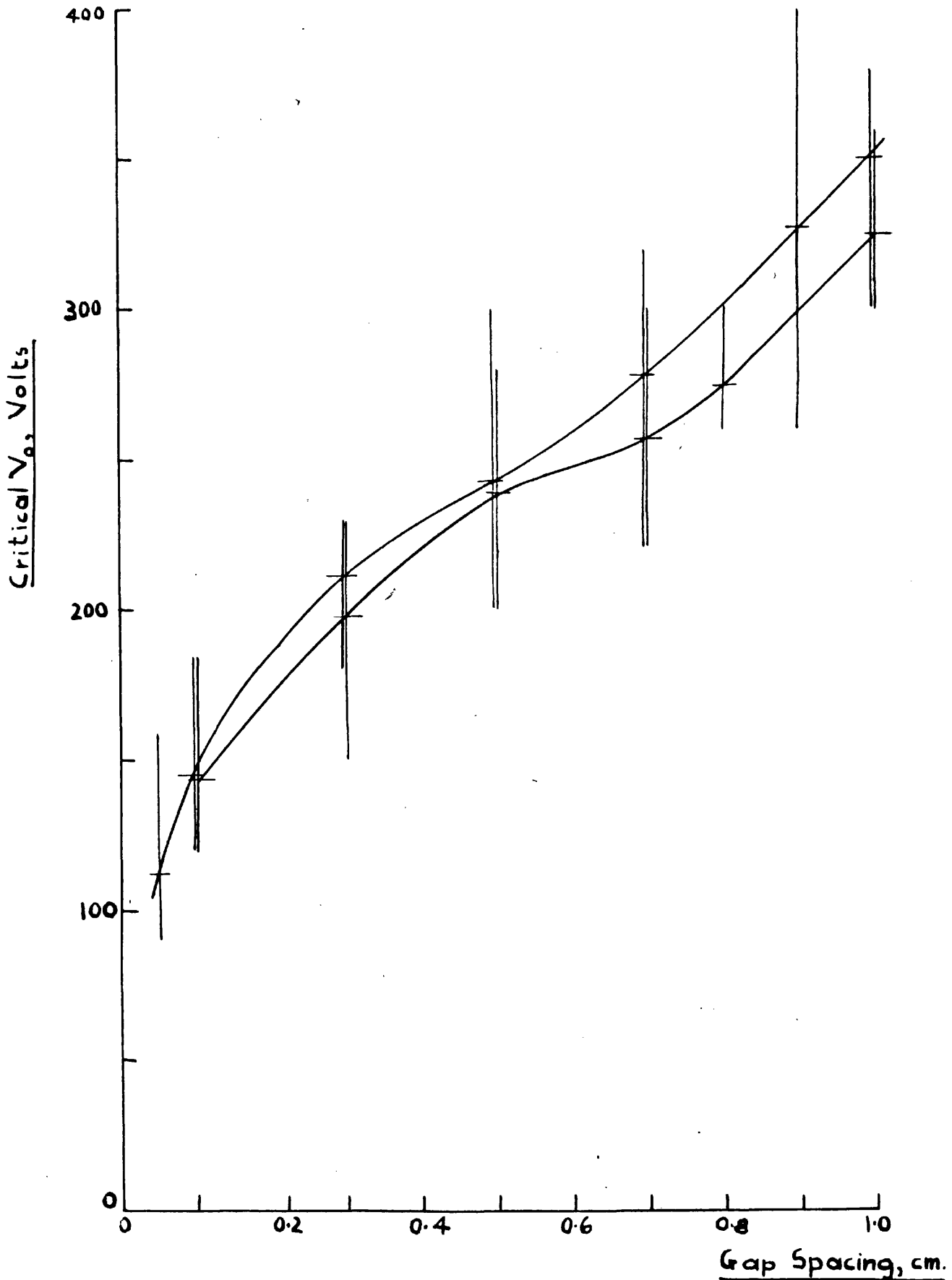


Fig. 37. Photograph of 2 cm brass spheres, showing arcing  
surfaces.

Standard Circuit; n = 5.

The two curves were obtained in two test runs carried out at an interval of 19 days.

Vertical lines give the scatter in  $V_0$ , and horizontal lines the mean, for each test.



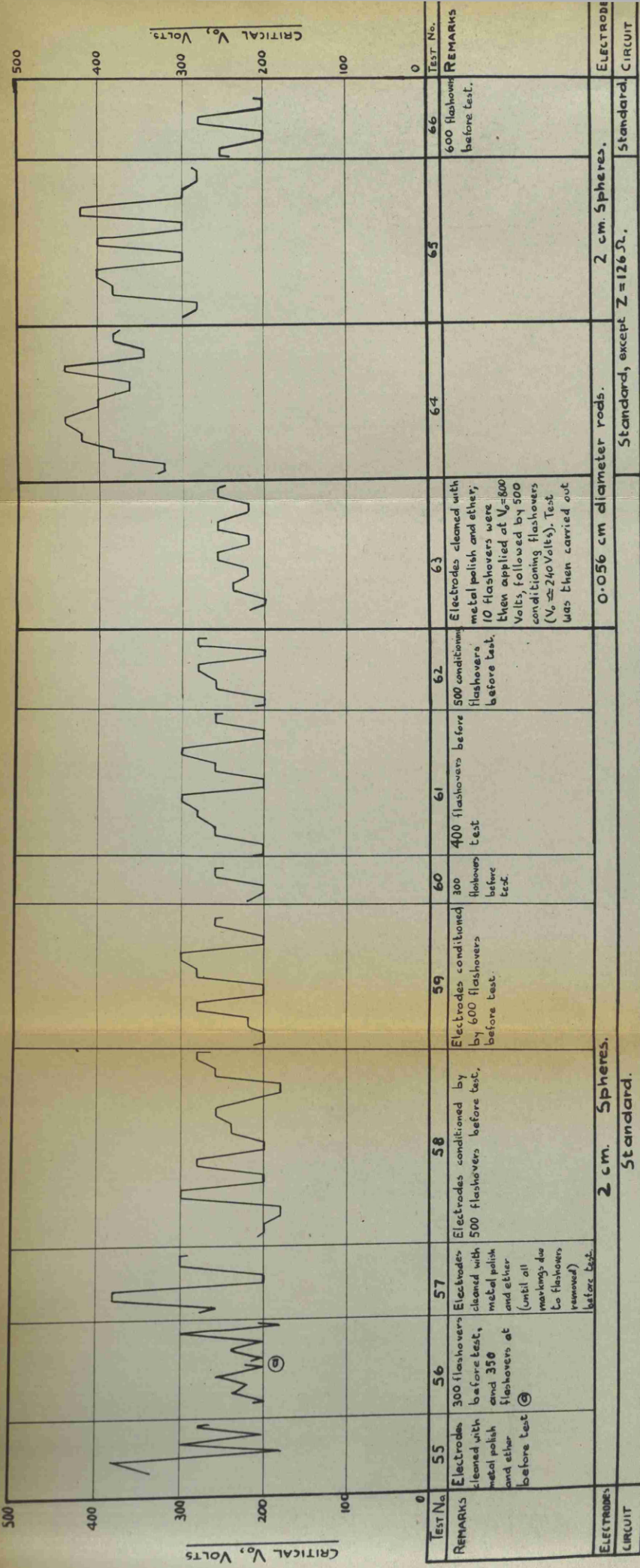


FIG. 39. SEQUENCE DIAGRAM FOR STEEL ELECTRODES, SPACED 0.5 CM APART.  
Conventions as in fig. 30.



Fig. 40. Photograph of 2 cm steel spheres, showing arcing surfaces.

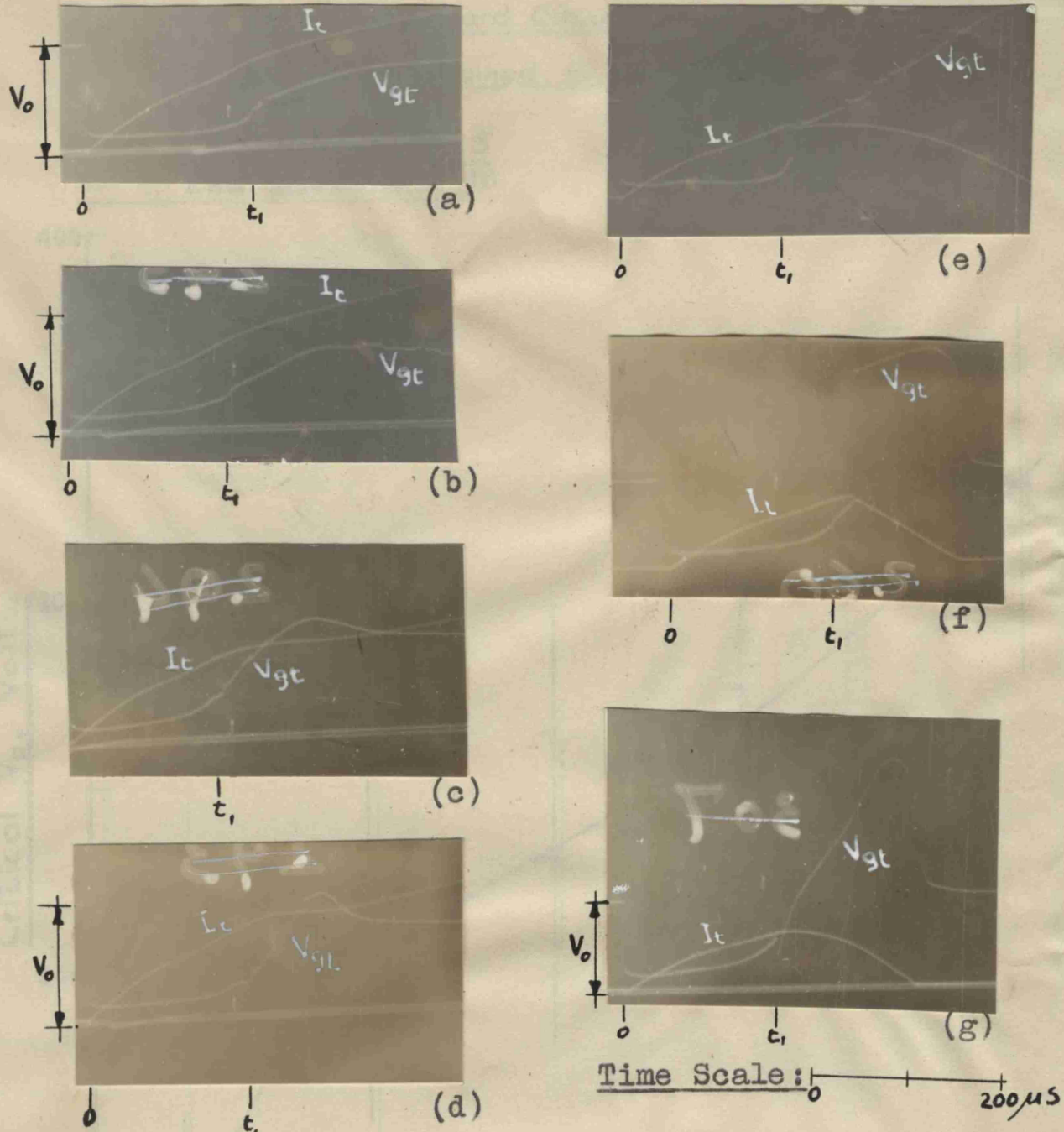


Fig. 41. Oscillograms obtained with conditioned steel spheres, 2 cm. diameter, spaced 0.5 cm. apart, when  $V_0$  was in the critical range. Standard Circuit.

(a)-(d) Follow Current established.

(e)-(g) Follow Current did not occur.

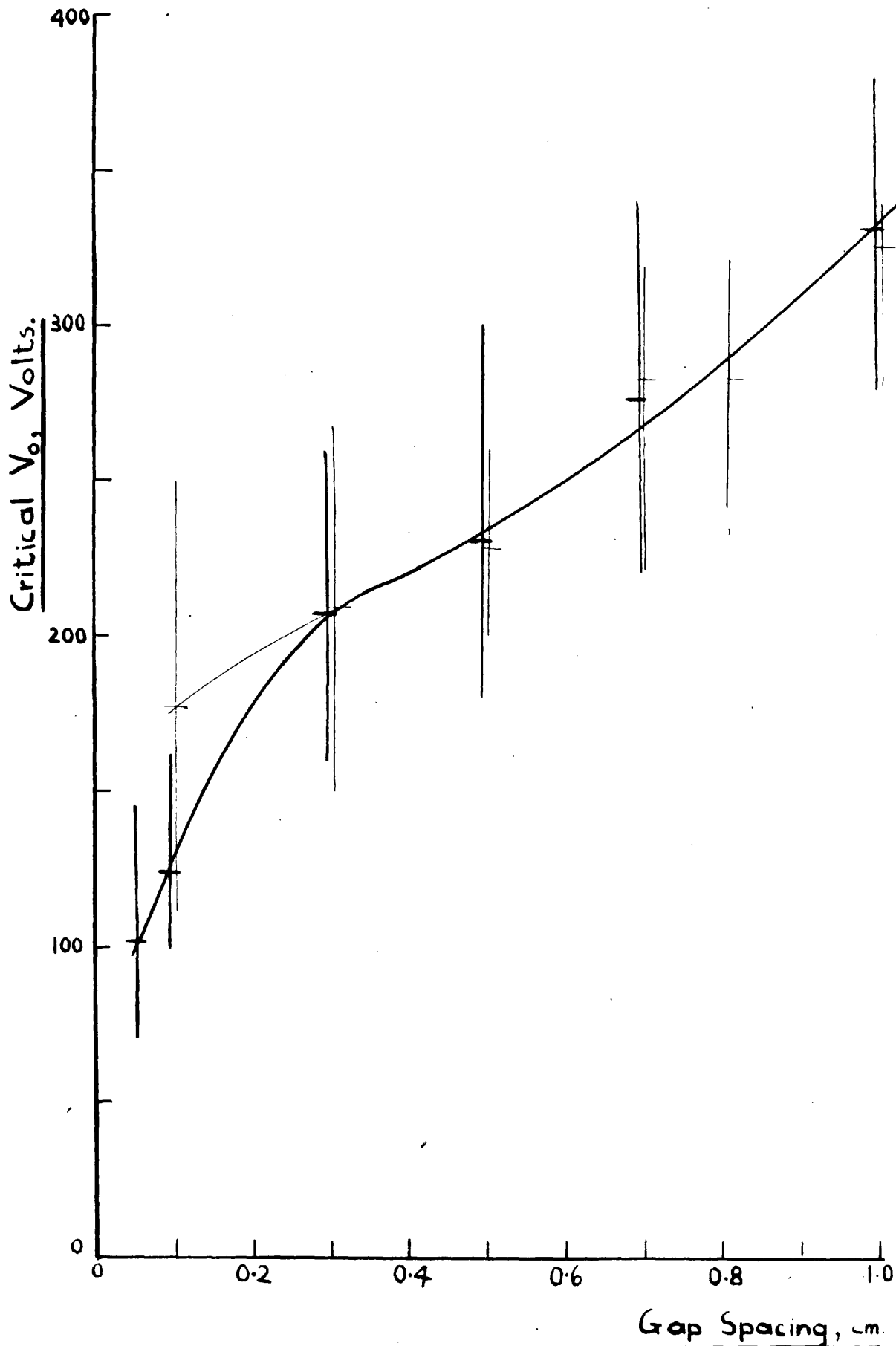
FIG. 42. SPACING DIAGRAM FOR 2 CM DIAMETER, HEAVILY OXIDISED

STEEL SPHERES. Standard Circuit.

These results were obtained in two test runs, at an interval of 7 weeks.

—— 1st test run, n=5

—— 2nd test run, n=10



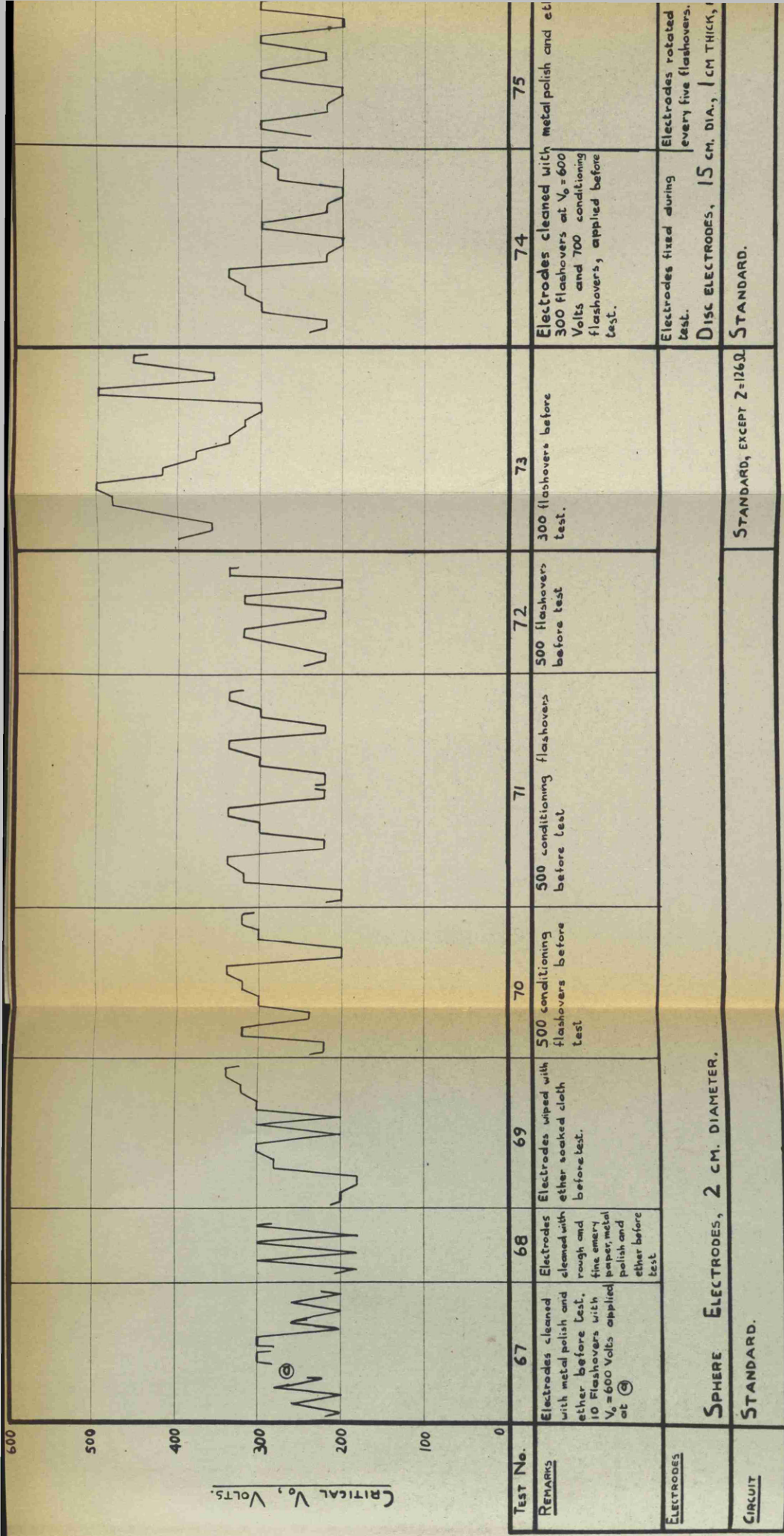
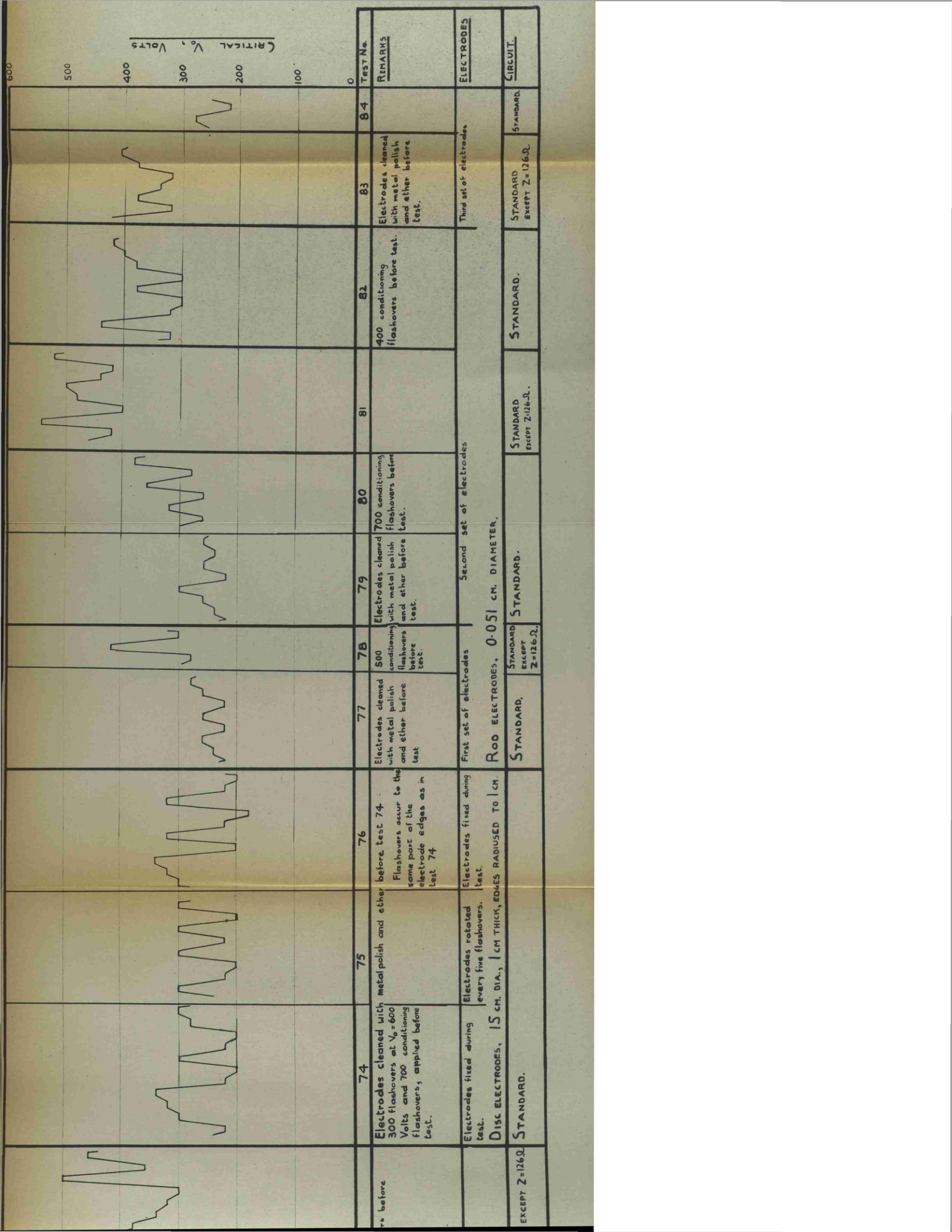


Fig. 43. SEQUENCE DIAGRAM FOR ALUMINIUM ELECTRODES SPACED 0.5 CM. APART. Conventions as on fig. 30.



Critical  $V_c$ , Volts

TEST No.	REMARKS	ELECTRODES
74	Electrodes cleaned with 300 flashovers at $V_c = 600$ Volts and 700 conditioning flashovers, applied before test.	First set of electrodes
75	Electrodes rotated every five flashovers.	Second set of electrodes
76	Flashovers occur to the same part of the electrode edges as in test 74.	ROD ELECTRODES, 0.051 CM. DIAMETER.
77	Electrodes cleaned with metal polish and other before test.	STANDARD, EXCEPT Z=126.02.
78	500 conditioning flashovers before test.	STANDARD, EXCEPT Z=126.02.
79	Electrodes cleaned with metal polish and other before test.	STANDARD.
80	700 conditioning flashovers before test.	STANDARD EXCEPT Z=126.02.
81	Electrodes cleaned with metal polish and other before test.	STANDARD EXCEPT Z=126.02.
82	400 conditioning flashovers before test.	STANDARD.
83	Electrodes cleaned with metal polish and other before test.	STANDARD EXCEPT Z=126.02.
84	Third set of electrodes.	STANDARD.

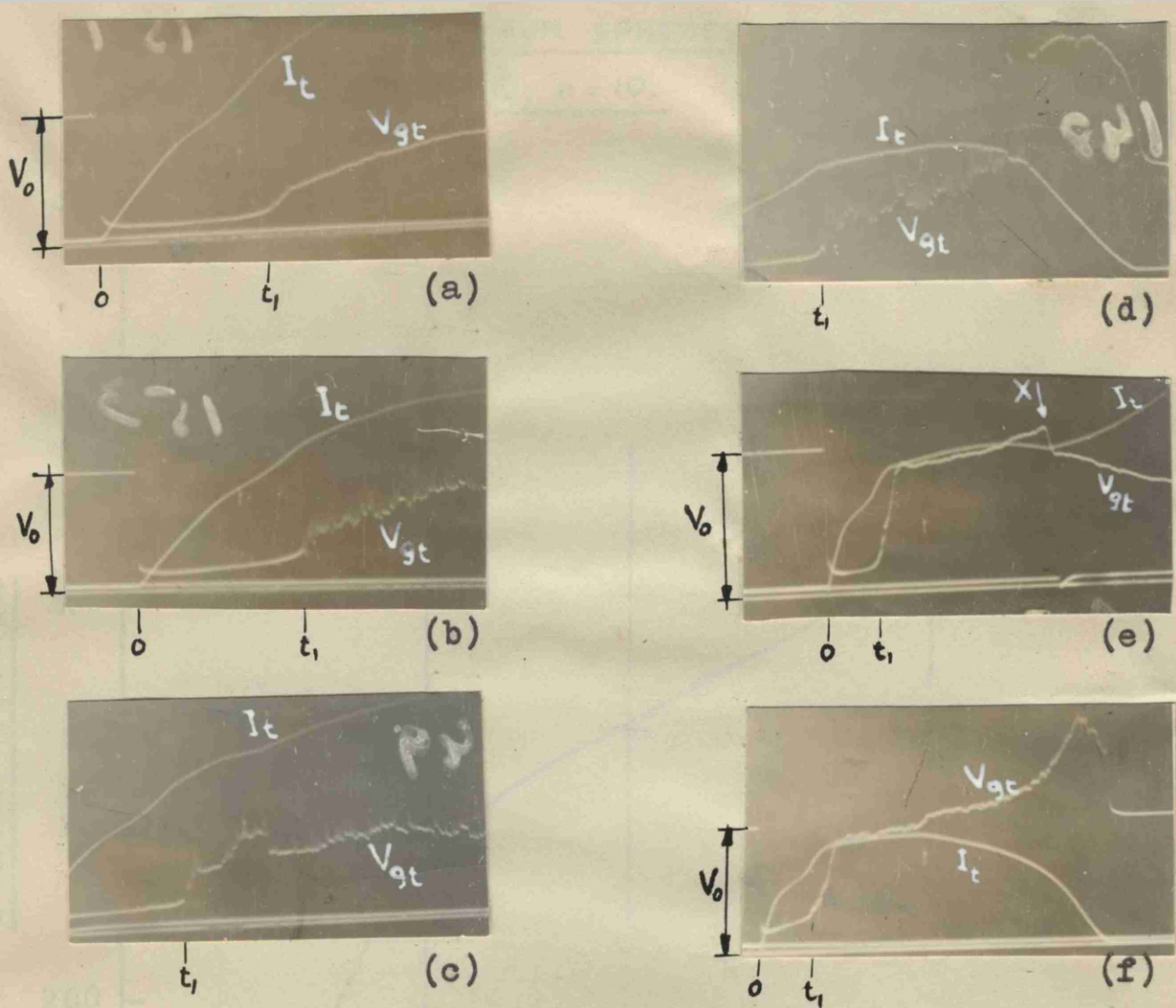
EXCEPT Z=126.02

DISC ELECTRODES, 15 CM. DIA., 1 CM THICK, EDGES RADIUSED TO 1 CM.

Electrodes fixed during test.



Fig. 44. Photograph of 2 cm diameter aluminium spheres, showing arcing surfaces.



Time Scales:

(a)-(d)

0 600  $\mu$ s

(e)-(f)

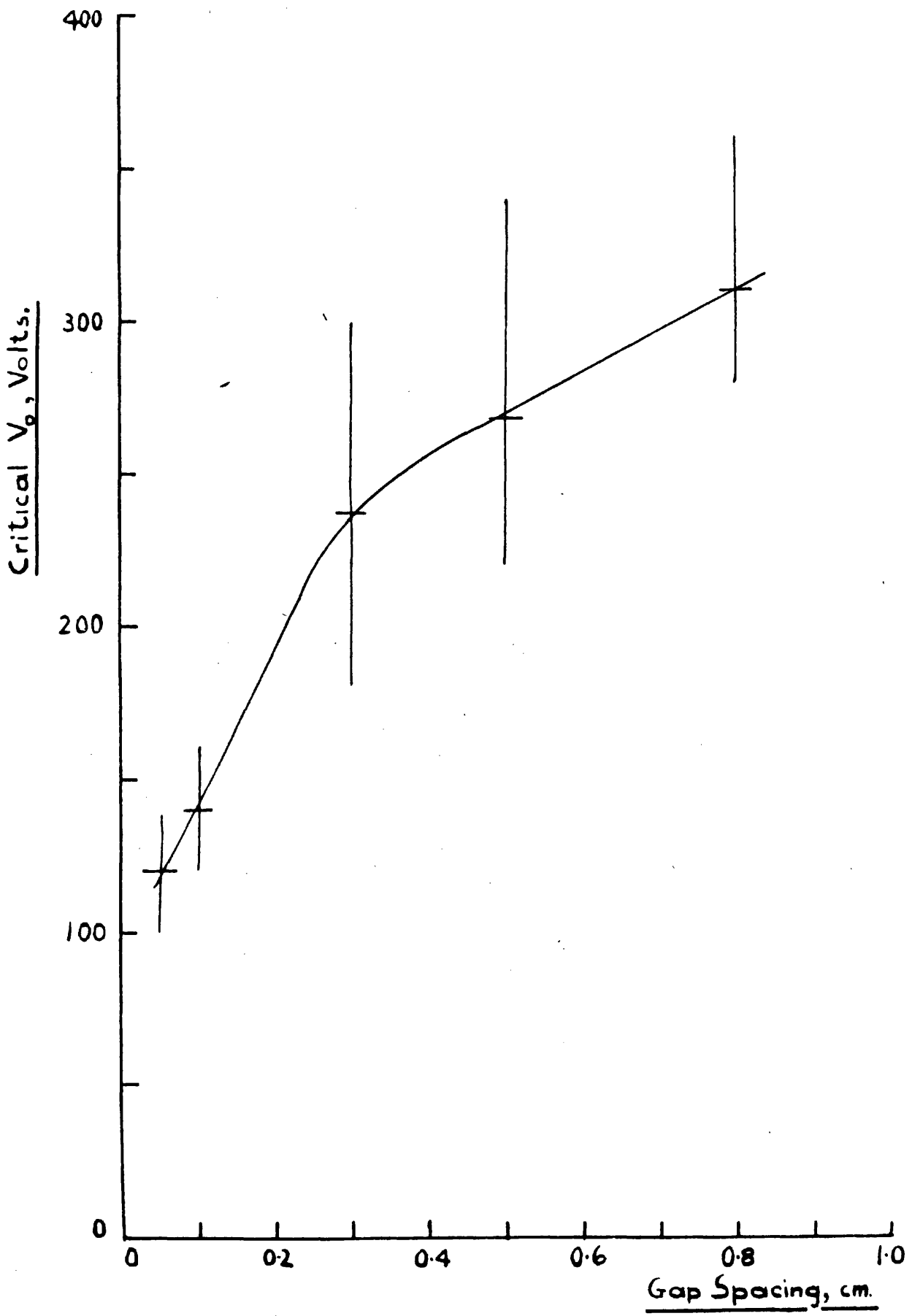
0 200  $\mu$ s

**Fig. 45.** Oscillograms obtained with aluminium spheres, 2 cm. diameter, spaced 0.5 cm. apart, when  $V_0$  was in the critical range. Standard Circuit.

(a)-(c) and (e) Follow Current established.

(d) and (f) Follow Current did not occur.

FIG. 46. SPACING DIAGRAM FOR 2 cm DIAMETER, HEAVILY OXIDISED ALUMINIUM SPHERES.  
Standard Circuit; n = 10.



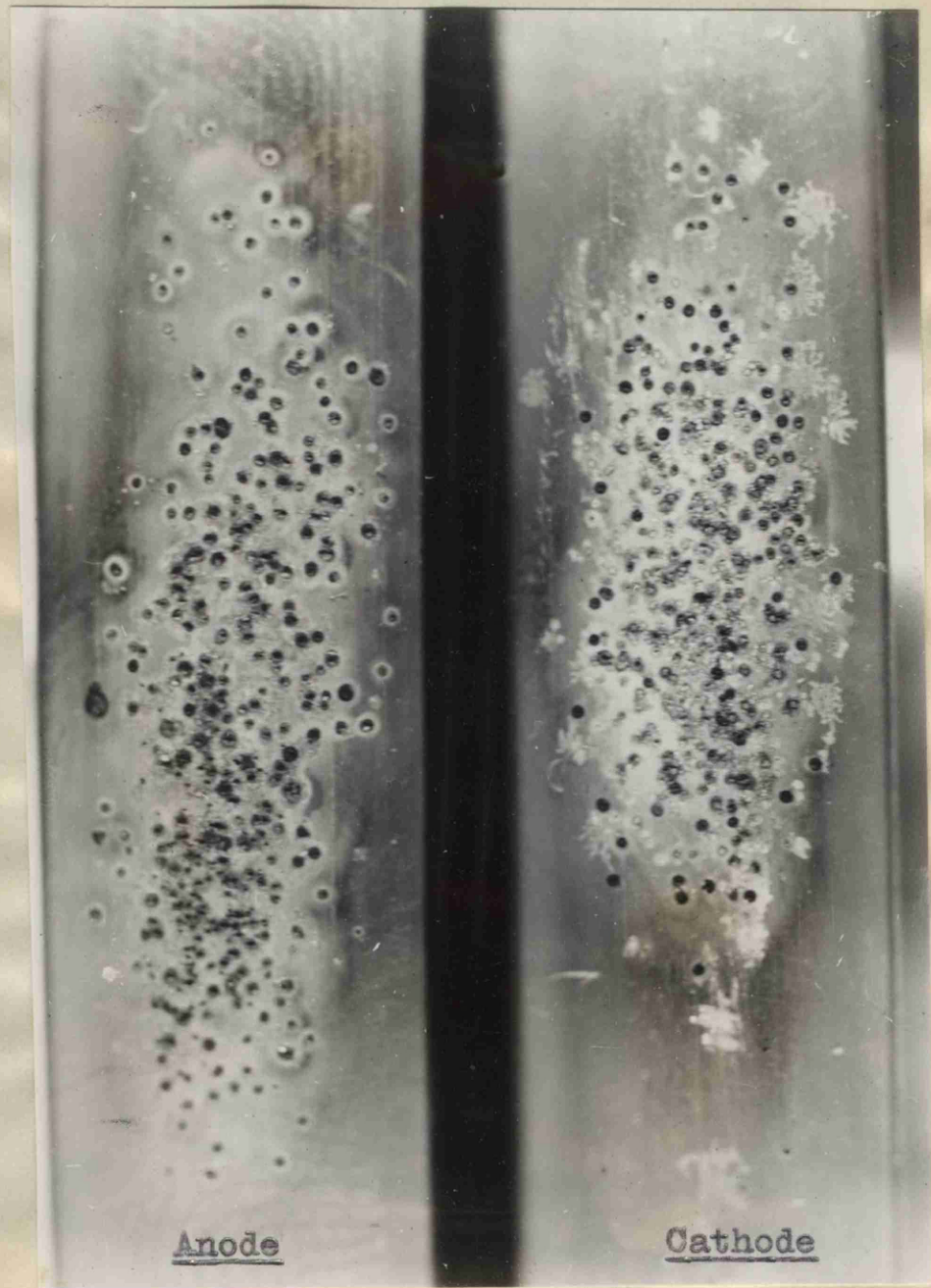


Fig. 47(a). Photograph of conditioned sections of aluminium disc electrodes. Flashovers 4.6 times full size.

(b) Some of the flashovers resulted in follow current.

(c) All flashovers resulted in follow current.



Anode

(b)

Cathode



Anode

(c)

Cathode

Fig. 47 ((b) and (c)). Photographs of sections of aluminium disc electrodes to which only five flashovers had been applied. 4.6 times full size.

(b) None of the flashovers resulted in follow current.

(c) All flashovers resulted in follow current.

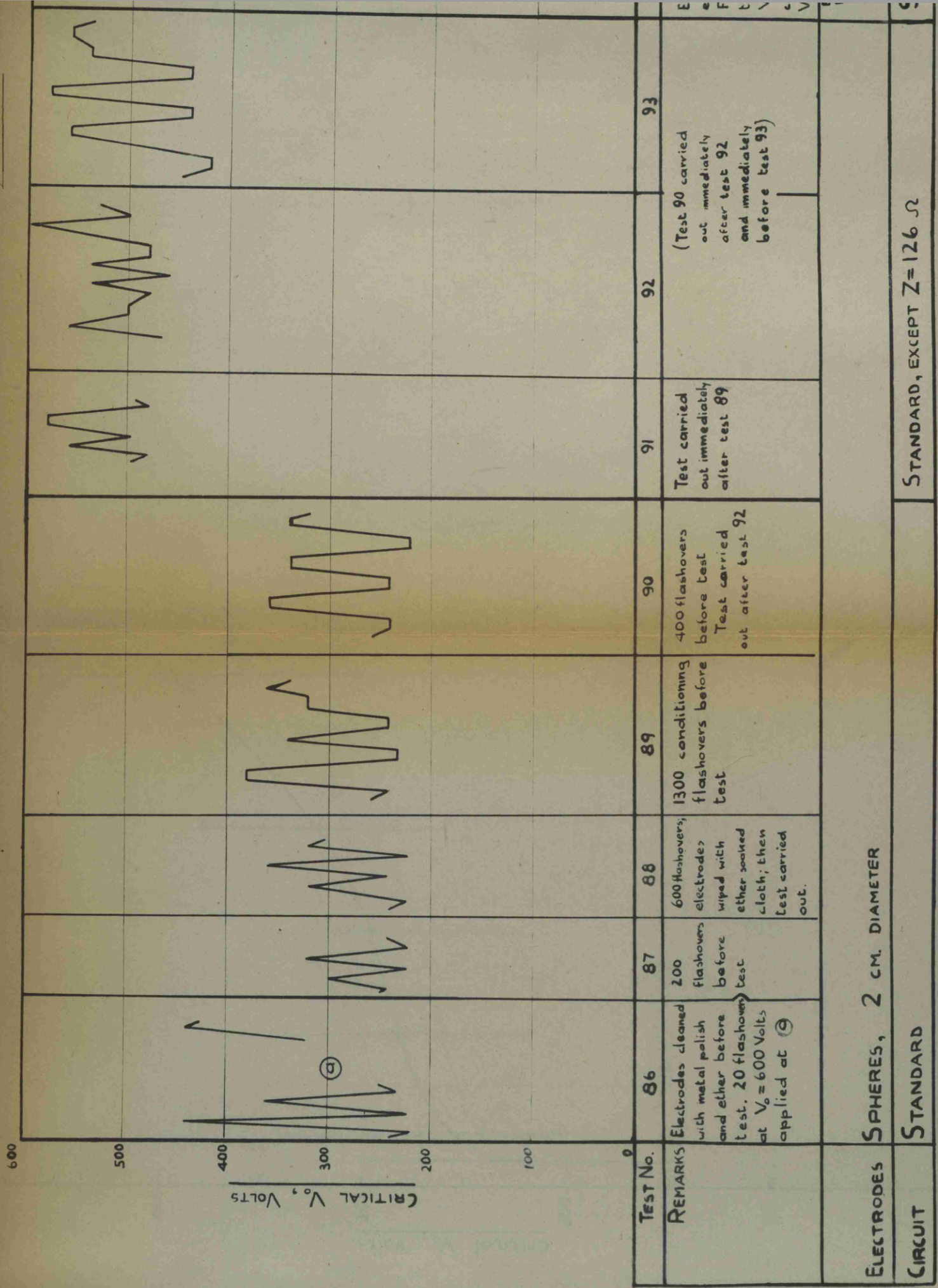
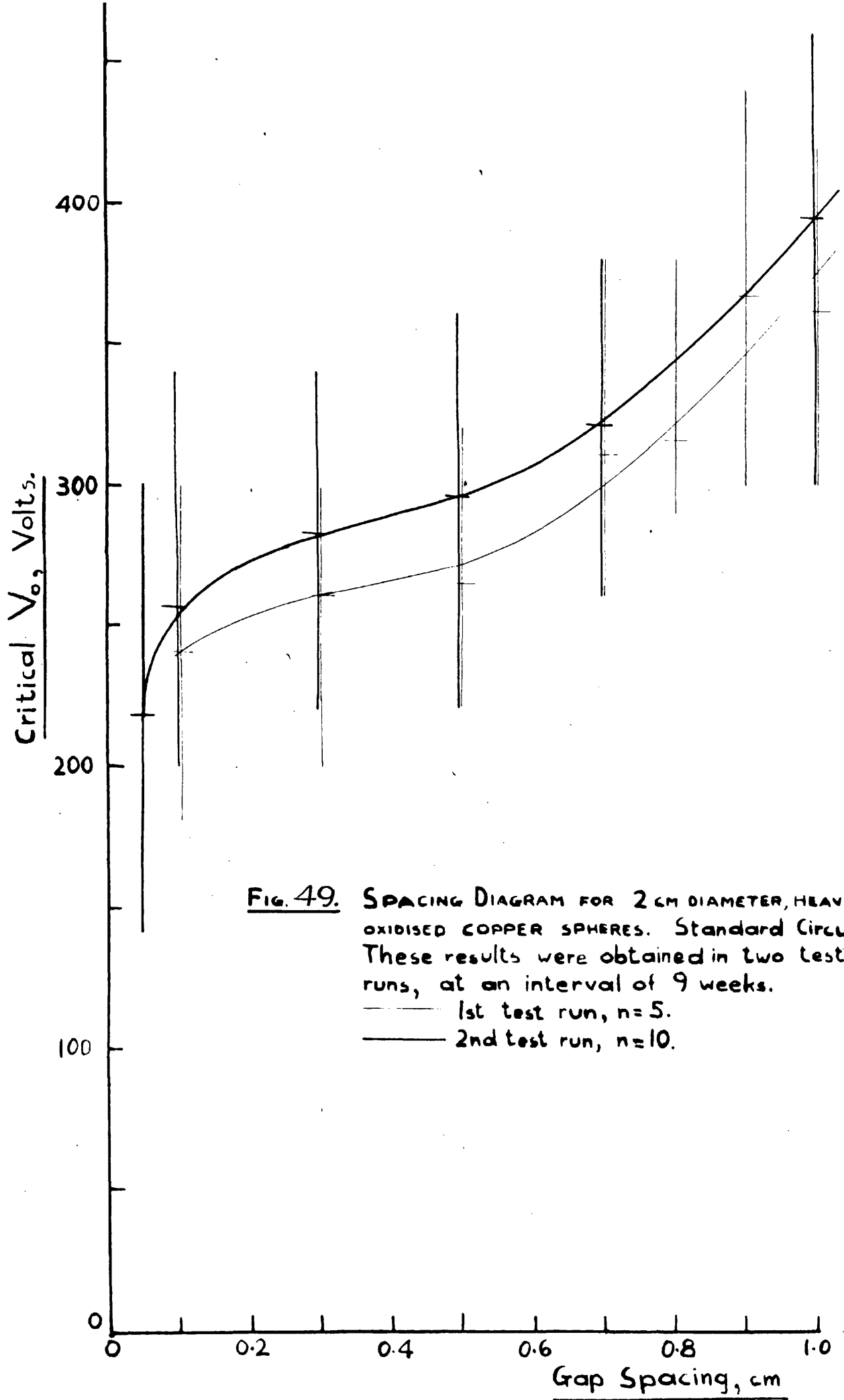


FIG. 48. SEQUENCE DIAGRAM FOR COPPER ELECTRODES SPACED 0.5 CM APART.  
Conventions as in fig. 30.





**FIG. 49.** SPACING DIAGRAM FOR 2 CM DIAMETER, HEAVILY OXIDISED COPPER SPHERES. Standard Circuit. These results were obtained in two test runs, at an interval of 9 weeks.  
 ——— 1st test run, n=5.  
 - - - 2nd test run, n=10.

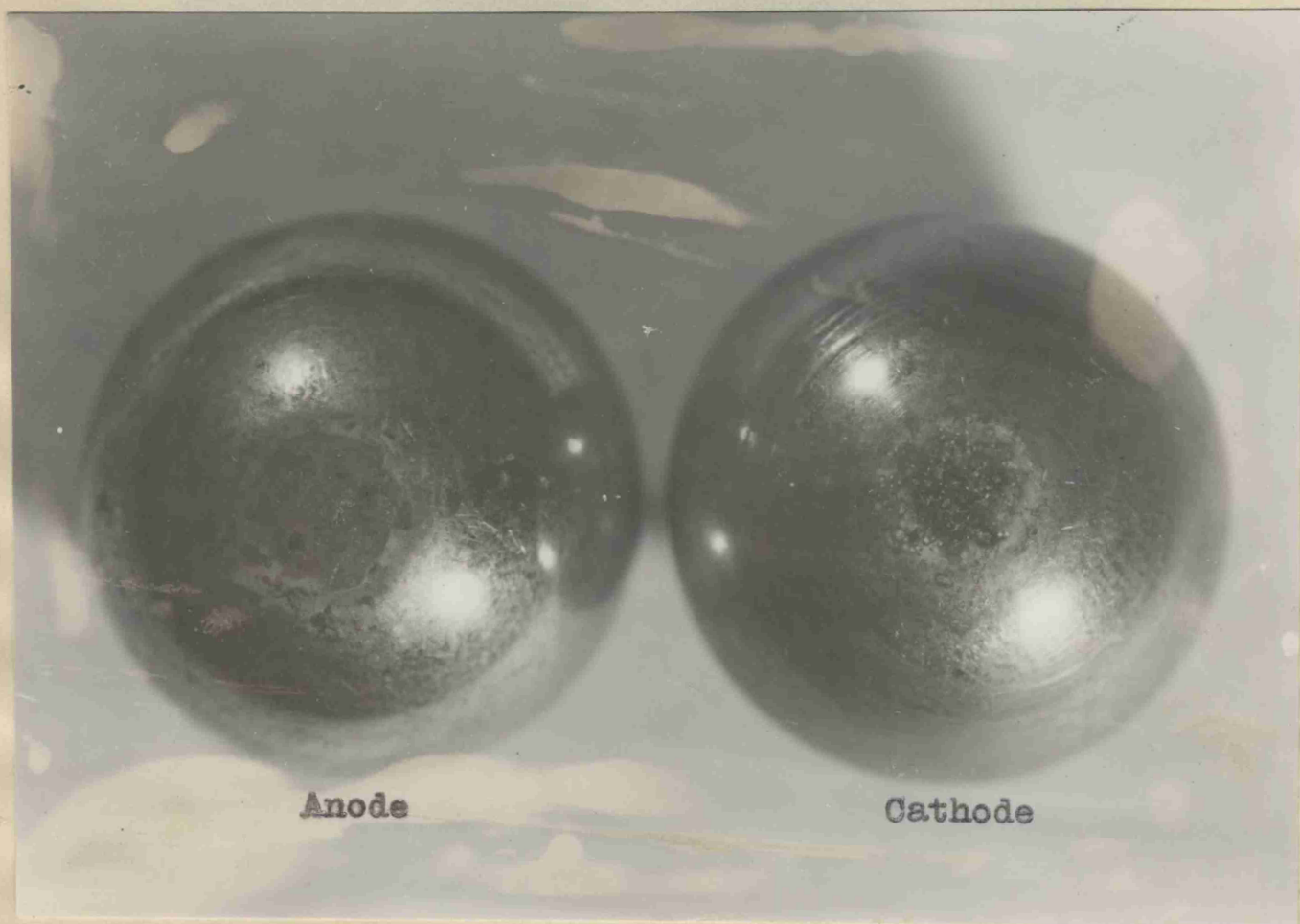
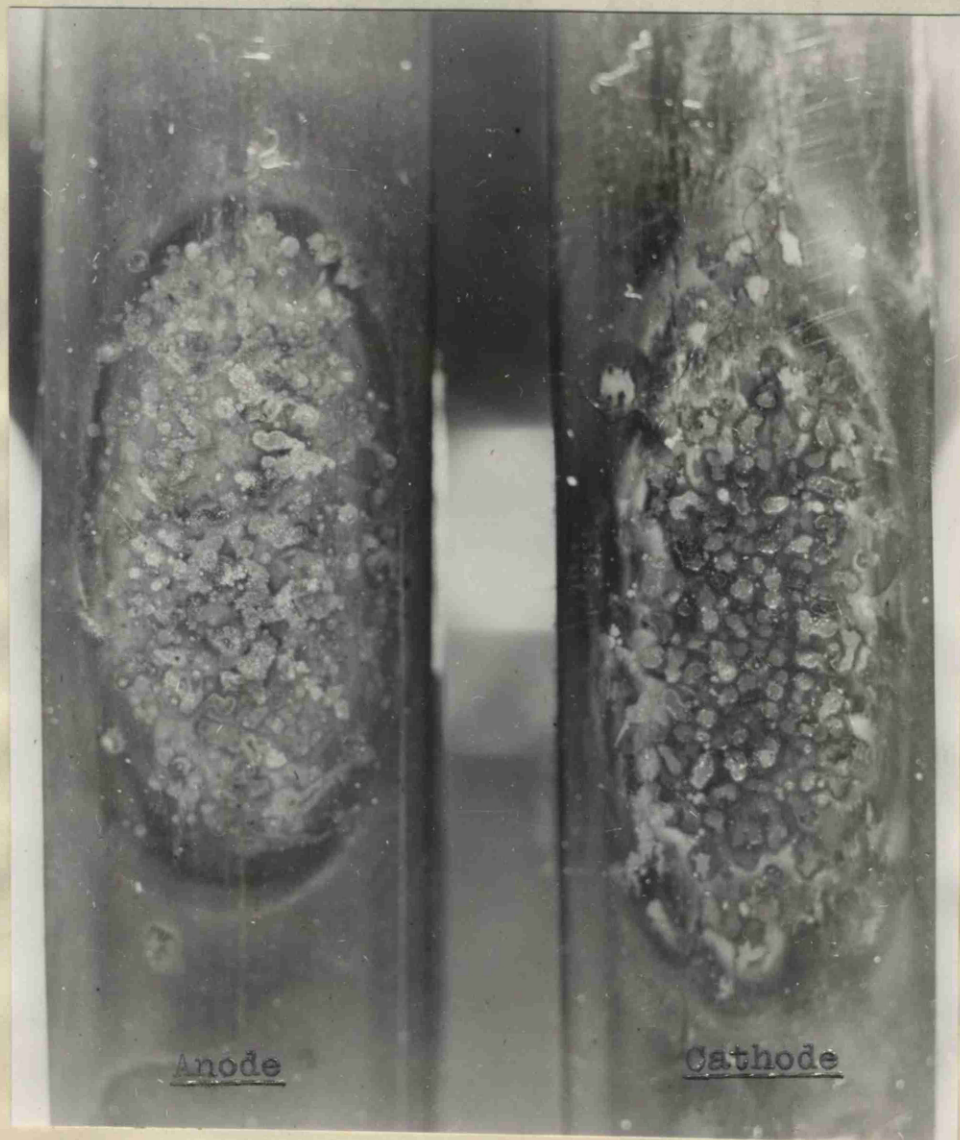


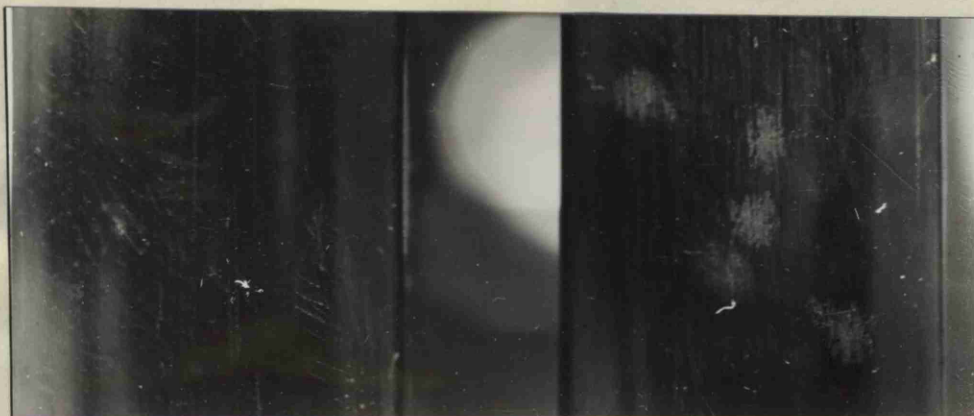
Fig. 50 Photograph of 2 cm copper spheres, showing arcing surfaces.



(8)  
Fig. 51. Photograph of conditioned sections  
of copper disc electrodes.  
4.3 times full size.

(a) None of the flashovers resulted  
in follow current.

(b) Follow current became established  
after every flashover.



Anode

Cathode

(a)



Anode

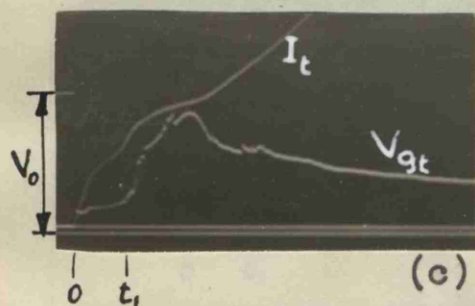
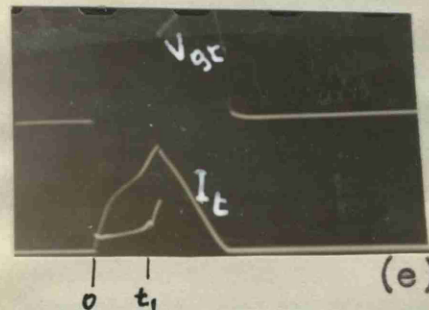
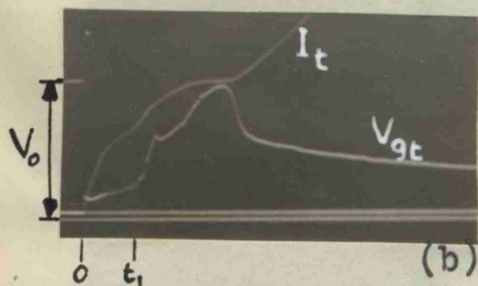
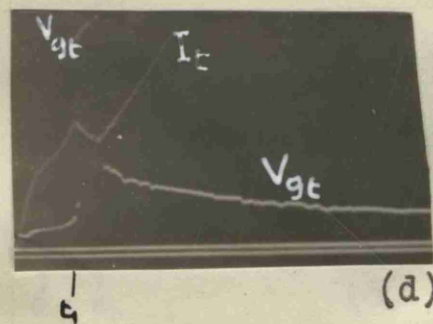
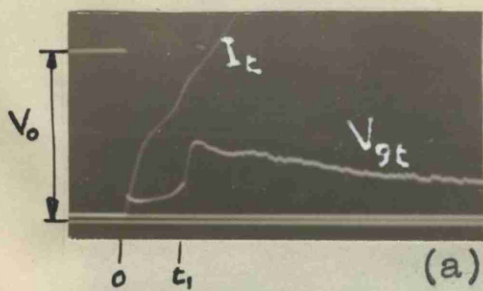
Cathode

(b)

Fig. 52. Photographs of sections of copper disc electrodes to which only five flashovers had been applied. 4.3 times full size.

(a) None of the flashovers resulted in follow current.

(b) Follow current became established after every flashover.

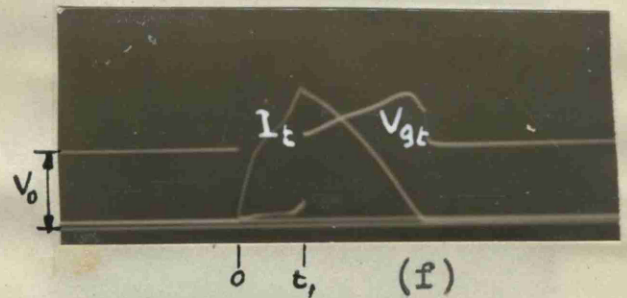
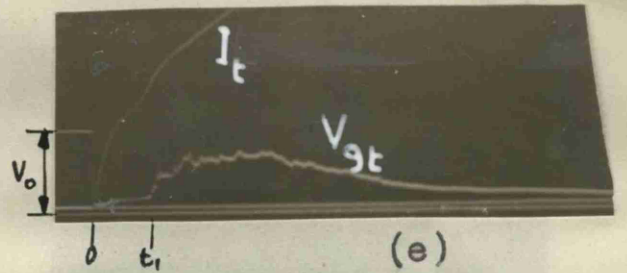
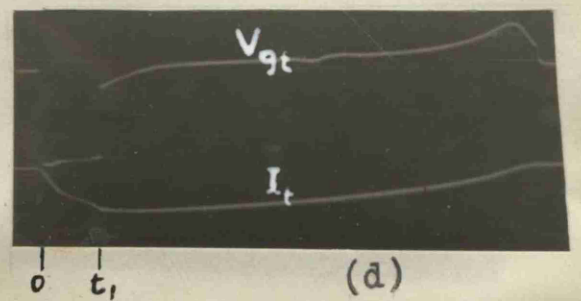
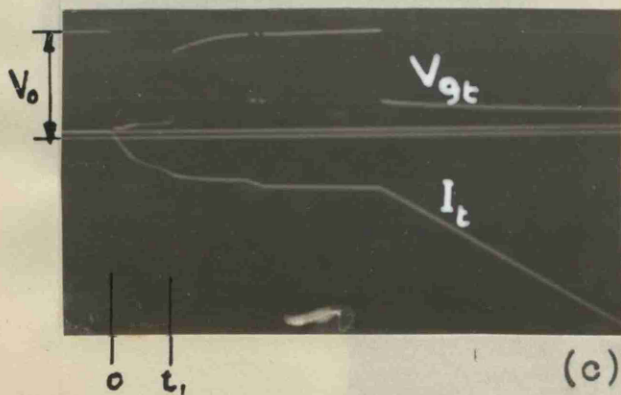
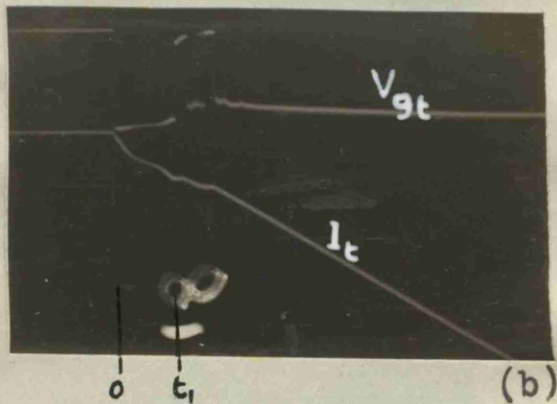
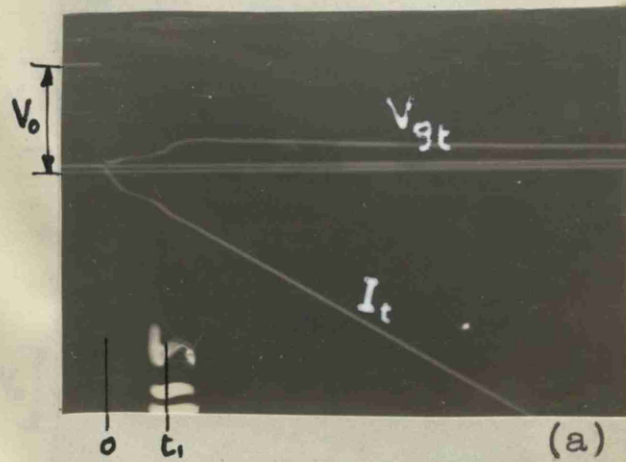


Time Scale: 0 ——— 600  $\mu$ s

Fig. 53. Oscillograms obtained with conditioned copper discs spaced 0.5 cm apart, when the value of  $V_0$  was in the critical range. Standard Circuit.

(a)-(d) Follow Current established.

(e) Follow Current did not occur.

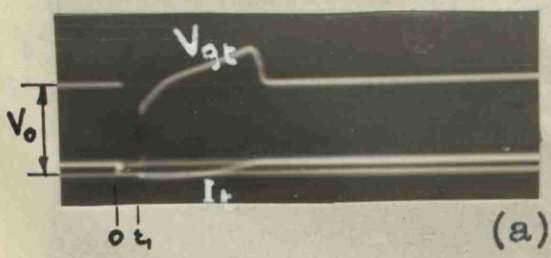


Time Scale: 0 ————— 600  $\mu$ s

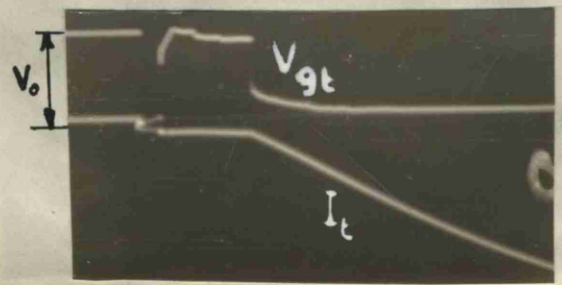
**Fig. 54.** Oscillograms obtained with unconditioned copper discs, spaced 0.5 cm. apart, when the value of  $V_0$  was in the critical range. Standard Circuit.

(a)-(c) and (e) Follow Current established.

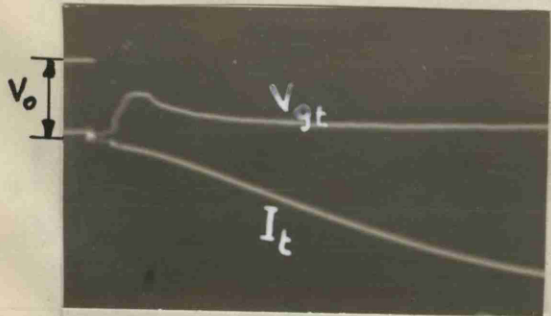
(d) and (f) Follow Current did not occur.



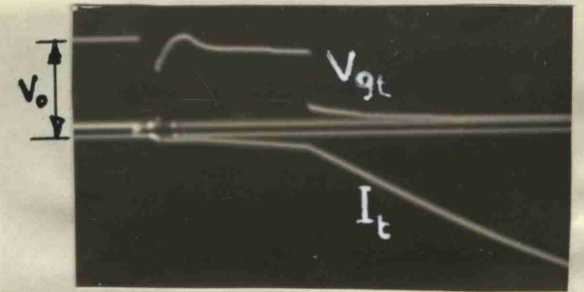
(a)



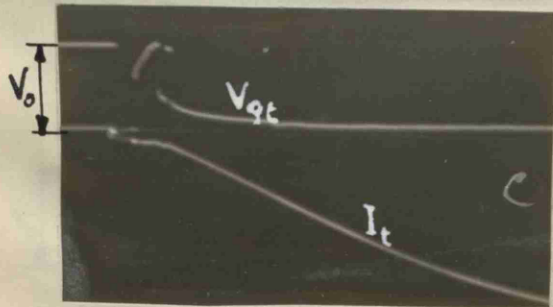
(d)



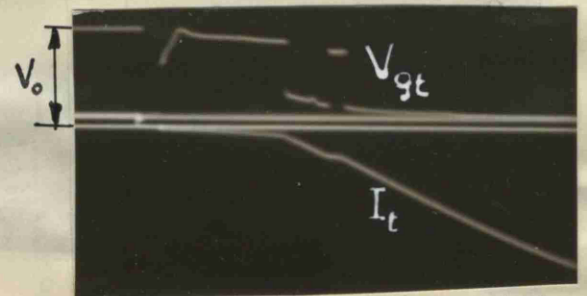
(b)



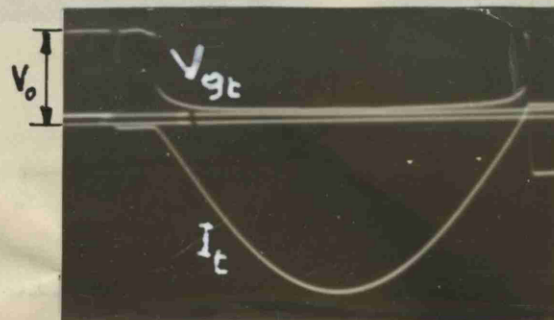
(e)



(c)



(f)



(g)

Time Scales:

(a)-(f) 4ms

(g) 10ms

Fig. 55. Oscillograms obtained with conditioned copper discs, spaced 0.5 cm apart, when the value of  $V_0$  was in the critical range. Standard Circuit, except that  $Z=126$  Ohms.

(a) Follow Current did not occur.

(b)-(g) Follow Current established.

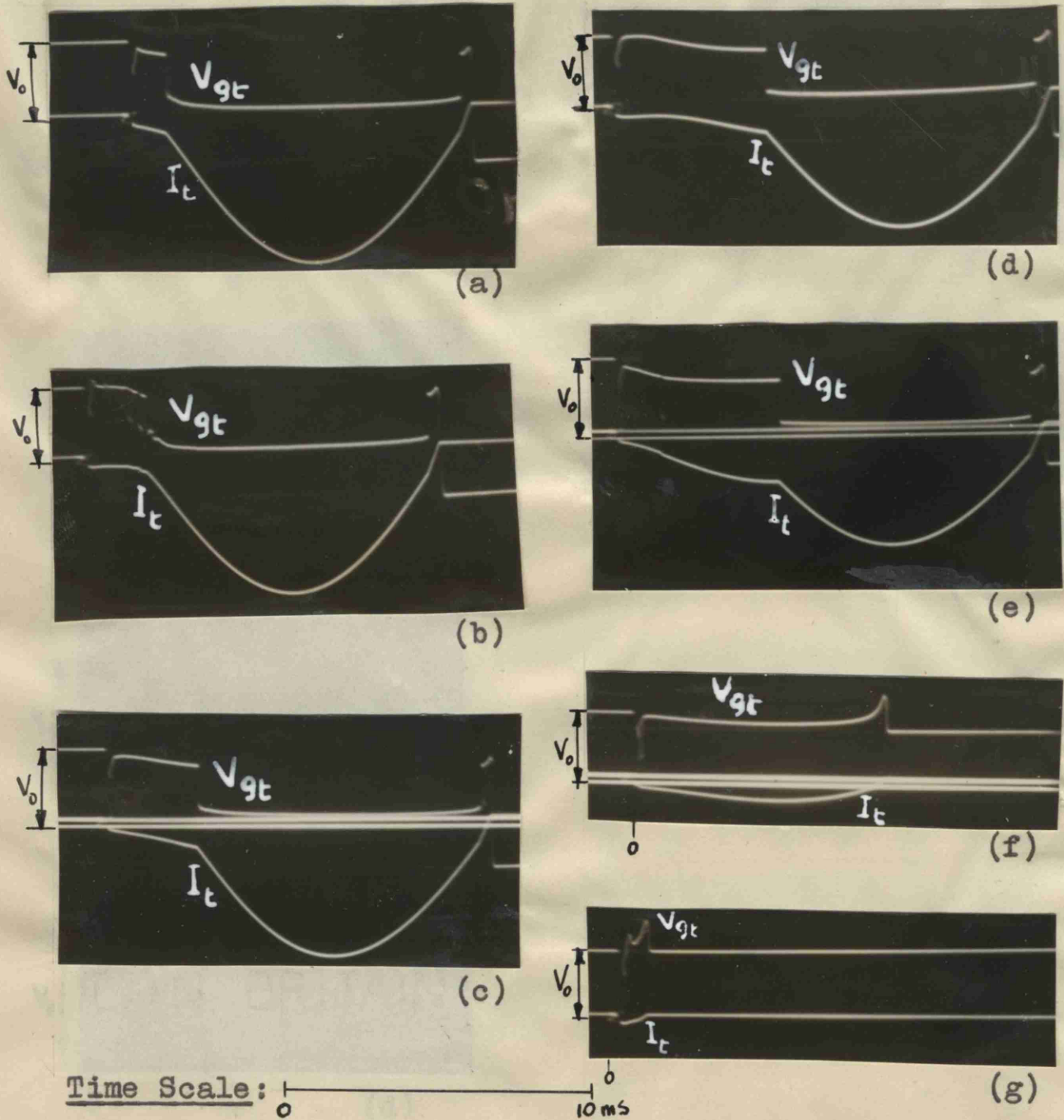
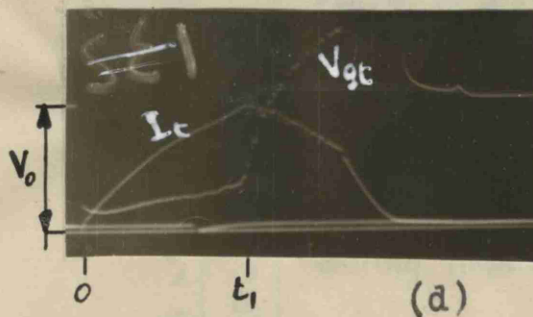
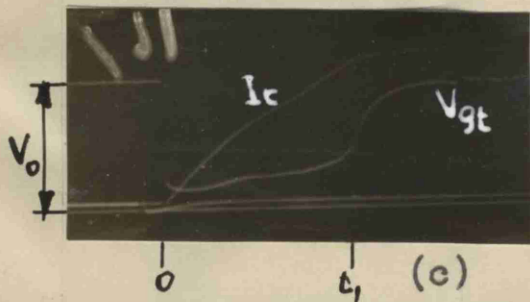
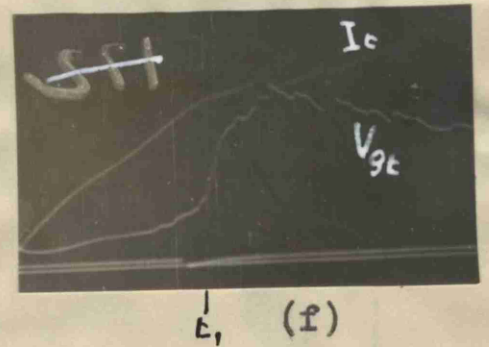
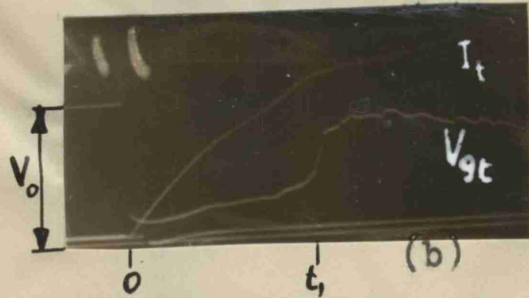
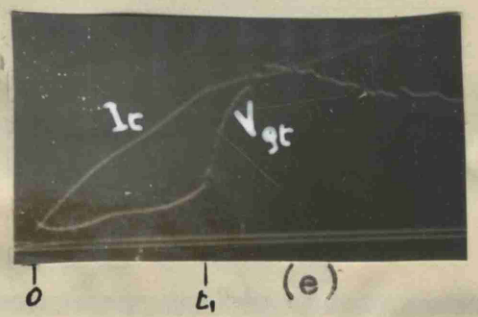
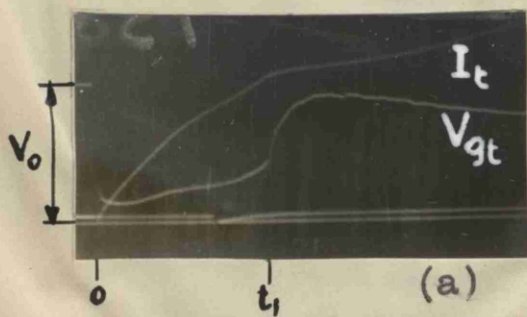


**Fig. 56.** Oscillograms obtained with unconditioned copper discs, spaced 0.5 cm. apart, when the value of  $V_0$  was in the critical range. Standard Circuit, except that  $Z=126$  Ohms.

(a)-(e) Follow Current established.

(f)-(g) Follow Current did not occur.



(a)-(d) Standard  
Circuit  
( $Z = 40$ ).

(e)-(f) Standard  
Circuit  
except  $Z = 126$

Time Scale: 500  $\mu$ s

**Fig. 57.** Oscillograms obtained with conditioned copper rods, 0.056 cm. diameter, spaced 0.5 cm. apart, when the value of  $V_0$  was in the critical range.

(a)-(c) and (e)-(f) Follow Current established.

(d) Follow Current did not occur.

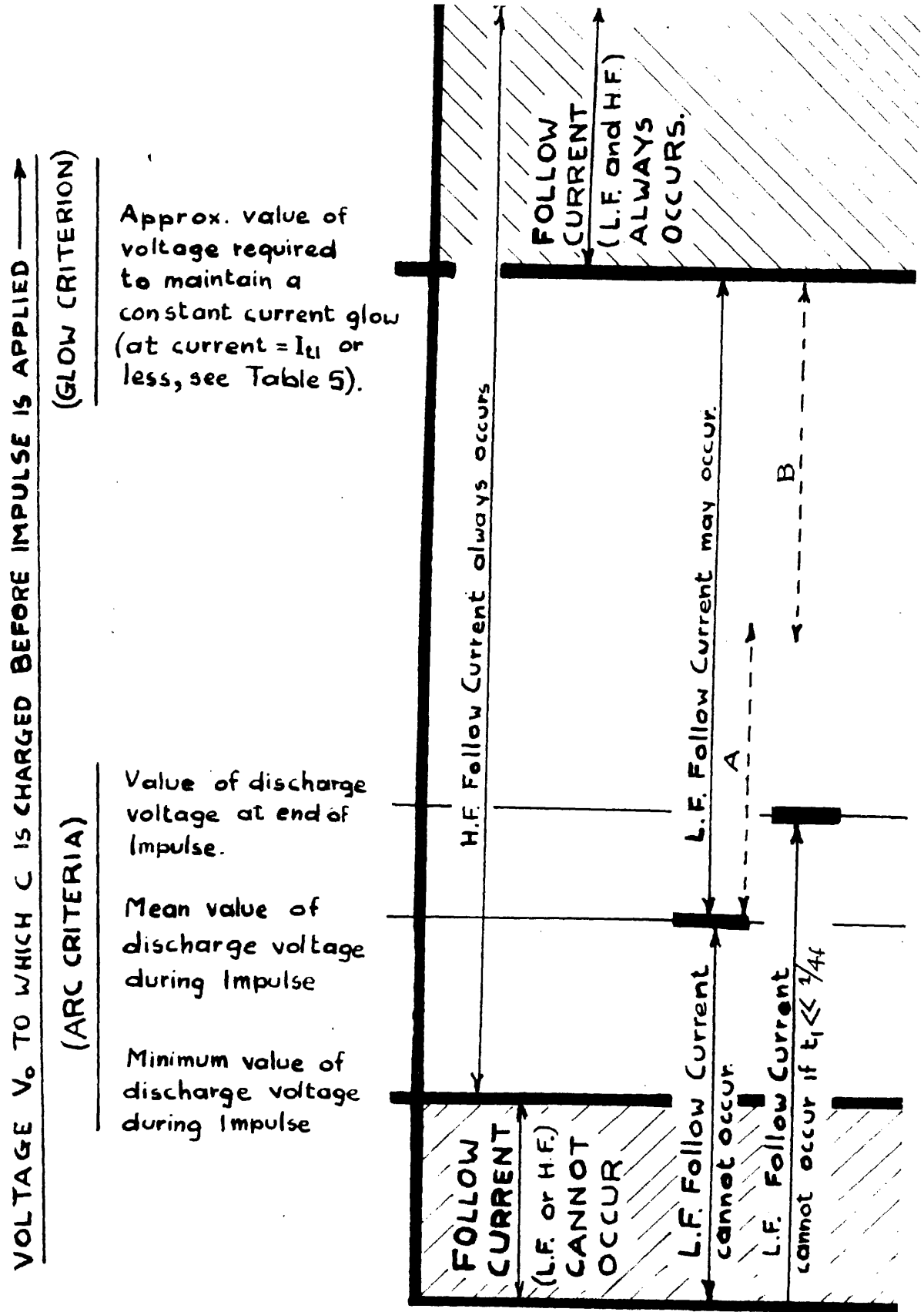


**FIG. 58** ILLUSTRATION OF THE CRITERIA OF FOLLOW CURRENT FOR THE CASE OF  $V_0$  AND  $V_{i0}$  HAVING THE SAME POLARITY TO EARTH AND  $I_0$  BEING NEGLIGIBLE.

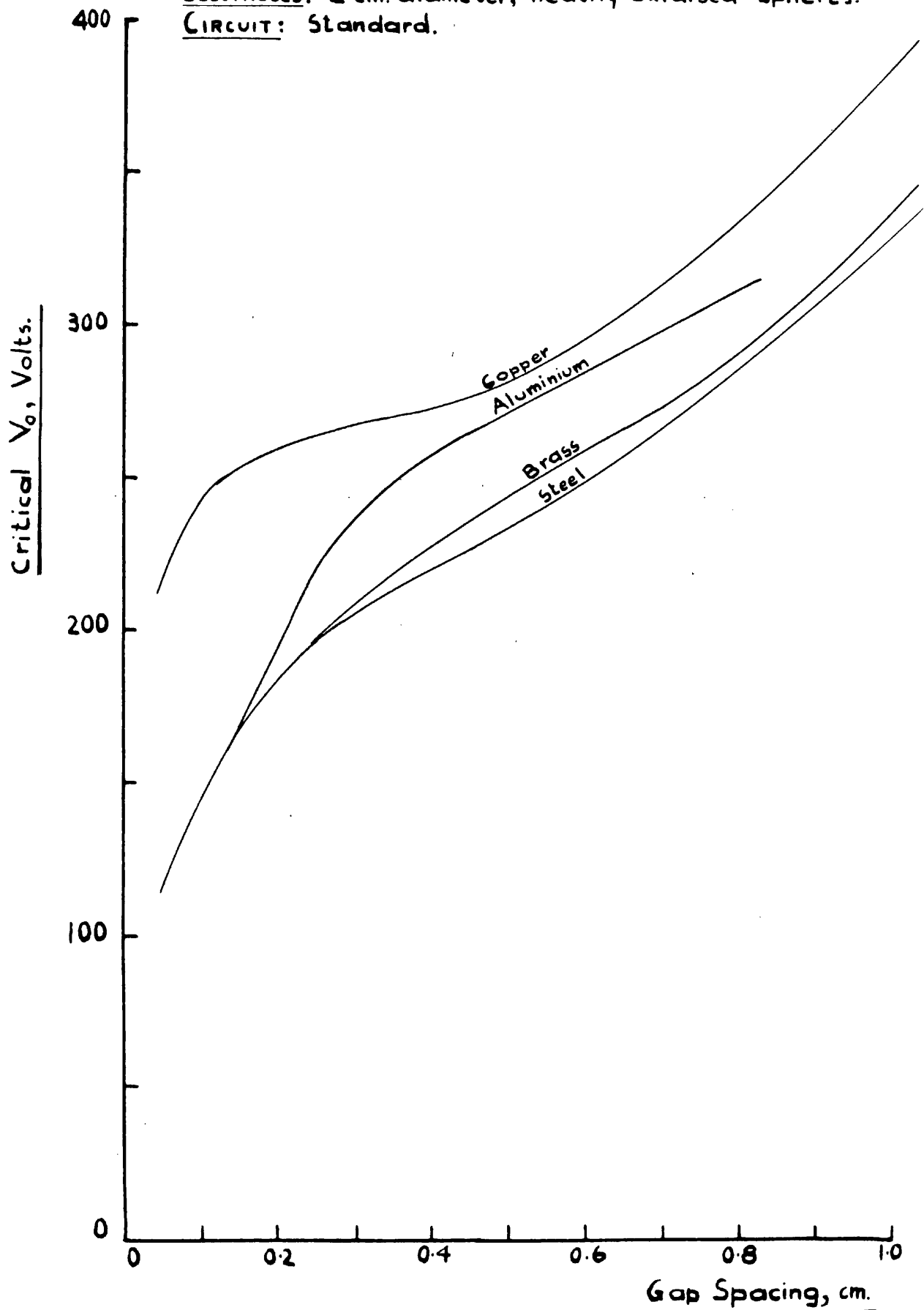
In this investigation the critical  $V_0$  ranges lay within A when Follow Current was of the H.C. type and within B when Follow Current was of the H.V. type.

**FIG. 59. COMPARISON OF SPACING DIAGRAMS.**

These curves have been drawn from the Spacing Diagrams, which have already been given. In the case of Copper, Brass and Steel, the curves given below have been drawn to lie evenly between those obtained in individual test runs.

ELECTRODES: 2 cm. diameter, heavily oxidised spheres.

CIRCUIT: Standard.



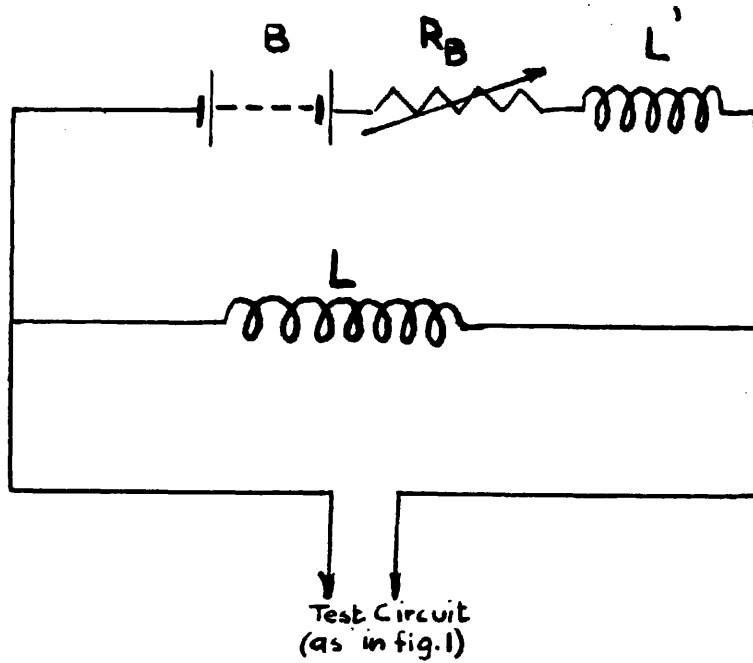


FIG. 60. MODIFICATION OF TEST CIRCUIT  
FOR 'POINT-ON-WAVE' TESTS.

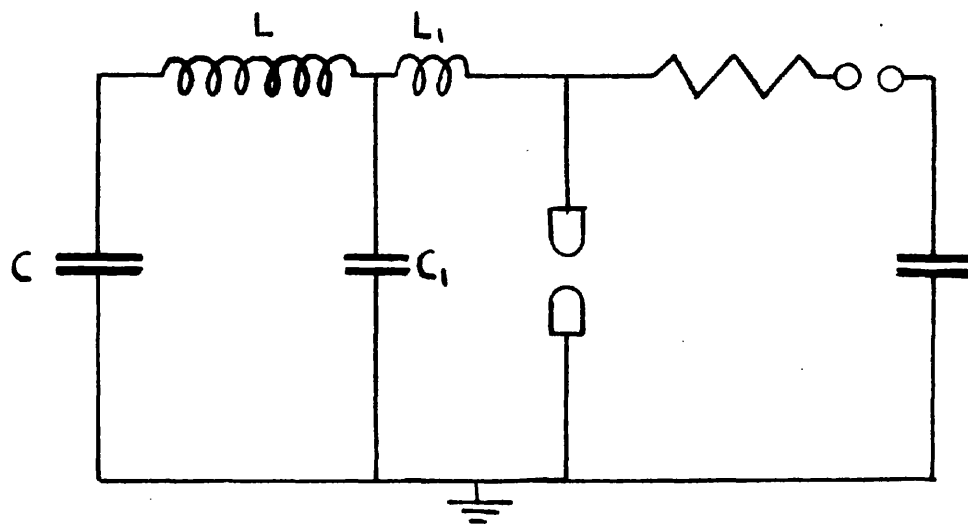
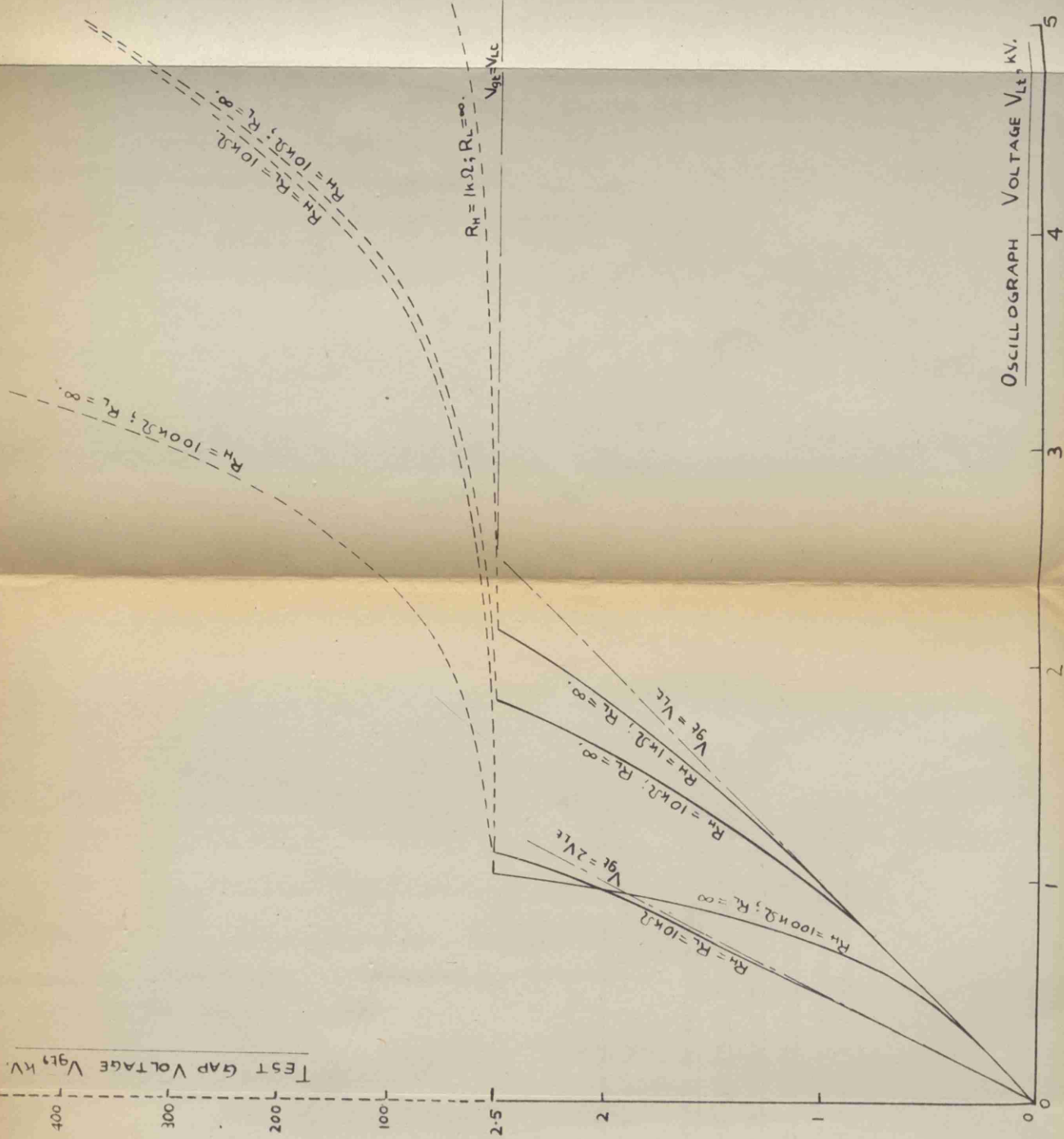


FIG. 61 CIRCUIT SUGGESTED FOR A STUDY OF THE EFFECT OF H.F. FOLLOW CURRENT ON THE ESTABLISHMENT OF L.F. FOLLOW CURRENT.

Fig. 62 Relation between the voltage  $V_{gt}$  at the test gap (and across the potential divider) and the voltage  $V_{It}$  at the oscillograph (and across the I.V. arm of the divider), calculated by taking  $R_{Mt} = 8 \times 10^4 \Omega$  and ignoring the stray capacitances associated with the divider.

The straight lines  $V_{gt} = V_{It}$  and  $V_{gt} = 2V_{It}$  show the relation between  $V_{gt}$  and  $V_{It}$  for the different  $R_H$  and  $R_L$  in the absence of  $R_{Mt}$ .

The  $V_{gt}$  scale is discontinuous at 2.5KV in order to illustrate both the protective and the measuring ranges of the divider.



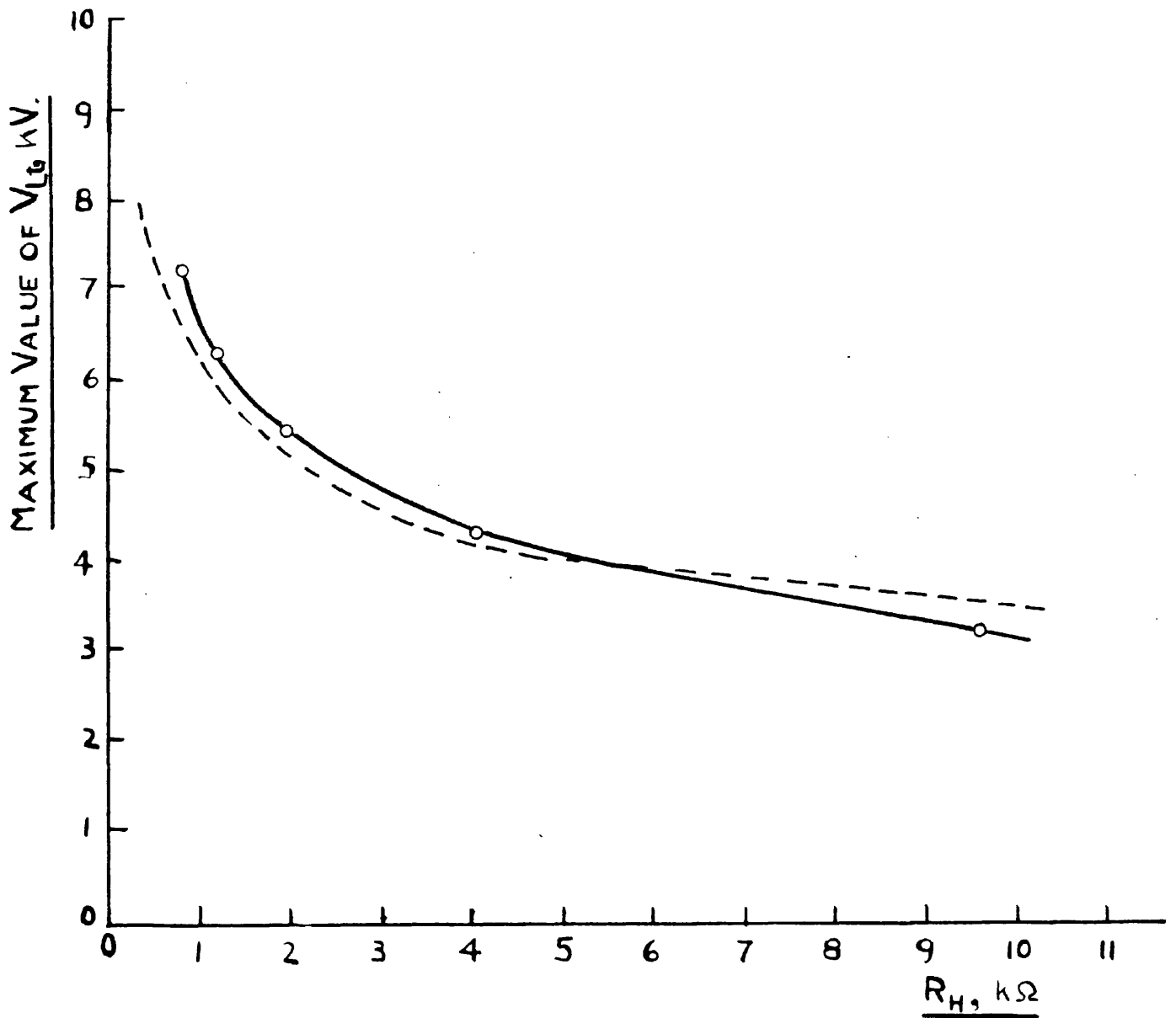
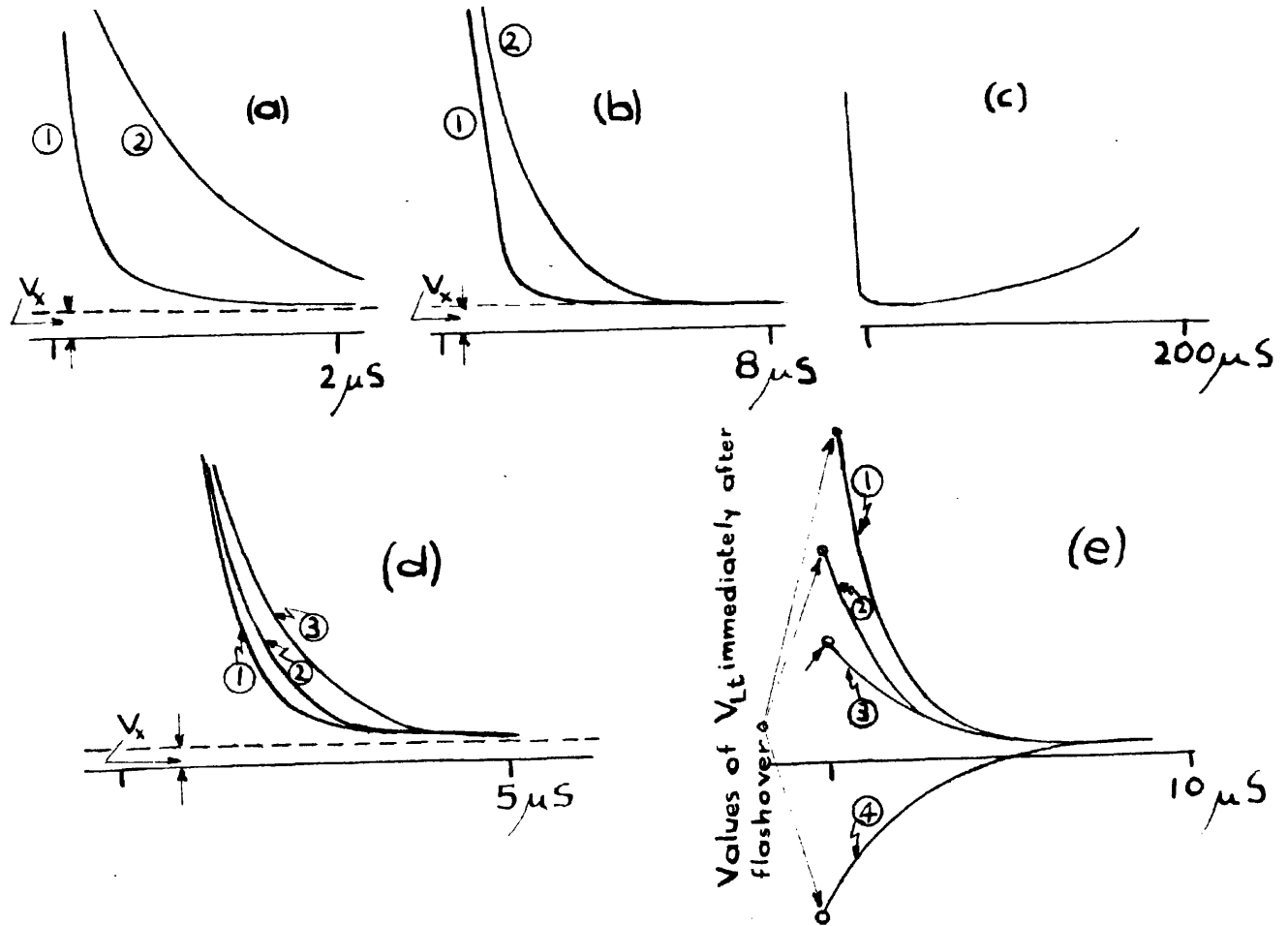


Fig.63. RELATION BETWEEN THE MAXIMUM VALUE OF  $V_{Lt9}$  AND THE VALUE OF  $R_H$ , WHEN A LONG DURATION PULSE WITH A PEAK VALUE OF 35 kV IS APPLIED ACROSS THE POTENTIAL DIVIDER.  $R_L = 11.9 \text{ k}\Omega$ .

The full curve was obtained by experiment.

The dotted curve was obtained from calculations.



**Fig. 64. Curves of  $V_{Lt}$  to a base of time, traced from oscillograms.**

- (a) Curve (1),  $R_H = 1 \text{ k}\Omega$ ; Curve (2),  $R_H = 10 \text{ k}\Omega$ , the straight line corresponding to  $V_x$  has been obtained from fig. 64(b). ( $R_L = 1 \text{ M}\Omega$ ) (No lumped  $C_H$  or  $C_L$ ).
- (b) Curve (1),  $R_H = 1 \text{ k}\Omega$ ; Curve (2),  $R_H = 10 \text{ k}\Omega$ . The figure shows how the voltage  $V_x$  is obtained (the test gap voltage  $V_{gt}$  is assumed to fall to  $n_\infty V_x$  at flashover, and to remain constant at that voltage until  $V_{Lt}'$  becomes negligible). ( $R_L = 1 \text{ M}\Omega$ ) (No lumped  $C_H$  or  $C_L$ ).
- (c) Curve obtained with  $R_H = 1 \text{ k}\Omega$ , and  $R_H = 10 \text{ k}\Omega$ . (Records are identical). ( $R_L = 1 \text{ M}\Omega$ ).
- (d) Curve (1),  $C_L = 40 \text{ }\mu\text{F}$ ; Curve (2),  $C_L = 50 \text{ }\mu\text{F}$ ; Curve (3),  $C_L = 79 \text{ }\mu\text{F}$ .  $V_x$  was obtained as for fig. 64(a). ( $R_H = 10 \text{ k}\Omega$ ;  $R_L = 150 \text{ k}\Omega$ ). (No lumped  $C_H$ ).
- (e)  $C_H$  is progressively increased for each of the subsequent curves (1), (2), (3) and (4).  $R_H = 10 \text{ k}\Omega$ ;  $R_L = 1 \text{ M}\Omega$ . (No lumped  $C_L$ ).

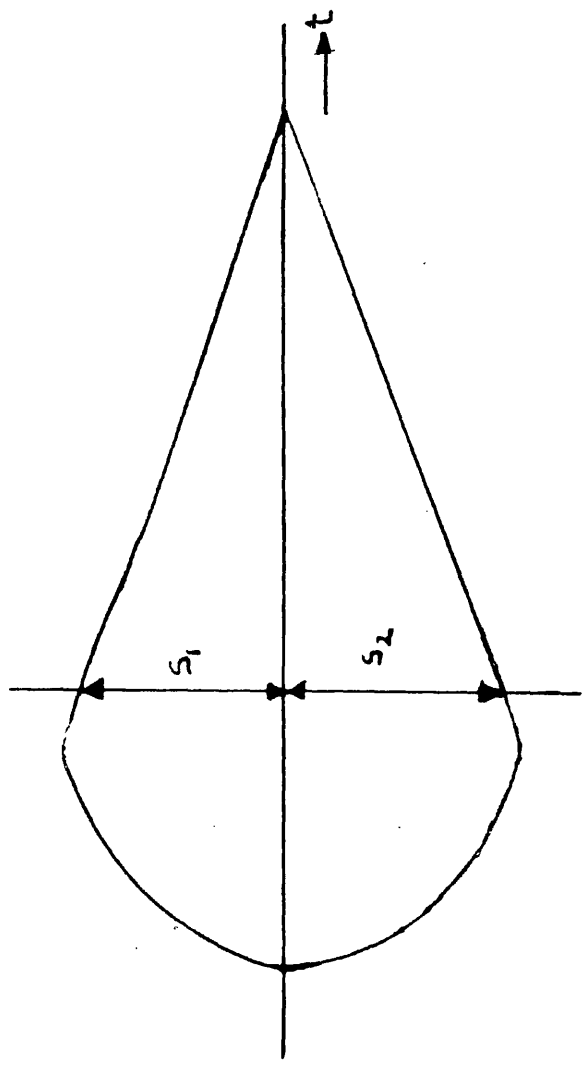
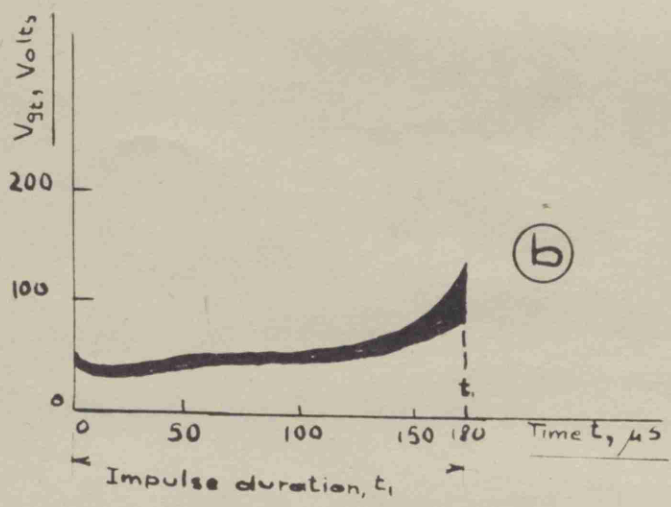
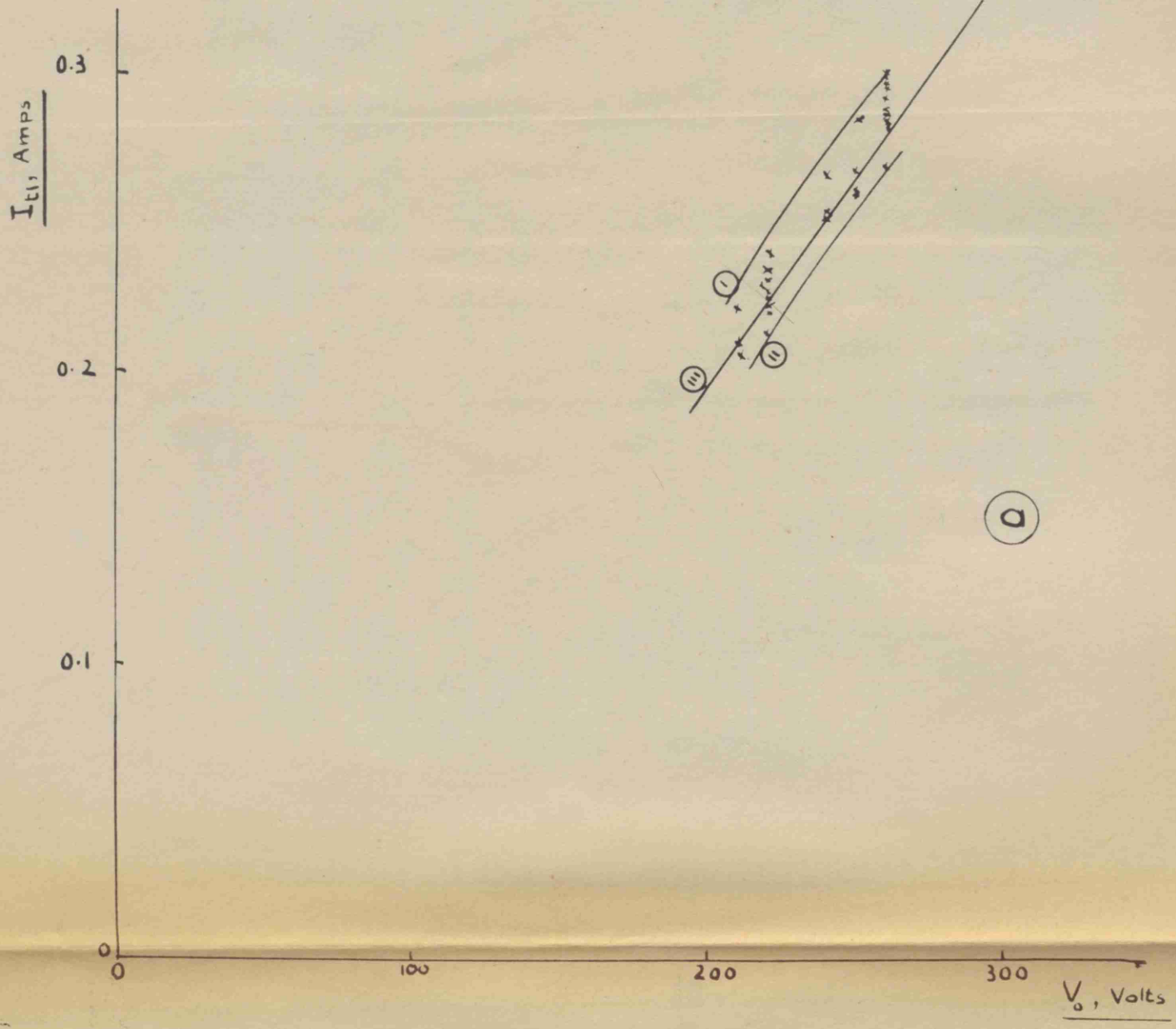


FIG. 65. Sketch of oscillogram used for calibrating the amplifier (Appendix II).



**FIG. 66. PREDICTION OF  $I_{t1}$**

The points shown in fig. (a) have been obtained from actual follow current tests. Lines (i) and (ii) indicate the limits of the region in which these points lie. Line (iii) has been obtained by calculation, as explained in Appendix VII.

Fig. 66